

**Department of Civil Engineering**

**Behaviour of Stiff Clayey Soils using Fracture  
Mechanics Approach**

**Miftahul Fauziah**

**This thesis is presented for the Degree of  
Doctor of Philosophy  
Of  
Curtin University of Technology**

**November 2009**

## DECLARATION

This thesis contains no material which has been accepted for the award of any other degree or diploma in any university.

To the best of my knowledge and belief, it contains no material previously published by any other person except where due acknowledgement has been made.

Following papers have resulted from this work:

1. Fauziah M and Nikraz H, 2009, *Influence of discontinuities on the behaviour of partially saturated compacted clay*, Jurnal dinamika TS UMS (national accredited Journal). (Paper submitted, under review).
2. Fauziah M and Nikraz H, Jun 2009, *Biaxial testing on the properties of pre-crack partially saturated clay*, Proc. of The 19th International Offshore (Ocean) and Polar Engineering Conference & Exhibition, Osaka, Japan, 21-26 Jun 2009.
3. Fauziah M and Nikraz H, Des 2008, *Plane testing on the properties of unsaturated compacted clay*, Proc. of the 3<sup>th</sup> International Conference on Geotechnical & GeoEnvironmental Engineering, Rock Mechanics & Engineering, Chiang Mai- Thailand, 10-12 Des 2008.
4. Fauziah M and Nikraz H, June 2008, *Behaviour of unsaturated compacted clay under plane strain condition*, Proc. of International Conference on Geo-Environment and Landscape Evolution 2008, The New Forest, United Kingdom, 16-18 June 2008
5. Fauziah M and Nikraz H, October 2007, *Stress strain behaviour of overconsolidated clay under plane strain condition*, Proc. of 10<sup>th</sup> Australian New Zealand Conference on Geomechanics, Brisbane, Queensland, Australia, 21-24 October 2007
6. Fauziah M and Nikraz H, Sept 2007, *Biaxial testing of overconsolidated clay*, Proc. of The 1st International Conference of European Asian Civil Engineering Forum, Jakarta, Indonesia, 26-27 September 2007
7. Fauziah M and Nikraz H, 2009, Comparison of Pre-crack and Intact Partially saturated stiff clay subjected to plane strain testing, Jurnal Rekayasa Sipil FTSP UII. (Paper submitted, under review).

Date : November 2009

Signature : .....



## ACKNOWLEDGEMENTS

First, I would like to thank my supervisors Prof. Hamid Reza Nikraz, principal supervisor, Prof. Kwang Wei Lo, and Dr.Min Min Zhao for initially giving me the chance to do research and then guiding me and assisting throughout the period of this work. The author also extend her gratitude to the Head of the Civil Engineering Department of Curtin University of Technology (2005-2008) Prof. David Scott and Prof. Hamid Reza Nikraz (2008-currently), and his secretaries, Mrs. Diane Garth, Ms Sucy Leong, and Ms Liz Field who patiently helped the author in any research-related matters.

The research presented in this thesis was funded by Indonesian Government, in the first stages through the Technological and Professional Skills Development Project (TPSDP) and the last stages by the Directorate General of Higher Degree (Dirjen Dikti), Department of National Education, Republic of Indonesia, as well as by Universitas Islam Indonesia (UII). Their support is gratefully acknowledged.

Many thanks are due to the laboratory staff: Rob Cutter, Mark Whittaker, Fonty, Ashley Hortle, Ashley Hughes, Michael Ellis, David Collier, Frank Cicoria, Jim Sherlock, Peter Bruce, Jeffrey Pickels and the general manager of the engineering laboratory, John Murray who had provided continuous assistance in preparing and carrying out the experiments. The author is also indebt to Mr Paisar Syakur and Mr Pontjo Utomo, both are former research students who used the same plane strain device, for their assistances, commitment and care.

The author would like to thank all the people that made the environment friendly and lively. Special thanks are due to Mr. Darmodjo Ruspanji, Mr. Murod Thontowi, Fitri and her family, Albani and his family, Monita, Rini, Jeny, Anas and his family, Dekar and his family, and Roman and his family for not only being friends from the very beginning but also helping me and my family in numerous ways.

To my beloved parents, Ayahanda, my father Achmad Tasliman, my mother Zumrodaturun, my father in-law Soebagi, my mother in-law Sri Hartati, without your continuous support, encouragements and prayer, I might not have reached this stage. Also to my sisters, Nani, Rofi and Umni and my brothers Shubhi and especially Rifqy, without whom I would never completed this thesis. I am fortunate to have encouragement and support from several other family members and many friends.

Finally, I wish to dedicate this thesis to my lovely family. It would not be possible to express here my gratitude to my husband Hari Wibowo, not only for loving me, supporting me and encouraging me in everything I have done in life, but also for assisting me in laboratory works as well as in computing works. Thank you for your great patience and for always being there for me. To my adorable daughter Qory'Aina Luthfia, you have shown your surprisingly deep understanding and patience (at such a young age) of your mother's research activity, even if it should spent our weekend at the laboratory. Thanks a lot to you and may Allah reward you.

Perth, November 2009

Miftahul Fauziah

## TABLE OF CONTENTS

<b>DECLARATION</b>	i
<b>ACKNOWLEDGEMENT</b>	ii
<b>TABLE OF CONTENTS</b>	iv
<b>ABSTRACT</b>	viii
<b>LIST OF FIGURES</b>	ix
<b>LIST OF TABLES</b>	xii

### **Chapter 1. Introduction**

1.1. Back ground of the study	1
1.2. Scope and aim of research	4
1.3. Outline of thesis	5

### **Chapter 2. Soil physics and testing device relevant to the study of stiff clay**

2.1. Introduction	7
2.2. Structure and composition of clay	9
2.3. Factors affecting soil stiffness	12
2.3.1. Current stress state-volume state	12
2.3.2. Soil structure	15
2.3.3. Ageing	17
2.3.4. Recent stress history	19
2.3.5. Stress path direction	21
2.4. Biaxial Apparatus	22
2.5. Summary	29

### **Chapter 3. Constitutive behaviour and failure of over consolidated clay**

3.1. Introduction	31
3.2. Constitutive models for over consolidated clays	32
3.2.1. Classical theory of elasto-plasticity	33
3.2.2. Elasto plastic constitutive model of over consolidated clay	37
3.3. Elastic plastic models of hard soil and soft rocks	44

3.4. Behavior of over consolidated clay based on critical state theory	47
3.5. Remark	55

#### **Chapter 4. Constitutive behaviour and failure of partially saturated clay**

4.1. Introduction	58
4.2. Constitutive models for partially saturated clays	59
4.2.1. The Barcelona-type models	59
4.2.2. Physical model of Leroueil and Barbosa (2000)	63
4.2.3. Models for the prediction of shear strength	65
4.3. Mechanical behavior of partially saturated clay	66
4.3.1. Stress state variables	67
4.3.2. Volume change	63
4.3.3. Pore Pressure Parameters	75
4.3.4. Matric suction	77
4.5. Concluding remark	78

#### **Chapter 5. Fracture mechanical approach**

5.1. Introduction	80
5.2. A basic concept of fracture mechanics theory	82
5.2.1. The pioneering work of Griffith (1920) and Irwin (1957)	82
5.2.2. Griffith energy balance	83
5.2.3. Irwin energy release rate	84
5.2.4. Stress Intensity factor and fracture toughness	85
5.2.5. Linear elastic fracture mechanics (LEFM) concept	87
5.3. Fracture mechanics theory applied in stiff clay	88
5.4. The unified mode	91
5.5. Behavior of partially saturated clay using fracture mechanical approach	95
5.5.1. Determination of degree of saturation and pore pressure parameter	95
5.5.2. Determination of matric suction	96
5.5.3. Determination of fracture toughness	96
5.5.4. Fracture criteria	97

5.5.5. Finite elemen analysis	106
5.5.6. Analytical procedure using the unified fracture model	111

## **Chapter 6. Experimental program**

6.1. Introduction	114
6.2. Biaxial compression device	115
6.2.1. Description of the apparatus	117
6.2.2. Components of the equipment	119
6.2.3. Loading system of biaxial apparatus	120
6.2.4. Data recording and instrumentation	121
6.3. Material and specimen preparation	123
6.3.1. Mixing the slurry and consolidation process	123
6.3.2. Preparation of plane strain test set up	126
6.4. Testing on saturated over consolidated clay specimen	129
6.4.1. Saturation and loading-unloading process	129
6.4.2. Biaxial compression process	130
6.5. Testing on partially saturated clay specimen	131
6.5.1. Set up of the biaxial and triaxial test	131
6.5.2. Saturation and suction process	133
6.2.3. Compression process	138
6.6. Testing on fracture toughness of partially saturated clay specimen	139
6.6.1. Specimen preparation	140
6.6.2. Mode I fracture test	141
Test verification of finite element analysis on pre-crack partially saturated clay	142
Specimen preparation and test apparatus set up	143
Test procedure for saturation, consolidation and loading the specimen	143

## **Chapter 7. Result, analysis and discussion**

7.1. Introduction	145
7.2. Behavior of saturated over consolidated kaolin clay specimen	146

7.2.1.	Normally consolidated undrained test	149
7.2.2.	Over consolidated undrained test	151
7.2.3.	Over consolidated drained test	157
7.3.	Behavior of partially saturated kaolin clay specimen	162
7.3.1.	Shear strength behaviour of partially saturated clay	162
7.3.2.	Volume change behaviour of partially saturated clay	166
7.4.	Fracture toughness of partially saturated clay specimen	179
7.5.	Crack propagation analysis on pre-crack partially saturated kaolin clay specimen	181
7.5.1.	Finite element analysis on crack development	181
7.5.2.	Experimental verification on crack development	183
 <b>Chapter 8. Conclusions and recommendations</b>		
8.1.	Conclusions	188
8.2.	Recommendations	190
 <b>REFERENCES</b>		191
 <b>APENDICES</b>		
Published paper resulting from this study		206

## ABSTRACT

Most of the conventional elastic plastic models of soils are based on continuum mechanics, however, for stiff, hard soils and soft rocks discontinuities develop under load, and since the models assume continuity, they would cease to apply. These discontinuities had not been accounted for in the continuum-based elastic plastic models. On the other hand, fracture mechanical theory may be used to advantage to replicate their behaviour. The behaviour of soil commonly is interpreted from conventional triaxial apparatus, whereas, testing of soil using the plane strain device would be more useful information, as more geotechnical field problems are basically occur in these situations.

The present study has dealt with the investigation on the behaviour of saturated over consolidated clay as well as partially saturated clay, which represent the stiff and hard brittle clay by the use of a new biaxial device modified from conventional triaxial apparatus. In general, the apparatus was able to produce data which are in a good accordance with known soil behaviour of stiff clay. Shear band localization occurred in all test specimens of over consolidated clay. Specimen initiated to be discontinuous upon reaching the peak stresses. It is evident that specimen of partially saturated containing fissures had weaker shear strength as well as compressive strength.

From point of view of the discontinuities that take places in the stiff clay, a model based on *the unified model* (Lo et al, 1996) and *the elasto-plastic shear fracture model* (Lo, et al, 2005) was used in this study. The problem may be dealt with one of brittle fracture of a three-phase specimen, where the matric suction is disrupted by tensile or shear loading. As a result the fracture toughness of the specimen would vary according to matric suction changes. A problem of plane strain compression testing was carried out to implement the model. The crack propagation simulation was resulted the same pattern with the experimental results on partially saturated kaolin clay.

## LIST OF FIGURE

	Page
Figure 2.1. Structural arrangements in clay minerals (after Baver et al, 1972)	10
Figure 2.2. Definition of isotropic over consolidation ratio (after Viggiani and Atkinson, 1995)	13
Figure 2.3. Effects of strain on stress level exponent $n$ (after Jardine, 1995)	14
Figure 2.4. Vallerica clay: initial shear modulus versus a) mean effective stress and b) specific volume (after Rampello and Silvestri, 1993)	15
Figure 2.5. Normalized shear stiffness of both natural and reconstituted Pappadai clay (after Cotecchia and Chandler (1997))	16
Figure 2.6. The effect of creep on the yield stress of normally consolidated clay (after Bjerrum (1967))	18
Figure 2.7. The effect of cementation on the yield stress of normally consolidated clay (after Bjerrum (1967))	18
Figure 2.8. The effect of ageing on the yield stress of normally consolidated clay (redrawn by Burland (1990) after Leonards and Ramiah (1959))	19
Figure 2.9. Stiffness versus strain measure in constant $p'$ tests of reconstituted London clay (after Atkinson, 1990)	20
Figure 2.10. Stress path followed in single sample of natural Bothkennar Clay (after Clayton and Heyman, 2001)	21
Figure 2.11. Stress path applied to: (a) Bothkennar Clay and (b) London clay (after Clayton and Heyman, 2001)	22
Figure 2.12. A schematic diagram of triaxial device (after Head, 1995)	23
Figure 2.13. Comparison between (a) triaxial/axis symmetric and (b) biaxial/plane strain condition (after Potts et al, 2002)	24
Figure 2.14. Stress strain curve of the specimen under triaxial and plane strain testing (after Mochizuki et al, 1993)	24



Figure 2.15. Kjelman's plane strain device (after Kjellman, 1936)	25
Figure 2.16. A schematic diagram of plane strain device (after Mita, 2003)	26
Figure 2.17. The view of The Vardoulakis-Drescher plane strain device (after Drescher et al, 1990)	27
Figure 2.18. A schematic diagram of Louisiana Plane strain device (after Alshibli and Akbas, 2007)	28
Figure 2.19. Double wall biaxial device (after Schanz and Alabdullah, 2007)	29
Figure 3.1. An illustration of Cap model (after Potts, 1999)	39
Figure 3.2. A schematic representation of bounding surface model (after Dafalias and Herrmann, 1982)	41
Figure 3.3. Conceptual model of unload-reload used by MIT-E3 for hydrostatic compression: a) perfect hysteresis b) hysteresis and bounding surface plasticity (after Whittle, 1993)	42
Figure 3.4. Two surface model (after Al-Tabaa, 1987)	43
Figure 3.5. States of failure and their related stress-strain behaviour on the Elastoplastic shear fracture model (after Lo, et al, 2005)	47
Figure 3.6. Isotropic compression line, swelling line and critical state line	48
Figure 3.7. State boundary surface of the critical state framework in normalized stress space (after Atkinson and Bransby, 1978)	49
Figure 3.8. State boundary surface of the critical state framework in $v$ - $p'$ - $q$ space (after Atkinson and Bransby, 1978)	50
Figure 3.9. Elastic wall (after Atkinson and Bransby, 1978)	50
Figure 3.10. Comparison of pore pressure: (a) dilation on over consolidated clay and (b) contraction on normally consolidated clay (after Ortigo, 1995)	52
Figure 3.11. Typical result of a drained test on heavily over consolidated Weald Clay ( after Bishop and Henkel, 1962)	53
Figure 3.12. Stress paths in $q$ ': $p'$ and $v$ : $p'$ of a drained test on over	

consolidated clay (after Atkinson and Bransby, 1978)	53
Figure 3.13. Typical result of triaxial undrained test on over	
consolidated clay (after Bishop and Henkel, 1962)	54
Figure 3.14. Stress paths in $q': p'$ and $v: p'$ of a drained test on over	
consolidated clay (after Atkinson and Bransby, 1978)	55
Figure 4.1. Limit state curves and elastic domains for unsaturated soil–	
BBM (after Alonso et al, 1990)	60
Figure 4.2. Yields surface in $q: p'': s$ surface (after Alonso et al, 1990)	61
Figure 4.3. Loading Collapsed Yield Curve (after Wheeler and	
Sivakumar, 1995)	62
Figure 4.4. Description of Leroueil and Barbosa model (after Leroueil	
and Barbosa, 2000)	63
Figure 4.5. Lc curve of Rosalie clay (after Ghorbel and Lerouiel, 2006)	65
Figure 4.6. Yielding and GFY-2 of Rosalie curve (after Ghorbel and	
Lerouiel, 2006)	65
Figure 4.7. Three dimensional void ratio and water content constitutive	
surfaces for unsaturated soil: (a) void ratio constitutive	
surface; (b) water content constitutive surfaces (after	
Fredlund and Rahardjo, 1993)	70
Figure 4.8 . Three dimensional plot showing the primary and secondary	
reference condition for the void ratio constitutive surface	
(after Fredlund et al, 2000)	71
Figure 4.9. Illustration of the definition the void ratio constitutive	
surface based on the slopes of the primary reference curve	
(after Fredlund et al, 2000)	72
Figure 4.10. Variation of constant void ratio contours when the surface	
is view along the void ratio axis (after Fredlund et al, 2000)	72
Figure 4.11. Effect of a variation in the air entry value on the void ratio	
contours (after Fredlund et al, 2000)	73
Figure 4.12. Variation of constant void ratio contours when the surface	
is viewd along the void ratio axis (after Fredlund et al,	
2000)	73

Figure 5.1. A through crack in an infinite plate under uniform tension (after Anderson, 2005)	83
Figure 5.2. The stress fields near a crack tip (after Anderson, 2005)	85
Figure 5.3. The three loading modes of a crack (after Broek, 1984)	86
Figure 5.4. Closure parameter of a crack tip (after Lo et al, 1996)	92
Figure 5.5: (a). Horizontal crack subjected to generalised stress system. (b). Inclined crack subjected to biaxial compressive loading (After Vallejo, 1988)	98
Figure 5.6. (a). Inclined crack subjected to biaxial compressive loading. (b). Inclined crack subjected to uniaxial compressive loading in infinite	99
Figure 5.7. $f(\theta)$ versus angle to parent crack plane around the crack tip	103
Figure 5.8. Formation of triangular crack-tip element from 8-noded quadratic quadrilateral element	107
Figure 5.9. The quarter-point elements modeled around crack tip	108
Figure 6.1. A schematic diagram of biaxial compression apparatus	118
Figure 6.2. A schematic diagram of principle stresses acting on the specimen under plane strain condition	118
Figure 6.3. Components of biaxial device	119
Figure 6.4. The Global Digital System (GDS) pressure generator unit	120
Figure 6.5. LVDT attached on top of the top cover of the cell	121
Figure 6.6. Laser sensor mounted to the triaxial cell	122
Figure 6.7. Four pore pressure transducers mounted to the base plate of the cell	122
Figure 6.8. Data logger and automatic volume change unit	123
Figure 6.9. Mixture of kaolin powder and water	124
Figure 6.10. Typical arrangement of consolidation unit	125
Figure 6.11. A view of consolidation unit machine	126
Figure 6.12. Inserting top cap to the rubber membrane	127
Figure 6.13. Placing the test specimen in rubber membrane	128
Figure 6.14. Rubber membrane slid over bottom pedestal	128

Figure 6.15. Perspex rigid wall assembled to the test specimen	129
Figure 6.16. Biaxial testing arrangement	130
Figure 6.17. Typical arrangement for biaxial device for unsaturated testing	132
Figure 6.18. A schematic diagram of plane strain condition of the pre-crack specimen	133
Figure 6.19. Constitutive surface of void ratio versus net normal stress and matric suction	134
Figure 6.20. Constitutive surface of water content versus net normal stress and matric suction	135
Figure 6.21. Side view of the triaxial test set up	135
Figure 6.22. Side view of the plane strain test set up	136
Figure 6.23. Typical geometry of Mode I test specimen (after Anderson, 1995)	140
Figure 6.24. Compact test specimen for Mode I test ( $K_{IC}$ test)	141
Figure 6.25. Mode I fracture test arrangement	141
Figure 7.1. The virgin compression line and swelling line of kaolin clay specimen	146
Figure 7.2. The Critical state line in $p': q$ plane	147
Figure 7.3. The Hvorslev surface in $p': q$ plane	148
Figure 7.4. Deviatoric stress versus axial strain of NC clay specimen	149
Figure 7.5. Pore pressure versus axial strain of NC clay specimen	150
Figure 7.6. Deviatoric stress versus axial strain of CU specimen	153
Figure 7.7. Deviatoric stress versus axial strain of CU specimen	154
Figure 7.8. Volumetric strain versus axial strain of CU specimen	155
Figure 7.9. Excess pore pressure versus axial strain of CU specimen	156
Figure 7.10. Deviatoric stress versus axial strain of CD specimen	159
Figure 7.11. Volumetric strain versus axial strain of CD specimen	160
Figure 7.12. Stress Path of CD Specimens	161
Figure 7.13. Deviatoric stress versus axial strain of specimen under matric suction 0 kPa and net normal stress 900 kPa	164
Figure 7.14. Deviatoric stress versus axial strain of specimen under net	

normal stress 0 kPa and matric suction 500 kPa	166
Figure 7.15. Void ratio against log matric suction of specimen under zero net normal stress	167
Figure 7.16. Void ratio against log net normal stress of specimen under zero matric suction	168
Figure. 7.17. Constitutive surface of void ratio versus net normal stress and matric suction of IB specimen (Intact, biaxial test)	170
Figure. 7.18. A-three dimensional constitutive surface of void ratio versus net normal stress and matric suction of IB specimen (Intact, biaxial test)	170
Figure. 7.19. Constitutive surface of void ratio versus net normal stress and matric suction of PCB specimen (Pre-crack, biaxial test)	171
Figure. 7.20. A-three dimensional constitutive surface of void ratio versus net normal stress and matric suction of PCB specimen (Pre-crack, biaxial test)	171
Figure. 7.21. Constitutive surface of void ratio versus net normal stress and matric suction of IT specimen (Intact, triaxial test)	172
Figure. 7.22. A-three dimensional constitutive surface of void ratio versus net normal stress and matric suction of IT specimen (Intact, triaxial test)	172
Figure 7.23. Water content against log matric suction of specimen under zero net normal stress	174
Figure 7.24. Water content against log net normal stress of specimen under matric suction zero	175
Figure. 7.25. Constitutive surface of water content versus net normal stress and matric suction of IB specimen (Intact specimen, biaxial test)	177
Figure. 7.26. A-three dimensional constitutive surface of water content versus net normal stress and matric suction of IB specimen (Intact specimen, biaxial test)	177
Figure. 7.27. Constitutive surface of water content versus net normal	

stress and matric suction of PCB specimen (Pre-crack specimen, biaxial test)	178
Figure. 7.28. A-three dimensional constitutive surface of water content versus net normal stress and matric suction of PCB specimen (Pre-crack specimen, biaxial test)	178
Figure. 7.29. Constitutive surface of water content versus net normal stress and matric suction of IT specimen (Intact specimen, triaxial test)	179
Figure. 7.30. A-three dimensional constitutive surface of water content versus net normal stress and matric suction of IT specimen (Intact specimen, triaxial test)	179
Figure. 7.31. Force against displacement of mode I fracture test of the partially saturated kaolin clay specimen under 500 kPa	181
Figure. 7.32. Finite element mesh of the pre-crack partially saturated specimen on plane strain test	182
Figure. 7.33. Crack pattern of the specimen using finite element analysis	183
Figure. 7.34. Constitutive surface of void ratio versus net normal stress And matric suction	184
Figure. 7.35. Constitutive surface of water content versus net normal stress and matric suction	185
Figure. 7.36. Crack pattern of the pre-crack partially saturated specimen under plane strain compression test	186

<b>LIST OF TABLES</b>	<b>Page</b>
Table 6.1. Plane strain compression tests on kaolin specimen	131
Table 6.2. Stages of varying matric suction for IBM, PCBM dan ITM specimen	137
Table 6.3. Stages of varying net normal stress for IBN, PCBN dan ITN specimen	138

Table 6.4. Compression tests on partially saturated kaolin clay specimen	139
Table 6.5. Mode I fracture toughness tests on partially saturated kaolin clay	142
Table 7.1. Material parameters of remoulded kaolin clay.	148
Table 7.2. Moisture content variation in failed CU tests specimen	152
Table 7.3. Result of biaxial compression test on undrained over consolidated clay	152
Table 7.4. Moisture content variation in failed CD tests specimen	157
Table 7.5. Result of biaxial compression test on drained over consolidated clay	158
Table 7.6. The peak stress versus axial strain of partially saturated clay specimen	163
Table 7.7. Void ratio variation with matric suction	167
Table 7.8. Void ratio variation with net normal stress	168
Table 7.9. Volume change index of the specimen correspond to void ratio	169
Table 7.10. Water content variation with matric suction	173
Table 7.11. Water content variation with net normal stress	173
Table 7.12. Volume change index of the specimen correspond to water content	176
Table 7.13. Result of mode I fracture test of partially saturated clay specimen	180
Table 7.14. Result of volumetric deformation indices of specimen	183

# **CHAPTER 1**

## **INTRODUCTION**

### **1.1. Background of the study**

The stress-strain behaviour of soil involving predictions of deformation and failure of soil is an important basis of soil mechanics. Experimental laboratory and field observations have indicated that an elastic-plastic model can approximate the behaviour of certain soils very well, as long as the soil deforms uniformly as a continuous medium. Most of the conventional elastic plastic models of soils, including the most widely used model, the Hvorslev-Modified Cam Clay (MCC) model (Roscoe and Burland, 1968) are based on the assumption of continuum mechanics, and therefore applies only if the material remains intact. For stiff or hard soils and soft rock, discontinuities develop under load, and since the models assume continuity, they would cease to apply.

Various studies have been conducted on detailed aspects of such discontinuities, notably on shear band localization failure but these are of limited practical application in an actual situation. And still, the presence of such discontinuities, which are clearly observable in soils and soft rock, is evidently a major feature to be taken into account in any reasonably consistent analytical model of the material behaviour. These discontinuities had not been accounted for in the continuum-based elastic plastic models.

The conventional failure criteria for soils (Atkinson and Bransby, 1982) may be partly appropriate to yield-dominant behaviour, but this is not a category of



brittle fracture. Conventional brittle fracture concept has been developed on the basis of the weakest link theory proposed by Pierce for cotton yarn, and Tucker for concrete, however, the major developments of the theory were made by Weibull (1939), who verified the results on many different brittle materials. In practice, there is the possibility that soil behaves more like a brittle material. The soil ruptures suddenly under compressive loading like soft rock, starting from the weakest crack in it. The existence of fissures and cracks, which are the result of mechanical, thermal and volume-change-induced stresses, such soils are non uniform and therefore not amenable to analysis by continuum mechanics. On the other hand, fracture mechanical theory may be used to advantage to replicate their behaviour.

The use of fracture mechanical theory to simulate the behaviour of stiff or hard soil which considered the discontinuities had been attempted by many researchers since few decades ago. Bishop (1967) and Skempton et al (1969) were the first ones to suggest that fracture mechanics concepts might shed light on the process of progressive failure of slopes made of stiff fissured clays. The principle of Linear Elastic Fracture Mechanics (LEFM) theory was applied by Vallejo (1985, 1986, 1987, 1988a, 1989) to investigate the failure mechanisms of stiff fissured kaolinite clay samples subjected to compression and direct shear stress condition. Saada et al (1985) also employed concepts of LEFM concept to over consolidated brittle clays with a crack tested under a combination of normal and shear loads and used a stability criterion to predict failure of infinite slopes. Chudnovsky et al (1988) studied the propagation of cracks in clays under sliding type of loading using the crack layer theory. Saada et al (1994) has conducted extensive laboratory tests on the mechanics of crack propagation in over consolidated clay samples.

Lo et al (2005) proposed an elasto-plastic shear fracture approach to the constitutive behaviour of soil and soft rock. The model took up from where Hvorslev-Modified Cam Clay (MCC) model leaves off, which is at the onset of localized shear banding. This model dealt with four distinct states of soil failure

and their related stress-strain behaviour. This model gives a rational basis for the prediction of such soil behaviour and applicable to the entire range of soils from normally consolidated to lightly over consolidated soil, which is a wet soil like marine clay, to stiff or hard soil like heavily over consolidated soil including soft rock as well as partially saturated soil.

The behaviour of partially saturated soil is different from those of fully saturated soil because of the influence of suction. Results obtained with the strength theory of fully saturated soil could not be directly applied to solve the partly saturated soil problems. Partially saturated soil is normally considered as a three-phase system consists of soil solids, fluid, and air gas. The presence of a fourth independent phase, a so called air–water interface was introduced by Fredlund and Morgenstern (1977). They concluded that any two of three possible normal stress variables can be used to describe the stress state of a partially saturated soil. This is in contrast to saturated soil, where it is possible to relate the behaviour of the soil to the effective stress only. Among the researchers Alonso et al (1987) were the first to propose an integrated framework incorporating both volume changes and shear strength model for partially saturated clays.

The most widely used elastic plastic model, The Modified Cam Clay (MCC) model and other such models are commonly formulated in triaxial stress space, therefore, their applications would be appropriated to the analysis of soil subjected to triaxial loading conditions. Commonly, the mechanical properties of soil is also interpreted from conventional triaxial apparatus; whereas, testing of soil using the plane strain device would be more useful information, as more geotechnical field problems such as landslide problems, failure of soils beneath shallow foundations, and failure of retaining structures are basically occur in these situations. It was reported by Mochizuki et al (1993) that when soil is tested under plane strain conditions, it, in general, exhibits a higher compressive strength and lower axial strain than that of triaxial case. Furthermore, Peters et al (1988) reported that for dense to medium dense sand, shear bands are more easily initiated under plane strain condition.

The biaxial testing on the behaviour of fined grained sands had been reported (Schanz and Alabdullah, 2007; Alshibli et al, 2004; Alshibli and Sture, 2000; Bizzarri, 1995; Han and Vardoulakis, 1991; Hans and Drescher, 1993; Lee, 1970; Marach et al, 1984; and Mochizuki et al, 1993). However, the plane strain testing of clay soils have only been initiated recently (Alshibli and Akbas, 2007; Mita, 2002, Lo et al, 2000; Viggiani, 1994; Drescher et al, 1990) and published data of such tests especially for stiff and hard partially saturated clay is very limited. This might be due to the lack of viable equipment to undertake the test under plane strain conditions.

## **1.2. Scope and aims of research**

The present work has been undertaken to investigate the constitutive behaviour and failure of saturated over consolidated clay as well as partially saturated clay, which represent the stiff and hard clay soils which also consider the discontinuities on the specimen by the use of a new biaxial device, which was a modification of conventional triaxial apparatus and previous plane strain apparatus. In particular, the scope and aims of the research project may be stated with the following terms:

- (1) Review on the basic concept of soil physics in particular to the clayey soil as well as factor affecting soil stiffness and the development of plane strain testing apparatus.
- (2) Review on the development of constitutive model and constitutive behaviour and failure of saturated over consolidated clay as well as partially saturated clay.
- (3) Review and analyse the use of fracture mechanical theory to predict the behaviour of stiff clay in particular to partially saturated clay.
- (4) Investigate the constitutive behaviour and failure of saturated over consolidated kaolin clay specimen from plane strain testing results.

- (5) Investigate the constitutive behaviour and failure of partially saturated kaolin clay specimen from plain strain testing as well as triaxial testing results.
- (6) Investigate the volume change behaviour of partially saturated kaolin clay specimen due to applied matric suction and net normal stress.
- (7) Conduct fracture test on partially saturated kaolin clay specimen under mode I fracture to determine their fracture load and fracture toughness.
- (8) Analysis and simulate crack propagation on pre-crack partially saturated kaolin clay specimen using finite element software as well as experimental investigation.

### **1.3. Outline of thesis**

The outline of the work presented in this thesis is the following:

Chapter I introduces the general idea of the study and the scope and aims of the research. In Chapter 2 a review of basic concept of soil physics in particular to the clayey soil is studied in the first part. The main features of factors affecting soil stiffness is also discussed and particular emphasis is given on the effect of recent stress history and stress path direction and the influent that ageing period have on them. The development of plane strain testing apparatus then is summarised in the last part.

Chapter 3 is subdivided in three main parts. The first part reviews the constitutive models for over consolidated clay, in which it begins with the current knowledge of the classical theory of elasto-plasticity and then it continue with the known elastic plastic model of over consolidated clay. The second part highlights the elastic-plastic models of soft rocks. A discussion on the behaviour of over consolidated clay within the critical state framework is presented in the third part.

Chapter 4 starts with the review of the constitutive models for partially saturated clay. The second part of this chapter which is concentrated on the main features of the mechanical properties of partially saturated soil, namely stress state

variables, volume change, pore pressure parameter and matric suction is discussed.

In Chapter 5 a brief of basic concepts of fracture mechanical theory including the linear elastic fracture mechanical (LEFM) approach is first be reviewed, then the use of fracture mechanical concept applied in stiff clay is discussed. The detail of the unified model, which in turn this study is based on will then be highlighted, thereafter, the fracture mechanical approach for the behaviour of partially saturated clay is then presented.

Chapter 6 explains the experimental program of this research. The detail description of the new biaxial equipment used in this study is presented. The specimen preparation and the procedures as well as method on carrying out the plane strain tests on saturated over consolidated clay as well as biaxial and triaxial tests on partially saturated clay is also included. The fracture toughness test and plane strain compression on partially saturated clay to obtain the crack pattern on the specimen is also described.

Chapter 7 analysis and discussion of the experimental results carried out in Chapter 6. Four studies are presented. The first part examines the behaviour of over consolidated clay under drained and undrained plane strain test based on the critical state frame work described in Chapter 3. The behaviour of partially saturated clay under biaxial and triaxial test set up based on theory presented in Chapter 4 is then discussed. The influence of the discontinuities on the specimen is highlighted. The volumetric change of partially saturated clay specimen due to applied matric suction and net normal stress is also explored. The third study deals with the fracture toughness of partially saturated kaolin clay specimen under mode I fracture test. Finite element analysis simulating crack propagation on pre-crack partially saturated kaolin clay specimen is then discussed in the last part.

Finally, Chapter 8 gives a summary of the work carried out in this research and the conclusion reached as well as the recommendation for further research.

## **CHAPTER 2**

### **SOIL PHYSICS AND TESTING DEVICE RELATED TO THE STUDY OF STIFF CLAY**

#### **2.1. Introduction**

The mechanical properties of soils depend on interactions between the components of the material. The soil is a system consists of solids, liquids and gaseous materials. The chemical and physical relationships between the solid, liquid and gaseous phases are influenced individual properties of each phase as well as its environmental condition such as temperature, pressure and light (Baver et al, 1972).

The solid phase may be formed of a mineral or organic nature. The mineral fraction constituted by particles of different sizes, shapes and chemical composition. The range of solid particles size varies from gravel and boulders to colloidal clay and is controlled mainly by its mineralogy (Mitchell, 1993). The organic fraction includes residues in decomposition and live organism. The liquid phase refers to the fluid, which fills part or all the pore spaces between the solid particles. The liquid phase varies in chemical composition according to the environment in which a particular soil is located. The gaseous, also called vapour phase, occupies that part of the pore space that is not filled with the pore fluid. Its composition may change within short intervals of time according to environmental conditions.

The consideration of an additional phase for unsaturated soil as so called the air-water interface or contractile skin was suggested by Fredlund and Morgernstern (1977). For a material to qualify as an independent phase it must have different properties than those of surrounding material and definite bounding surface. Therefore, the contractile skin qualifies as an independent phase because of its distinct physical properties. The most important property is its ability to exert a tensile pull, such as a surface tension.

An element of partially saturated soil can be visualised as, if the fourth phase is included, a mixture of two phases that come to equilibrium under applied stress gradients, which are soil particles and contractile skin, and two phases that flow under applied stress gradients, which are air and water. However, the contractile skin can be considered part of the water phase without incurring a significant error (the thickness of the contractile skin is of the order of a few molecular layers). As a result, the physical sub division of the contractile skin is unnecessary when establishing volume-mass relationships for partially saturated soil (Fredlund and Rahardjo, 1993).

Most laboratory experiments on the mechanical behaviour of soils are performed under axis symmetric or conventional triaxial conditions. However, most geotechnical field problems such as landslide problems, failure of soils beneath shallow foundations, and failure of retaining structures are cases that can generally be considered as plane strain situation and hence data obtained from triaxial testing would not apply. It would be more appropriate using data from biaxial compression testing. As mentioned in preceding 1.1, the plane strain testing on the behaviour of fined grained sands had been reported (Alshibli et al, 2004; Alshibli and Sture, 2000; Bizzarri, 1995; Han and Vardoulakis, 1991; Hans and Drescher, 1993; Lee, 1970; Marach et al, 1984; and Mochizuki et al, 1993). However, the plane strain testing of clay soils have only been initiated recently (Lo et al, 2000; Mita, 2002; and Drescher et.al (1990)) and published data of such tests especially for stiff clay material is very limited.

This chapter is divided into three parts. The first part presents a summarised of the structure and composition of clay. The main features of factors affecting soil stiffness then will be reviewed in the second part. The third part dealt with the soil testing in particular to the study of plane strain device.

## **2.2. Structure and composition of clay**

Clays are formed mainly of crystalline minerals. The primary components of clay belong to the phyllosilicates mineral family (Mitchel, 1993). Elements which form the minerals are silicon, aluminium, ferrous and ferric iron, magnesium and oxygen atoms plus hydroxyl group. There are two basics units that are responsible in the construction of clay mineral, namely the silicon tetrahedron in which oxygen atoms are arranged in such a way that each forms a corner of a tetrahedron held together by a silicon atom in the centre (Figure 2.1 a). The silicon atom is possible to be substituted by an aluminium atom. In an idealised structure, the tetrahedra are kinked in a sheet known as the silica or tetrahedral sheet. The three oxygen atoms that form the base of the tetrahedron are shared by three adjacent tetrahedra.

The second unit is the aluminium octahedron, in which six hydroxyl group (OH) or oxygen atoms are arranged in such a way that each forms a corner of an octahedron held together by an aluminium atom in the centre (Figure 2.2 c). The aluminium atom is possible to be substituted by magnesium, ferrous and /or ferric iron atoms. The six OH groups that form the octahedron are shared by three adjacent octahedra.

There are two steps to be followed to form a clay mineral. In the first step the OH groups in the upper plane of Figure 2.2 e corresponding to position 1 to 9 are removed. Secondly, the silica sheet shown in Figure 2.2.b is place on top of the octahedral sheet so that the oxygen atoms on the apex position 1 to 9 occupy the corresponding positions in Figure 2.2 e. The two sheets are held together by



sharing the oxygen atoms that are on the apexes of the silica tetrahedra. The oxygen-hydroxyl boundary layer between the alumina and silica sheet can be seen in Figure 2.2e. The aluminium in each octahedron is now surrounded by four OH groups and two oxygen atoms.

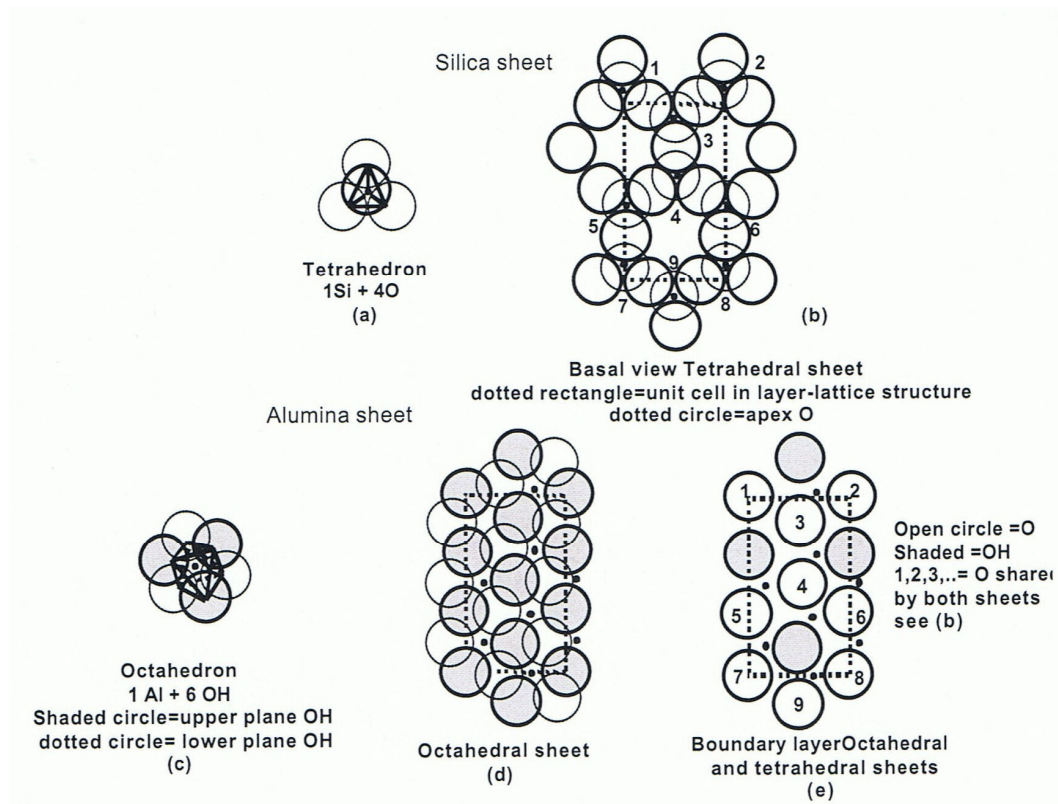


Figure 2.1. Structural arrangements in clay minerals  
(after Baver et al, 1972)

As mention earlier, there are possibilities to substitute the crystal atoms that can change the properties of the clay mineral. For example, the bigger trivalent aluminium atom can substitute the trivalent silicon atom forcing the oxygen atoms of the tetrahedron apart, introducing a strain in the crystal. This substitution also decreases the positive charge of that particular tetrahedron by one, which increases the negative charge by the same extra cation. The cations that balance the negative charges originating from substitutions within the crystal can be replaced by other cation from the planar surfaces of the minerals, called exchangeable cations. The total number of exchangeable cations is expressed as

the Cation Exchangeable Capacity (CEC) and it reflects the degree of substitution within the crystal (Baver et al, 1972).

The principles of interlinking of specific number of silicon tetrahedron sheets and aluminium octahedron into various layer lattice structures along with the origin and nature of isomorphous substitution account for the occurrence of many types of clay minerals.

Cristaline clay minerals may be divided into four main groups, as follow:

1. Kaolin groups, is characterized by having one silica and one alumina sheet. Members are kaolinite, dicktite, nacrite and halloysite. The unit layers are bonded together so tighly, through hydrogen bonding, that ions or water molecules ca not permeate the interlayer positions between adjacent kaolinite layers. This means that their colloidal properties are determined by external surfaces only. There is little swelling or shrinkage and low plasticity. The CEC is less than 10 meq /100 g of clay (Baver et al, 1972)
2. Hydrous mica groups, consists of two silica sheet and one of alumina. Two main members are illite and vermiculite. The major substitutions of illite occur in the silica sheet (Al for Si). The negatives charges produced are balanced by potassium ion. The CEC varies between 20 and 40 meq /100 g of clay. However in this mineral the CEC does not reflect the degree of isomorphous substitution in the crystal. This is because the unit layers are held together by the potassium ions and its exchange capacity resides on the external surface.
3. Smectite groups, consist of octahedral sheet sandwiched between two silica sheets. The crystal lattice expands or contracts depending on the amount of water and interlayer cations present. The main members of the groups are montmorillonite, beidellite, and nontronite. In montmorilonite there is some substitution of Al for Si in the silica sheet and Fe and Mg for Al in the alumina sheet. The negative charges generated are balance by exchangeable cation that found between the unit layers. Bonding between successive layers is weak and they are easily separated by cleavage or adsorption of water or other polar liquids. Because of the large amount of unbalanced substitution, they have high CEC of

80-150 meq/100 g of clay. This exchange capacity has tremendous impact on swelling, plasticity and other physical properties (Mitchell, 1993)

4. Paligorskite or fibrous clay group. The silica tetrahedra occur in alternate strips on both sides of the basal oxygen plane resulting from the apexes of tetrahedra being systematically but alternately inverted. This produces a chain like structure. There are two of this group, attapulgite and sepiolite.

### **2.3. Factors affecting soil stiffness**

There are many factors that affect soil stiffness, but only the most important ones will be reviewed as follows: current stress state-volume state, soil structure, ageing, recent stress history and stress path direction. A more detailed review of factors that affect soil stiffness can be found in Atkinson and Salfors (1991), Jardine (1995), Heymann (1998) and Grammatikopoulou (2004).

#### **2.3.6. Current stress state-volume state**

The dependence of the soil stiffness on the current stress state has been approached by either idealizing the soil as an assembly of elastic spheres or considering its mechanical behaviour to be essentially frictional. If the mechanical behaviour of the soil is assumed to be purely frictional then its strength and stiffness is directly proportional to the mean effective stress,  $p'$ . If the soil is idealized as an assembly of elastic spheres then the theoretical work by Hertz and Mindlin (as reported by Richart et al, 1970) suggests that the soil stiffness varies with the mean effective stress  $p'$ , raised to the power of  $n$  equal to 1/3. Viggiani and Atkinson (1995) suggested that at very small strains the soil is expected to follow the theory of the elastic spheres while at large strains the purely frictional case is expected to apply.

*(i) Very small strains*

Experimental evidence suggests that at very small strains the power coefficient,  $n$ , is higher than  $1/3$ . Apart from small slippage and rearrangement, which would indicate inelastic behavior, this could also be attributed to the soil particles having different sizes, shapes and angularity within a real soil (Jovicic, 1997). A number of equations have been proposed in the literature for the calculation of stiffness at very small strains. These relationships are generally derived from dynamic tests and therefore are semi-empirical. Based on the results of resonant column tests on normally consolidated kaolin and Boston Blue clay, Hardin and Black (1968) proposed the relationship for the shear stiffness at very small strains, which showed the dependence of the stiffness on the mean effective stress and the void ratio.

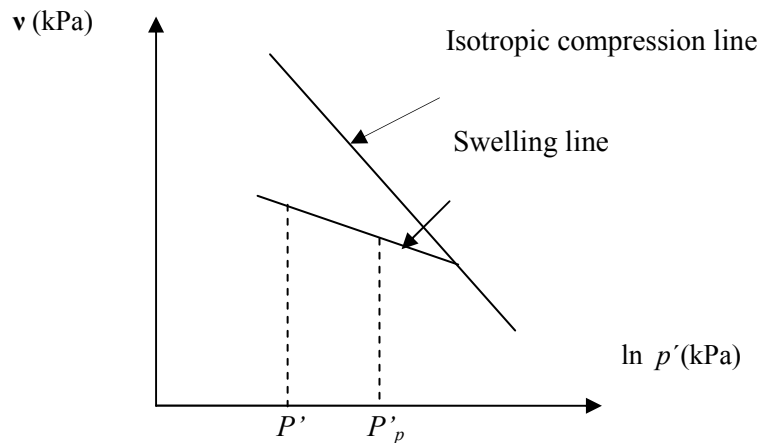


Figure 2.2. Definition of isotropic over consolidation ratio  
(after Viggiani and Atkinson, 1995)

Based on the results of resonant column tests on a range of clays, Hardin and Black (1969) extended Black's equation to account for over consolidated stress states, which depends on the over consolidated ratio and the corresponding power coefficient which depends on the plasticity index. A more general equation proposed by Hardin (1978) by combining the work of Jambu (1963) and the elastic stress-strain relationships by Rowe (1971). Within the framework of

critical state soil mechanics the three variables, there are mean effective stress, void ratio and over consolidation ratio can be interrelated. The over consolidation ratio is redefined as the isotropic over consolidation ratio,  $Ro$ , which is equal to the ratio of the maximum past mean effective stress,  $P'_p$  (kPa) , to the current mean effective stress,  $P'$  (kPa),  $Ro = P'_p/P'$ , as shown in Figure 2.2.

### (ii) Small to large strains

The behaviour of normally consolidated and over consolidated samples under undrained triaxial tests at large strains is linearly normalisable by the mean effective stress. At large strains the soil is expected to resemble an assembly of rigid frictional particles, in which case the stiffness varies linearly with the mean effective stress, and  $n$  is equal to 1.

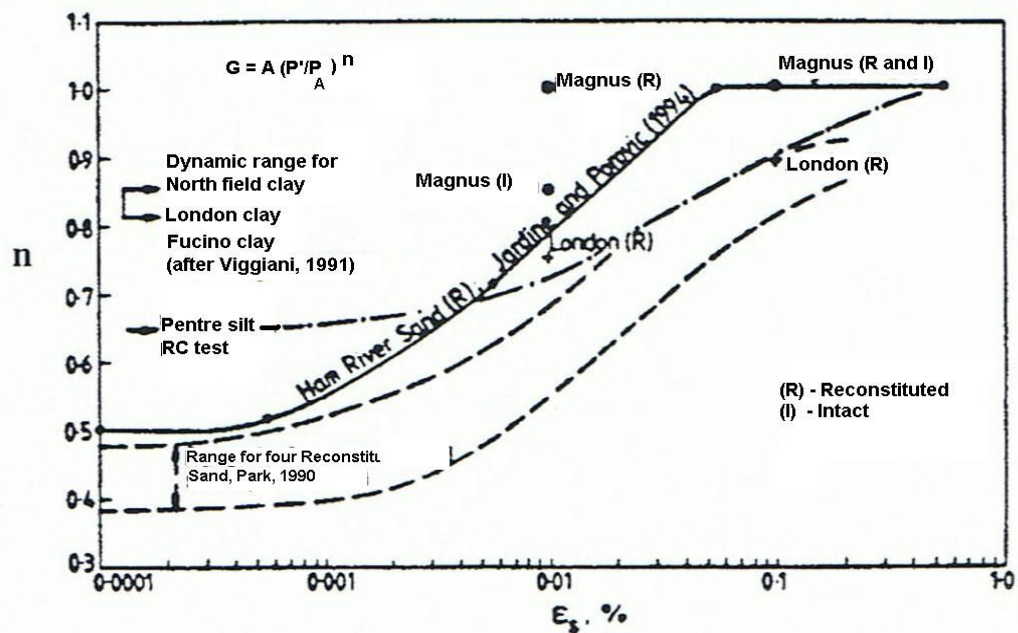


Figure 2.3. Effects of strain on stress level exponent  $n$  (after Jardine, 1995)

It is expected that the stress level dependency of the stiffness varies with strains level, from the value of  $n$  at very small strains to the value of  $n = 1$  at large strains. Jardine (1995) presents a summary of the way the exponent  $n$  varies with strain level, for a range of soils (Figure 2.3). It can be seen that  $n$  increases with

strain level tending to unity at large strains.

### 2.3.7. Soil structure

Two issues of the influence of soil structure on soil stiffness are the effect of the different structure between natural clays compared to the reconstituted clays and the effect of the anisotropic fabric both natural and reconstituted clays.

#### *(i) Effect of different structure between natural and reconstituted clays*

The very small strain stiffness of natural and reconstituted Vallerica clay, a stiff over consolidated clay was observed by Rampello and Silvestri (1993) using resonant column tests. The stiffness of the natural samples was shown to be generally higher than the stiffness of the reconstituted samples as shown in Figure 2.4. This difference was attributed to the different location of the isotropic compression lines. The natural isotropic compression line plotted well to the right of the reconstituted one (termed intrinsic, after Burland (1990)), showing the effect of the difference in structure between the natural and the reconstituted material. Rampello and Silvestri (1993) went on to show that when the stiffness data was normalized with respect to the equivalent pressure on the appropriate isotropic compression line then the stiffness of the natural and reconstituted samples plot very closely.

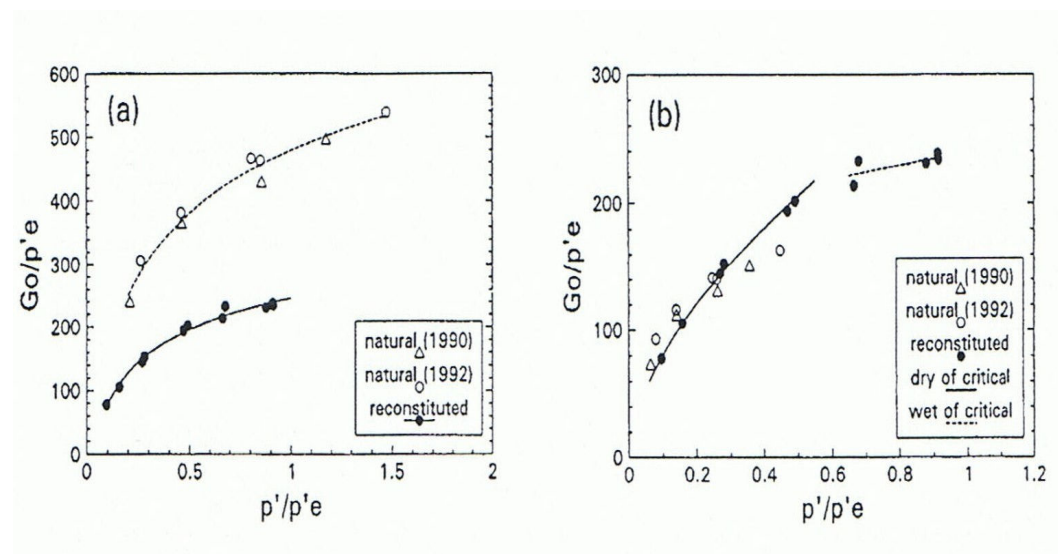


Figure 2.4. Vallerica clay: initial shear modulus versus a) mean effective stress

and b) specific volume (after Rampello and Silvestri, 1993)

The pre-failure behaviour of natural compare to the reconstituted Pappadai clay, a stiff over consolidated clay in undrained triaxial compression tests were investigated by Cotecchia and Chandler (1997). The results showed that there is little difference between the normalized stiffness  $G/(p')^n$  of the natural reconstituted samples of in the small to intermediate strain range, if this is plotted against either the isotropic over consolidation ratio,  $R_o$ , in the case of the reconstituted samples or the yield stress ratio in isotropic compression,  $YSR_{is}$ , in the case of the natural samples as shown in Figure 2.5. Similar findings were reported by Coop et al (1995), who showed that if the state relative to the appropriate natural or intrinsic isotropic compression line was taken account of, there was no clear distinction between the stiffness of natural and reconstituted Boom clay, a stiff over consolidated clay, in the small to intermediate strain range.

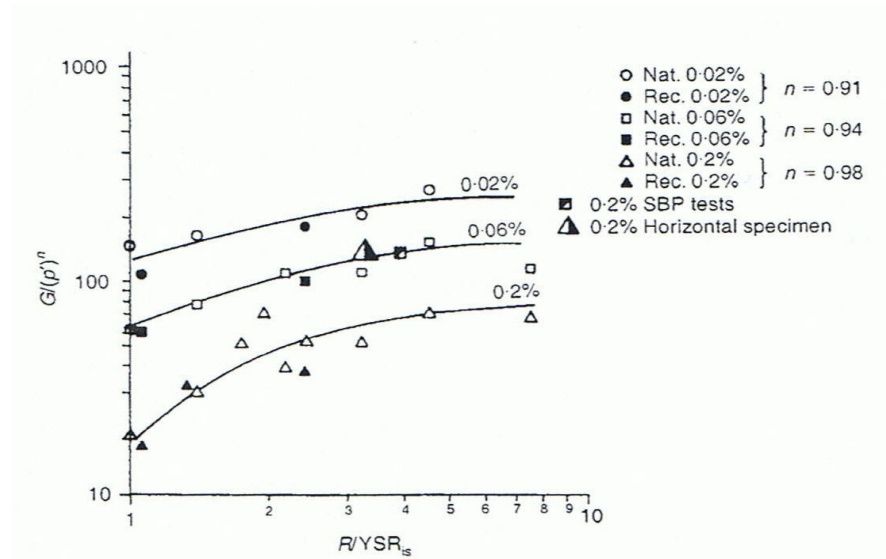


Figure 2.5. Normalized shear stiffness of both natural and reconstituted Pappadai clay (after Cotecchia and Chandler (1997))

### (ii) Effect of anisotropic fabric

As a result of deposition, anisotropic consolidation and subsequent stress history, such soil commonly posses an anisotropic fabric. On macro scale this anisotropic fabric gives rise to mechanical anisotropy of the soil, which means that its properties become directional dependent (Mitchell, 1993). Anisotropy of

the soil results in an anisotropic state boundary surfaces that are no more centred around the isotropic axis, as is the case for the state boundary surfaces of isotropically consolidate soils (Parry and Nadarajah (1973) and Graham et al (1983)).

Due to the way they were deposited, soils are often assumed to behave as cross-anisotropic materials, which mean that they are assumed to have symmetry around the vertical axis. Therefore, they behave the same way in any of the two horizontal directions and differently in the vertical direction. Jamiolkowsky et al (1995) investigated the anisotropy of the very small strain stiffness of natural clays. It had found that the ratio of the shear modulus in the horizontal plane to the shear modulus in the vertical plane,  $G_{hh}/G_{hv}$ , which is an expression of the degree of anisotropy, varied between 1.2 and 2. Jovicic and Coop (1998) examined the very small strain stiffness anisotropy of London Clay by conducting bender element tests on natural and reconstituted samples. The reconstituted samples followed the geological history of the natural deposit. The degree of anisotropy was found to be equal to 1.5 for both natural and reconstituted samples.

#### **2.3.8. Ageing**

Commonly ageing increases the soil stiffness with two mechanisms, increased inter particle bonding and volume reduction under constant stress due to creep. Since there is lack of data for over consolidated clays, only work on normally consolidated clays will be reviewed.

The effects of ageing on the soil stiffness were first investigated experimentally by Bjerrum (1967). He studied the effect of ageing on the compressibility of soft Norwegian clays. It was shown that when normally consolidated clay was kept under constant effective stress, volume reduction occurred due to secondary consolidation and the yield stress recorded on subsequent loading was much higher than the current stress (Figure 2.6).



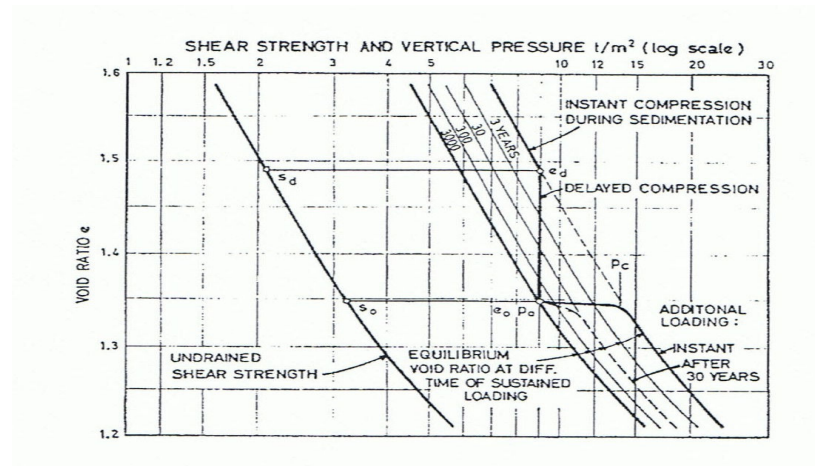


Figure 2.6. The effect of creep on the yield stress of normally consolidated clay (after Bjerrum (1967))

It can be seen from Figure 2.7 that when a soil element is loaded after a certain rest period then this yields on the compression line that the same soil element would have followed if no creep had occurred. This demonstrates only the effect of ageing due to volumetric creep. Bjerrum (1967) recognized that apart from the effect of creep, increased inter particle bonding can develop during the rest period which leads to the further increase of the yield stress (Figure 2.7).

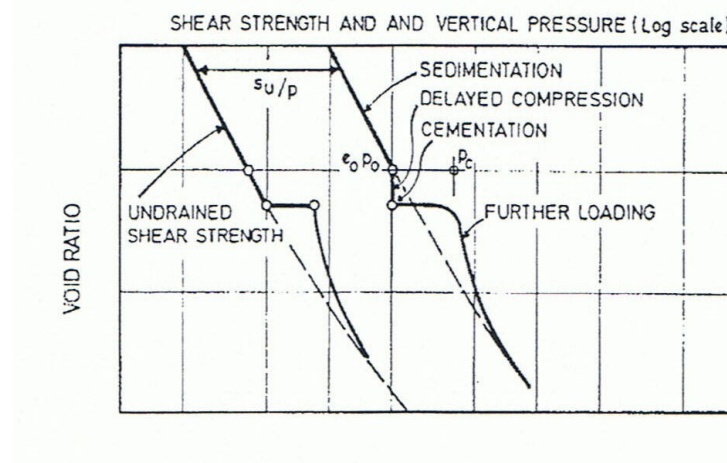


Figure 2.7. The effect of cementation on the yield stress of normally consolidated clay (after Bjerrum (1967))

The effect of ageing on the one dimensional compression of normally consolidated reconstituted clays was investigated by Leonards and Ramiah

(1959). Figure 2.8 shows some of the results (Burland, 1990). It can be seen that after the rest period there is an increase in the yield stress irrespective of whether or not creep was allowed. This is evidence that the increased resistance due to ageing is not just because of the effect of creep but also because of the bonding developing during the rest period.

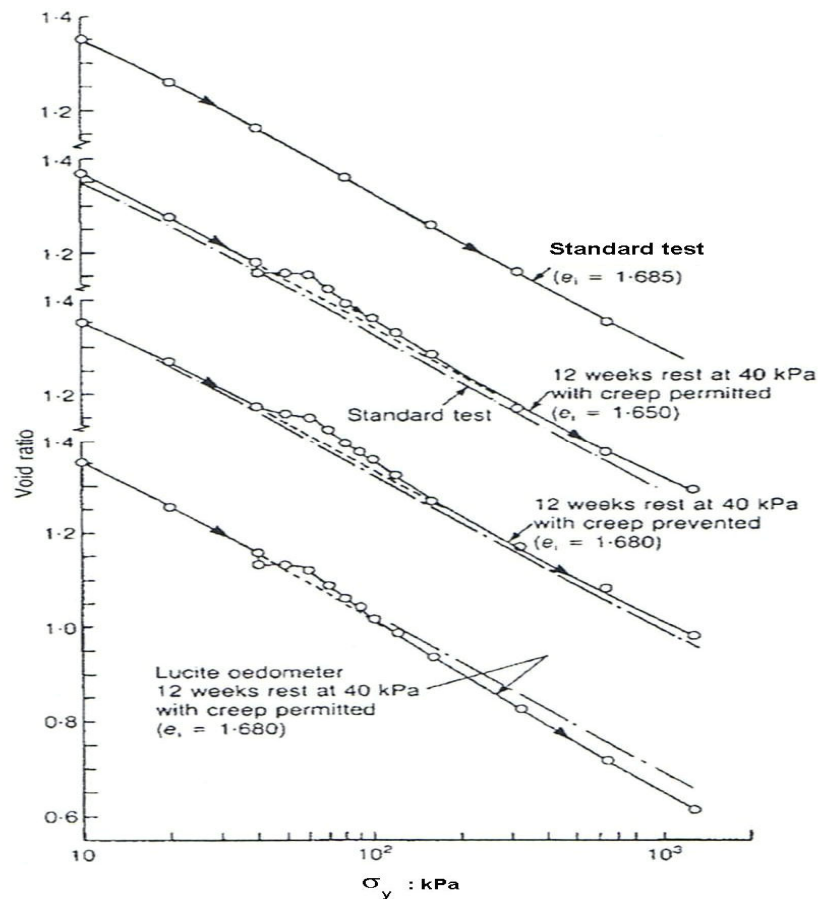


Figure 2.8. The effect of ageing on the yield stress of normally consolidated clay (redrawn by Burland (1990) after Leonards and Ramiah (1959))

### 2.3.9. Recent stress history

The effect of recent stress history on the stiffness of over consolidated soil was studied by Atkinson et al (1990) by performing drained triaxial constant  $p'$  and constant  $q$  tests on reconstituted over consolidated samples of London Clay. The tests involved bringing the samples to a common stress state by following different approaching paths and then shearing along a common loading path in the

constant  $p'$  tests. The effect on the direction of the approaching path relative to the direction of the loading path is term the effect of recent stress history. Figure 2.9 shows that this effect seems to decrease as the soil is loaded and becomes negligible after strains of less than 0.5 %. It is possible that the results presented by Atkinson et al (1990) are influenced by the effect of creep and in this case it is reasonable to measure an increased stiffness after a stress path reversal and a reduce stiffness in the case of no stress path reversal.

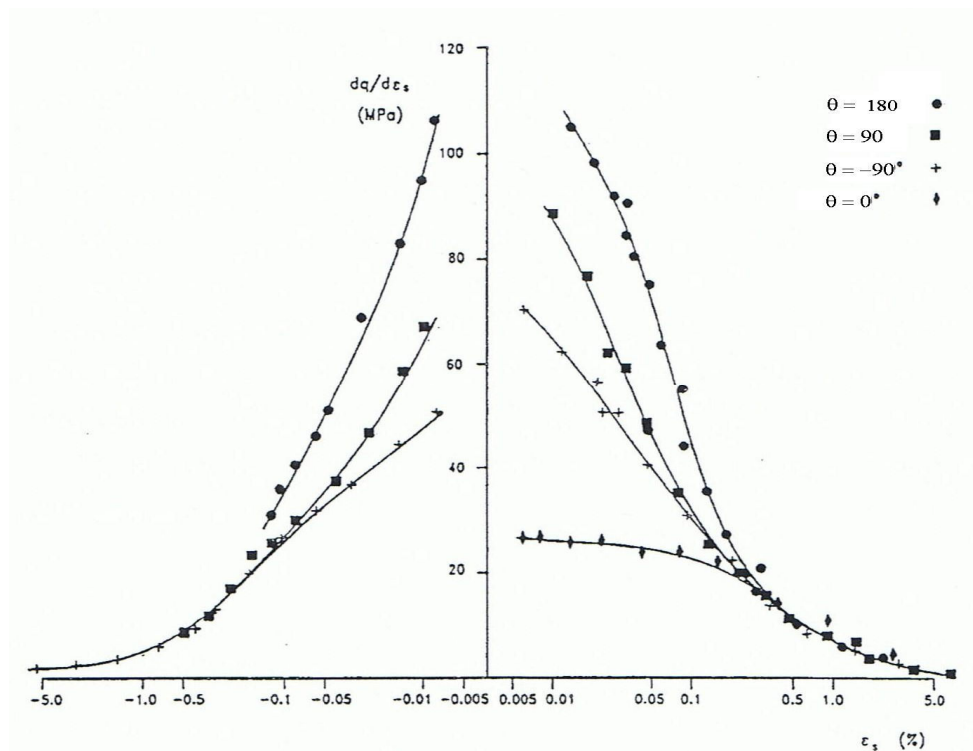


Figure 2.9. Stiffness versus strain measure in constant  $p'$  tests of reconstituted London clay (after Atkinson et al, 1990)

The effect of recent stress history on the stiffness of natural Bothkennar clay was conducted by Clayton and Heyman (2001) similar to Atkinson et al (1990). Figure 2.10 presents the stress path followed in single sample. The incoming stress path BA, CA, and DA had relative angle to the outgoing stress path starting from A equal to  $180^\circ$ ,  $+90^\circ$ , and  $-90^\circ$  respectively. A rest period was applied at point A before the beginning of the common loading stage. This rest period was varied from 1 to 3 days and ensure that the locally measure creep rates were less than 0.01 % per day at the start of each sharing stage. From the evidence

above it was concluded that the recent stress history is an effect which it self depend on time.

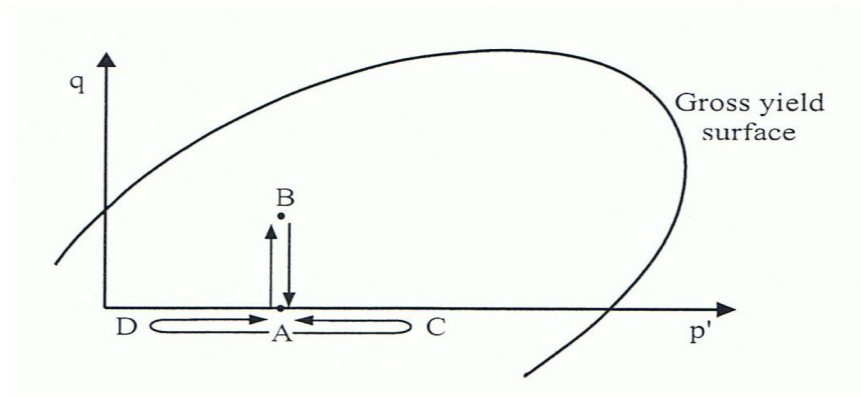


Figure 2.10. Stress path followed in single sample of natural Bothkennar Clay  
(after Clayton and Heyman, 2001)

### 2.3.10. Stress path direction

The effect of stress path direction on the stiffness of soil was investigated by Clayton and Heyman (2001). Based on the result of the undrained triaxial compression and extension tests on natural Bothkennar and London clay, they suggested that what really influent soil stiffness is the direction of stress path rather than recent stress history. As can be seen in Figure 2.11, sample was initially reconsolidated to its estimated in situ stresses and was used for both compression and extension test. Clayton and Heyman (2001) suggested that their results are reminiscent of those reported by Atkinson et al (1990), in the sense that the stress path that shows the higher stiffness in the small strain range is also the one involving a stress path reversal (Figure 2.11). It seems that in both cases the stress path that takes the loading close to the gross yield surface shows softer behaviour than the stress path that takes it away from the gross yield surface. Therefore it can be concluded that the direction of stress path is really important effect on the stiffness of soil.

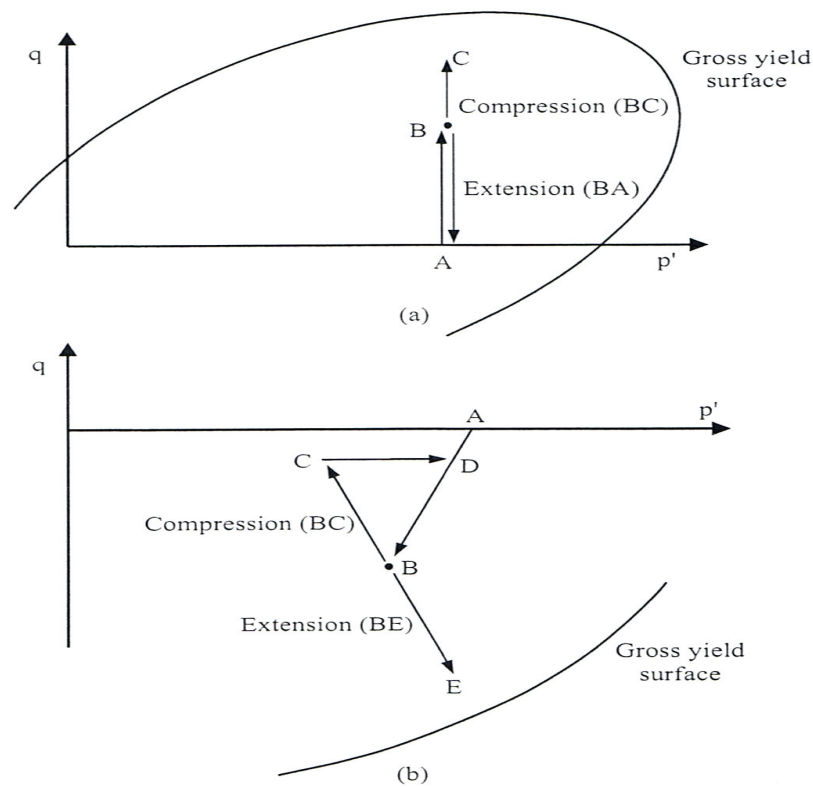


Figure 2.11. Stress path applied to: (a) Bothkennar Clay and (b) London clay  
(after Clayton and Heyman, 2001)

The direction of stress path effect on the stiffness of soil can also be seen in other work, for example, Jardin (1985) who studied the behaviour of reconstituted London clay and Smith (1992), who investigated the stress strain curve of undrained compression and extension of natural Bothkennar clay, but in some cases it seems difficult to isolate it from the effect of recent stress history. However, since as recent stress history seems to diminish with ageing time, one could postulate that the effect of stress path direction becomes more pronounced.

## 2.4. Biaxial apparatus

The behaviour of soil is routinely interpreted from triaxial testing using triaxial device (Figure 2.12). However, most geotechnical field problems such as

failure of retaining structures, failure of soils beneath shallow foundations, and landslide problems are truly or close to plane strain situations and hence data obtained from biaxial apparatus would be more appropriate. The comparison between triaxial and biaxial condition are shown in Figure 2.13.

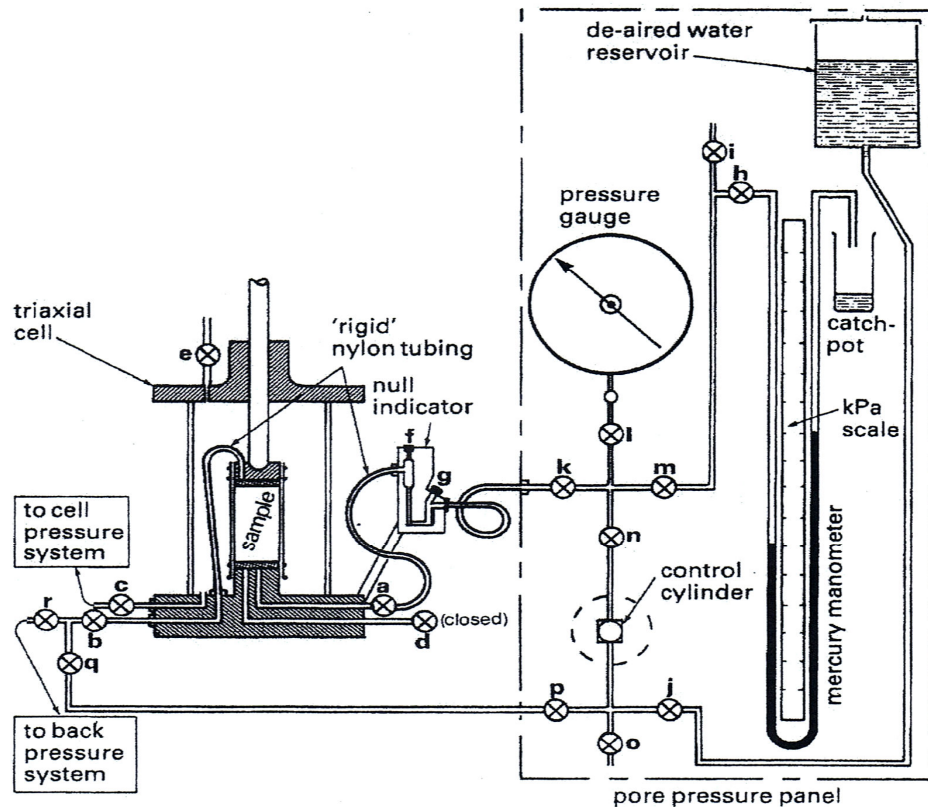


Figure 2.12. A schematic diagram of triaxial device (after Head, 1995)

It has been reported by Mochizuki et al (1993) that when soil is tested under plane strain conditions, it, in general, exhibits a higher compressive strength and lower axial strain than that of axis symmetric condition. Figure 2.14 shows the comparison between triaxial and biaxial testing results of dense to loose sands. Furthermore, Peters et al (1988) found out that for dense to medium dense sand, shear bands are more easily initiated under plane strain condition than that of triaxial case.

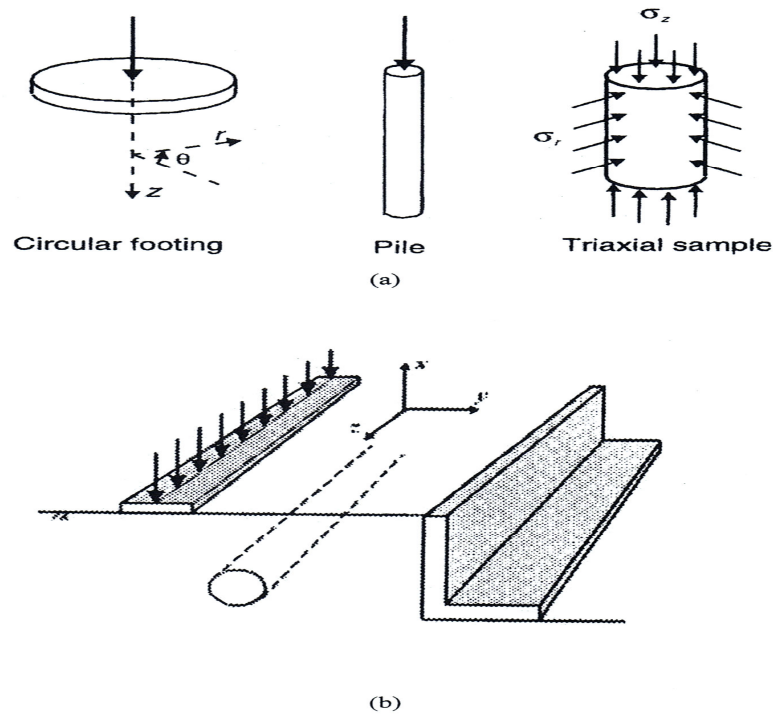


Figure 2.13. Comparison between (a) triaxial/axis symmetric and (b) biaxial/plane strain condition (after Potts et al, 2002)

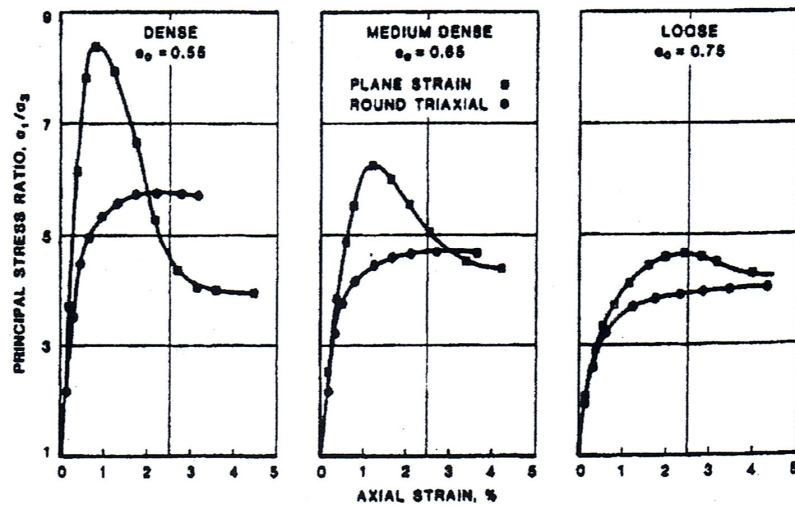
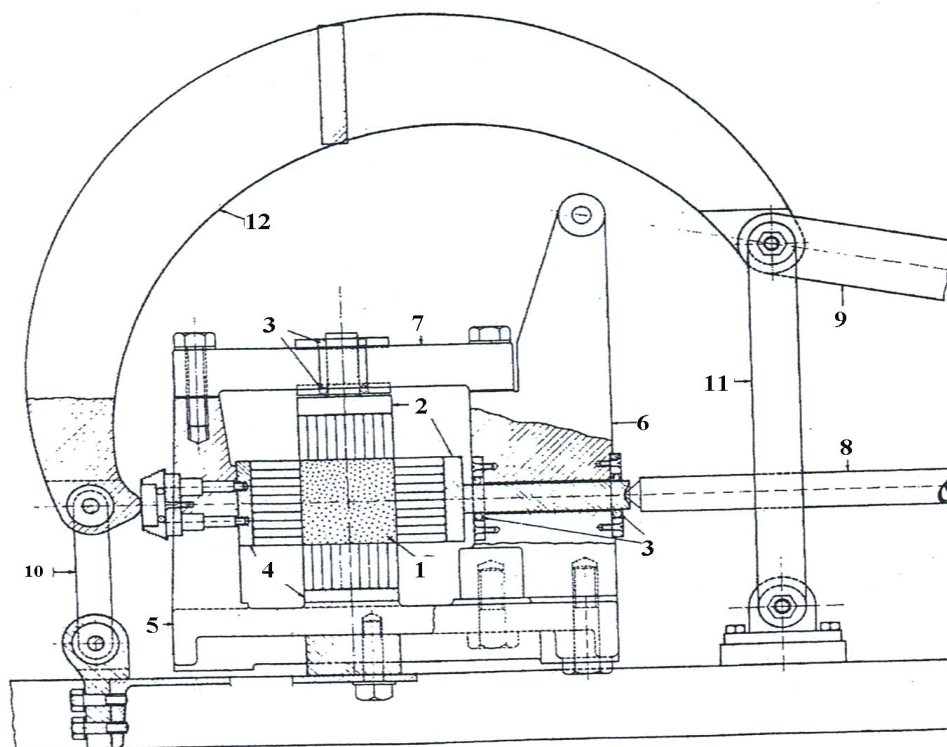


Figure 2.14. Stress strain curve of the specimen under triaxial and plane strain testing (after Mochizuki et al, 1993)

Plane strain testing of soil was performed firstly by Kjellman (1936), in which a principle stress-controlled device was used by combining three pairs of rigid plates as shown in Figure 2.15. Jakobson (1957), Lorenz et al (1965) and



Hambly and Roscoe (1969) who adopt this testing device found the corner junction problem occurring in the intersection of the rigid plates, insurmountable. On the other hand, the use of a long rectangular specimen, which plane strain was believed to be easier to control had proposed by Wood (1958). Cornforth (1964) proposed a similar device, which was known as “Bishop-Cornforth” device. However, inaccuracy in the measurements of stresses and strains caused by the friction force arising from axial loading surface was found by Finn et al (1968), Lee (1970) and Marach et al (1981) when adopt this method.



- |                                |                            |
|--------------------------------|----------------------------|
| 1. Specimen                    | 7. Top platen              |
| 2. Unfixed end platen          | 8. Load cell               |
| 3. Bolt and nut                | 9. Flexible horizontal arm |
| 4. Fixed end platen            | 10. Short vertical arm     |
| 5. Base of plane strain device | 11. Long vertical arm      |
| 6. Vertical platen             | 12. Curve arm              |

Figure 2.15. Kjellman's plane strain device (after Kjellman, 1936)



A plane strain test device using a rectangular specimen of 84 mm x 76 mm x 53 mm was developed by Green (1971), after which test apparatus using small rectangular specimen developed increasingly. However, Bishop (1981) pointed out that Green's method, which had the  $\sigma_2$  loading surface suspended by wires, could not perform as expected. Taylor (1941), Rowe and Barden (1964), Lee and Seed (1964) and Bishop and Green (1965) found that if the aspect ratio was bigger than 2, the effect of loading platen friction and the restraint of loading frame would be negligible. Mita (2003) developed plane strain device for conduct testing on over consolidated clay with the specimen size of 85 mm high, 36 mm wide, and 72 mm thick. In this test the deformations specimen was restrict along the long direction of the cross section of the specimen. A schematic diagram of this apparatus can be seen in Figure 2.16.

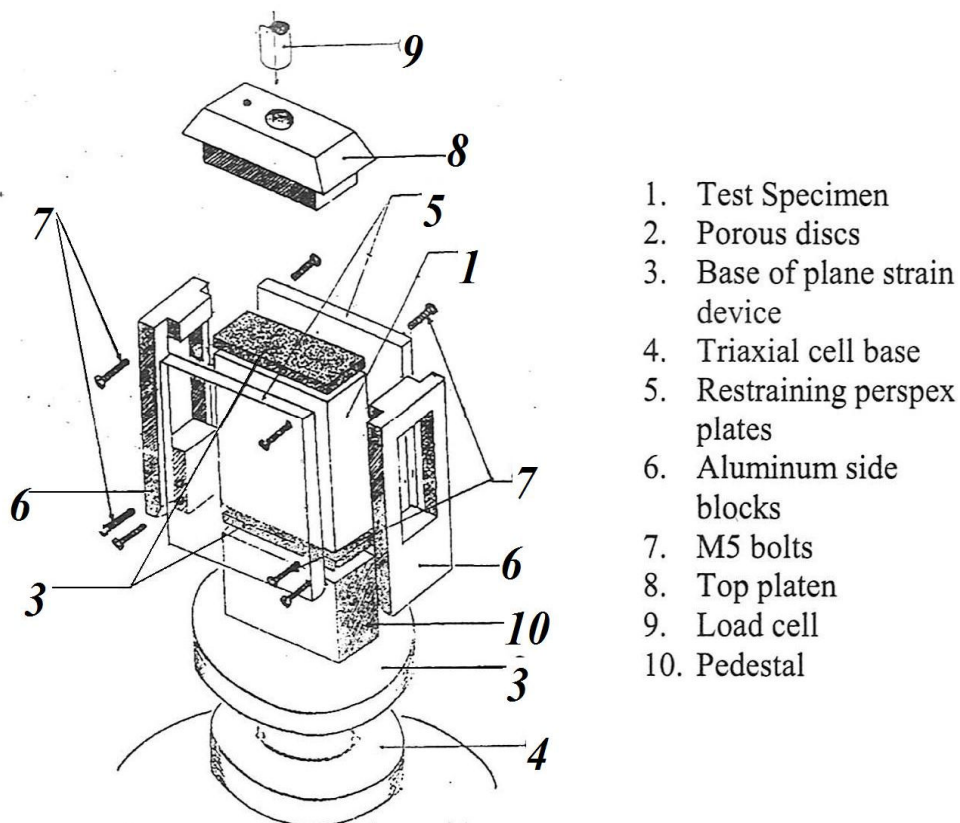


Figure 2.16. A schematic diagram of plane strain device (after Mita, 2003)

Most of the plane strain apparatus (Green and Reades, 1975; Mochizuki et al, 1993; Peters et al, 1988; Drescher, et al 1990 (Figure 2.17); Han and Vardoulakis, 1991; Viggiani et al, 1994; Mita, 2004, Alshibli et al, 2004; Schanz, and Alabdullah, 2007) had the common feature of using rigid walls and tie-rods to impose zero strain boundary condition in one of the principles axes. This method was found to be satisfactory and by the use of a silicon lubricant, friction between the rigid walls and the test specimen could be adequately mitigated. However, shape of all these devices had to be customized. This resulted in slackness and the formation of air pockets. Some researches have resorted to apply suction to remove the air pocket. However, this application may cause swelling and destruction of the sample, resulting in unacceptable disturbance.



Figure 2.17. The view of The Vardoulakis-Drescher plane strain device  
(after Georgopoulos and Vardoulakis, 2005))

Almost recently, the use of plane strain device were studied by Alshibli and Akbas (2007) and Alshibli et al, (2004), which known as Lousiana plane strain apparatus (Figure 2.18). The design of this device took into consideration flexibility in accomodating different specimen sizes. A new double wall biaxial device was proposed by Schanz, and Alabdullah (2007) for plane strain testing of unsaturated granulated material. Figure 2.19 shows the schematic diagram and view of the double wall biaxial device.

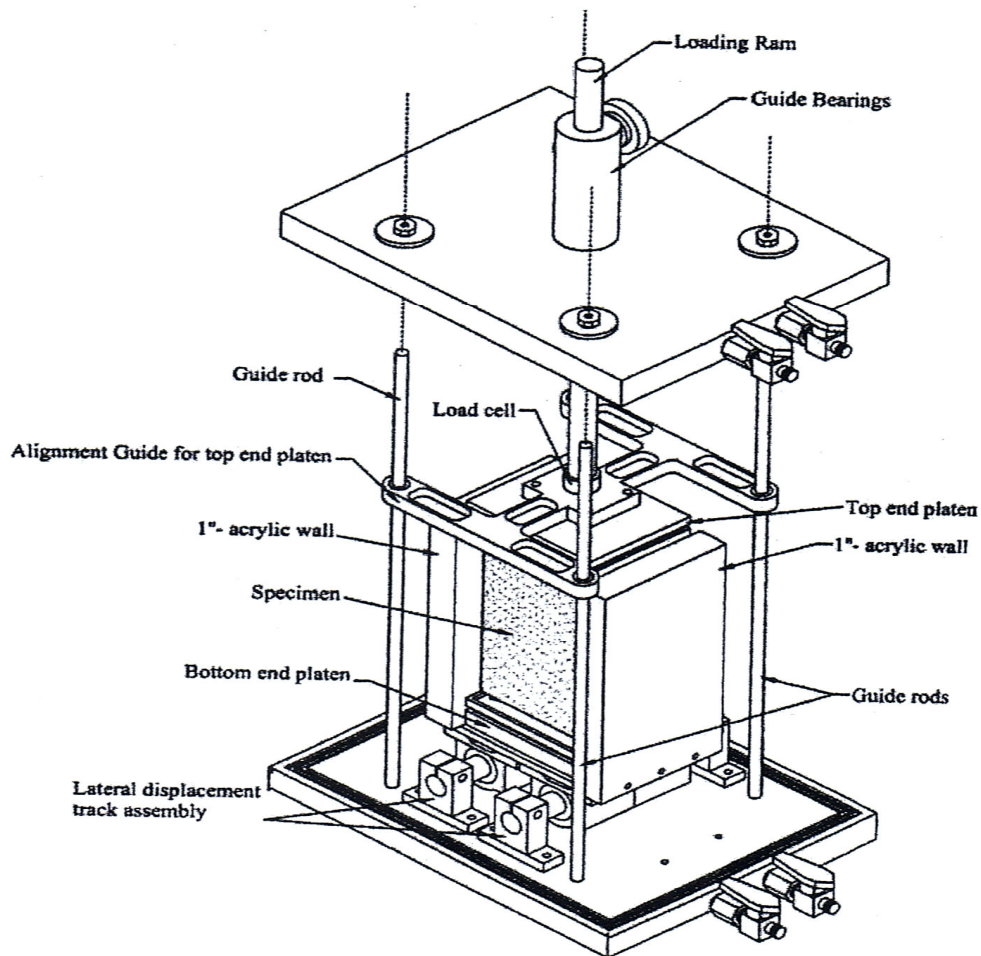


Figure 2.18. A schematic diagram of Lousiana Plane strain device  
(after Alshibli and Akbas, 2007)

To the best knowledge of the author, as mentioned earlier in previous sub sequent 1.1 and the last part of sub section 2.1, the plane strain testing on the behaviour of fined grained sands had been reported (Schanz and Alabdullah, 2007; Alshibli et al, 2004; Alshibli and Sture, 2000; Bizzarri, 1995; Han and

Vardoulakis, 1991; Hans and Drescher, 1993; Lee, 1970; Marach et al, 1984; and Mochizuki et al, 1993). However, the plane strain testing of clay soils have only been initiated recently (Alshibli and Akbas, 2007; Mita, 2002, Lo et al, 2000; Drescher et.al, 1990) and published data of such tests especially for stiff and brittle clay material is very limited.

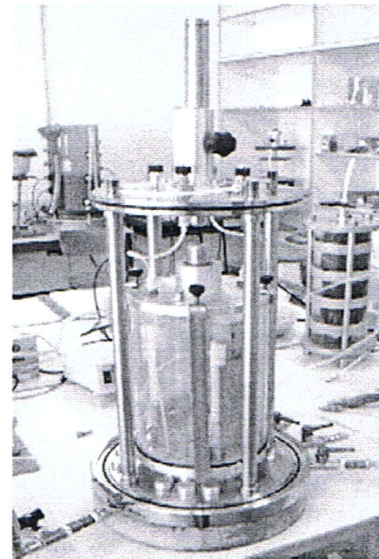
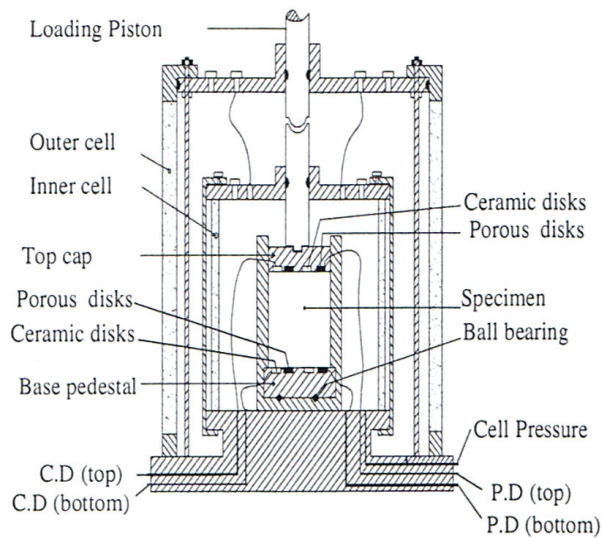


Figure 2.19. Double wall biaxial device (after Schanz and Alabdullah, 2007)

## 2.5. Summary

Soils are a system consists of solid (minerals and organic matter), liquids and gases. The understanding of its behaviour requires the study of interactions between the components of the material. The mineral component of solid phase is controlled mainly by its mineralogy. Clays are formed primarily of crystalline minerals. Two basic units are responsible in the construction of clay mineral, namely the silicon tetrahedron and the aluminium octahedron. In an idealised structure the tetrahedra are linked in a sheet known as alumina or octahedral sheet. Four main groups of cristaline clay minerals are kaolin groups, hydrous mica groups, Smectite groups, and Smectite groups.

The stiffness of soil in particular to the clay soil is influenced by a great number of factors. The most important ones were identified and reviewed as follows: current stress state-volume state, soil structure, ageing, recent stress history and stress path direction. The soil stiffness on the current stress state had been approached at very small strains and small to large strains. Two issues of the influence of soil structure on soil stiffness are the effect of the different structure between natural clays compared to the reconstituted clays and the effect of the anisotropic fabric both natural and reconstituted clays. The effects of ageing on the soil stiffness increases with two mechanisms, increased inter particle bonding and volume reduction under constant stress due to creep. The effect of recent stress history and stress path direction on the stiffness of clay can be seen in many works, but in some cases it seem difficult to isolated each other. However, since as recent stress history seems to diminish with ageing time, it can be concluded that the effect of stress path direction becomes more pronounced. From the review of the factors influenced the soil stiffness it can be summarised that each of these factors seems to affect the stress strain behaviour of clays in different way.

The study of biaxial apparatus showed that plane strain devices have been developed since the early 1930's until today. The use of this apparatus is aimed to improve the accuracy of the data used for the analysis of the geotechnical structures under plane strain situation. Until now, there is no single biaxial device has been accepted universally by the geotechnical society around the world. Unlike the triaxial apparatus, most of the biaxial apparatus developed in the past were built in the research laboratory and were not available commercially. Further more, most of the apparatus were not easy to set up to carry out testing due to their inherent complexities. From the study presented above, it is obvious that more research to improve the biaxial apparatus is still required.

## **CHAPTER 3**

### **CONSTITUTIVE BEHAVIOUR AND FAILURE OF OVER CONSOLIDATED CLAY**

#### **3.1. Introduction**

The majority of naturally-aged in-situ materials, often described as soil, actually refers to soft rocks. These are characterised by certain degree of lithification or cementation. The presence of anisotropy and discontinuities are other major of soft rocks that demand special consideration in their constitutive modelling (Vaughan, 1997). The stress-strain response of soft rock or hard soil, in general, is similar to that of over consolidated soils (ISSMFE, 1989). The shear stress-strain curves commonly observed under triaxial compression tests of soft rocks in the range of low confining pressures indicated that brittle deformation is dominant and softening behaviour occurs. However, the behaviour becomes ductile and only strain hardening occurs with increase in the confining pressure.

The stress-strain behaviour of soil involving predictions of deformation and failure of soil is an important basis of soil mechanics. Experimental laboratory and field observations have indicated that an elastic-plastic model can approximate the behaviour of certain soils very well, as long as the soil deforms uniformly as continuous medium. The most widely used elastic plastic model, The Modified Cam Clay (MCC) model (Roscoe and Burland, 1968), appears to be the best choice of basic, conventional soil modelling, mainly because of its simplicity and adequacy in predicting soil behaviour. This, and other such models are

commonly formulated in triaxial stress space, therefore, their applications would be appropriate to the analysis of soil subjected to triaxial loading conditions. The generalized three dimensional formulation of Cam clay models have been the subject of research, but only in limited form (Zdravkovich, 2000). Potts and Zdravkovich (1999) presented the full formulation of the MCC model in a generalized stress system, adopting a circular yield surface in the deviatoric plane.

It has been the goal of many researchers to combine the two fundamental aspects of soil behaviour, namely plasticity and density dependence, within a single constitutive model. The works of Rendulic (1937) on normally consolidated clays combined with that of Hvorslev (1937) on over consolidated clays were the first to produce a predictive constitutive framework known as critical state soil mechanics. The framework was developed from the results of tests on reconstituted clays. The first elastic-plastic critical state models were the series of Cam Clay formulations originally developed by Roscoe and Burland (1968). The formulation of the original Cam Clay model, completely in terms of incremental elastic-plasticity, was undertaken by Schofield and Wroth (1968). Afterwards, Roscoe and Burland (1968) proposed the modified Cam Clay models (MCC) that has been proven to describe the behaviour of normally to lightly over consolidated clay.

In the following discussion, a review of the constitutive models for over consolidated clay, in which it begins with the classical theory of elasto-plasticity and continue with the elastic plastic model of over consolidated clay will be presented, then followed by several elastic-plastic models of soft rocks will be highlighted. The behaviour and failure of over consolidated clay based on the critical state theory then will be discussed.

### **3.2. Constitutive models for over consolidated clays**

One of the drawbacks of the basic Cam clay formulation is that it



significantly overestimates the failure stresses in the supercritical (dry region). Furthermore, Hvorslev (1937) had found experimentally, that a straight line approximates the failure envelope for over consolidated soils satisfactorily. Therefore, it is not surprising that in one of the earliest computations based on the Cam clay models, Zienkiewicz and Naylor (1973) adopted a straight line as the yield surface in the supercritical side called the Hvorslev surface. Likewise for soft rock materials, most of the soils constitutive models have been developed within the frame work of elasto-plasticity. According to this reason, a description of the classical theory of elasto-plasticity will first be reviewed, following this the existing model for over consolidated soils will be presented.

### **3.2.1. Clasical theory of elasto-plasticity**

A description of the basic concepts of the elasto-plastic theory will present in this section, followed by the formulation of the elasto-plastic constitutive matrix. A more detailed description is well documented by Potts and Zdravkovic (1999) and Zienkiewicz et al (1999).

There are four basic requirements of an elasto-plastic constitutive model to cater for, as follows: coincidence of axes, an equation for the yield surface, a plastic potential or flow rule, and finally a hardening/softening rule. These will be explained briefly as follows:

#### **(i) Coincidence of axes**

The principles directions accumulated stress and incremental plastic strain must coincide. This differs from elastic behaviour where the principal directions of incremental stress and incremental strain are coincided.

#### **(ii) Yield Surface**

A Yield surface separates purely elastic behaviour from elasto-plastic behaviour. The yield function,  $F$ , is defined as scalar function of the stress (expressed in term of either the stress components or invariants),  $\{\sigma\}$ , and the hardening (or otherwise termed state) parameters,  $\{k\}$ , that is,



$$F(\{\sigma\}, \{k\}) = 0. \quad (3.1)$$

(iii) A plastic potential function or flow rule

For multi-axial stress state, it is necessary to have a flow rule in order to specify the direction of plastic straining at any stress state. The flow rule determines the plastic strain increments. This is usually constructed with the assumption of a plastic potential surface, whose outward normal vector at the current stress state represents the plastic strain increments vector. The flow rule can be expressed as follows:

$$\{d\varepsilon_i^p\} = \Lambda \left\{ \frac{\partial P(\{\sigma\}, \{m\})}{\partial \sigma_i} \right\} \quad (3.2)$$

where  $\{d\varepsilon_i^p\}$  represents the plastic strain increment vector,  $P(\{\sigma\}, \{m\}) = 0$ , is the plastic potential function, and  $\Lambda$  is an unknown scalar multiplier.  $\{m\}$  is, essentially, a vector of the state parameters, the values of which are immaterial since only the differentials of  $P$ , with respect to the stress components, are needed in the flow rule.

A further simplification is introduced by assuming the plastic potential function to be the same as the yield function,  $P(\{\sigma\}, \{m\}) = F(\{\sigma\}, \{k\})$ , therefore flow rule is said to be associated and normally condition applies. In general case, where the plastic potential function is different from the yield function,  $P(\{\sigma\}, \{m\}) \neq F(\{\sigma\}, \{k\})$ , the flow rule is said to be non-associated.

(iv) Hardening/softening rule

The evolution of the yield surface in the course of plastic deformation is described by the hardening rule. For materials which harden and/or soften, during plastic straining, rules are required to specify how the yield function changes, and this is achieved by prescribing how the state parameters,  $\{k\}$ , vary with plastic straining,  $\varepsilon^p$ . If the elasto-plastic model is assumed to be perfectly plastic then the hardening parameters,  $\{k\}$  are constant and no hardening rule is needed.

Otherwise the hardening parameters are usually assumed to be a function of either the plastic work or the plastic strains.

#### *Determination of the scalar multiplier, $\Lambda$*

The scalar multiplier,  $\Lambda$ , is determined by employing the consistency condition. When the soil is yielding the consistency condition requires the stress state to remain always on the yield surface, so that  $dF = 0$ . As mention previously the yield function depends on the stress state,  $\{\sigma\}$ , and the hardening parameter,  $\{k\}$ , so the chain rule of differentiation gives :

$$dF = \left\{ \frac{\partial F}{\partial \sigma} \right\}^T \{d\sigma\} + \left\{ \frac{\partial F}{\partial k} \right\}^T \{dk\} = 0. \quad (3.3)$$

The above equation can be rearranged to give

$$\left\{ \frac{\partial F}{\partial \sigma} \right\}^T \{d\sigma\} = - \left\{ \frac{\partial F}{\partial k} \right\}^T \{dk\}. \quad (3.4)$$

If the hardening parameters are function of the plastic strains then:

$$\{dk\} = \left\{ \frac{\partial k}{\partial \varepsilon_i^p} \right\} \{d\varepsilon_i^p\}. \quad (3.5)$$

So equation (3.4) becomes

$$\left\{ \frac{\partial F}{\partial \sigma} \right\}^T \{d\sigma\} = \left\{ \frac{\partial F}{\partial k} \right\}^T \left\{ \frac{\partial k}{\partial \varepsilon_i^p} \right\} \{d\varepsilon_i^p\} \quad (3.6)$$

Hence, combining the flow rule and equation (3.6) would result in

$$\left\{ \frac{\partial F}{\partial \sigma} \right\}^T \{d\sigma\} = \left\{ \frac{\partial F}{\partial k} \right\}^T \left\{ \frac{\partial k}{\partial \varepsilon_i^p} \right\} \left[ \Lambda \left\{ \frac{\partial P}{\partial \sigma} \right\} \right]. \quad (3.7)$$

The scalar quantity,  $A$ , is obtained after a simple manipulation as:

$$\Lambda = \frac{1}{A} \left\{ \frac{\partial F}{\partial \sigma} \right\}^T \{d\sigma\}, \quad (3.8)$$

where  $A$  denotes the hardening modulus (or otherwise termed plastic modulus) given by the following equation :

$$A = - \left\{ \frac{\partial F}{\partial k} \right\}^T \left\{ \frac{\partial k}{\partial \varepsilon_i^p} \right\} \left\{ \frac{\partial P}{\partial \sigma} \right\}. \quad (3.9)$$

Based on the foregoing four basic requirements described above, the elasto-plastic constitutive model can be formulated. Accordingly, the relationship between incremental stresses,  $\{d\sigma\}$ , and strain,  $\{d\varepsilon\}$ , may be stated in terms of the elasto-plastic constitutive matrix,  $[D^{ep}]$ , as

$$\{d\sigma\} = [D^{ep}] \{d\varepsilon\}. \quad (3.10)$$

The changes in total strains,  $\{d\varepsilon\}$ , may be divided into two component, the elastic strains,  $\{d\varepsilon^e\}$  and the plastic strains,  $\{d\varepsilon^p\}$  that is,

$$\{d\varepsilon\} = \{d\varepsilon^e\} + \{d\varepsilon^p\} \quad (3.11)$$

The incremental stresses,  $\{d\sigma\}$ , are related to the changes in elastic strains,  $\{d\varepsilon^e\}$ , through the elastic constitutive matrix,  $[D]$ , such that

$$\{d\sigma\} = [D] \{d\varepsilon^e\}. \quad (3.12)$$

Hence, combining equation (3.11) into equation (3.12) would result in

$$\{d\sigma\} = [D] \{d\varepsilon - d\varepsilon^p\}. \quad (3.13)$$

Substitution of the flow rule in equation (3.13) would lead to

$$\{d\sigma\} = [D] \{d\varepsilon\} - [D] \Lambda \left\{ \frac{\partial P}{\partial \sigma} \right\} \quad (3.14)$$

If equation (3.14) is substituted in equation (3.8) then the scalar multiplier,  $\Lambda$ , becomes

$$\Lambda = \frac{\left\{ \frac{\partial F}{\partial \sigma} \right\}^T [D] \{d\varepsilon\}}{\left\{ \frac{\partial F}{\partial \sigma} \right\}^T [D] \left\{ \frac{\partial P}{\partial \sigma} \right\} + A} \quad (3.15)$$

Substitution of equation (3.15) in equation (3.14), would result in

$$\{d\sigma\} = [D] \{d\varepsilon\} - \frac{[D] \left\{ \frac{\partial P}{\partial \sigma} \right\} \left\{ \frac{\partial F}{\partial \sigma} \right\}^T [D] \{d\varepsilon\}}{\left\{ \frac{\partial F}{\partial \sigma} \right\}^T [D] \left\{ \frac{\partial P}{\partial \sigma} \right\} + A} \quad (3.16)$$

Equation (3.16) provides a relationship between changes in stress and strains. Therefore from equation (3.10), the elasto-plastic constitutive matrix,  $[D^{ep}]$ , may be deduced as

$$[D^{ep}] = [D] - \frac{[D] \left\{ \frac{\partial P}{\partial \sigma} \right\} \left\{ \frac{\partial F}{\partial \sigma} \right\}^T [D]}{\left\{ \frac{\partial F}{\partial \sigma} \right\}^T [D] \left\{ \frac{\partial P}{\partial \sigma} \right\} + A}. \quad (3.17)$$

### 3.2.2. Elasto plastic constitutive model of over consolidated clay

A basic formulation for critical state modelling based on the classical concepts of the elasto-plasticity has been presented in previous section. The

original critical state model, the Cam Clay model and the modified Cam Clay (MCC) model, are the classical example. These types of constitutive modelling do not satisfactorily describe the actual behaviour of soil in all aspects, especially in the supercritical region or on the dry side of critical state, as the softening, undergone by the models, results in excessively high peak stress and large volume expansion (ISSMFE, 1985). Another important problem of the MCC model is its poor prediction of shear strain. Moreover, problems involving cyclic loading, stress reversals, anisotropy and so on are not handled well by these simple models. As a result, various models for improving the basic critical state models have been made over the past several years.

There have been numerous models developed to simulate the behaviour of over consolidated clay, only the most significant ones will be reviewed in the following discussion, as follows: models that assume elastic strain within the yield surface based on the classical theory of elasto-plasticity and models that are based on extensions of the classical theory of elasto-plasticity, which allow for plastic strain to develop within the conventionally defined yield surface. A more detailed description and review of over consolidated clay behaviour models are well documented by Potts and Zdravkovic (1999), Zienkiewicz et al (1999) and Grammatikopoulou (2004). These models will be briefly reviewed as follows:

***(i) Models based on the classical theory of elasto-plasticity***

These models commonly adopt non-linear stress strain behaviour pre-yield to reproduce the highly non linear behaviour of over consolidated clay from early stages of loading. The simplest model that avoids the problem on the dry side of critical state was proposed by DiMaggio and Sandler (1971) known as a ‘Cap’ model. In this model the softening portion of the MCC model was replaced with a spindle-shaped failure surface which is assumed to be fixed, without expansion or contraction. Thus, a stress increment on this surface would give rise to perfectly plastic deformation only. For the hardening portion, an ellipsoidal yield surface with D-hardening is used as the yield cap. As the yield cap surface moves within

the changes in plastic volumetric strain, the failure surface is fix (Figure 3.1). Although this model primarily proposed for prediction of sand behaviour, application has been made to wide range of geo-materials, including clays and rocks by Sandler et al (1976, Baladi and Rohani (1979) and Baladi and Sandler (1980).

An empirical soil pre-yield model based on the results of high quality test data obtained with local measurements of strain was proposed by Jardine et al (1986) and Jardine et al (1991). This model adopted periodic logarithmic functions which related the shear and bulk modulus to the shear and volumetric strains. This pre-yield model is independent of the way plastic behaviour is modelled at large strains. Jardine et al (1991) used it in conjunction with a Mohr Coulomb yield surface. The model has been used in a wide range of geotechnical problems and the results have compared satisfactorily with field observations, including deep excavations, tunnels and off shore structures, highlighting the importance of modelling the highly non linear behaviour of over consolidated clay.

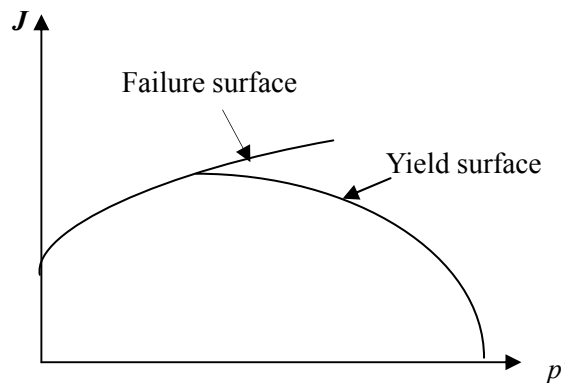


Figure 3.1. An ilustration of Cap model (after Potts, 1999)

The stress strain behaviour of heavily over consolidated Oxford clay modelled by Hird and Pierpoint (1997) using a cross-anisotropic non linear elastic model. In this model the material non linearity was independent on the incremental strain energy which was suggested by Burland (1989) for the definition of the kinematic regions proposed by Jardine (1985) and Jardine (1992).

The model was used in the numerical analysis of trial excavations in Oxford Clay. Based on the concept of kinematic regions proposed by Jardine (1985) and Jardine (1992), Puzrin and Burland (1998) developed a small strain pre-yield model. This model was concentrated on the behaviour within the small strain region (SSR) boundary. However, they noted that it is possible to use an elasto-plastic model for the SSR boundary or alternatively this model can be used in conjunction with any plastic model that can model the bounding surface. Results of triaxial test on undisturbed Bothkennar Clay have been used satisfactorily to validate this model.

**(ii) *Models based on extensions of classical theory of elasto-plasticity***

The models that are based on extensions of the conventional elasto-plastic framework allow for plastic deformation developed within the classically define yield surface of elasto-plasticity classical theory. In these models, the hardening modulus,  $A$ , varies within the yield surface, therefore, the variation of the hardening modulus within the yield surface is an extra ingredient has to be defined in this types of models, in addition to the four main ingredients required in the classical theory of elasto-plasticity.

As mention earlier, elastic behaviour is assumed within the yield surface in the original and MCC and Cap models. Poorooshasb (1966) first point out that small plastic deformation takes place naturally, even within the yield surface. Research dealt with over consolidated soil and studied their small deformation before failure, which is ignored in the MCC and Cap model. The introduction of a 'Hvorslev surface' as means of modifying the supercritical yield surface has been made by various researchers. Based on elastic, perfectly plastic behaviour in triaxial plane, Houlsby et al (1982) proposed the 'Roscoe-Hvorslev' model, and Tanaka et al (1987) adopted Hvorslev yield surface for the supercritical side and used a non associated flow rule, with dilatancy increasing linearly from zero, at the critical state point, to some fixed value at  $p'=0$ .

The bounding surface model was initially developed by Dafalias and Herman (1980, 1982). In this model, a bounding surface is introduced, which resembles a conventional yield surface. Under the framework of bounding surface plasticity, during unloading only elastic behaviour was predicted, whereas elastic plastic behaviour was predicted upon loading. The magnitude of such elastic-plastic behaviour depends on the gradients of the yield function and the hardening modulus. The hardening modulus for each stress point within the bounding surface depended on the distance between this stress point and the image point and reduced to the bounding surface hardening modulus when the stress point reached the bounding surface (Figure 3.2). These quantities are related to those of the bounding surface, using a simple radial rules that are dependent on the proximity of the current stress state to the bounding surface.

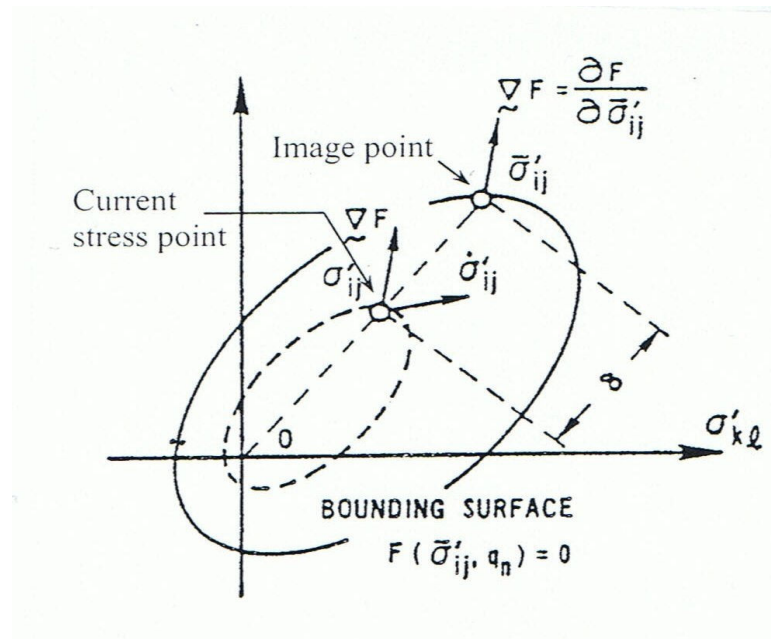


Figure 3.2. A schematic representation of bounding surface model (after Dafalias and Herrmann, 1982)

Whittle (1993) presented the MIT-E3 model for over consolidated clays adopted from modified Cam clay formulation. The model dealt with an anisotropic yield surface, kinematic plasticity and significant strain softening under undrained conditions. A closed symmetric, hysteresis loop during



unloading combined with bounding surface plasticity to develop plastic strains during reloading were used in this model (Figure 3.3). The model requires 15 input parameters, some of which are difficult to evaluate and it is inordinately complex. This model demonstrated accurately to represent the behaviour of three different clays, subjected to a variety of loading path. It has also shown to adequately predict the behaviour of a deep excavation in Boston Blue Clay (Whittle et al, 1993). The model has been used in parametric study of the pull-out capacity of bucket foundations in soft clay (Zdravkovic et al, 2001), and was shown to predict successfully the failure height of an embankment founded on soft clay at Saint-Alban, Quebec (Zdravkovic et al, 2002). The constitutive laws of the model have been clearly set out by Ganendra and Potts (1995).

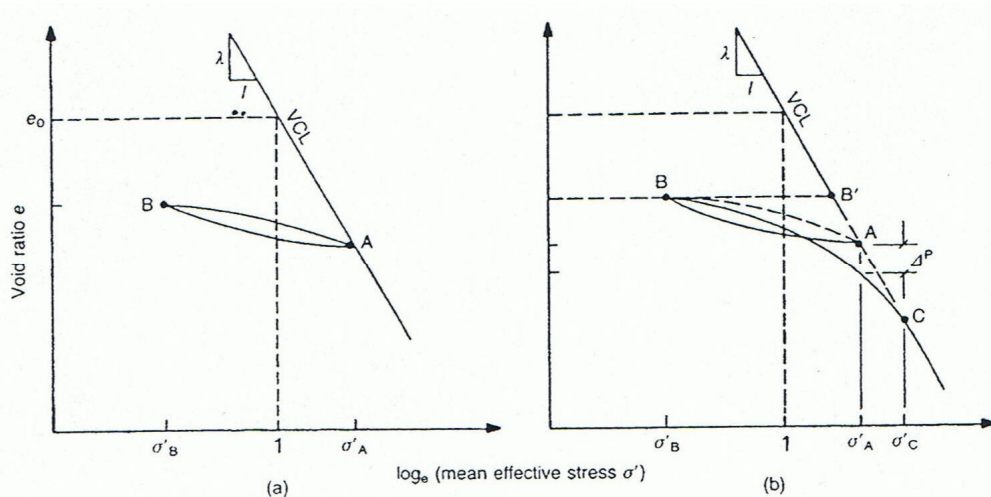


Figure 3.3. Conceptual model of unload-reload used by MIT-E3 for hydrostatic compression: a) perfect hysteresis b) hysteresis and bounding surface plasticity (after Whittle, 1993)

A two-surface model within the framework of critical state soil mechanics was formulated by Al-Tabaa (1987) and Al-Tabaa and Wood (1989) based on the model of Mroz et al (1979) and Hashiguchi (1985). In this model, a single kinematic yield surface, which is acted as the bounding surface, was introduced within the modified Cam Clay yield surface (Figure 3.4). The behaviour within the kinematic yield surface was assumed to be isotropic elastic. This model degenerates to the modified Cam Clay model for monotonic loading and for

continuous yielding. The model demonstrated accurately to predict the cyclic behaviour of spetwhite kaolin clay. Stallebrass (1990) and Stallebrass and Taylor (1997) extended this model by incorporating a third surface within the modified Cam Clay bounding surface. This surface was introduced to provide a more realistic simulation of the recent stress history effect on the behaviour of over consolidated clay. The two surface model (Al-Tabaa, 1987) and three surface model (Stallebrass, 1990) have been implemented into finite element program and in parametric study of the over consolidated clay and were shown to predict successfully the behaviour of tunnel excavation within over consolidated London Clay (Grammatikopoluou, 2004).

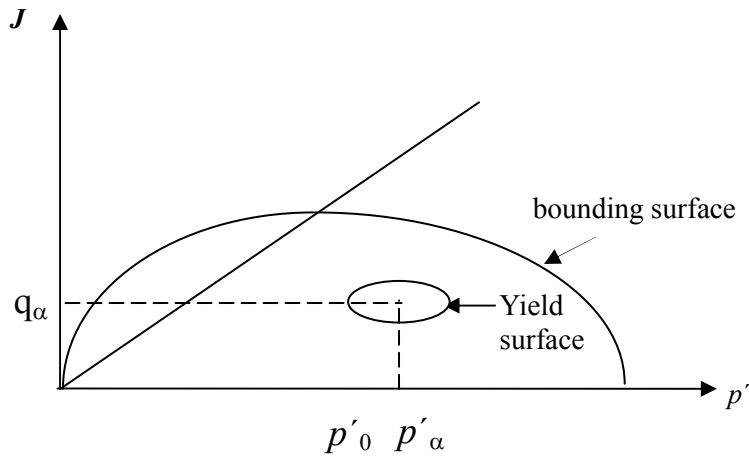


Figure 3.4. Two surface model (after Al-Tabaa, 1987)

An extension developing of Kinematic hardening plasticity model was formulated by Puzrin and Burland (2000) incorporating the small strain pre-yield, which was developed earlier (Puzrin and Burland, 1998). In this model the boundaries of the linear elastic region and small strain region were assumed to be kinematic yield surface and were represented by rotated ellipses of the same shape. To account for the effect of structure in natural soil, the extension of kinematic hardening models have been presented by Kavvadas and Amorosi (2000) which is an extension of the two surface model (Al-Tabaa, 1987) and Baudet (2001), which is an extension of the three surface model (Stallebrass,

1990). Moreover, an additional effect of anisotropy on the model was presented by Gajo and Wood (2001 and Callisto et al (2002).

### **3.3. Elastic plastic models of hard soil and soft rocks**

The concepts of critical state theory may be applicable to soft rocks at relatively low stresses have been shown by Chiu and Johnson (1984) and Johnston and Novello (1985). At higher stresses, cracking and dilatation takes places and the behaviour of soft rocks tend to deviate significantly from critical state model predictions. Johnston and Novello (1985) introduced a “crack volume” concept to account for the influence of crack propagation, and demonstrated that the intact material of the specimen failure. In their later work Johnston and Novello (1995) showed the equivalence of over consolidated and normally consolidated behaviour of soils with the brittle-ductile transition of rock, and suggested that all these apparent different geotechnical materials may related within the critical state framework. Price and Farmer (1979) examined the applicability of the critical state concept to the yielding of soft rocks, and found that the critical state is the ultimate state that can be reached by the homogenous deformation of soft rocks.

A model based on elastic-viscoplastic theory for sedimentary soft rock has been developed by Akai et al (1978). The functional form of the yield surface with an associated flow rule (af<sub>r</sub>) have been determined and verified experimentally. Hirai and Masao (1982) proposed a yield function in terms of first and second stress invariants, similar to Mroz’s theory (1967), in which the hardening parameter was expressed in terms of the deviatoric and volumetric parts of the plastic work. Maekawa and Miyakita (1983) showed that the shape of the initial yield surface for diatomaceous mudstone, when subjected to triaxial testing, is very similar to that of the Cam clay model (Roscoe et al, 1963). This suggested the fact that the stress-strain relation, for soft rocks, may also be similar to those of natural over consolidated clay. Okamoto (1985) modified the multi-surface

model proposed by Mroz et al (1981), so that it could be applied to predict the stress-strain behaviour of sands, over consolidated clays and soft rocks.

The homogenous deformation of soft rocks usually requires a significant increase in the confining pressure of soft rocks. Price and Farmer (1981) reported that a “Hvorslev surface” exist for soft rocks. In order to explain the brittle behaviour of soft rocks, Gerogiannopoulos and Brown (1978) proposed to modify the Cam clay model. Based on this approach and verified experimentally, Elliot and Brown (1986) obtained the yield surface of Bath Stone and showed that the proposed methods are applicable to rock. In the model, an associated flow rule (afr) was adopted and later extended to incorporate a non-afr yield surface (Michelis and Brown, 1986). Elastic-plastic models applicable to soft rocks with non-afr yield surface were also proposed by Ichikawa et al. (1987, 1988).

The non-afr (non associated flow rule) model proposed by Adachi and Oka (1982) was extended for application to soft rocks (Adachi et al., 1987), and it was shown to describe the behaviour of soft sedimentary rock during triaxial compression test. A general simplified model for soft rock based on elastic-plasticity theory that can characterize the behaviour of soft rock was proposed by Desai and Salami (1987). The model has successfully characterized the behaviour of soft rock, such as hardening/softening, dilatancy, stress path dependency, cohesive and tensile strengths.

The existence of fissures and cracks which are the result of mechanical, thermal and volume-change-induced stresses, such soils are non uniform. In general, the structural nature of soil material is such that it can sustain very little or no tensile stress under drained loading condition. This phenomenon can be observed with a fissured or jointed rock mass in its varying degrees of weathering. An appropriate constitutive model for such a material should not permit the soil's tensile strength to be exceeded, and it should also control the way tensile cracks initiate and then develop (Potts and Zdravkovic, 1999). Based on elasto-plastic theory, Nyaoro (1989) developed such a model that allows for crack formation

and subsequent rotation of the crack orientation in a systematic manner. The model accommodates elements within the material, which simultaneously undergo tensile and shear failure.

Lo et al (2005) proposed an elasto-plastic shear fracture approach to the constitutive behaviour of soil and soft rock. The model took up from where Hvorslev-Modified Cam Clay (MCC) model leaves off, which is at the onset of localized shear banding. This model dealt with four distinct states of soil failure and their related stress-strain behaviour (Figure 3.5). State I, which is applicable to normally to lightly over consolidated soils, consist of two phases. The first phase follows the behaviour of the MCC model up to the peak stress. Phase 2 behaviour simulates state A to B of Figure 3.5. In the State II, an elasto-plastic shear, or  $J_{ii}$  fracture of the specimen follows the Hvorslev-MCC model behaviour either pre- or post-peak stress. This behaviour is attributable to soils on the dry side of critical state, such as heavily over consolidated clay. The stress-strain trace follows the elastic curve of critical state theory up to point A and it moves on the peak at point B. Following this, the plastic zone start to grow more slowly, so that the specimen strain softens until point C is reached, at which the crack would have cut through the specimen. The upper portion of soil then slide down along the discontinuity and only frictional resistance would be offered at their interface as the curve follows the ultimate path CD. In the State III the test specimen is sufficiently brittle to exhibit elastic only fracture, which is the case of hard, partially saturated soils and soft rock. A vertical crack would develop from the initial flaw or defect grows in the test specimen under biaxial compression in plane strain. Finally, the fourth state is the transition of State II and State III. A vertical crack firstly develops from defect in the specimen, similarly as state III until such a stage is reached when a diagonal elasto-plastic shear fracture develops preferentially, as in the case of State II.

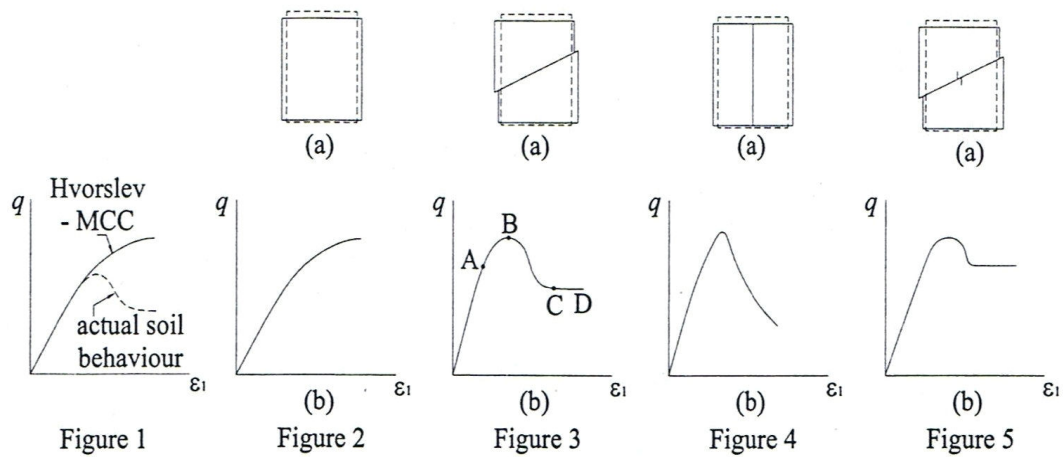


Figure 3.5. States of failure and their related stress-strain behaviour on the Elastoplastic shear fracture model (after Lo, et al, 2005)

In spite of the various attempts to model the strain-softening behaviour of naturally over consolidated clays and soft rocks using the theory of plasticity (Prevost and Hoeg, 1977; Bannerjee and Stipho, 1979), such an approach has been criticized mainly from the strain-localization point of view. Read and Hegemier (1984) argued that the strain-softening behaviour does not exist locally on the continuum level. Sandler (1986) concluded that strain softening is not a material property, but simply a manifestation of the effects of the progressively increasing inhomogeneity of deformation. The continuum-based, elastic-plastic models can not deal with the actual kinematics of strain softening, and thus, do not have a sound basis for application to soils on the dry side of critical state. In this context an elasto-plastic fracture model proposed by Lo et al (2005) probably can provide a rational basis for the prediction of such soil behaviour.

### 3.4. Behaviour of over consolidated clay based on critical state theory

The critical state framework essentially combined the work of Rendulic (1937) for normally consolidated clays and that of Hvorslev (1937) for over consolidated clays. The framework was developed from the results of tests on reconstituted clays. The first elastic-plastic critical state models were the series of

Cam Clay formulations originally developed by Roscoe and Burland (1968). The formulation of the original Cam Clay model, completely in terms of incremental elastic-plasticity, was undertaken by Schofield and Wroth (1968). Afterwards, Roscoe and Burland (1968) proposed the modified Cam Clay models (MCC). A more detailed description is well documented by Potts and Zdravkovic (1999) and Zienkiewicz et al (1999). The main hypotheses of critical state frame work are the following:

- (i) When the normally consolidated clay sample is compressed isotropically then this will follow the isotropic compression line and when the sample is isotropically swelled then this will move up a swelling line. As can be seen in Figure 3.6, and are described by equation 3.18 and 3.19, respectively, the compression line and the swelling line are assumed to be a straight line in the  $v$ - $\ln p'$  space:

$$v = N - \lambda \ln p' \quad (3.18)$$

and

$$v = v_k - \kappa \ln p' \quad (3.19)$$

in which  $N$  is the specific volume of the isotropic compression line for  $p' = 1$  kPa,  $\lambda$  is the slope of the line in the  $v$ - $\ln p'$  space,  $v_k$  is the specific volume of the swelling line for  $p' = 1$  kPa and  $\kappa$  is the slope of the line in the  $v$ - $\ln p'$  space.

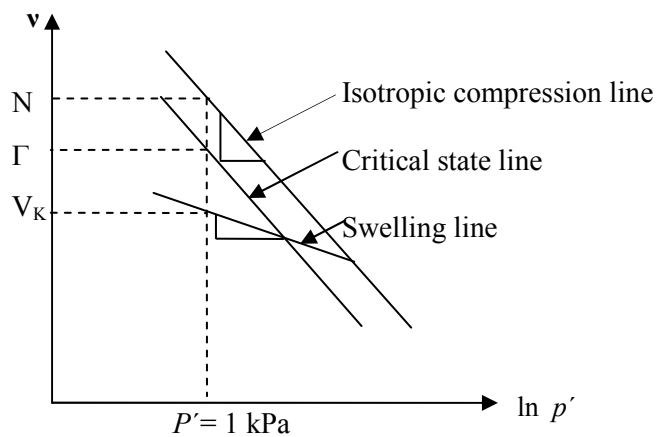


Figure 3.6. Isotropic compression line, swelling line and critical state line (after Potts and Zdravkovic, 1999)

(ii) If sheared, all soils ultimately reach a critical state at which large shear distortions occur with no change in stress or specific volume. The critical state line projection onto the  $q$ - $p'$  space and the  $v$ - $\ln p'$  space, as can be seen in Figure 3.6, is described by the Equations 3.20 and 3.21, respectively:

$$q = Mp' \quad (3.20)$$

and

$$v = \Gamma - \lambda \ln p' \quad (3.21)$$

where  $M$  is the gradient of the critical state line in the  $q$ - $p'$  space and  $\Gamma$  is the specific volume of the critical state line for  $p' = 1$  kPa.

(iii) When a clay sample is sheared then its stress path will climb up to the state boundary surface and then it will traverse the surface until it reaches the critical state line. A unique state boundary surface of the soil presents, which is described by the stress parameters  $p', q$  and  $v$  fall within or on the state boundary surface. The state boundary surface in normalized stress space as shown in Figure 3.7 consists of the Hvorslev surface for heavily over consolidated clays and the Roscoe surface for normally consolidated and lightly over consolidated clays (Atkinson and Bransby, 1978). The state boundary surface in  $v$ - $p'$ - $q$  space can be seen in Figure 3.8.

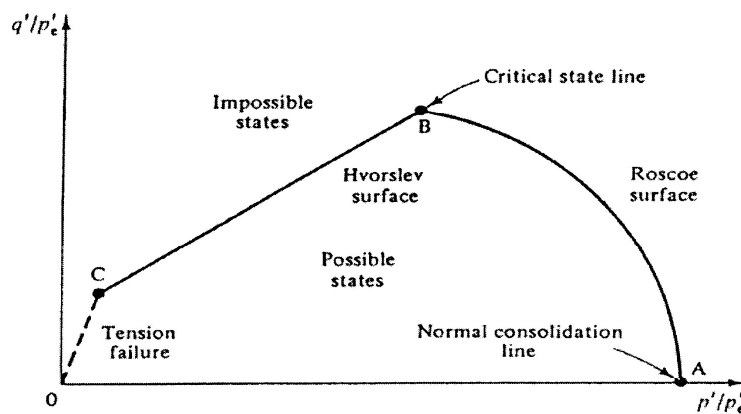


Figure 3.7. State boundary surface of the critical state framework in normalized stress space (after Atkinson and Bransby, 1978)



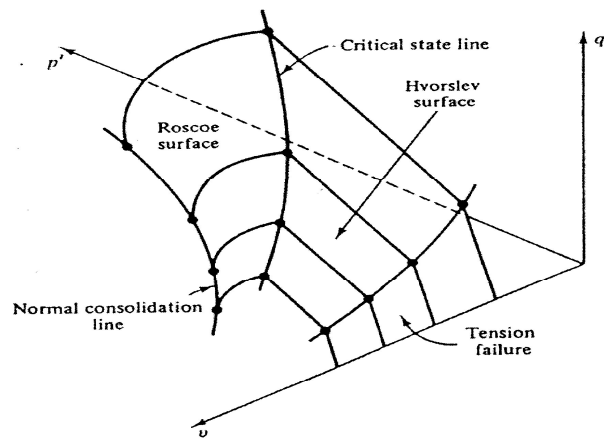


Figure 3.8. State boundary surface of the critical state framework in  $v$ - $p'$ - $q$  space  
(after Atkinson and Bransby, 1978)

(iv) If the behaviour of the sample within the state boundary surface is assumed to be elastic, this means that only recoverable strains occur. When the behaviour of the sample on the state boundary surface is assumed to be elastoplastic, this means that both recoverable (elastic) and irrecoverable (plastic) strains develop. As can be seen in Figure 3.9 an “elastic wall” exists within which behaviour is purely elastic. This elastic wall intersects the state boundary surface along a line which is called yield locus. The critical state models of Cam Clay (Roscoe and Schofield, 1963) and modified Cam Clay (Roscoe and Burland, 1968) give an equation to this line.

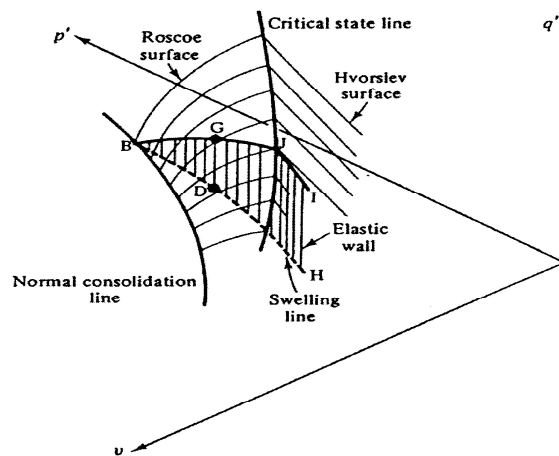


Figure 3.9. Elastic wall (after Atkinson and Bransby, 1978)

The critical state framework predicts that when an over consolidated soil is sheared, elastic behaviour occurs until the stress state reaches the state boundary surface. The condition of over consolidated soil is the result of unloading the soil and is represented by stress states within the state boundary surface. Thereafter elasto-plastic behaviour is predicted. The elastic bulk modulus  $K$ , is linked to the values of the mean effective stress,  $p'$ , and the specific volume,  $v$ , as stated in Equation 3.22:

$$K = \frac{vp'}{\kappa} \quad (3.22)$$

The elastic shear stiffness,  $G$ , is related to the elastic bulk modulus,  $K$ , through the Poisson's ratio,  $\mu$ , as formulated in Equation 3.23:

$$\frac{G}{K} = \frac{3(1-2\mu)}{2(1+\mu)} \quad (3.23)$$

The initial formulations of the critical state models assumed an infinite shear modulus. In the applications of the model either a constant shear modulus,  $G$ , or a constant Poisson's ratio,  $\mu$ , was usually assumed. For a constant Poisson's ratio,  $\mu$ , the shear stiffness is also linked to  $p'$  and  $v$ . It has been demonstrated by Zytynski et al (1978) that this formulation is not conservative and can lead to the development of permanent shear strains for a loading-unloading cycle that remains within the yield surface. Since no significant changes in both  $p'$  and  $v$  are expected until the stress path reaches the state boundary surface, the dependence of the stiffness on  $p'$  and  $v$  results in a slightly non-linear elastic behaviour.

Behaviour of over consolidated clay is different from normally consolidated clay, due to their stress history underwent in the past. The state of normally consolidated clays lies on the wet side of critical state line while the state of over consolidated clay is on the dry side of critical state line. The behaviour differences of over consolidated clay and normally consolidated clay in terms of volume change and pore water pressure shown in Figure 3.10. As can be

seen in Figure 3.10 (a), when over consolidated clay is subjected to load, it exhibits dilation during shearing, the pore water will be in tension as the effort to hold the soil particles in their initial positions. As a consequence, the pore water will drop. The opposite behaviour will occur in normally consolidated clay as shown in Figure 3.10 (b). When normally consolidated clay is subjected to load, the volume will decrease during shearing, as the particles tend to compress. The pore water will oppose to this movement and pore pressure will increase.

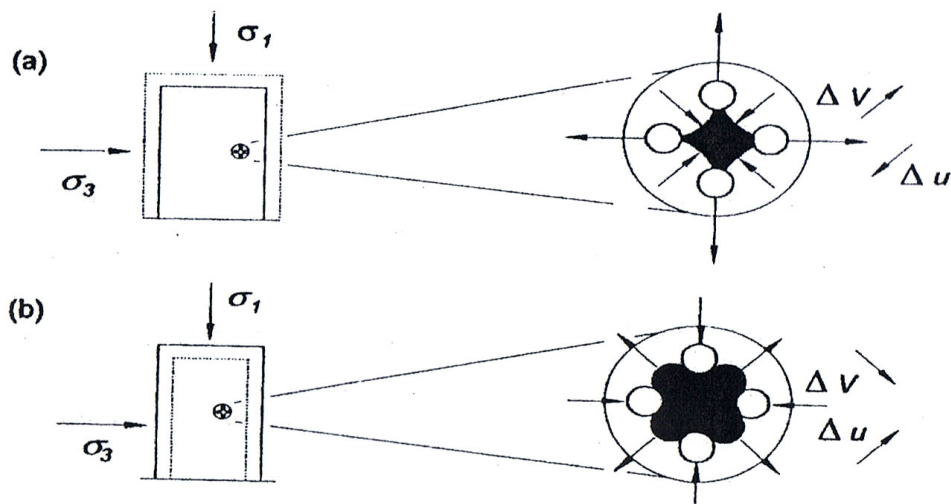


Figure 3.10. Comparison of pore pressure: (a) dilation on over consolidated clay and (b) contraction on normally consolidated clay (after Ortigo, 1995)

Bishop and Henkel (1962) investigated the behaviour of heavily over consolidated Weald Clay. The typical stress strain curve of triaxial drained on over consolidated clay presented in Figure 3.11. It can be seen from the graph that the samples experienced a peak strength which is denoted by  $q_f'$  after which the value of  $q'$  decreases as the strain increases. The volumetric strain curve showed that the sample was initially contracted and dilated at the end of the test.

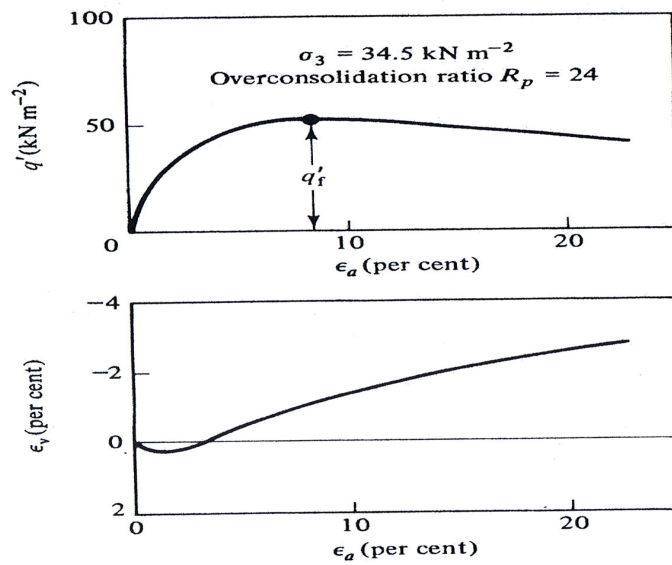


Figure 3.11. Typical result of a drained test on heavily over consolidated Weald Clay ( after Bishop and Henkel, 1962)

The stress path of the result showed in Figure 3.11 is plotted in Figure 3.12. It can be seen from the graph that the stress path moves above the projection of critical state line to failure point before moving back along the same path approaching the projection of the critical state line.

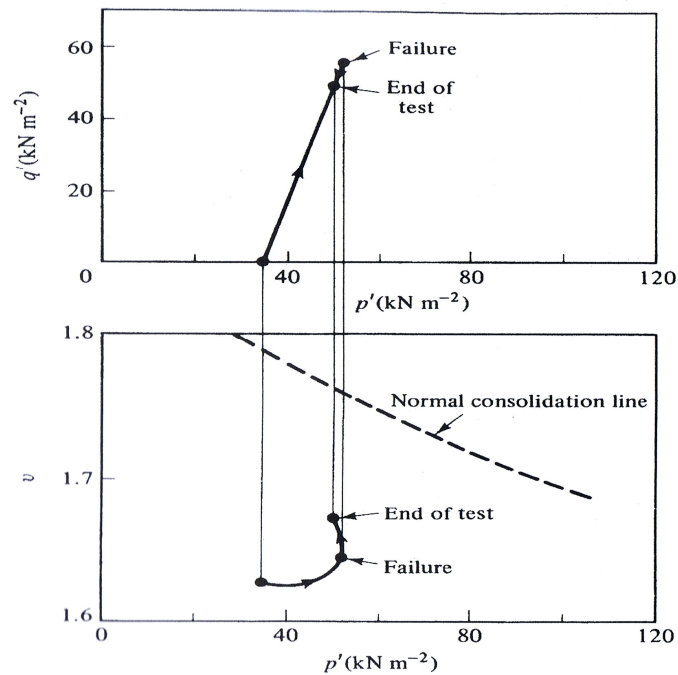


Figure 3.12. Stress paths in  $q': p'$  and  $v: p'$  of a drained test on over consolidated clay (after Atkinson and Bransby, 1978)

A typical stress strain behaviour of triaxial undrained test result of an over consolidated clay studied by Bishop and Henkel (1962) can be seen in Figure 3.13. It can be seen from the graph that the failure of the sample had occurred in very large strain. The pore pressure change in undrained test is different manifestation of the same physical phenomenon that exists in drained test, which is described the increase of the specific volume.

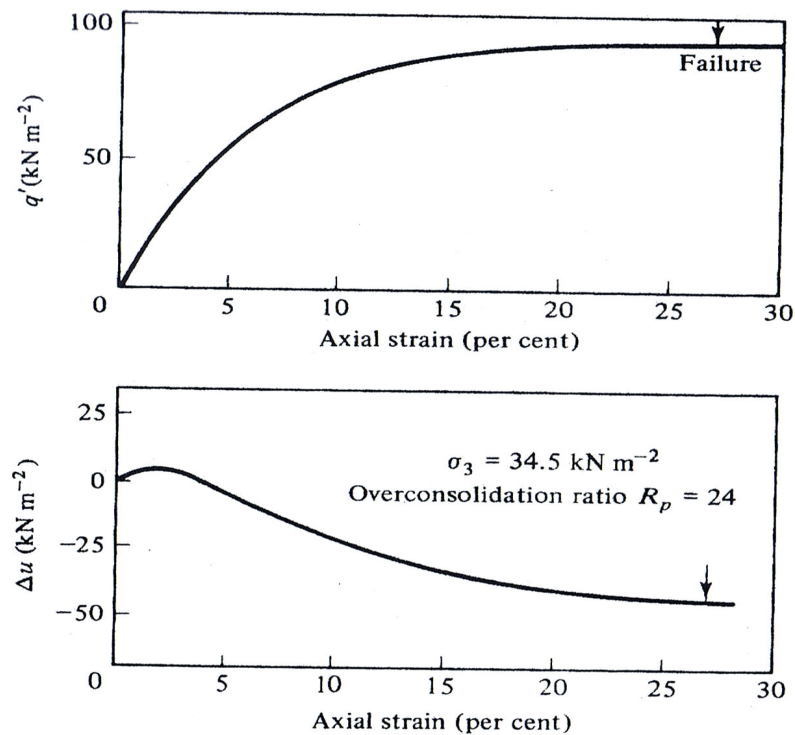


Figure 3.13. Typical result of triaxial undrained test on over consolidated clay  
(after Bishop and Henkel, 1962)

Figure 3.14 shows the typical stress path of the undrained test on over consolidated clay. The easiest way to draw the effective stress path is to offset the path by pore pressure to the left of the total stress path which moves up with the slope of 3 from the initial point that represents the initial state of the sample.

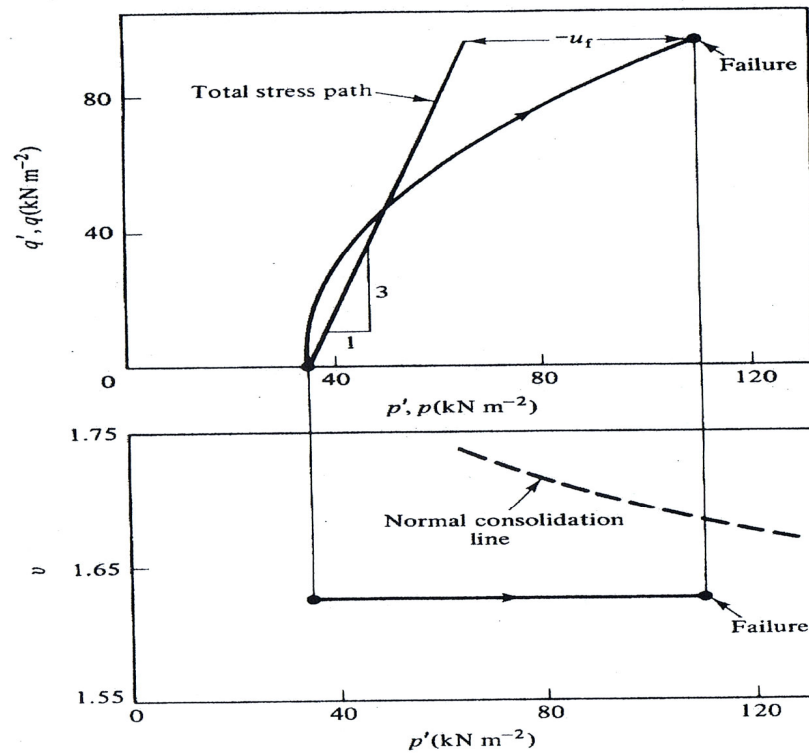


Figure 3.14. Stress paths in  $q': p'$  and  $v: p'$  of a drained test on over consolidated clay (after Atkinson and Bransby, 1978)

### 3.5. Remark

The constitutive behaviour of elastic plastic deformation and failure of over consolidated clay, including their application to soft rock that has been developed over the past forty years, have been reviewed. There have been numerous exertions made to describe the complex nature of irreversible soil deformation that involves mainly pressure dependence and plastic volume changes or softening. Among the available elastic-plastic models, the series of Cam Clay models have been proved in providing a fundamental and rational framework for understanding soil behaviour in a relatively simple way. Nowadays, we still do not have a single constitutive model, acknowledged by everyone as satisfactorily describing all facets of real soil behaviour.

The review of the classical theory of elasto plasticity showed that there are four basic requirements needed, there are coincidence of axes, an equation for the yield surface, a plastic potential or flow rule, and finally a hardening/softening rule. Based on these four basic requirements, the elasto-plastic constitutive model can be formulated.

There have been numerous models developed of more realistic models on the behaviour of over consolidated clay. Two categories of models have been presented. The first categories include the models that assume elastic strain within the yield surface based on the classical theory of elasto-plasticity. These models assume elastic pre-failure behaviour and usually simulate high pre-yield non linearity. The second categories models based on the extensions of the classical theory of elasto-plasticity. These extension models allow for plastic strain to develop within the conventionally defined yield surface, which is known as the bounding surface. In these models plastic deformations occur in a progressive rate within the bounding surface.

In the discussion of the various attempts to model the strain-softening behaviour of naturally over consolidated clays and soft rocks, such an approach has been criticized mainly from the strain-localization point of view. It should be emphasised that all of the elastic plastic models discussed so far, including the most widely used model, the Hvorslev-MCC model, are based on the assumption of continuum mechanics, and therefore apply only if the material remains intact. For stiff or hard soils and soft rock, discontinuities develop under load, and since the models assume continuity, they cease to apply. In this effort, an elasto-plastic fracture model proposed by Lo et al (2005) probably can give a rational basis for the prediction of such soil behaviour and applicable to the entire range of soils from normally consolidated to lightly over consolidated soil, which is a wet soil like marine clay, to stiff or hard soil like partially saturated soil, as well as heavily over consolidated soil including soft rock, in which is a dry soil.

The study of the behaviour of over consolidated clay based on the critical

state frame work exhibited that there are four main hypotheses of critical state theory. The first hypothesis stated that the isotropic compression line occur when the normally consolidated clay sample is compressed isotropically and a move up swelling line occur when it is isotropically swelled. The second hypothesis concise that when the soils are sheared, they will reach a critical state at which large shear distortions occur with no change in stress or specific volume. The third theory point out that the stress path of clay will climb up to the state boundary surface and then it will traverse the surface until it reaches the critical state line. The fourth theory mentioned that when elastic behaviour is assumed within the state boundary surface then only recoverable strains occur. However, when the behaviour of the sample on the state boundary surface is assumed to be elasto-plastic, this means that both recoverable (elastic) and irrecoverable (plastic) strains develop.



## **CHAPTER 4**

### **CONSTITUTIVE BEHAVIOUR AND FAILURE OF PARTIALLY SATURATED CLAY**

#### **4.1. Introduction**

The behaviour of partially saturated soil is quite different from those of fully saturated soil because of the influence of suction. Partially saturated soils form the largest category of materials that cannot be classified by classical saturated soil mechanics concepts. Any soil near the ground surface in a relatively dry environment will be subjected to negative pore-water pressure and possible desaturation. Although soils are generally assumed fully saturated below the groundwater table, they may be semi saturated near the state of full saturation under certain conditions. The situation of partial saturation may be caused by several factors, such as variation of water table level due to natural or manmade processes.

The presence of matric suction pressure is the main difference between saturated and unsaturated soil mechanics. It has been observed that several stability problems, involving soils used as construction materials, are due to water content changes and therefore to matric suction changes that occur periodically in nature. Commonly it is the presence of more than two phases that results in a media that is difficult to deal with in engineering applications. Results obtained

with the strength theory of fully saturated soil could not be directly applied to solve the partly saturated soil problems.

Partially saturated soil is normally considered as a three-phase system, there are soil solids, water (fluid), and air (gas). The presence of a fourth independent phase, a so called air–water interface or contractile skin was introduced (Fredlund and Morgenstern, 1977). Based on multiphase continuum mechanics, a theoretical stress analysis of an unsaturated soil has been presented (Fredlund and Morgenstern, 1977; Fredlund and Morgenstern, 1976). The analysis concluded that any two of three possible normal stress variables can be used to describe the stress state of a partially saturated soil. This is in contrast to saturated soil, where it is possible to relate the behaviour of the soil to the effective stress only.

This chapter is divided into two parts. The first part presents a reviewed of the constitutive models for partially saturated clay. The main features of the mechanical behaviour and failure of partially saturated clay then will be studied and discussed in the second part.

## **4.2. Constitutive models for partially saturated clays**

The importance of partially saturated soil in geotechnical engineering has long been recognised and efforts have been made to model their mechanical behaviour. However, unified elasto-plastic constitutive models for partially saturated soil using the overall framework of critical state concept have only been initiated in the last decade. On the basis of the literature review, the existing models can be divided into three categories. The distinction between them is discussed in the following sub sequent.

### **4.2.1. The Barcelona-type models**

Among the researchers Alonso et al (1987) were the first to propose an integrated framework incorporating both volume changes and shear strength models for partially saturated clays. The proposed framework was based on the theory of elasto-plasticity and was initially in a qualitative way rather than with full mathematical development. Alonso et al (1987, 1990) proposed a critical state framework involving two independent set of stress variables, namely the net stress and the matric suction. The proposed model, called Barcelona Basic Model (BBM), is an extension of the modified Cam-clay model developed for saturated clay ((Roescoe and Burland, 1968). The BBM model presents a simple and powerful conceptual framework to describe and predict the behaviour of unsaturated soils. The model generally relating the compressibility of soils to matric suction by the Loading- Collapse curve, called LC curve. The concept of Loading-Collapse (LC) is depicted in Figure 4.1.

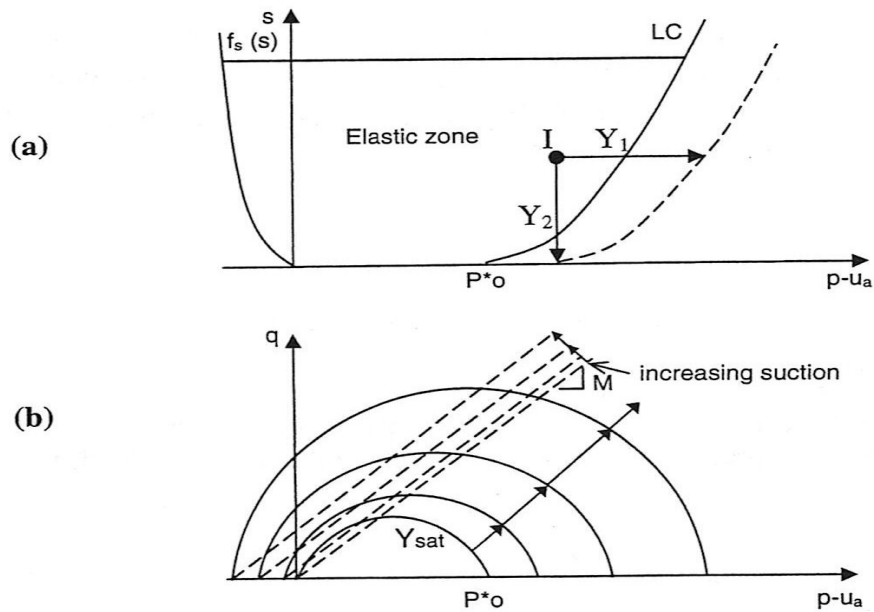


Figure 4.1. Limit state curves and elastic domains for unsaturated soil-BBM (after Alonso et al, 1990)

A fully developed mathematical formulation in the form of a critical state type model for partially saturated soils presented by Alonso et al (1990) was

developed for non expansive and moderately expansive clays. The model is formulated in terms of four state variables, namely: mean net stress, deviator stress, matric suction and specific volume for the conditions of triaxial test. Based on the concept of a yield surface in  $p'' : q : s$  space the model is presented. In this model elastic behaviour occurs within the yield surface and on reaching the yield surface the onset of plastic volumetric and shear strains occurs. For isotropic loading to virgin states, plastic strains occur and the soil state lies on normal compression line for particular value of suction. For isotropic stress states, the intersection of the yield surface with the  $q=0$  plane gives a yield curve, termed the 'loading collapsed' *LC* yield curve. Alonso et al (1990) considered the Modified Cam Clay model as a limiting condition corresponding to the saturated case. Consequently, extension of the model to anisotropic stress state resulted in elliptical yield curve in the  $p'' : q : s$  plane for each value of suction, as presented in Figure 4.2.

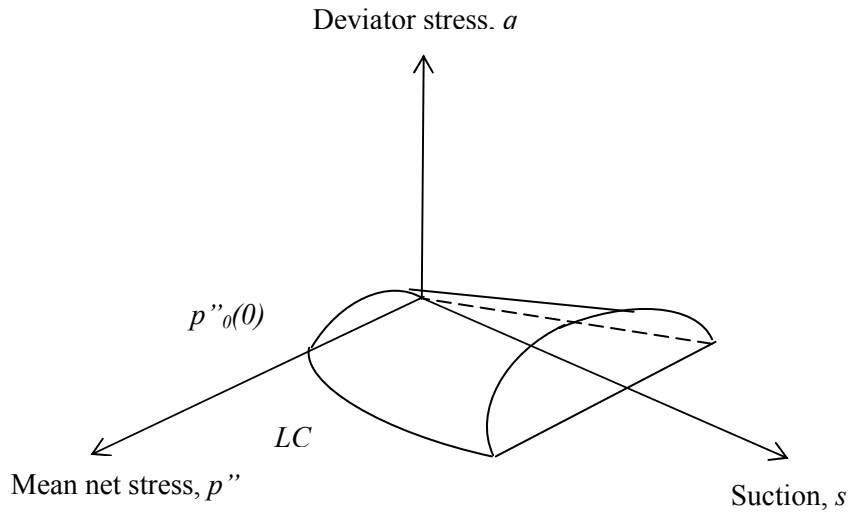


Figure 4.2. Yields surface in  $q : p'' : s$  surface (after Alonso et al, 1990)

Wheeler and Sivakumar (1995), Maatouk et al (1995) and Cui and Delage (1996) reported result from an experimental investigation of compacted kaolin clay. These results provided support for the main features of the model proposed by Alonso et al (1990). However, aspects of the experimental data suggested

minor modifications to the original model. A revised model was therefore proposed by Wheeler and Sivakumar (1995). An existence of a unique normal compression line for each value of suction was indicated from an experimental data obtained from controlled-suction triaxial test on speswhite kaolin. The data reported by Wheeler and Sivakumar (1995) relate to a limited range of stresses, which for compacted kaolin clay, presumably corresponds to stresses above that where the maximum collapse occurs. They also showed that the form of normal compression lines in the  $v:p''$  plane is inextricably linked with the development of the shape of the LC yield curve in the  $S:p''$  plane as the curve expand (Figure 4.3). This implies that defining either the normal compression line for different values of suction or the changing shape of the yield curve as it expands is sufficient for the developing these aspect of an elasto-plastic model. It should be noted that A and C lie on the same yield curve at different values of suction (Figure 4.3 (a)), and that each lies on the normal compression line for the appropriate value of suction.

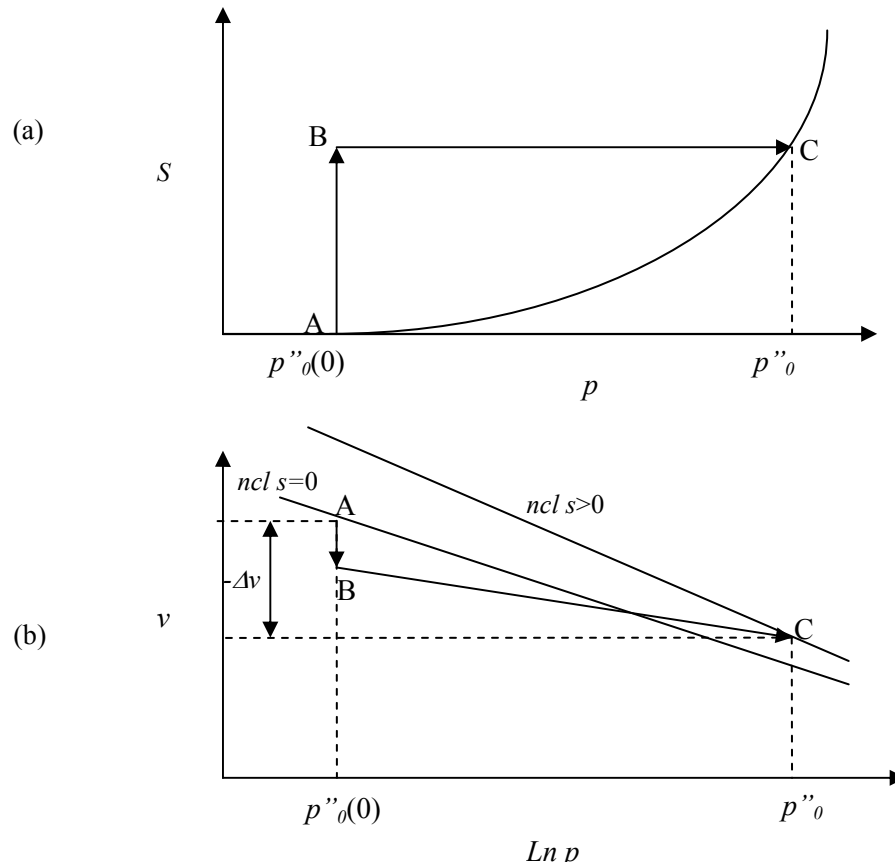


Figure 4.3. Loading Collapsed Yield Curve (after Wheeler and Sivakumar, 1995)

#### 4.2.2. Physical model of Leroueil and Barbosa (2000)

Leroueil and Barbosa (2000) proposed the model called GFY model. The model assumed that yield curves for saturated soil can be schematised by four segments shown in Figure 4.4. Two segments are corresponding to the strength envelopes in compression and in extension, while other two segments are corresponding to  $\sigma'_a = \sigma^*_{ayo}$  and  $\sigma'_r = \sigma^*_{ryo} = K_{AL} \sigma^*_{ayo}$ . In these equations  $\sigma^*_{ayo}$  is the axial net yield stress,  $\sigma^*_{ryo}$  is the radial net yield stress, and  $K_{AL}$  is the anisotropy ratio. In the diagram shown in Figure 4.4, the line reflecting the anisotropy is called the anisotropy line (AL) and is characterised by  $K_{AL} = \sigma^*_{ryo} / \sigma^*_{ayo}$ . By increasing the axial yield stress from  $\sigma^*_{ayo}$  to  $\sigma^*_{ays}$ , matric suction increases the shear strength of soil in compression from  $B_o$  to  $B_s$ , or from  $B_o$  to  $B'$ . In extension, the shear strength increase due to a given matric suction is associated with an increase in radial yield stress from  $\sigma^*_{ryo}$  to  $\sigma^*_{rys}$ .

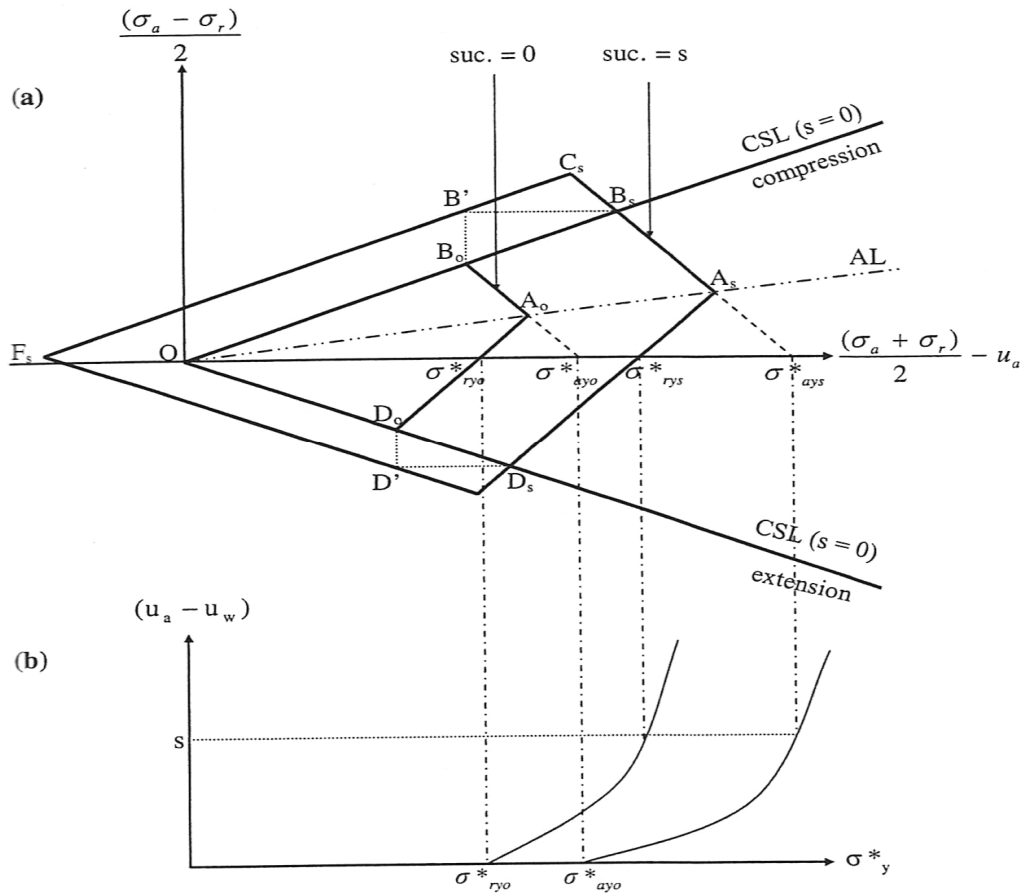


Figure 4.4. Description of Leroueil and Barbosa model (after Leroueil and Barbosa, 2000)

For partially saturated soil, the model considers that matric suction generates a resistance to slippage at the contacts between particles or aggregates. Its global effect should thus reflect the distribution of these contacts, and the anisotropy line (AL) should be the same as for the saturated soil. Then if soil in saturated condition has a yield curve such as  $OB_0A_0D_0$  in Figure 4.4a, is given suction should extend  $B_0A_0D_0$  to  $B_sA_sD_s$ , with increases in axial net yield stress from  $\sigma^*_{ay0}$  to  $\sigma^*_{ays}$  and in radial net yield stress from  $\sigma^*_{ry0}$  to  $\sigma^*_{rys}$ . The variation of the axial and radial yield stresses with suction defines two Loading-Collapse curves,  $LC_a$  and  $LC_r$  respectively, as depicted in Figure 4.4b. Leroueil and Barbosa (2000) showed that this idealised and approximate model well represents the behaviour of partly saturated isotropic or anisotropic soils.

Ghorbel and Lerouiel (2006) proposed a yield model, known as GFY-2 model, based on the GFY model proposed by Leroueil and Barbosa (2000) to relate the Loading-collapse (LC) curve to the soil-water characteristic curve and to the behaviour of soils in strength and volumetric changes within a generalized elasto-plastic model. The model takes into account the anisotropy and kinematic hardening and applies to saturated and unsaturated soils. GFY-2 model shows that the increase in axial and radial yield stresses depends on the water characteristic curve. The axial and radial modified net yield stresses determined by the experimental results on Ste-Rosalie clay as a function of matric suction are plotted in Figure 4.5, while the yielding points obtained on Ste-Rosalie clay from odometer and triaxial tests under certain matric suction are depicted in Figure 4.6. It is shown from the graph that the LC curve obtained from GFY-2 model well fit the experimental data points obtained at yielding. The behaviour in compression can be related to the shear strength behaviour, as demonstrated by Leroueil and Barbosa (2000) and both of them depend on the water characteristic curve.

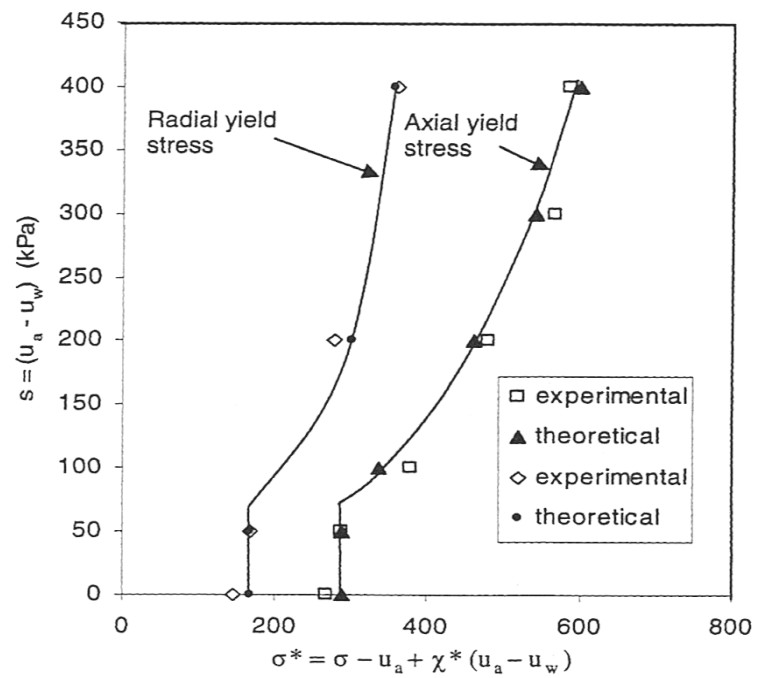


Figure 4.5. Lc curve of Rosalie clay (after Ghorbel and Lerouiel, 2006)

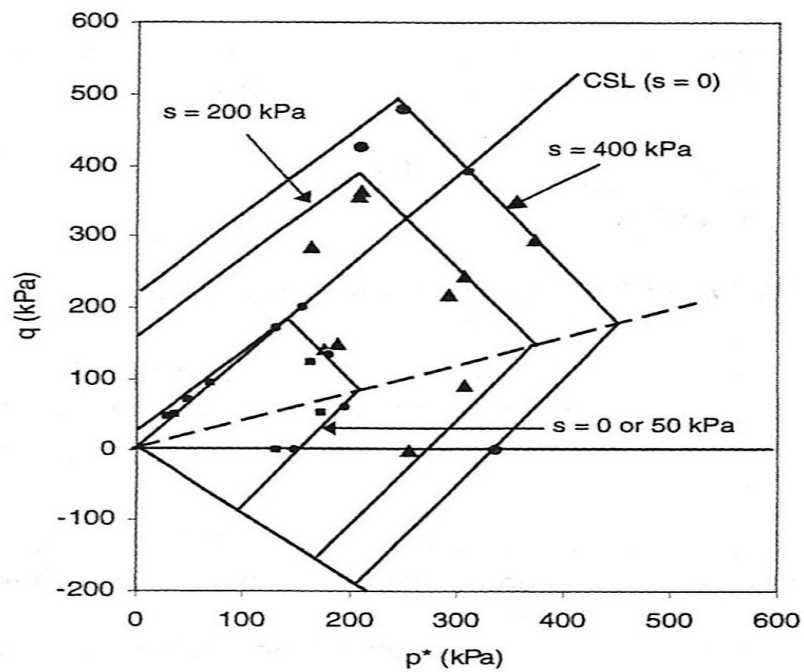


Figure 4.6. Yielding and GFY-2 of Rosalie curve  
(after Ghorbel and Lerouiel, 2006)



#### 4.2.3. Models for the prediction of shear strength

Several formulations have been proposed to study the shear strength of unsaturated soils. One of the most important modelling for predicting the shear strength of soils is reported by Fredlund et al (1995) who proposed to describe the shear strength of unsaturated soil at any suction as follows:

$$\tau_f = c' + (\sigma_n - u_a) \tan \Phi' + (u_a - u_w) \Theta^K \tan \Phi' \quad (4.1)$$

where  $c'$  is the effective cohesion,  $\Phi'$  is the effective friction angle of the saturated soils,  $(\sigma_n - u_a)$  is the net normal stress on the plane of failure at failure,  $(u_a - u_w)$  is the matrix suction,  $\kappa$  is a fitting parameter and  $\Theta$  is the normalized volumetric water content of the soils, which is defined as follows:

$$\Theta = \frac{\phi}{\phi_s} \quad (4.2)$$

in which  $\theta$  and  $\theta_s$  are the volumetric water contents at the considered suction and at saturation respectively.

Extending the same concept, a slightly different equation was proposed by Vanapalli et al (1996) for predicting the shear strength without using the fitting parameter  $\kappa$ . The equation is giving below:

$$\tau_f = c' + (\sigma_n - u_a) \tan \Phi' + (u_a - u_w) \left( \frac{\phi - \phi_r}{\phi_s - \phi_r} \right) \tan \Phi' \quad (4.3)$$

in which  $\theta_r$  is the residual volumetric water content.

### 4.3. Mechanical behaviour of partially saturated clay

The main features of the mechanical behaviour and failure of partially saturated clay will be reviewed and discussed in the following sub sequent.

#### 4.3.1. Stress state variables

There have been many argument about the stress state which partially saturated should take. Experimental results have shown that the soil properties measured so not yield a single valued relationship to the proposed effective stress. In other words, the soil property in the proposed effective stress equation has different magnitudes for different problems. There has been a tendency now to use the stress state variables for partially saturated soil in an independent manner. That is, adopting two independent stress state variables to describe the effective stress. Consideration of the contractile skin as an independent phase proposed by (Fredlund and Morgenstern, 1977) lends support to the theoretical justification for two independent stress state variables for partially saturated soil. Biot (1941) proposed a general theory of consolidation for unsaturated soil with occluded air bubbles.

The constitutive equations relating stress and strain were formulated in terms of effective stress,  $(\sigma - u_w)$ , and the pore water. Croney et al (1958) then proposed the following form of an effective stress equation for unsaturated soil:

$$\sigma' = \sigma - \beta u_w \quad (4.4)$$

in which  $\sigma'$  represents the effective normal stress,  $\sigma$  is the total normal stress,  $\beta$  is bonding factor, which is measured of the number of bonds under tension effective in contributing to the shear strength of soil, and  $u_w$  is pore water pressure. Bishop (1959) suggested a tentative expression for effective stress has gained widespread reference:

$$\sigma' = (\sigma - u_a) + X(u_a - u_w), \quad (4.5)$$

in which  $u_w$  represents pore air pressure and  $X$  is a parameter related to the degree of saturation of the soil.

A theoretical stress analysis of partially saturated soil on the basis of multi-phase continuum mechanics was demonstrated by Fredlund and Morgenstern (1977). The partially saturated soil was considered as a four system. The soil particles were assumed to be incompressible and the soil was treated as though it was chemically inert. These assumptions are consistent with those used in the saturated soil mechanics. The analysis concluded that any two of three possible normal stress variables can be used to describe the stress state of a partially saturated soil. The possible combinations of the stress state variables are (1)  $(\sigma - u_a)$  and  $(u_a - u_w)$ , (2)  $(\sigma - u_w)$  and  $(u_a - u_w)$ , and (3)  $(\sigma - u_a)$  and  $(\sigma - u_w)$ . The partially saturated soil equation was thus evolved:

$$\sigma' = (\sigma - u_a) + (u_a - u_w) \quad (4.6)$$

where  $(\sigma - u_a)$  is net normal stress and  $(u_a - u_w)$  is matric suction.

#### 4.3.2. Volume change

Partially saturated soil consists of two phases that are mobile, known as the air and the water phases. Upon the application of stress, the phases will come to equilibrium consequent to the dissipation of the pressures built up in the phases. This can be fulfilled by the actual flowing of the phases out of the soil body, which in turn constitutes volume change in soil. Soil particles are assumed not to undergo any deformation during loading and their size is large, therefore, the volume changes of partially saturated soil would be due to the migration and deformation of air and water. It has been found that there is no relationship

between volume change and effective stress for many partially saturated soils. Coleman (1962) point out that the volume change would be given by:

$$\frac{dV}{V} = C_1(du_w - du_a) + C_2(d\sigma_m - du_a) + C_3(d\sigma_1 - d\sigma_3), \quad (4.7)$$

where  $dV$  is change in the total volume,  $V$  is the total volume of soil,  $u_a$  is pore air pressure,  $u_w$  is pore water pressure,  $\sigma_1$  is major principle stress,  $\sigma_3$  is minor principle stress,  $C_1$ ,  $C_2$ ,  $C_3$ , are coefficient parameters and  $\sigma_m$  is mean total normal stress.

The stress versus deformation path of both stress state variables to be considered in an independent manner was pointed out by Bishop and Blight (1963), and hence, they proposed that volume change to be plotted against net normal stress and matric suction in three-dimensional space. The used of net normal stress,  $(\sigma - u_a)$  and matric suction,  $(u_a - u_w)$  as stress state variables for partially saturated soil was later presented by by Fredlund (1975) and Fredlund and Morgernstern (1977). The semi empirical constitutive relations for partially saturated soil using the two stress state variables, which was similar to those of proposed by Coleman (1962) was proposed by Fredlund and Morgernstern (1977). The stress and deformation state variables were combined using suitable constitutive relations for the soil structure, air phase, and water phase. The proposed constitutive relations were presented graphically to form constitutive surfaces by plotting the deformation state variables with respect to the two stress state variables.

The overall volume change of partially saturated soil can be defined as a change in void ratio in response to a change in the stress state (Fredlund and Morgernstern, 1976).

$$de = \frac{\partial e}{\partial(\sigma - u_a)} d(\sigma - u_a) + \frac{\partial e}{\partial(u_a - u_w)} d(u_a - u_w), \quad (4.8)$$

where  $e$  represents void ratio,  $\sigma$  is total normal confining stress,  $u_a$  is pore air pressure,  $u_w$ , and is pore water pressure.

Equation 4.8 can be viewed as having two parts, namely a part that is designation of the stress state (i.e., net normal stress,  $(\sigma - u_a)$  and matric suction,  $(u_a - u_w)$ ) and a part that is designation of the soil properties. The soil properties can be viewed as the slope of the void ratio constitutive surfaces as shown in Figure 4.7. The soil properties are moduli that vary as a function of the stress state. The moduli associated with the net normal stress,  $(\sigma - u_a)$  and matric suction,  $(u_a - u_w)$ . At a particular state, the compressibility modulus for the void ratio constitutive surface with respect to matric suction can be designated as a constant.

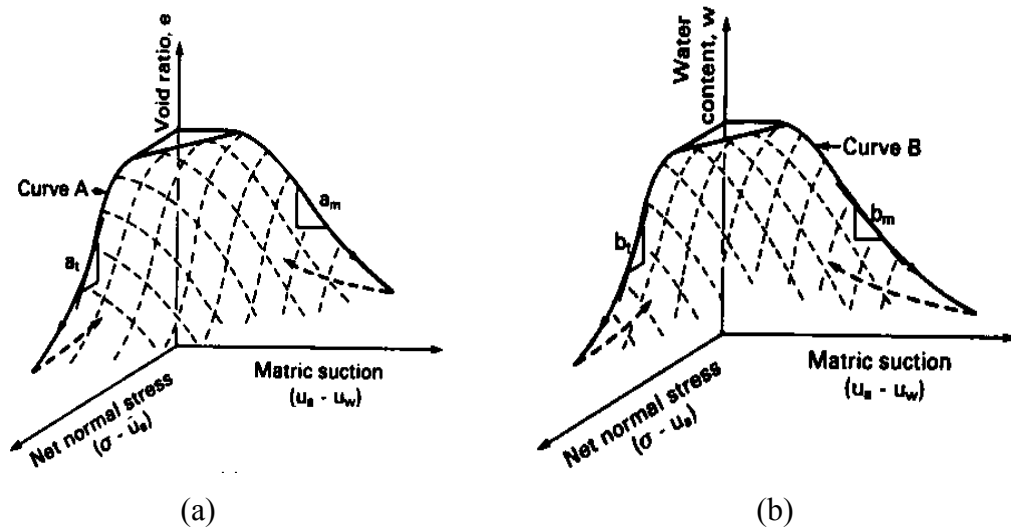


Figure 4.7. Three dimensional void ratio and water content constitutive surfaces for unsaturated soil: (a) void ratio constitutive surface; (b) water content constitutive surfaces (after Fredlund and Rahardjo, 1993)

A series of postulates have been provided for the estimation of the volume change constitutive surfaces for unsaturated soil for the case of monotonic loading

(Fredlund et al, 2000). The postulates will be summarised as follows:

- (1) Postulate 1: The overall volume change constitutive relationship require a primary reference condition determined by applying a net (isotropic) total stress loading of the soil with the pore-water and pore-air pressures maintained as zero, while measuring the change in void ratio
- (2) Postulate 2: The overall volume change constitutive relationship require a secondary reference condition determined by applying various soil suction to the soil with the net isotropic stress equal to zero, while measuring the change in void ratio
- (3) Postulate 2a: The relationship of void ratio versus soil suction can also be computed using the soil-water characteristic curve for the soil along with the shrinkage curve associated with the drying of a clay soil
- (4) Postulate 3: A unique volume change constitutive is defined for conditions of monotonic deformation (Figure 4.8).

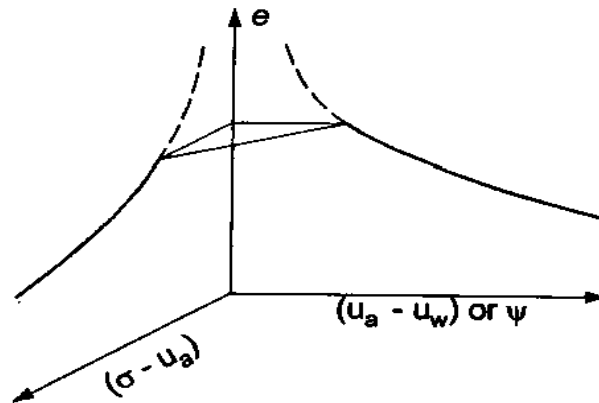


Figure 4.8. Three dimensional plot showing the primary and secondary reference condition for the void ratio constitutive surface (after Fredlund et al, 2000)

- (5) Postulate 4: As defined on the zero soil suction plane, the slope along any constant net total stress plane on the volume change constitutive surface is a function of the void ratio (Figure 4.9). In which  $(m_1^s)_{e_1}$  is coefficient of volume change with respect to a change in net normal stress at void ratio of  $e_1$ , while  $(m_2^s)_{e_1}$  is coefficient of volume change with respect to a change in matric suction

at void ratio of  $e_1$ . A more detail determination of these parameters will be discussed in the next section of 4.3.3. (ii).

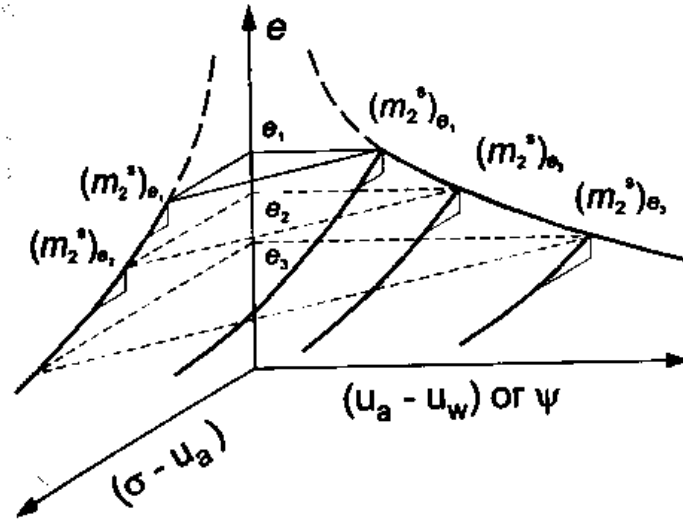


Figure 4.9. Illustration of the definition the void ratio constitutive surface based on the slopes of the primary reference curve (after Fredlund et al, 2000)

(6) Postulate 5: A one-to-one relationship between the effects of changes in net total stress and a change in soil suction is less than the air entry value of the soil (Figure 4.10).

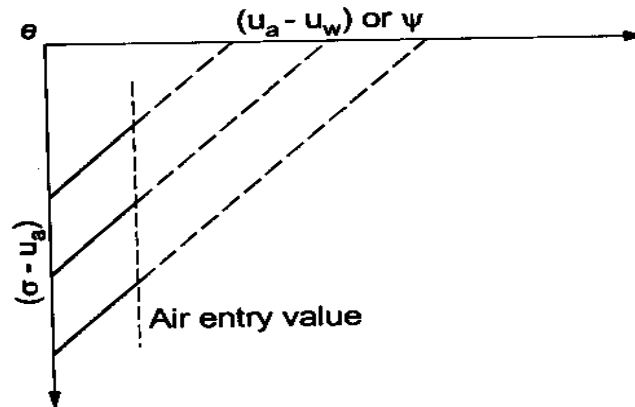


Figure 4.10. Variation of constant void ratio contours when the surface is viewed along the void ratio axis (after Fredlund et al, 2000)

(7) Postulate 5a: The soil air entry value can be assumed to be a constant for a first approximation, then for greater refinement, the air entry value may need to be defined as a function of void ratio or the net isotropic stress (Figure 4.11).

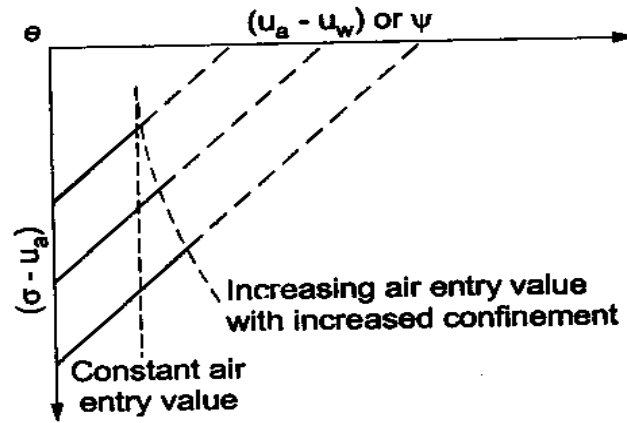


Figure 4.11. Effect of a variation in the air entry value on the void ratio contours  
(after Fredlund et al, 2000)

(8) Postulate 6: There is a gradual curve forms from the air entry value to the secondary reference condition, corresponding to a particular void ratio on the soil structure constitutive surface (Figure 4.12).

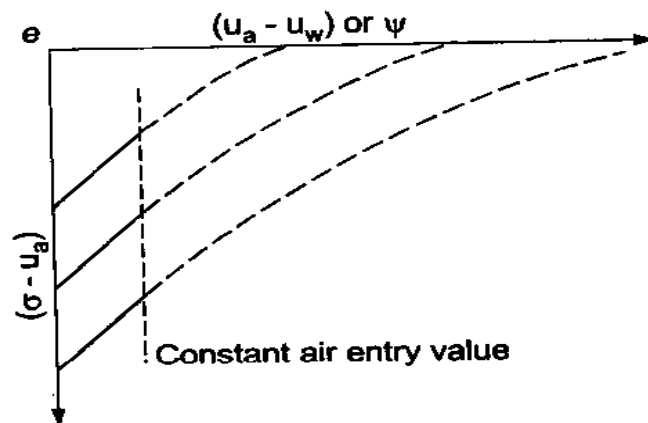


Figure 4.12. Variation of constant void ratio contours when the surface is viewed  
along the void ratio axis (after Fredlund et al, 2000)



### 4.3.3. Pore Pressure Parameters

#### *(i) Degree of saturation*

The degree of saturation, commonly expressed as a percentage, is defined as the ratio of the volume of water to the volume of voids. The degree of saturation effect on the permeability of soil with respect to water is highly significant. It has been found by Brooks and Coorey (1964) that a change in matric suction would produce a greater effect on the degree of saturation or water content than a change in the net normal stress. Due to the desaturation processes, air, which is introduced into the soil medium, becomes occluded when the degree of saturation is lowered to about 90 % (Matyas, 1967). Corey (1957) found that upon reaching 85 % of saturation, the air phase becomes continuous and air would flow through the soil as this stated. In contrast with the permeability of water, the permeability of air increases with decreasing the degree of saturation.

The degree of saturation of the partially saturated soil-rock  $S$  and its matric suction ( $u_a - u_w$ ) can vary as the soil-rock body is loaded. Thus, it would be necessary to keep track of these changes in parameters in all stages of loading. For instance, when brittle fracture takes place, the fracture toughness would depend on their ambient values. As a consequent, unlike the applied loading would not only raise the level of total stresses required to cause further crack extension, but also influence the properties of the medium which determined whether a crack would extend.

In determining the pore pressure parameters, the value of the degree of saturation  $S$  at any stage of net normal stress and matric suction may be obtained from the constitutive surfaces of void ratio  $e$  and water content  $w$  which are themselves obtained experimentally. The degree of saturation is required since the pore pressure parameters which are determined according to the following subparagraph depend on it. Following the procedure proposed by Fredlund and Rahardjo (1993) although adapted to plane strain condition (Lo, et al, 2005), the

pore pressure parameters may be deduced from the volumetric deformation coefficients  $C_t$   $C_m$   $D_t$   $D_m$ , which in turn, be determined experimentally in Chapter 6. According to the fundamental phase relationships of soil,

$$S = w \frac{G_s}{e} \quad (4.9)$$

in which  $G_s$  is the specific gravity of the soil.

### ***(ii) Pore Pressure Parameters***

The compression indices  $C_t$  and  $C_m$ , from which parameters  $B_a$  and  $B_w$  may be derived, have to be determined under plane strain loading condition. The pore pressure parameters  $D_a$  and  $D_w$  would likewise have to be determined in plane strain in principle, although with  $\sigma_1$  and  $\sigma_3 = 0$ . However, it may be readily that the parameters  $D_a$  and  $D_w$  are not independent of parameters  $B_a$  and  $B_w$ . Therefore  $B_a$  and  $B_w$  would together be sufficient to obtain the changes in pore pressure under generalised plane strain loading, where

$$B_a = \frac{R_2 R_3 - R_4}{1 - R_1 R_3}, \quad (4.10)$$

and

$$B_w = \frac{R_2 - R_1 R_4}{1 - R_1 R_3}, \quad (4.11)$$

in which

$$R_1 = \frac{R_s - 1 - [(1 - S + hS)n / (\bar{u}_a m_{1p}^s)]}{R_s + (SnC_w / m_{1p}^s)}, \quad (4.12)$$

$$R_2 = \frac{1}{R_s + (SnC_w / m_{1p}^s)}, \quad (4.13)$$

$$R_3 = \frac{R_a}{R_a - 1 - [(1 - S + hS)n / (\bar{u}_a (m_{1p}^s - m_{1p}^w))]} , \quad (4.14)$$

$$R_4 = \frac{1}{R_a - 1 - [(1 - S + hS)n / (\bar{u}_a (m_{1p}^s - m_{1p}^w))]} , \quad (4.15)$$

and

$$R_s = \frac{m_2^p}{m_{1p}^s} , \quad (4.16)$$

where

$$R_a = \frac{m_2^p - m_2^w}{m_{1p}^s - m_{1p}^w} , \quad (4.17)$$

$C_w$  is the water compressibility,  $h$  is the proportion of dissolved air in the water,  $\bar{u}_a$  is the absolute air pressure,  $n$  is the porosity and  $m_{1p}^s, m_2, m_{1p}$  and  $m_2$  are the volumetric deformation coefficients which may be evaluated from the compressive indices  $C_t$ ,  $C_m$ ,  $D_t$  and  $D_m$  obtained from laboratory testing in Chapter 6, as follows:

$$m_{1p}^s = \frac{0.435C_t}{(1 + e_0)(\sigma_{ave} - u_a)_{mean}} , \quad (4.18)$$

$$m_2^s = \frac{0.435C_m}{(1 + e_0)(u_a - u_w)_{mean}} , \quad (4.19)$$

$$m_{1p}^w = \frac{0.435D_t G_s}{(1 + e_0)(\sigma_{ave} - u_a)_{mean}} , \quad (4.20)$$

and

$$m_2^w = \frac{0.435D_m G_s}{(1 + e_0)(u_a - u_w)_{mean}} . \quad (4.21)$$

In which  $(\sigma_{ave} - u_a)_{mean}$  and  $(u_a - u_w)_{mean}$  are the averages of the initial and final net normal stresses and matric suction for increment. The subscript  $m$  on the

compression indices  $C_m$  (void ratio) and  $D_m$  (water content) are corresponding to matric suction, while the subscript  $t$  on the compression indices  $C_t$  and  $D_t$  are corresponding to net normal stress.

#### 4.3.4. Matric suction

The soil suction is an important part in the behaviour of partially saturated soil, especially in the volumetric deformation of the soil structure. Soil suction is actually a quantity of energy that signifies the capability of a soil to retain water. When free water migrates into a soil, the water will either be retained or adsorbed by the soil. To release the adsorbed water, external energy has to be applied to counteract the water retention forces. There are two components of total suction, namely osmotic suction, which is caused by the salt dissolved in the water and matric suction. In the absence of salt the relative humidity increases and therefore the total suction reduces to a value equal to the matric suction. The matric suction is known as a measure of the energy required to remove a water molecule from the soil matrix without changing state (Ridley, 1993). Matric suction is the dominant component compared to osmotic suction, therefore the emphasis will be on the former.

The direct method that can be used to determine the matric suction is to measure the pore water suction. The matric suction ( $u_a - u_w$ ) can be measured as the difference between the pore air pressure  $u_a$  and pore water pressure  $u_w$ , which are applied individually at the beginning of each loading stage. It is required in order to determine the fracture toughness of the soil-rock specimen. The pore pressures may be in turn be deduced from their respective pore pressure parameters  $B_a$ ,  $D_a$  and  $B_w$ ,  $D_w$  based on the following relationships:

$$du_a = B_a d\sigma_{ave} \quad (4.22)$$

and

$$du_w = B_w d\sigma_{ave} , \quad (4.23)$$

where the pore pressure parameters are determined according to sub sequent 4.3.3 and normal stress of

$$\sigma_{ave} = \frac{\sigma_1 + \sigma_3}{2} . \quad (4.24)$$

In the initial state of the soil-rock specimen, the degree of saturation  $S_0$ , and hence porosity  $n_0$  may be determined from the constitutive surfaces of subsequent Figure 4.9, Figure 6.19 and Figure 6.20, where the pore air pressure  $u_{a0}$  and the pore water pressure  $u_{w0}$  would be presetting of the test and the loading would be set at zero net normal stress, that is  $\sigma_1 = \sigma_3 = u_{a0}$ .

#### 4.4. Concluding remark

The review of the constitutive behaviour model for partially saturated clay at the first part of this chapter showed that although the importance of partially saturated soil has long been recognised, unified elasto-plastic constitutive models for partially saturated soil using the overall framework of critical state concept have only been initiated in the last decade (Alonso et al (1987, 1990); Fredlund et al (1995); Wheeler and Sivakumar (1995); Maatouk et al (1995); Cui and Delage (1996); Vanapalli et al (1996); Leroueil and Barbosa (2000); and Ghorbel and Lerouiel (2006)). The existing models for unsaturated soils can be divided into three categories. The first models are Barcelona type models, such as Barcelona Basic Model (BBM), which is the extension of MCC model and generally relating the compressibility of soils to the matric suction by Loading-Collapse curve. The second category is the physical models which apply to saturated and unsaturated soils, including the model proposed by Leroueil and Barbarosa (2000) known as

GFY-1 model, and GFY-2 model presented by Ghorbel and Leroueil (2006). The third category dealt with the prediction of shear strength of unsaturated soils presented by Fredlund et al (1995) and Vanapalli et al (1996).

The second part of this chapter concentrated on the main features of the mechanical properties of partially saturated soil. The four main features of mechanical properties of partially saturated soil had been presented, namely stress state variables, volume change, pore pressure parameter and matric suction. There has been a tendency now to use the stress state variables for partially saturated soil in an independent manner. The possible combinations of the stress state variables are (1) effective stress and matric suction, (2) net normal stress and matric suction, and (3) effective stress and net normal stress. The volume change of partially saturated soil can be related to net normal stress and matric suction, as there is no relationship between volume change and effective stress. In determining the pore pressure parameters, the value of the degree of saturation at any stage of net normal stress and matric suction be obtained from the constitutive surfaces of void ratio and water content.

## **CHAPTER 5**

### **FRACTURE MECHANICS APPROACH**

#### **5.1. Introduction**

The present modelling of soil is based on principles of continuum mechanics in spite of the fact that discontinuities are known to develop when such materials are subject to loading. However, in the case of strong rock, there has been considerable interest to account for such discontinuities using fracture mechanical approach (Ingraffea, 1987). Many studies have been conducted on detailed aspect of such discontinuities, but these are of limited practical application in an actual situation. The existence of cracks and fissures, which are the results of mechanical, thermal and volume-change-induced stresses, such soils are non uniform and therefore not amenable to analysis by continuum mechanics. On the other hand, fracture mechanical theory may be used to advantage to replicate their behaviour.

Atkinson and Bransby (1982) proposed the conventional failure criteria for soils which might be partly appropriate to yield-dominant behaviour, but not this category of brittle fracture. In practice, there is the possibility that soil behaves more like a brittle material. The soil ruptures suddenly under compressive loading like soft rock, starting from the weakest fracture in it. A basic premise of fracture theory is that crack like imperfections are inherent in engineering materials. These defects have the tendency to make stresses higher, which eventually trigger off

fractures when a material body is subjected to a critical load or undergoes damage under cyclic loading (Anderson, 2005).

The study on behaviour of stiff and hard soil which considered the discontinuities by the use of fracture mechanical theory had been attempted by many researchers since few decades ago. Among the researchers, Bishop (1967) and Skempton et al (1969) were the first ones to suggest that fracture mechanics concepts might shed light on the process of progressive failure of slopes made of stiff fissured clays. The principle of Linear Elastic Fracture Mechanics (LEFM) theory was applied by Vallejo (1985, 1986, 1987, 1988a, 1989) to investigate the failure mechanisms of stiff fissured kaolinite clay samples. Saada et al (1985) also employed concepts of LEFM concept to over consolidated brittle clays with a crack tested under a combination of normal and shear loads. An extensive laboratory tests on the mechanics of crack propagation in over consolidated clay samples were then also been conducted (Saada et al, 1994). Chudnovsky et al (1988) studied the propagation of cracks in clays under sliding type of loading using the crack layer theory.

In 1994 Lo and Tamiselvan published the unified model for fracture for the first time (Lo et al, 1996), which is a generalized of Irwin's stress intensity factor refers to the  $\theta_0$  plane to be applicable to the  $\theta$  plane. The analytical basis and experimental verification of this model were formally reported in 1996 (Lo et al, 1996) for pure mode stress intensity factor as well as mixed modes of deformation. Based on Modified Cam Clay model, Lo et al (2005) modelled an elasto-plastic shear fracture for hard soil-soft rock. This model employed linear elastic fracture mechanics (LEFM) as well as elastic plastic fracture mechanics (EPFM) and is applicable to the entire range of soils from normally consolidated to lightly over consolidated soil to stiff or hard soil like heavily over consolidated soil including soft rock as well as partially saturated soil accordingly and thereby provided a rational basis for the prediction of such soil behaviour.



A brief of basic concepts of fracture mechanical theory including the linear elastic fracture mechanical (LEFM) approach will firstly be reviewed then the use of fracture mechanical concept applied in stiff clay will be discussed. The detail of the unified model, which in turn this study is based on will then be presented, thereafter, the fracture mechanical approach of the present work will be set out.

## **5.2. A basic concept of fracture mechanics theory**

### **5.2.1. The pioneering work of Griffith (1920) and Irwin (1957)**

The founding of fracture mechanics is generally attributed to Griffith (1920), who deduced the critical rates of energy release,  $G_C$  as material constants for determining crack extension. Griffith (1920) formulated that the reduction in strain energy upon crack formation would transform into surface energy at the crack face. Furthermore, he showed that the surface energy of glass obtained from fracture testing was in good agreement with the surface energy of glass obtained by measuring its surface tension experimentally. However, Griffith's theory was considered to have limited application since it was applicable only to brittle materials such as glass, whereas most of the structural materials exhibit ductile properties during failure.

The next significant development to fracture mechanics was Irwin's (1957) quasi-brittle theory. He found that Griffith's theory would be applicable to most materials, if the surface energy were replaced by irreversible energy dissipated in a thin layer of plastic strain beneath the surface of the crack. Irwin proposed the energy release rate or crack driving force,  $G$ , as the total energy which released during cracking per unit increase in crack size. He also introduced another major advance, the concept of stress intensity factors  $K$  and showed that it related directly to Griffith's corresponding critical rates of energy release,  $G_C$ , according to which fracture occurs when critical stress distribution a head of the

crack tip is reached. These models by Irwin (1957) started the foundation of linear elastic fracture mechanics (LEFM).

### 5.2.2. Griffith energy balance

The model was developed by Griffith (1920) which recognized that fracture is associated with the balance of energy. Once a crack is propagated throughout a material, the extension of the crack resulted in the creation of new crack surface. New free surfaces are created at the faces of a crack, which increases the surface energy of the system. The Griffith energy balance for an incremental increase in the crack area,  $dA$ , under equilibrium conditions can be expressed as follows:

$$\frac{dE}{dA} = \frac{d\Pi}{dA} + \frac{dW_s}{dA} = 0 , \quad (5.1)$$

in which  $E$  is the total energy,  $\Pi$  is the potential energy that provided by strain energy and external forces and  $W_s$  is the work needed to create a new surface.

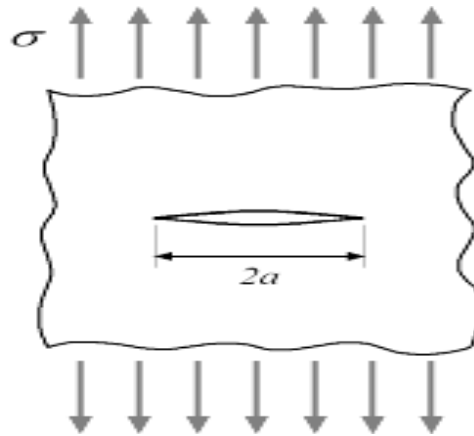


Figure 5.1. A through crack in an infinite plate under uniform tension (after Anderson, 2005)

For the crack infinite plate containing a crack of  $2a$ , with the width of  $> 2a$ , and the condition of plane stress is applied, shown in Figure 5.1, the stress analyses is given by Griffith as follows:

$$\Pi = \Pi_0 - \frac{\pi\sigma^2 a^2 B}{E}, \quad (5.2)$$

where  $\Pi_0$  is the potential energy of uncracked plate and  $B$  is the thickness of the plate. The creation of the two surfaces needs for a crack formation, so that

$$W_s = 4aB\gamma_s, \quad (5.3)$$

$\gamma_s$  is specific surface energy of the material, then:

$$-\frac{d\Pi}{dA} = \frac{\pi\sigma^2 a}{E}, \quad (5.4)$$

and

$$-\frac{dW}{dA} = 2\gamma_s. \quad (5.5)$$

Equating formula (5.4) and (5.5) results in

$$\sigma_f = \sqrt{\frac{2E\gamma_s}{\pi a}}. \quad (5.6)$$

in which  $\sigma$  is the applied plane stress and  $\sigma_f$  is the stress release.

### 5.2.3. Irwin energy release rate

An energy approach for fracture, known as energy release rate, that basically similar to the Griffith model was proposed by Irwin (1957). The energy release rate often denoted by  $G$  is the amount of energy, per unit length along the

crack edge that is supplied by the elastic energy in the body and by the loading system in creating the new fracture surface area, formulated as follows:

$$G = -\frac{d\Pi}{dA} . \quad (5.7)$$

$G$  is obtained from a potential crack extension force or crack driving force. Based on equation (5.4), for a wide plate in plane stress with the length crack of  $2a$ , shown in Figure 5.1, the energy release rate is given by:

$$G = \frac{\pi\sigma^2 a}{E} . \quad (5.8)$$

#### 5.2.4. Stress Intensity factor and fracture toughness

The stress intensity factor  $K$  is commonly expressed in terms of the applied stresses  $\sigma$  at  $r \rightarrow 0$  and  $\theta = 0$ . The stress fields near a crack tip of an isotropic linear elastic material can be expressed as a product of  $1/\sqrt{r}$  and a function of  $\theta$  with a scaling factor  $K$  in the following equations:

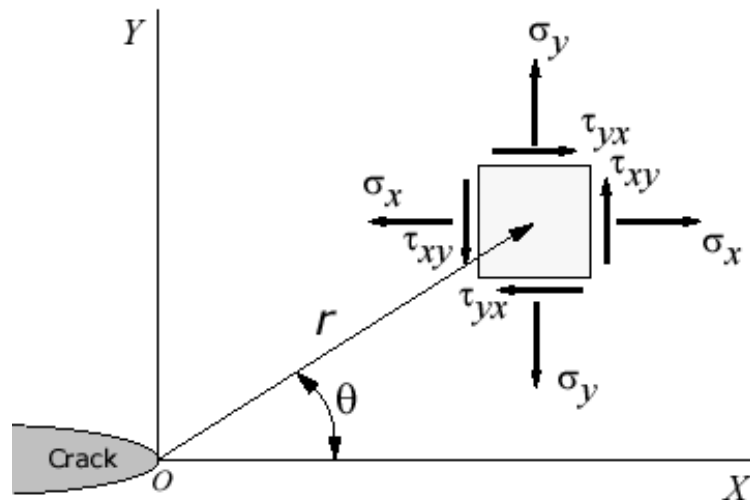


Figure 5.2. The stress fields near a crack tip (after Anderson, 2005)

$$\lim_{r \rightarrow 0} \sigma_{ij}^{(I)} = \frac{K_I}{\sqrt{2\pi r}} f_{ij}^{(I)}(\theta), \quad (5.9)$$

$$\lim_{r \rightarrow 0} \sigma_{ij}^{(II)} = \frac{K_{II}}{\sqrt{2\pi r}} f_{ij}^{(II)}(\theta), \quad (5.10)$$

and

$$\lim_{r \rightarrow 0} \sigma_{ij}^{(III)} = \frac{K_{III}}{\sqrt{2\pi r}} f_{ij}^{(III)}(\theta). \quad (5.11)$$

where  $r$ ,  $\theta$  and the cylindrical polar co-ordinates of a point with respect to the crack tip are shown in Figure 5.2. The superscripts and subscripts  $I$ ,  $II$ , and  $III$  denote the [three different modes](#) that different loadings may be applied to a crack as seen in Figure 5.3. Based on the Griffith analysis, the stress intensity factor can be express in term of:

$$K = \sigma \sqrt{\pi a} \cdot f(a/W), \quad (5.12)$$

in which  $f(a/W)$  is a dimensionless parameter obtained from the dimension of the specimen crack,  $W$  is the width of the plane and  $\sigma$  is remote applied stress.

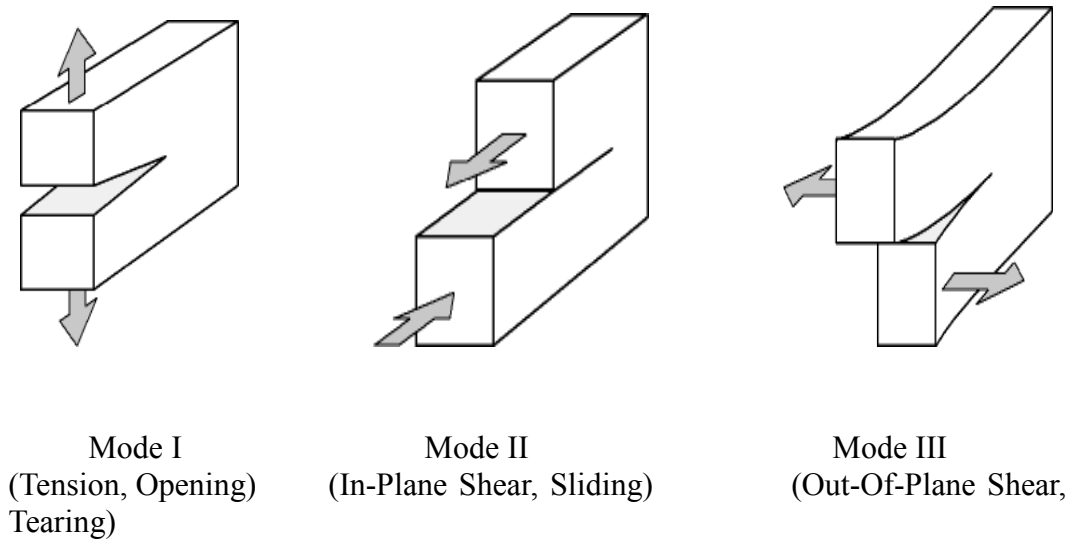


Figure 5.3. The three loading modes of a crack (after Broek, 1984)

In terms of the stress intensity factor there is relationship called the Irwin

relationship. There are two models for the stress intensity factor for plane stress and plane strain as follows.

(i) plane strain:

$$G = \frac{(1-\nu^2)}{E} K^2, \quad (5.13)$$

(ii) plane stress:

$$G = \frac{K^2}{E}, \quad (5.14)$$

where  $G$  is the energy release rate,  $\nu$  represents Poisson's Ratio,  $K$  is the stress intensity factor, and  $E$  is the modulus of elasticity.

Based on the linear theory the stresses at the crack tip are infinity however in reality there is always a plastic zone at the crack tip that limits the stresses to finite values. It is very difficult to model and calculate the actual stresses in the plastic zone and compare them to the maximum allowable stresses of the material to determine whether a crack is going to grow or not. An engineering approach is to perform a series of experiments and reach at a critical stress intensity factor  $K_c$  for each material, called the fracture toughness of the material. One can then determine the crack stability by comparing  $K$  and  $K_c$  directly.

#### **5.2.5. Linear elastic fracture mechanics (LEFM) concept**

Based on linear elasticity theories, the stress field near a crack tip is a function of the location, the loading conditions, and the geometry of the specimen or object (Anderson, 2005). In practice, engineers calculate the stress intensity factor,  $K$ , based on the stress field at the crack tip and compare it against the known fracture toughness of the material. The basic LEFM analysis can be outline as follows:

1. The crack tip stress field is a function of the location, loading, and geometry

$$\begin{aligned}\sigma_{ij}^{Tip} &\equiv \sigma_{ij}^{Tip} (Location, Loading, Geometri) \\ &\equiv \sigma_{ij}^{Tip} (r, \theta, K)\end{aligned}$$

where location can be represented by  $r$  and  $\theta$  using the polar coordinate system whereas the loading and geometry terms can be grouped into a single parameter *stress intensity factor*,  $K$ .

$$K \equiv K(\sigma^{Loading}, Geometri)$$

2. The fracture toughness of a material can be obtained by experiment. It is material specific.

$$\sigma_{ij}^{Toughness} \equiv \sigma_{ij}^{Toughness} (Material).$$

The stress intensity factor associated with the fracture toughness of the material is called the critical stress intensity factor  $K_c$  where  $K_c$  is material dependent.

$$K_c \equiv K_c (Material)$$

3. The stress intensity factor  $K$  should not exceed  $K_c$ :  $K < K_c$ .

### 5.3. Fracture mechanics theory applied in stiff clay

A fissure in clay is defined as small macroscopic surface of rupturing that divides an otherwise continuous material without separating it into units or blocks of intact material (Fookes and Denness, 1969). From an extensive literature review William and Jennings (1977) found that fissures in stiff clays can develop under the following circumstances: (1) as a result of consolidation process, (2) due to a decrease in overburden pressure during swelling of the clay, (3) as a result of syneresis, a colloidal phenomenon, (4) as a result of chemical reactions

in the clay which induce volumetric distortions with fissures forming, (5) as a result of tectonic stresses, (6) due to the dessication of clay, (7) the extension of fissures in bedrock into the clay layer and (8) due to large lateral stresses.

The fissures play a major role in the way geotechnical structures fail (Vallejo 1988b, 1993). Earlier, Gregory (1844) had already begun research on the relationship of the presence of fissure in stiff clays and the geotechnical properties of the materials. He found that the instability of slopes was directly related to the fissures in them. Terzaghi (1936) presented the first quantitative data on the role of fissures on the strength of clay from the study of instabilities of gentle slopes in fissure clay. Despite the high compressive strength of fissured clay, it was found that failures still occurred on the intact clay. Terzaghi (1936) establish that the overall strength of the fissured clays represented a fraction of the strength of the same clay without fissures.

Bishop (1967) and Skempton et al. (1967) were the first ones to suggest that fracture mechanics concepts might shed light on the process of progressive failure of slopes made of stiff fissured clays. Bjerrum (1967) discussed progressive failure in term of stress concentration at the tip of a slip surface. The observation that most landslides and foundation failures in over consolidated clay are concentrated in narrows zones (shear bands) which lies between region that appear hardly to deform and which are bounded at their distant edges, led Palmer and Rices (1973) to model a shear band as a crack and attempted to asses its propagation using the J-integral approach of fracture mechanics.

Covarrubias (1969) used the three modes of fracture described in figure 5.3 to interpret the propagation characteristics of cracks in cohesive materials forming part of earth dams. The propagation of the cracks was found by Covarrubias (1969) to be the result of tensile stresses normal to the plane of the cracks (mode I type of loading). Lee et al. (1988), Fang et al. (1989), and Morris et al (1992) have also used LEFM theory to analyze the crack propagation in soils as a result of tensile stresses.



Vallejo (1985, 1986, 1987, 1988, 1989) also used the principle of LEFM theory to interpret the failure mechanisms of stiff fissured kaolinite clay samples subjected to compression and direct shear stress condition. Failure was the result of stress concentration induced by the tips of the fissures. These stress concentrations caused the propagation and interaction of the fissures in the clay samples. The fissures in the samples were subjected to a combination of normal and shear stresses (mode I plus mode II type of loading). Saada et al (1985) also applied concepts of LEFM theory to over consolidated brittle clays with a crack tested under a combination of normal and shear loads, and used a stability criterion to predict failure of infinite slopes. Chudnovsky et al (1988) studied the propagation of cracks in clays under mode II type of loading using the crack layer theory. More recently, Saada et al (1994) has conducted extensive laboratory tests on the mechanics of crack propagation in over consolidated and consolidation as well as the degree of anisotropy of the clay samples had an effect on the way the cracks propagated in the clay samples.

The analysis of crack kink (Cotterell and Rice, 1980; Hayashi and Nemat-Nasser, 1981) apparently evolved out of a reaction to the lack consensus in traditional fracture mechanics, particularly with regard to the need to determine non self-similar crack extension. Accordingly, whereas the notion of an Irwin-type stress intensity factors (which is referred to the current crack plane) is maintained as the basis for determining crack extension, it is, in contrast with the traditional approach, applied to both self-similar and non self-similar crack extension. However, the closure analysis of a non self-similar crack extension becomes unnecessarily elaborated, in that it is necessary to provide an a priori kinked branch crack, thereby distinguishing it from that of a self-similar crack extension, which according to Irwin effectively takes place directly from the existing crack tip.

Lo et al (2005) proposed an elasto-plastic shear fracture approach to the constitutive behaviour of soil and soft rock. The model took up from where

Hvorslev-Modified Cam Clay (MCC) model leaves off, which is at the onset of localized shear banding. This model dealt with four distinct states of soil failure and their related stress-strain behaviour. This model gives a rational basis for the prediction of such soil behaviour and applicable to the entire range of soils from normally consolidated to lightly over consolidated soil, which is a wet soil like marine clay, to stiff or hard soil like heavily over consolidated soil including soft rock as well as partially saturated soil.

#### 5.4. The Unified Model

The *unified model* which essentially is a natural extension as well as generalization of Irwin's approach was first developed by Lo and Tamiselvan in 1994. The analytical basis and experimental verification of this model were formally reported in 1996 (Lo et al, 1996) for pure mode stress intensity factor as well as mixed modes of deformation. By applying Weierstrass' (Belding and Mitchell, 1991) limiting condition to the rate of energy release  $G$ , in the closure analysis of a small crack extension in the generalised  $\theta$  direction, the problem of non self-similar crack extension was solved exactly on the basis of the near field stresses of the existing crack tip, contrary to the requirement of crack kink analysis. In doing so the unified pure mode stress intensity factor  $K_I$  and  $K_{II}$  were derived consistently and shown to contain the same expression as the earlier proposal for  $K_{I\theta}$  and  $K_{II\theta}$ .

According to the unified model (Lo et al, 1996), the closure analysis of the crack extension in Figure 5.4, which is oriented in the generalised  $\theta$  direction and subjected to mixed mode I and II loading for which

$$G_0 = \frac{1}{\partial a} \int_0^{\partial a} [\sigma_{00}(r, \theta) u'_{00}(\partial ar, -\pi) + \tau_{r\theta}(r, \theta) u'_{rr}(\partial ar, -\pi)] dr, \quad (5.15)$$

in which  $G_0$  is the mix mode rate of energy release in the  $\theta$  plane,  $a$  the pre-crack length,  $\theta$  the direction of the plane of interest with respect to pre-crack plane,

$\theta_0 = 0$  and  $u'_{\theta\theta}$  and  $u'_{rr}$  the circumferential and radial displacements in polar coordinates respectively.

Irwin (1958) deducted  $K_{I0}$  and  $K_{II0}$  as:

$$K_{I0} = \sigma \sqrt{2\pi a} \quad , \quad (5.16)$$

$$K_{H0} = \tau \sqrt{2\pi a} \quad . \quad (5.17)$$

Notes : notation referred to crack  
extension tip is primed;  
e.g.  $r' = r - \delta a$  when  $\theta' = 0$

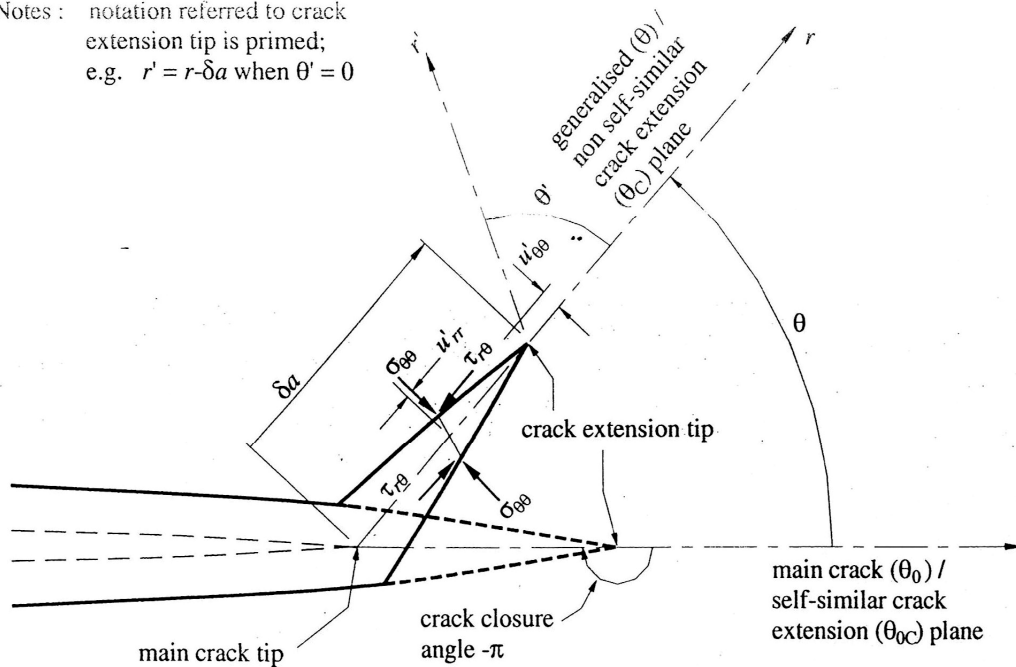


Figure 5.4. Closure parameter of a crack tip (after Lo et al, 1996)

Based on Westergaards's (1939) stress function, Irwin (1958) expressed the stress and displacement in the near field of a crack tip in an otherwise a continuous body shown in Figure 5.4, for  $\theta_0 = 0$  as:

$$\sigma_{\theta\theta}\sqrt{2\pi r} = K_{I0} \ , \quad (5.18)$$

$$\tau_{r\theta} \sqrt{2\pi r} = K_{II0} , \quad (5.19)$$

Substituting the expressions given by Irwin (1958) for  $\sigma_{\theta\theta}$ ,  $u'_{00}$ ,  $\tau_{r\theta}$  and  $u'_{rr}$  in equation (5.15) would result in:

$$G_0 = \frac{1}{\partial a} \int_0^{\partial a} \left[ \frac{K_{I\theta}}{\sqrt{2\pi r}} \frac{(1+\nu)(1+\kappa)}{4} \sqrt{\frac{\partial a - r}{2\pi}} K_I' + \frac{K_{II\theta}}{\sqrt{2\pi r}} \frac{(1+\nu)(1+\kappa)}{4} \sqrt{\frac{\partial a - r}{2\pi}} K_{II}' \right] dr , \quad (5.20)$$

in which  $\nu$  is Poisson's ratio and  $\kappa$  known function of  $\nu$ . In view of equation (5.18) and (5.19),  $K_{I0}$  and  $K_{II0}$  would represent the mode I and mode II stress intensity factors corresponding to the generalised  $\theta$  plane, given as:

$$K_{I\theta} = \lim_{r \rightarrow 0} \sigma_{\theta\theta} \sqrt{2\pi r} = K_I \cos^3 \frac{\theta}{2} - K_{II} \sin \frac{\theta}{2} \cos^2 \frac{\theta}{2} , \quad (5.21)$$

and

$$K_{II\theta} = \lim_{r \rightarrow 0} \tau_{r\theta} \sqrt{2\pi r} = K_I \sin \frac{\theta}{2} \cos^2 \frac{\theta}{2} + K_{II} \cos \frac{\theta}{2} (1 - 3 \sin^2 \frac{\theta}{2}) , \quad (5.22)$$

rather than Irwin's  $K_{I0}$  and  $K_{II0}$  which pertain to the  $\theta_{0C}$  plane only, while

$$K_I' = \lim_{(r-\partial a) \rightarrow 0} \sigma_{\theta\theta} \sqrt{2\pi(r-\partial a)} , \quad (5.23)$$

and

$$K_{II}' = \lim_{(r-\partial a) \rightarrow 0} \tau_{r\theta} \sqrt{2\pi(r-\partial a)} , \quad (5.24)$$

also similar as in the traditional analysis of the  $\theta_{0C}$  plane, although now referred to generalised  $\theta$  plane. It can be seen that  $K_{I0}$  and  $K_{II0}$  are the counter parts in generalised  $\theta$  plane and therefore a necessary condition would be that  $\theta_0 = 0$ ,  $K_{I\theta} = K_I$  and  $K_{II\theta} = K_{II}$ . As indicated earlier, it would be more appropriate to

refer as  $K_{I\theta}$  and  $K_{II\theta}$  specifically to the  $\theta$  plane, rather than  $K_I$  and  $K_{II}$ . Since  $K_I' = K_{I\theta}$  and  $K_{II}' = K_{II\theta}$  when  $\partial a \longrightarrow 0$ , the energy release in the  $\theta_C$  plane would be

$$G_c = (K_{I\theta}^2 + K_{II\theta}^2) \frac{(1+\nu)(1+\kappa)}{4E}, \quad (5.25)$$

in which  $E$  represents Young's modulus. As in the case of Irwin's (1958) analysis of mode I crack extension along the generalised  $\theta_C$  plane  $K_{II\theta} = 0$ ,  $K_{I\theta} \longrightarrow K_{IC}$  as  $G_\theta \longrightarrow G_{IC}$ , the pure mode I energy release in the  $\theta_C$  plane would be

$$G_{Ic} = (K_{IC}^2) \frac{(1+\nu)(1+\kappa)}{4E}. \quad (5.26)$$

Likewise, for pure mode II crack extension along the generalised  $\theta_C$  plane  $K_{I\theta} = 0$ ,  $K_{II\theta} \longrightarrow K_{IIC}$  as  $G_\theta \longrightarrow G_{IIC}$ , so that the pure mode II energy release would be

$$G_{IIc} = (K_{IIC}^2) \frac{(1+\nu)(1+\kappa)}{4E}. \quad (5.27)$$

The fundamental physical requirement as specified by equation (5.26) and (5.27) should be applicable to any  $\theta_C$  plane in an isotropic, homogeneous medium by employing the unified stress intensity factors as defined by equation (5.21) and (5.22).

## **5.5. Behaviour of partially saturated clay using fracture mechanics approach**

Partially saturated soil is normally considered as a three-phase system, there are soil solids, water (fluid), and air (gas). The degree of saturation of the partially saturated soil-rock  $S$  and its matric suction ( $u_a - u_w$ ) can vary as the soil-rock body is loaded. Thus, it would be necessary to keep track of these changes in parameters in all stages of loading. For instance, when brittle fracture takes place, the fracture toughness would depend on their ambient values (Lo et al, 2005). As a consequent, unlike the applied loading would not only raise the level of total stresses required to cause further crack extension, but also influence the properties of the medium which determined whether a crack would extend. Based on the above consideration, a fracture mechanical approach for the partially saturated clay will be presented in the following discussion.

In the determination of degree of saturation, pore pressure and matric suction will be based on the procedure proposed by Fredlund and Rahardjo (1993) although adapted to plane strain condition, while in the determination of fracture toughness and fracture criteria will be based on the elasto plastic shear fracture model (Lo et al, 2005) and the unified model (Lo, et al. 1996) and Lo (2001) as the basis of analysing how a crack would develop in this situation.

### **5.5.1. Determination of degree of saturation and pore pressure parameter**

The value of the degree of saturation  $S$  at any stage of net normal stress and matric suction would be obtained from the constitutive surfaces of void ratio  $e$  and water content  $w$  which are themselves obtained experimentally. The degree of saturation is determined according to the equation (4.9) in the sub sequent 4.3.3.

The pore pressure parameters may be deduced from the volumetric

deformation coefficients  $C_t$ ,  $C_m$ ,  $D_t$ ,  $D_m$ . As shown in Figure 6.19 and Figure 6.20, the compression indices  $C_t$  and  $C_m$  from which parameter  $B_a$  and  $B_w$  be determined according to the equation (4.10) and (4.11) respectively, have to be determined under biaxial loading conditions. The pore pressure parameters  $D_a$  and  $D_w$  would likewise have to be determined in plane strain in principle, although with  $\varepsilon_z = 0$ .

### 5.5.2 Determination of matric suction

The matric suction  $(u_a - u_w)$  can be measured as the difference between the pore air pressure  $u_a$  and pore water pressure  $u_w$ , which are applied individually at the beginning of each loading stage. It is required to determine the fracture toughness of the soil-rock specimen. The pore pressures may be in turn be deduced from their respective pore pressure parameters  $B_a$ ,  $D_a$  and  $B_w$ ,  $D_w$  based on the equation (4.22) and (4.23).

### 5.5.3. Determination of fracture toughness

It is necessary to obtain an update on the value of the fracture toughness  $K_c$ , at any given stage of crack developments, which is generally dependant on the matric suction, or alternatively the degree of saturation of the soil medium by way of the pore size distribution index  $\lambda$ . It is noteworthy that this dependency may be established fundamentally on the basis of Griffith's analogy of the critical rate of energy release  $G_c$  and the surface tension  $\gamma$  for glass, in which it may be shown that a relationship may be obtained between  $G_c$ , the matric suction  $(u_a - u_w)$  and characteristic pore size  $D_p$ , given by:

$$G_c = k \frac{(u_a - u_w) D_p}{4}, \quad (5.28)$$

where  $k$  is a parameter which reflects the mode of fracture. The pore size is

related to the pore distribution index, which depends on the effective degree of saturation  $S_e$  and matric suction. Accordingly, it may be shown that  $K_{Ic}$  depends directly on matric suction  $(u_a - u_w)$ . Hence, a relationship exists between the mode I fracture toughness,  $K_{Ic}$  and the matric suction.

In view of the preceding consideration, for a complete specification of the fracture model, the fracture toughness  $K_{Ic}$  would have to be determined a priori by laboratory testing at various value of matric suction  $(u_a - u_w)$  of specimens of the soil adopted as deal with in 4.3 of subsequent Chapter 4.

#### **5.5.4. Fracture criteria**

##### **5.5.4.1. An earlier solution of Brittle soil under compressive loading**

To solve the problem of brittle soil fracture under compressive loading, the following approach was suggested by Vallejo (1988). A crack may be subjected to the generalised stress pattern of Figure 5.5 (a) or it may be set at some angle to the biaxial principle stress system shown in Figure 5.5 (b). It may be deduced that the two configurations are interchangeable. Hence, it would be sufficient to address the problem of the fracture of an inclined crack subjected to a biaxial stress system on the basis of Figure.5.6.(a).

Various criteria have been proposed in traditional fracture mechanics to determine the direction under pure as well as mixed mode loading. The most commonly adopted appears to have been the maximum tangential stress criterion developed by Erdogan and Sih (1963). Accordingly, under mixed mode loading, crack extension would take place in a brittle material in some radial direction from the parent crack tip which is normal to that of the maximum tangential stress  $\sigma_{\theta_{\max}}$ . The maximum tangential criterion predicts that the direction of crack extention  $\alpha$  maybe obtained from the relationship



$$K_{I0} \sin \alpha + K_{II0} (3 \cos \alpha - 1) = 0 , \quad (5.28)$$

in which  $K_{I0}$  and  $K_{II0}$  are the respective modes I and II stress intensity factor which are specific to a particular boundary value problem.

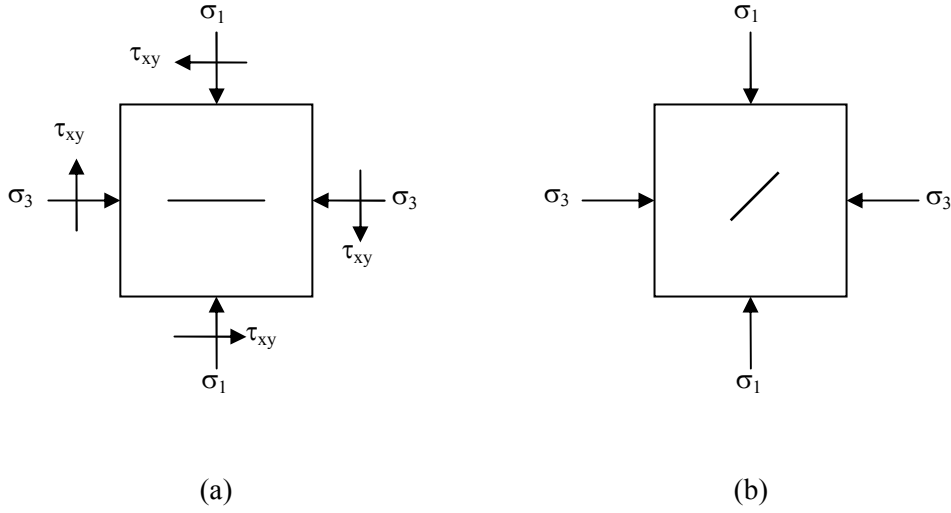


Figure 5.5. (a). Horizontal crack subjected to generalised stress system.  
(b). Inclined crack subjected to biaxial compressive loading (After Vallejo, 1988)

Consider the uniaxial loading case of Figure 5.6 (b). The state of stress in the near field of the crack tip would be given by the expression:

$$\begin{bmatrix} \sigma_r \\ \sigma_\theta \\ \tau_{r\theta} \end{bmatrix} = \frac{K_{I0}}{\sqrt{2\pi r}} \begin{bmatrix} \cos \frac{\theta}{2} (1 + \sin^2 \frac{\theta}{2}) \\ \cos^3 \frac{\theta}{2} \\ \sin \frac{\theta}{2} \cos^2 \frac{\theta}{2} \end{bmatrix} + \frac{K_{II0}}{\sqrt{2\pi r}} \begin{bmatrix} \sin \frac{\theta}{2} (1 - 3 \sin^2 \frac{\theta}{2}) \\ -3 \sin \frac{\theta}{2} \cos^2 \frac{\theta}{2} \\ \cos \frac{\theta}{2} (1 - 3 \sin^2 \frac{\theta}{2}) \end{bmatrix}. \quad (5.29)$$

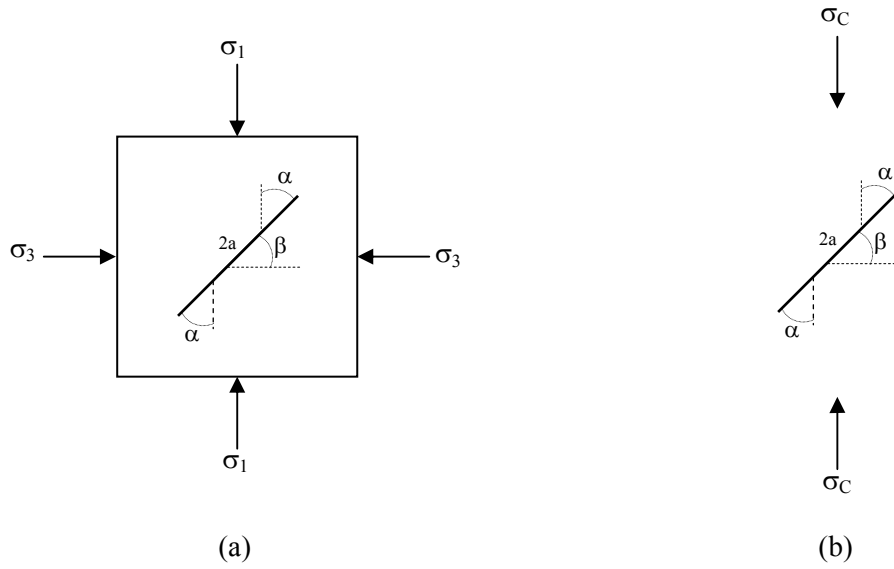


Figure 5.6. (a). Inclined crack subjected to biaxial compressive loading.  
 (b). Inclined crack subjected to uniaxial compressive loading in infinite  
 (After Vallejo, 1988)

For the case of an infinite plate containing an inclined crack under compressive loading,  $K_{I0}$  and  $K_{II0}$  may be expressed as

$$K_{I0} = \sigma \sqrt{\pi a} \sin^2 \beta \quad (5.30)$$

$$K_{II0} = \sigma \sqrt{\pi a} \sin \beta \cos \beta \quad (5.31)$$

in which  $a$  is one-half the length of the crack. Hence, substituting equation (5.30) and (5.31) in equation (5.28), it may be shown that

$$\tan \beta \sin \alpha + (3 \cos \alpha - 1) = 0 \quad (5.32)$$

Two possible solutions of  $\alpha$  in any given value of  $\beta$ , in which  $0 \leq \beta \leq \pi/2$ . The variation of crack extension angle  $\alpha$  with pre-crack angle  $\beta$ , when the applied stress is compressive and the tangential near field stress of the parent crack trip is positive. Since the crack would extend when the maximum

tangential stress reached its critical value, it would follow from equation (5.28) that

$$\sigma_{crit} = \frac{K_{I0}}{\sqrt{2\pi r}} \cos^3 \frac{\alpha}{2} - \frac{K_{II0}}{\sqrt{2\pi r}} 3 \sin \frac{\alpha}{2} \cos^2 \frac{\alpha}{2}, \quad (5.33)$$

where the value of  $K_{I0}$  and  $K_{II0}$  would then correspond to the critical state of crack extension. Thus, for the particular case shown in Figure 5.6 (a), substituting  $K_{I0}$  and  $K_{II0}$  of equations (5.30) and (5.31) into equation (5.32) when  $\sigma = \sigma_{crit}$  would result in

$$\sigma_{crit} = \sigma \sqrt{\frac{a}{2r}} \sin \beta \cos^2 \frac{\alpha}{2} \left[ \sin \beta \cos \frac{\alpha}{2} - 3 \sin \frac{\alpha}{2} \cos \beta \right]. \quad (5.34)$$

#### 5.5.4.2. Analysis of brittle soil fracture under biaxial compression

##### *(i) Special consideration of soil behaviour*

In view of the preceding consideration, the maximum tangential stress criterion has two components,  $K_{I0}$  and  $K_{II0}$ , both of which are the results of the developments of a stress singularity at the crack tip. According to Irwin (1957), a crack in a body may be defined as a line across which the displacement fields exhibits a discontinuity. The stress intensity factor is evaluated directly on the basis of the displacements computed at the crack tip element, which in the case of would have to take account the development of frictional resistance at the crack tip. In contrast with non-particulate materials, shear resistance play an important role in soil behaviour when slip occurs along a crack surface and must be considered when crack behaviour is analysed.

Based on the above discussion, when a crack is located in compressive stress field, two following condition would apply. Firstly, the compressed crack

surface would deform in the normal direction without giving rise to displacement discontinuity. As a consequent, no singularity would develop in the near stress field of the crack tip and hence  $K_{I0} = 0$  there. Secondly, in the tangential direction, frictional stresses could develop on crack surface because of the normal stress along their line of contact. If a shear stress were applied at the same time and the available resistance exceeded, the crack surfaces would start to slip relative to each other. A displacement discontinuity would then develop which would result in a  $K_{II0}$  value than zero and the possibility of crack extension

***(ii) Brittle fracture of partially saturated clay***

In the following discussion, the unified model (Lo, et al. 1996a) and Lo (2001) will be used as the basis of analysing how a crack would develop in this situation. The plane strain problem of a crack of length  $2a$  which is subjected to biaxial compression loading shown in figure 3.6.(b). The crack forms an angle of  $\beta$  to the horizontal direction. Hence, the normal and shear stresses along the crack interface would be given by

$$\sigma_{\beta} = \frac{\sigma_1 + \sigma_3}{2} + \frac{\sigma_1 - \sigma_3}{2} \cos 2\beta, \quad (5.35)$$

and

$$\tau_{\beta} = \frac{\sigma_1 - \sigma_3}{2} \sin 2\beta, \quad (5.36)$$

in which compressive stresses are taken to be positive, provided that there is no relative displacement of the crack face at the interface of the crack, otherwise,  $\tau_{\beta}$  would be equal to the shear resistance of the interface.

It is evident that  $\sigma_{\beta}$  would always be compressive as long as  $\sigma_1$  and  $\sigma_3$  were likewise compressive, which is the case in the laboratory testing of soil when the pre-crack is small compared to the overall specimen. Under such loading, the

normal compressive stress  $\sigma_\beta$  along the crack surface would cause the crack to close, so that  $K_{I0} = 0$  and would not contribute to the stresses in the near field of the trip. That is to say that  $K_{I0} = 0$  would not play a part in the crack extension, which would leave only  $K_{II0}$  to activate extension, although  $K_{II0}$  would also be zero if the shear resistance due to friction were higher than the shear stress along the crack face.

Due to the compressive and shear stresses along the crack surface,  $K_{I0} = 0$  and  $K_{II0} > 0$  provided that  $0 \leq \beta \leq 90^\circ$  and  $\sigma_1 \geq \sigma_3$  respectively; otherwise  $K_{II0}$  would be less than zero. Hence, on the generalised  $\theta$  plane, the corresponding modes I and II stress intensity factors would be given by

$$K_{I0} = -3K_{II0} \sin \frac{\theta}{2} \cos^2 \frac{\theta}{2} \quad (5.37)$$

and

$$K_{II0} = K_{II0} \cos \frac{\theta}{2} \left( 1 - 3 \sin^2 \frac{\theta}{2} \right) \quad (5.38)$$

Let the  $K_{CR} = K_{IC} / K_{IIC}$ , then the tendency to fracture may be expressed in term of

$$\begin{aligned} \left( \frac{K_{I\theta}}{K_{IC}} \right)^2 + \left( \frac{K_{II\theta}}{K_{IIC}} \right)^2 &= \left( \frac{-3K_{II0} \sin \frac{\theta}{2} \cos^2 \frac{\theta}{2}}{K_{IC}} \right)^2 + \left( \frac{K_{II0} \cos \frac{\theta}{2} (1 - 3 \sin^2 \frac{\theta}{2})}{K_{IIC}} \right)^2 \\ &= \frac{K_{II0}^2}{K_{IC}^2} f(\theta) \end{aligned} \quad (5.39)$$

where

$$f(\theta) = \left( -3 \sin \frac{\theta}{2} \cos^2 \frac{\theta}{2} \right)^2 + K_{CR}^2 \left( \cos \frac{\theta}{2} (1 - 3 \sin^2 \frac{\theta}{2}) \right)^2 \quad (5.40)$$

For a given boundary value problem and material properties represented by  $K_{II0}$ ,  $K_{IC}$  and  $K_{CR}$ , the angle where the crack would most readily extend may be

determined from Figure 5.7. in which  $\theta$  is angle to parent crack plane and  $n$  is defined as  $K_{IIc}/K_{IC}$ .

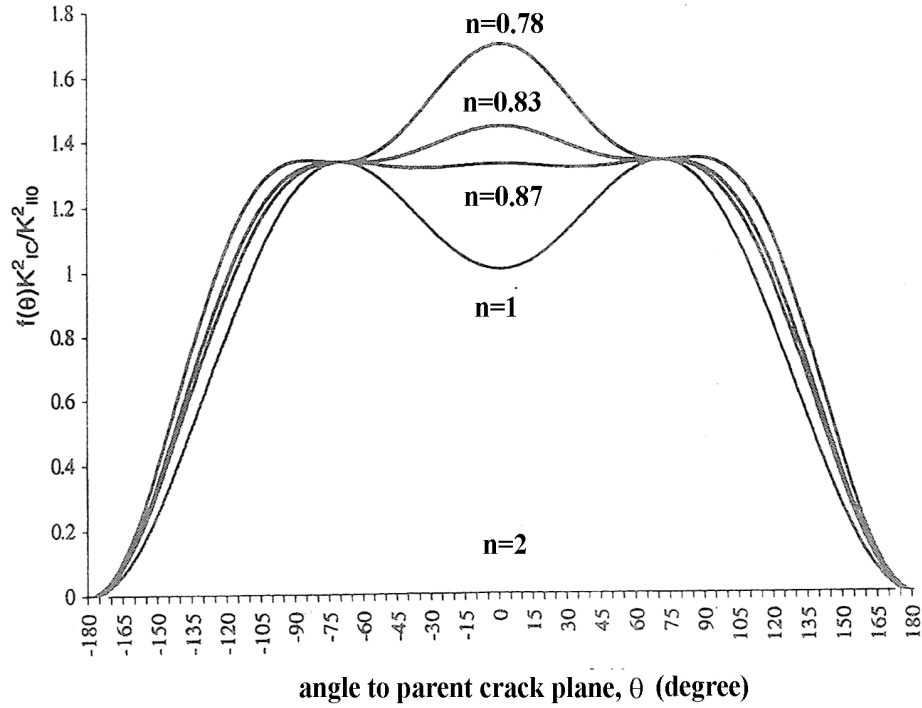


Figure 5.7.  $f(\theta)$  versus angle to parent crack plane around the crack tip  
(after Lo, 2001)

It shown from the graph that  $f(\theta)$  would attain the maximum value of  $1.33 K_{II0}^2 / K_{IC}^2$  at either  $\theta=70.5^\circ$  or  $\theta=-70.5^\circ$  when  $K_{IIc} > 0.87 K_{IC}$ . When  $\theta=70.5^\circ$ ,  $K_{I0}$  is negative, which means that the stress at this stage would be compressive and it would be impossible for the crack to extend. On the other hand, it would be easier for the crack to extend along  $\theta=-70.5^\circ$ , under pure mode II loading at the crack tip. In this case,  $1.33 K_{II0}^2 / K_{IC}^2 = 1$ , therefore, for the kaolin clay to fracture under pure mode II loading at the crack tip

$$K_{II0} = \frac{K_{IC}}{1.15} \quad (5.41)$$

**(iii) Fracture envelope of brittle soil for the case of compressive along the crack surface**

For a pre crack which is significantly smaller than the length of the soil specimen, in view of equations (5.30) and (5.35)

$$\frac{K_{I0}}{\sqrt{\pi a}} = -\sigma_\beta = -\frac{\sigma_1 + \sigma_3}{2} - \frac{\sigma_1 - \sigma_3}{2} \cos 2\beta \quad (5.42)$$

when  $\sigma_\beta$  is tensile, while  $K_{I0} = 0$ , when  $\sigma_\beta$  is compressive along the crack surface. Similarly, in view of equations (5.31) and (5.36)

$$\frac{K_{II0}}{\sqrt{\pi a}} = \tau_\beta - \sigma_\beta \mu = \frac{\sigma_1 - \sigma_3}{2} \sin 2\beta - \left( \frac{\sigma_1 + \sigma_3}{2} + \frac{\sigma_1 - \sigma_3}{2} \cos 2\beta \right) \mu, \quad (5.43)$$

where  $\mu$  is coefficient of friction along the crack surface.

Since the problem is one of plane strain, the preceding criteria of failure may be restated in terms of the normal stress  $p = (\sigma_1 + \sigma_3)/2$  and deviatoric stress  $q = \sigma_1 - \sigma_3$ , so that

$$\frac{K_{I0}}{\sqrt{\pi a}} = -p - \frac{q}{2} \cos 2\beta \quad (5.44)$$

when  $\sigma_\beta$  is tensile, whereas  $K_{I0} = 0$ , when  $\sigma_\beta$  is compressive, while

$$\frac{K_{II0}}{\sqrt{\pi a}} = \frac{q}{2} \sin 2\beta - \left( p + \frac{q}{2} \cos 2\beta \right) \mu \quad (5.45)$$

Except when  $\tau_\beta \leq \tau_\beta \mu$  where upon  $K_{II0} / \sqrt{(\pi a)} = 0$ . This would then translate to the condition that equation (5.45) would be valid when

$$\frac{\sigma_1 - \sigma_3}{\sigma_1 - \sigma_3} > \frac{\mu}{\sin 2\beta - \mu \cos 2\beta}. \quad (5.46)$$

It is noteworthy that this condition indicates that when the friction coefficient is high and  $\beta$  is small,  $K_{II0} > 0$  only when  $\sigma_1$  is very much greater than  $\sigma_3$ . In this particular condition, for the case of  $\mu = 0.4$ ,  $\sigma_1$  is equal to  $2.33 \sigma_3$ .

According to foregoing equation (5.41)

$$K_{II0} = \frac{K_{IC}}{1.15}, \quad (5.41)$$

for the crack to extend. Hence, by substituting the expression for  $K_{II0}$  in equation (5.45),

$$\frac{K_{IC}}{1.15\sqrt{\pi a}} = \frac{q}{2} \sin 2\beta - \left( p + \frac{q}{2} \cos 2\beta \right) \mu, \quad (5.47)$$

where upon

$$q = \frac{2\mu}{\sin 2\beta - \mu \cos 2\beta} p + \frac{K_{IC}}{1.15\sqrt{\pi a}(\sin 2\beta - \mu \cos 2\beta)}. \quad (5.48)$$

Thus, equation (5.48) would represent the fracture envelope of a brittle hard soil-soft rock in the  $p - q$  loading plane when pure mode II loading existed at the crack tip, for which the basic parameters would be the coefficient of friction  $\mu$ , half-crack length  $a$  and angle of pre-crack  $\beta$ , provided that the condition of equation (3.35) can be satisfied. However, taking into consideration the test result of Vallejo (1993) that a crack would extend most readily when  $\beta = \beta_c = 45^\circ$ , equation (3.37) might be simplified as

$$q = 2\mu p + \frac{K_{IC}}{1.15\sqrt{\pi a}}. \quad (5.49)$$



According to equation (5.49), the slope of the fracture envelope in a  $p - q$  plot would be influenced by  $\mu$  while the intercept on the  $q$ -axis would be governed by the half-crack length  $a$ .

#### **5.5.5. Finite element analysis**

There are three basic methods to evaluate the stress intensity factors, namely the classical, numerical (analytical) and photo elastic (experimental) methods. Among the numerical methods, the finite element (FE) method is probably the most widely used due to a comparatively practical and effective, especially in determining the stress intensity factors of test specimens. The basic concept, formulation and solution of the FE method adopted herein may be found in various texts (Barsoum, 1976; Cheung and Yeo, 1979; Zienkiewicz and Taylor, 1989; Lo et al, 1997 and Lo, 2001). Hence, only the analytical aspects of the present problem will be highlighted in the subsequent discussion.

The model determines the relevant stress intensity factors at the crack tip numerically and employs the *unified model* to address the condition of fracture. The software package ABAQUS version 6.6 (Simulia Inc., 2006) has been used to generate the finite element mesh of the model. The stress intensity factors at the crack tip then have been calculated from the displacement field obtained from this software package. Eight-node isoparametric plane strain elements were chosen with the mid-side nodes of elements surrounding the crack tips moved to the quarter point of each element side, so that a square root singular deformation field at the crack tip might simulated according to Barsoum (1976). To simulate friction at the crack surface, interface elements were included whenever the crack surfaces came into contact.

##### **5.5.5.1. Quadratic isoparametric element.**

The provision of square-root singular stresses at the crack tip is one of the main requirements in the computational of stress intensity factors by the Finite

Element methods. The triangular quarter-points element of Barsoum (1976), which is a modification of an isoparametric quadratic quadrilateral element, will be adopted to satisfy this condition. Following the usual notation, the geometry of the 8-node plane, isoparametric element in Figure 5.8 is mapped onto normalised curvilinear square space  $(\xi, \eta)$ , where  $-1 \leq \xi \leq 1$  and  $-1 \leq \eta \leq 1$ , by the transformations

$$x = \sum_{i=1}^8 N_i(\xi, \eta) x_i \quad (5.50)$$

and

$$y = \sum_{i=1}^8 N_i(\xi, \eta) y_i \quad (5.51)$$

where  $N_i$  is the shape function corresponding to node  $i$  whose co-ordinates are  $(x_i, y_i)$  in the  $x$ - $y$  system and  $(\xi_i, \eta_i)$  in the transformed  $\xi$ - $\eta$  system, and is given by

$$N_i = [(1 + \xi\xi_i)(1 + \eta\eta_i) - (1 - \xi^2)(1 + \eta\eta_i) - (1 - \eta^2)(1 + \xi\xi_i)] \frac{\xi_i^2 \eta_i^2}{4} + [(1 - \xi^2)(1 + \eta\eta_i)(1 - \xi^2)] \frac{\eta_i^2}{2} + [(1 - \eta^2)(1 + \xi\xi_i)(1 - \eta^2)] \frac{\xi_i^2}{2} \quad (5.52)$$

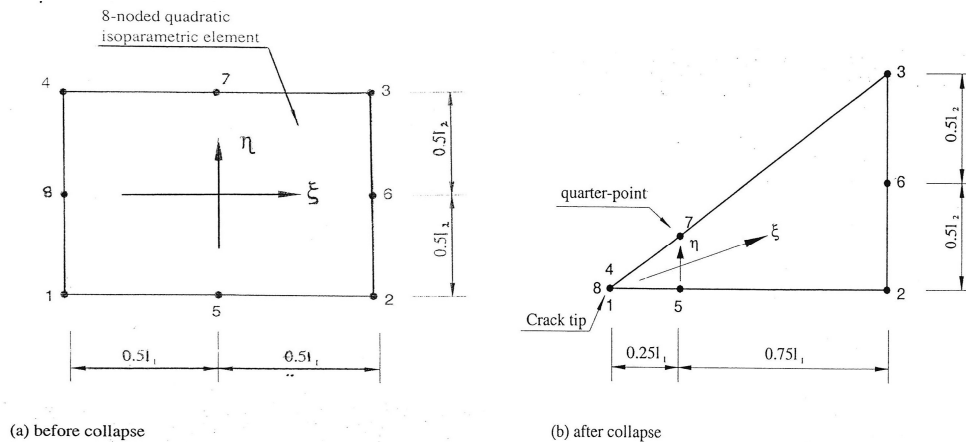


Figure 5.8. Formation of triangular crack-tip element from 8-noded quadratic quadrilateral element

At the corner points,  $\xi_i, \eta_i = \pm 1$ , while for the mid-side nodes,  $\xi_i, \eta_i = 0$ . Accordingly, the displacements may be interpolated as

$$u = \sum_{i=1}^8 N_i(\xi, \eta) u_i \quad (5.53)$$

and

$$v = \sum_{i=1}^8 N_i(\xi, \eta) v_i \quad (5.54)$$

The plane triangular quarter-point crack tip element of Figure 5.7 has been formed by collapsing side 1-8 of the original quadrilateral, then moving the two adjacent mid-side nodes to corresponding quarter points as shown. The strain in the x-direction may be determined as

$$\begin{aligned} \varepsilon_x = \frac{\partial u}{\partial x} = & \left( \frac{1}{l_1} - \frac{1}{2\sqrt{x}l_1} \right) (u_1 + u_2 + u_3 + u_4) + \frac{1}{2\sqrt{x}l_1} u_6 \\ & + 2 \left( \frac{1}{l_1} - \frac{1}{2\sqrt{x}l_1} \right) (u_5 + u_7) - \frac{1}{2\sqrt{x}l_1} u_8 \end{aligned} \quad (5.55)$$

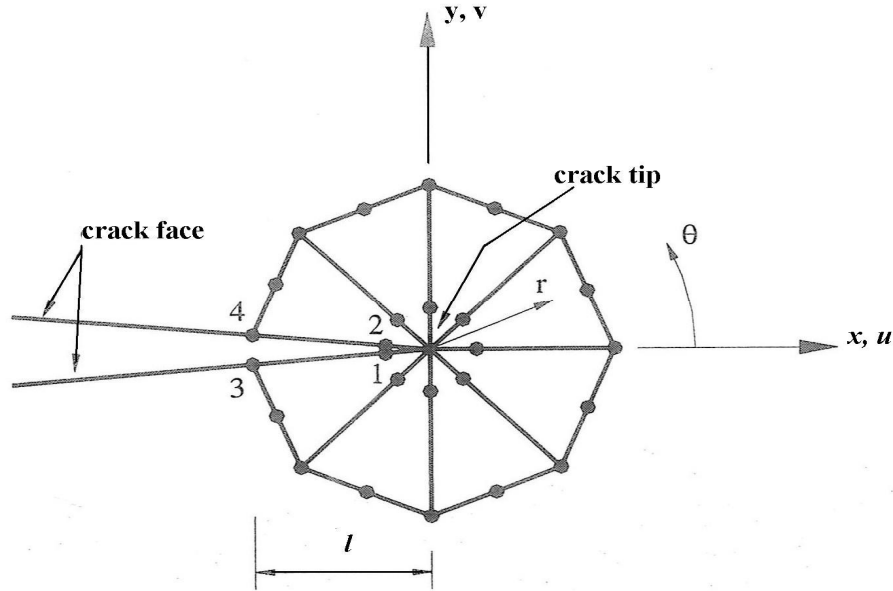


Figure 5.9. The quarter-point elements modelled around crack tip

Since it may be inferred from equation (5.55) that the strain along x-axis would vary as  $1/\sqrt{r}$ , the requirement of singularity in LEFM would be satisfied. It may be similarly shown that the strain along any axis radiating from the collapsed side of the FE would exhibit such a singularity. The quarter-point elements modelled around crack tip is shown in Figure 5.8 and Figure 5.9, in which  $l_1$  is the step length of a crack to extend.

#### 5.5.5.2.Determination of $K_{I0}$ from nodal displacements around crack tip

The expression for displacement around crack tip in LEFM for pure mode I loading may be stated as follows

$$u = \frac{K_{I0}}{8\pi G} \sqrt{2\pi r} \left[ (2\kappa - 1) \cos \frac{\theta}{2} - \cos \frac{3\theta}{2} \right] \quad (5.56)$$

and

$$v = \frac{K_{I0}}{8\pi G} \sqrt{2\pi r} \left[ (2\kappa + 1) \sin \frac{\theta}{2} - \sin \frac{3\theta}{2} \right]. \quad (5.57)$$

Based on the above equations, it may be shown that a curve of  $K$  versus  $\sqrt{r}$ , which is obtained by determining  $K$  at various radial distances  $r$  along the crack tip, may be extrapolated to obtain  $K$  at  $r = 0$ . Accordingly, as shown in Figure 5.8,  $\theta = -\pi$  and  $r_1 = l/4$  at node 1, hence

$$v_1 = \frac{K_{I0}(\kappa + 1)}{4\pi G} \sqrt{2\pi r_1}, \quad (5.58)$$

while at node 2,  $\theta = \pi$  and  $r_2 = l/4$ , hence

$$v_2 = \frac{K_{I0}(\kappa + 1)}{4\pi G} \sqrt{2\pi r_2}. \quad (5.59)$$

Therefore

$$v_2 - v_1 = \frac{K_{I0}(\kappa + 1)}{4\pi G} \sqrt{2\pi} (r_2 - r_1) = \frac{K_{I0}(\kappa + 1)}{4\pi G} \sqrt{2\pi} \cdot \sqrt{l}. \quad (5.60)$$

Similarly, it can be shown that

$$v_4 - v_3 = \frac{K_{I0}(\kappa + 1)}{4\pi G} \sqrt{2\pi} (r_4 - r_3) = \frac{K_{I0}(\kappa + 1)}{4\pi G} \sqrt{2\pi} \cdot 2\sqrt{l}. \quad (5.61)$$

Next, let  $K_{I0} = A\sqrt{r} + B$ , where A and B are factors which may be determined once  $K_{I0}$  is known as two points. Accordingly, when  $r = l/4$ ,

$$K_{I0} = \frac{2\pi G(v_2 - v_1)}{(\kappa + 1)\sqrt{2\pi r}} \frac{1}{\sqrt{l/4}}, \quad (5.62)$$

so that

$$\frac{2\pi G(v_2 - v_1)}{(\kappa + 1)\sqrt{2\pi r}} \frac{1}{\sqrt{l/4}} = A\sqrt{l/4} + B, \quad (5.63)$$

while when  $r = 1$ ,

$$K_{I0} = \frac{2\pi G(v_2 - v_1)}{(\kappa + 1)\sqrt{2\pi r}} \frac{1}{\sqrt{l}}, \quad (5.64)$$

in which case

$$\frac{2\pi G(v_4 - v_3)}{(\kappa + 1)\sqrt{2\pi r}} \frac{1}{\sqrt{l}} = A\sqrt{l} + B. \quad (5.65)$$

Thus it may be shown that

$$B = \frac{2G}{(\kappa + 1)} \sqrt{\frac{\pi}{2l}} [4(v_2 - v_1) - (v_4 - v_3)]. \quad (5.66)$$

Hence, when  $r = 0$ ,

$$K_{I0} = B = \frac{2G}{(\kappa + 1)} \sqrt{\frac{\pi}{2l}} [4(v_2 - v_1) - (v_4 - v_3)]. \quad (5.67)$$

Equation (5.67) may be used to obtain the corresponding  $K$  value once the displacements of the four relevant nodes in the vicinity of the crack tip have been determined.

#### 5.5.6. Analytical procedure using the unified fracture model

The soil specimen is initially subjected to stress states of  $\sigma_{10}$  and  $\sigma_{30}$ , while maintained at a pore pressure of  $u_{a0}$  and pore water pressure of  $u_{w0}$ . Computation under loading then takes place according to the following stages:

##### Stage 1

The degree of saturation  $S_0$  is evaluated from the void ratio and water content constitutive surfaces via the phase relationship of equation (4.9.). The pore pressure parameters of the initial state of stress  $B_{a0}$  and  $B_{w0}$  then be determined from equations (4.10) and (4.11) respectively.

##### Stage 2

The pore air and pore water pressure increments  $\Delta u_a$  and  $\Delta u_w$  under load increments  $\Delta \sigma_1$  and  $\Delta \sigma_3$  may be determined as

$$\Delta u_a = B_a \Delta \sigma'_{ave} \quad (5.68)$$

and

$$\Delta u_w = B_w \Delta \sigma'_{ave}, \quad (5.69)$$

where

$$\Delta \sigma'_{ave} = \frac{\Delta \sigma'_1 + \Delta \sigma'_3}{2}, \quad (5.70)$$

in which the prime is used to signify the internal rather the applied stresses. This distinction is necessary in view of the non-uniformity of the internal stresses that would developed from crack extension, bearing in mind that the foregoing formulation of the proposed fracture model is based on the outset of fracture.

Hence, the updated pore air and water pressures  $u_{a1}$  and  $u_{w1}$  may be obtained as

$$u_{a1} = \mu_{a0} + \Delta\mu_a \quad (5.71)$$

and

$$u_{w1} = \mu_{w0} + \Delta\mu_w, \quad (5.72)$$

where the fracture toughness ( $K_{IC}$ ) for this loading stage may be determined from the  $G_C$  versus  $(u_a - u_w)$  relationship. Furthermore, for small increments, it would be suffice to adopt the initial matric suction at the start of the increment in determining the fracture toughness, namely  $(u_{a0} - u_{w0})$ .

### Stage 3

Determine whether the unified fracture criterion is satisfied in this stage of loading the criterion, which is based on total stresses of equation (5.47), is given by

$$\frac{(K_{IC})_1}{1.15\sqrt{\pi a}} = \frac{q_1}{2} \sin 2\beta_c - \left( p_1 + \frac{q_1}{2} \cos 2\beta_c \right) \mu, \quad (5.73)$$

in which

$$p_1 = \frac{\sigma'_{11} + \sigma'_{31}}{2} \quad (5.74)$$

and

$$q_1 = \frac{\sigma'_{11} - \sigma'_{31}}{2}, \quad (5.75)$$

where  $\sigma'_{11} = \sigma'_{10} + \Delta\sigma'_1$  and  $\sigma'_{31} = \sigma'_{30} + \Delta\sigma'_3$ .

If the criterion is satisfied, then allow crack increment to take place accordingly until the next load increment is required, updating the stresses and displacements, and hence the degree of saturation and matric suction, with each crack increment as before. However, if the criterion is not satisfied, the stresses and displacements could be determined and updated throughout the soil specimen

by FE analysis, and keep loading up and carrying out stage 1 to stage 3 until the criterion is satisfied. Note, however, that after crack extension has taken place, the criterion of fracture of equation (5.73) would have to be amended accordingly. In other words, the condition  $K_{I0} = K_{IC}$  would then be appropriate.

In the analysis of the crack propagation, following procedure is required:

### Stage 1

Prescribe vertical displacement  $d$  on the model, then determined  $K_{I0}$  and  $K_{II0}$  from the displacement field as outline in foregoing 5.5.5.2. Check if the angle of 70.5 applied to the parent crack plane that

$$f(\theta) = \left( \frac{K_{I0}}{K_{IC}} \right)^2 + \left( \frac{K_{II0}}{K_{IIC}} \right)^2, \quad (5.76)$$

where  $K_{I0}$  be determined by equation (5.37) and (5.38). If it is equal to 1, the vertical displacement  $d = d_l$ , would be just required magnitude for crack extension in this stage and the angle where  $f(\theta)$  attained its maximum value may then be denote as  $\theta_1$ . To obtain the correct  $d_l$  and  $\theta_1$  at the first step, If  $f(\theta)_{\max}$  is not equal to 1, then  $d$  would need to modify until  $f(\theta)_{\max}$  is equal to 1.

### Stage 2

Allow the crack to extend at angle  $\theta_1$  for step length  $l = 1$  mm and then re-mesh the model. A new pair of  $K_{I0}$  and  $K_{II0}$  value would results from the vertical displacement  $d_l$ . The same procedure as in stage 1 then be determined if the new  $f(\theta)_{\max} = 1$ . If  $f(\theta)_{\max} \geq 1$ , the crack would extend without additional prescribed displacement, whereupon, the critical displacement  $d_2 = d_l$ , and  $\theta_2$  may be obtained similarly as before. Following this stage 2 is repeated until the crack extends to the edge of the model. The load displacement curve then is drawn from the results of the various steps of the analysis.



## **CHAPTER 6**

### **EXPERIMENTAL PROGRAM**

#### **6.1. Introduction**

Experimental tests to determinate constitutive behaviour of soil are based on the premise that the specimen deforms uniformly in spite of the fact that laboratory evidence of localization phenomena has existed for some time. Strain localization had been experienced by heavily over consolidated clays when they are subjected to shear (Hvorslev, 1960). Localized failure, which is commonly observed in feature of slope and underground failures in soft rock and over consolidated clays, is manifested by relatively large shear deformations within a thin layer of material known as “shear band” which are accompanied by dilation (Viggiani et al, 1994). The occurrence of such failure zones; therefore, affect the experimental techniques as well as the numerical implementation of the constitutive equations of soil.

The behaviour of soil is routinely interpreted from triaxial testing, whereas testing of soil under plane strain condition would be more useful information, as more geotechnical problems basically occur under these conditions. There were very limited researches data under plane strain condition derived from customized device, which do not find their way elsewhere, due to their sophistication and high cost (Lo et al, 2000 and Mita, 2003).

A new biaxial device has been used in this present research. This apparatus is believed to be able to produce reliable test results and the condition of plane strain can be maintained during the tests. Due to its simplicity and toughness, malfunction or inaccuracy of the test results caused by leakage and other deficiencies are minimized. This device is not only easy to set up but it also easy to carry out the testing with minimum disturbances. In addition, unlike other devices that used customized O-ring and rubber membrane, the standard O-ring and rubber membrane can be used in this apparatus. Furthermore, the used of laser sensors to measure lateral displacement and volume change is also able to detect the onset of such localized deformation.

Plane strain device adapted from triaxial testing apparatus to biaxial testing apparatus was used as well as the standard tests which adopted from any available standard, such as ASTM, British Standard and Australian Standard. A series of experimental works had been carried out to achieve the research objectives, those are the basic engineering properties tests of kaolin clay, plane strain compression tests on saturated over consolidated clay, biaxial and triaxial tests on partially saturated clay, and fracture testing on partially saturated clay.

## **6.2. Biaxial compression device**

It was fairly recently that systematic studies were undertaken to analyse and describe the occurrence and patterns of localized failure zone, in spite of the fact that this phenomena has existed frequently (Drescher et al, 1990). For the purposes of evaluating constitutive behaviour and stability properties of soil, most laboratory experiments on soils in particular to the clayey soils are performed under axis symmetric or conventional triaxial conditions. However, most geotechnical field problems such as landslide problems, failure of soils beneath shallow foundations, and failure of retaining structures are truly or close to biaxial situations and hence data obtained from triaxial testing would not apply. It would be more appropriate using data from plane strain tests.

Mochizuki et al (1993) reported that when soil is tested under plane strain conditions, it, in general, exhibits a higher compressive strength and lower axial strain. Peters et al (1988) found out that shear bands are more easily initiated under plane strain condition, for dense to medium dense sand. The plane strain testing on the behaviour of fine grained sands had been reported (Alshibli et.al, 2004; Bizzarri, 1995; Han and Vardoulakis, 1991; Hans and Drescher, 1993; Mochizuki et al, 1993; Schanz and Alabdullah, 2007). The plane strain testing of clay has only been initiated recently (Drescher et al, 1990, Lo, et al, 2000; Viggiani et al, 1994). However published data of such tests especially for hard stiff clay material is very limited.

Plane strain testing of soil was performed firstly by Kjellman (1936), then Jakobson (1957), Lorenz et al (1965) and Hambly and Roscoe (1969) who adopt this testing device found the “corner junction “ problem. Wood (1958) and Cornforth (1964) proposed a long rectangular specimen for ease of controlling the plane strain condition, which was known as “Bishop-Cornforth” device. However, inaccuracy in the measurements of stresses and strains caused by the friction force arising from axial loading surface was found by Finn et al (1968), Lee (1970) and Marach et al (1981) when adopt this method. A plane strain test device using a rectangular sample of 84 mm x 76 mm x 53 mm was developed by Green (1971). However, Bishop (1981) pointed out that Green’s method, which had the  $\sigma_2$  loading surface suspended by wires, could not perform as expected.

Most of the plane strain apparatus (Green and Reades, 1975; Mochizuki et al, 1993; Peters et Al, 1988; Drescher, 1990; Han and Vardoulakis, 1991; Viggiani et al, 1994) had the common feature of using rigid walls and tie-rods to impose zero strain boundary condition in one of the principal axes. This method was found to be satisfactory, and friction between the rigid wall and test specimen could be adequately mitigated. Taylor (1941), Rowe and Barden (1964), Lee and Seed (1964) and Bishop and Green (1965) found that if the aspect ratio was bigger

than 2, the effect of loading platen friction and the restraint of loading frame would be negligible and the specimen would maintain constant strength.

An adaptation of a plane strain testing apparatus is being used in this research. The specimen size is 72 mm high x 36 mm wide x 72 mm thick, so that the aspect ratio (height to width) is 2. A commonly-available cylindrical rubber membrane may be used. This would allow some flexibility in the specimen height and prevent the air pockets formation in the specimen vicinity. The rubber membrane is secured to the rectangular loading platens by means of O-rings and O-ring clamps. The water tightness of the system has been tested to a very high pressure (1000 kPa) and found to be satisfactory. Plane strain conditions are maintained using acrylic rigid walls and tie rods, while the friction between the rigid walls and the specimen is mitigated by the use of silicone lubricant. The lateral displacements of the specimen are monitored by laser sensors which allow for remote measurements, while doing away with cumbersome reflectors, which would be required for the more commonly used gap sensors. The volume change of the specimen could be measured by a volume-change gauge.

#### **6.2.1. Description of the apparatus**

An initial prismatic specimen with the width of 36 mm, height of 72 mm, and thickness of 72 mm, so that the aspect ratio is 2, is placed on the base pedestal where it is restrained laterally by two rigid perspex plates to restrain its out-of plane movement, which make  $\varepsilon_2=0$ . Therefore, only major ( $\sigma_1$ ) and minor ( $\sigma_3$ ) principal stresses acting on the soil specimen. A schematic diagram of the biaxial apparatus can be seen in Figure 6.1, while a schematic diagram of principle stresses acting on the specimen under plane strain condition is presented in Figure 6.1.

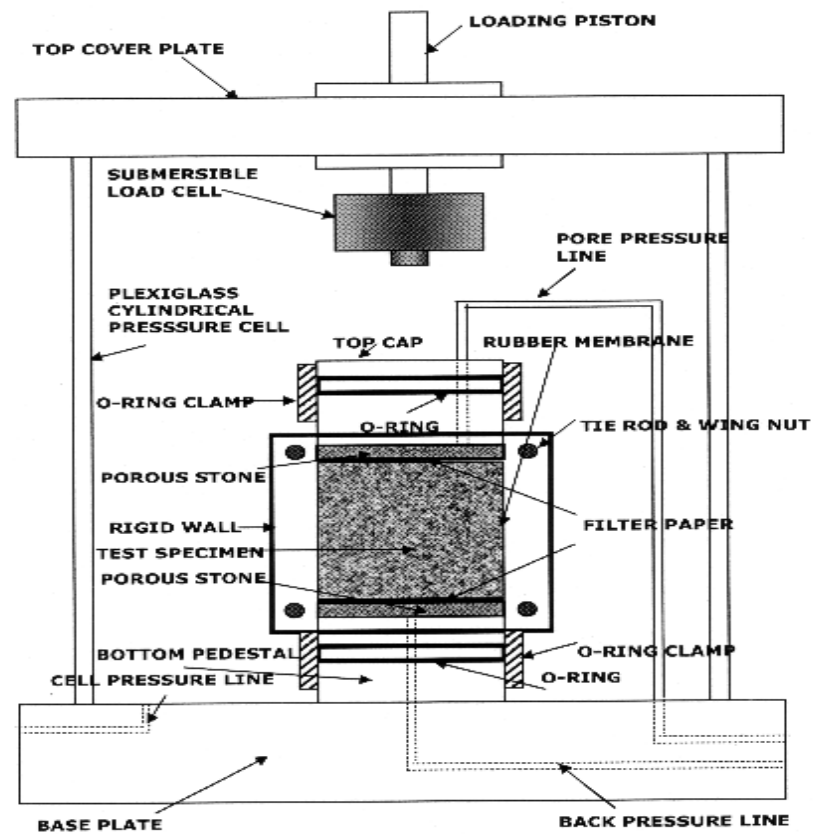


Figure 6.1. A schematic diagram of biaxial compression apparatus

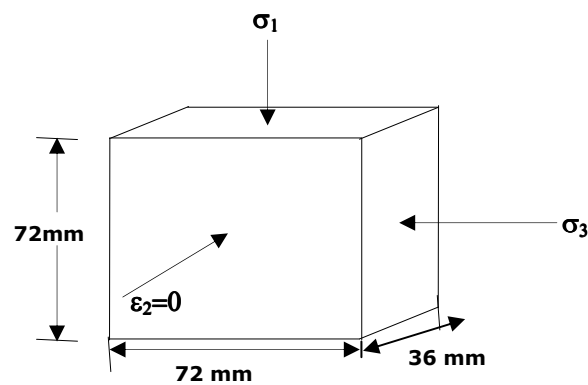


Figure 6.2. A schematic diagram of principle stresses acting on the specimen under plane strain condition

### 6.2.2. Components of the equipment

The biaxial equipment consists of 9 components, there are top cap, high air-entry disc (head), bottom pedestal, O-rings, O-ring clamps, rigid walls, tie rods with wing nuts, rubber membrane, and rectangular porous plate, which are assembled inside the triaxial chamber and 2 other components that used to help assembling. Figure 6.3 shows the component of the biaxial equipment. These 9 components were placed in cell, with the height of 300 mm, 200 mm internal diameter and 30 mm wall. Rubber membrane that used for this apparatus has length of 180 mm, with the thickness of 3 mm and 65 mm in diameter while the O-ring used has diameter of 45 mm with the wall thickness of 3 mm. The rectangular porous stone plate of 5 mm thickness has the same plan dimension as the top cap. The 2 other components that used to help assembling those 8 component are O-ring stretcher which made from stainless steel and sleeve stretcher, made of Aluminium.

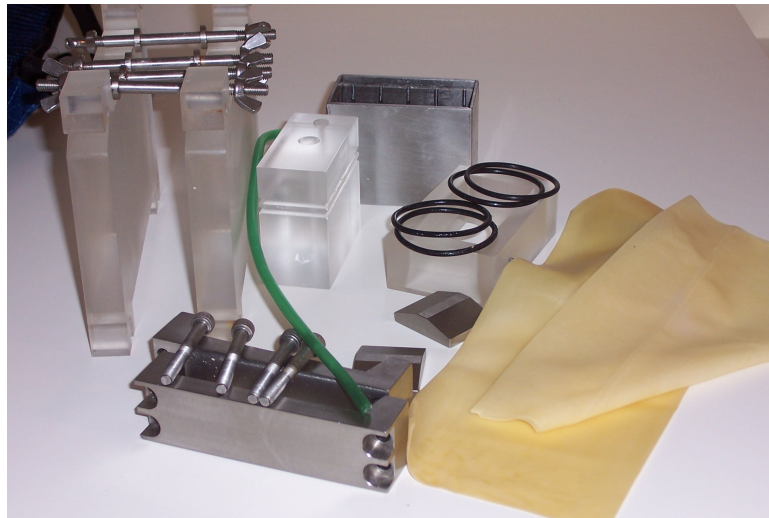


Figure 6.3. Components of biaxial device

For conducting the test of unsaturated clay specimen, a high air-entry disc (HAED) was used and it was sealed to the base pedestal of the triaxial cell. The HAED is a porous, ceramic disc which allowed only the passage of water, but prevented the entry of air if the matric suction within the specimen is less than the air-entry value of the HAED. The HAED act as a membrane between air and

water and has small pores of relatively uniform size. Once the disc is saturated with water, air can not pass through the disc due to the ability of the contractile skin to resist the flow of air. The ability of a HAED to prevent the flow of air arises from the surface tension,  $T_s$ , developed by the contractile skin. The contractile skin acts as a thin membrane joining the small pores of radius,  $R_s$ , on the surface of the ceramic disc. The difference between the air pressure above the contractile skin and the water pressure below is defined as matric suction. The ability of a HAED to withstand the difference between air and water pressure makes it suitable for direct measurement of the negative pore water pressure in a specimen which is undergoing consolidation by matric suction.

### 6.2.3. Loading system of biaxial apparatus

The biaxial apparatus is placed inside a plexiglass confining pressure cell, with the height of 300 mm, 200 mm internal diameter and 30 mm wall thickness. To enable the specimen to be pressurized laterally up to 1000 kPa, the cell is filled up by water, which is supplied by a pressure generator device which is a product of Global Digital System Ltd (GDS instruments), as shown in Figure 6.4. It can generate pressure up to 24 MPa. A Hitachi compressor with the capacity of 1000 kPa was also used to supply to the back pressure. A 50 kN capacity of Wykeham Farrance displacement-controlled compression machine is used for the application of axial load for plane strain testing.

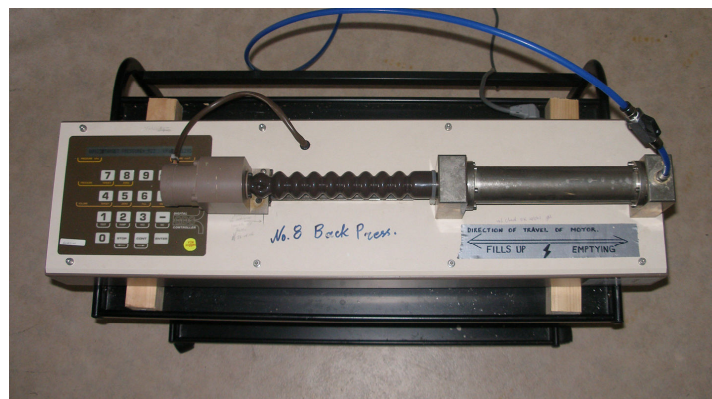


Figure 6.4. The Global Digital System (GDS) pressure generator unit

#### 6.2.4. Data recording and instrumentation

A 5 kN capacity of A Wykeham Farrance WF 17109 submersible load cell is used to measure the axial load applied to the test specimen. The axial displacement of the test specimens are measured by 35-mm range LVDT (Linear Vertical Displacement Transducer) attached on top of the top cover of the cell (Figure 6.5). Lateral displacement is measured by two laser sensors which are mounted to the triaxial cell (Figure. 6.6). This laser sensors is used to monitor any change in distance between the test specimen and the sensor along the height of the specimen, which indicated by voltage readings on the voltage controllers. Stepper motor is used to control the movement of the laser sensors up and down, along the lead screw such that every cycle of travel consist of upward and downward motion. The data recorded are transferred to the data logger and converted to actual distance captured by the laser sensors.



Figure 6.5. LVDT attached on top of the top cover of the cell



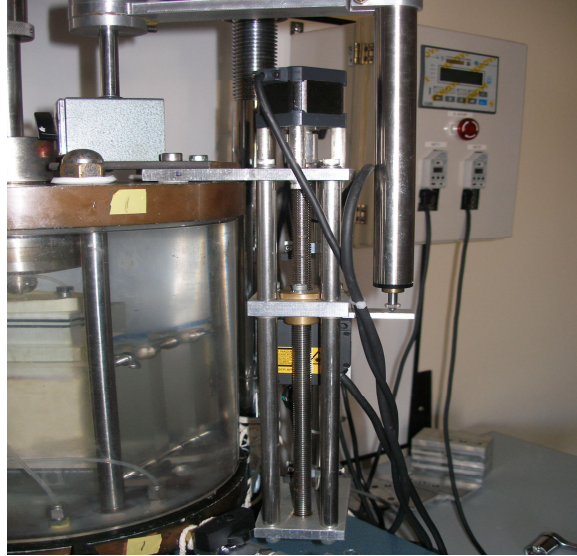


Figure 6.6. Laser sensor mounted to the triaxial cell

For the purpose of measuring the applied cell pressure, back pressure and pore pressure of the specimen four pore pressure transducers were used and mounted to the base plate of the cell (Figure 6.7). The pore pressure transducers are connected to the drainage line, for pore pressure measurement in the test specimen, it is located on the top cap. The drainage line for back pressure located at the bottom pedestal and for cell pressure measurement is directly connected to the triaxial chamber. The global volume change of the water-saturated soil specimens are monitored by an automatic volume change unit which is connected to the back-pressure line (Figure 6.8).

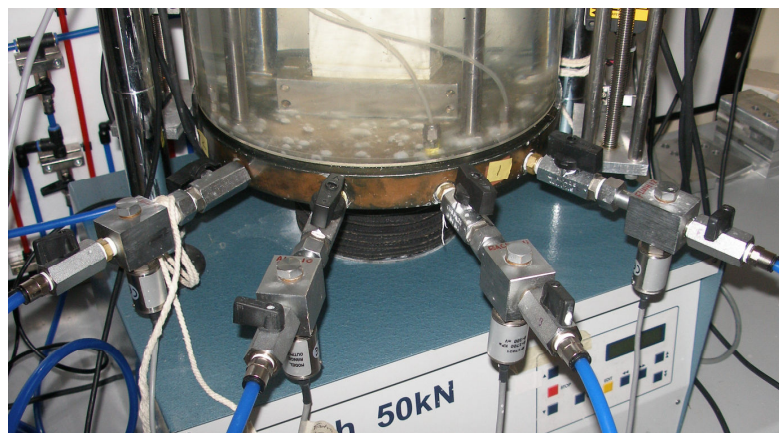


Figure 6.7. Four pore pressure transducers mounted to the base plate of the cell

To record the displacement, loads, pressure and volume change reading a data acquisition system consisting of an MPX 300 data logger (Figure 6.8) and a set of microcomputer were used. A WINHOST 2.0 package software (VJ Technology product) is used to convert digital bit data from the ADU (Analogue digital Unit) to engineering units based on the calibration of the relevant measuring unit, which was done before running the plane strain test.

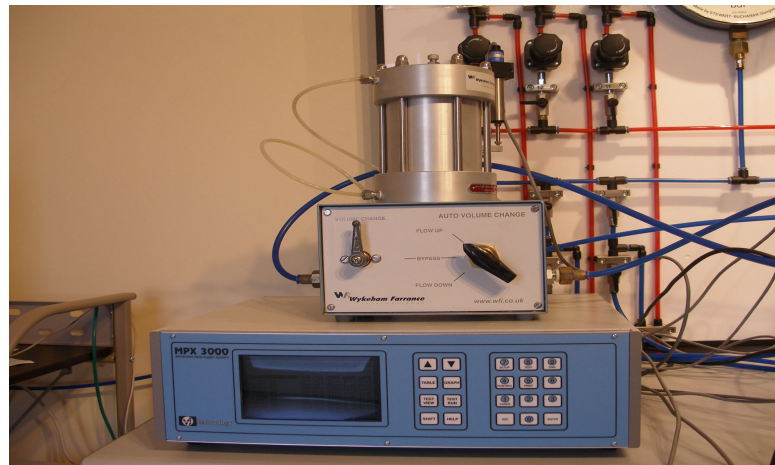


Figure 6.8. Data logger and automatic volume change unit

### 6.3. Material and specimen preparation

Similar to that of axi-symmetric triaxial testing, the sample could either be obtained in-situ, or reconstituted and consolidated cohesive soil. In the present research, remoulded kaolin clay was used for all of the specimens. The source of clay was kaolin clay which was a product of UNIMIN PTY LTD, Australia, with a specific gravity  $G_s = 2.6$ , Liquid Limit  $LL = 53.5\%$  and plastic limit  $PL = 30.76$  (British Standards Institution, 1990). Following the procedure herein is adopted from previous researcher (Mita, 2003; Lo, 2001; and Boon and Suen, 2001).

#### 6.3.1. Mixing the slurry and consolidation process

It was taken few weeks to complete and consisted of the preparation of soil specimen. Initially, a kaolin clay sample was slurried to a uniform consistency

of 1 ½ times its liquid limit using an electrical soil mixer. This slurry was obtained by mixing 8 kg of kaolin powder with 6 kg of water using the electric mixer for about 2 hours (Figure 6.9). To ease the extrusion of the sample from the mould at the end of consolidation, the inner wall of the cylinder mould was greased before pouring the kaolin slurry to the consolidation unit.

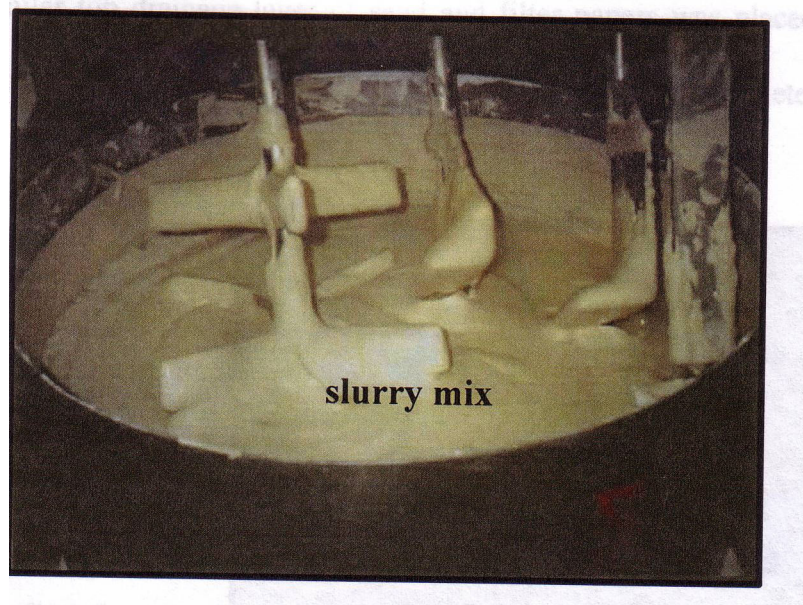


Figure 6.9. Mixture of kaolin powder and water

A steel cylindrical mould with the height of 600 mm and 150 mm in diameter was used to consolidate the slurry using a hydraulic tester in over a period of one to two weeks which the maximum of 300 kPa was applied in three stages. To accelerate the consolidation process a layer of sand and geosynthetic were placed on the top and the bottom of this slurry. Two circular perspexes were placed at both ends of the slurry in the mould to apply the pressure evenly to the slurry. The slurry was allowed to consolidate by its own weight and small pressure was applied to prevent the slurry being squeezed out between the circular perspexes and the mould. A higher vertical pressure was applied when there was no further settlement change.

Once the consolidation process had completed, the soil was then extruded from the mould into lubricated formers. Following this, the specimen and the



former were wrapped in plastic film sheeting after sealing both their faces with liquid wax. To obtain even pore water pressure, the specimens were placed in the dehumidifier for at least 2 days until it is tested. Figure 6.10 shows typical arrangement of the consolidation unit, while Figure 6.11 shows the graph of the consolidation unit.

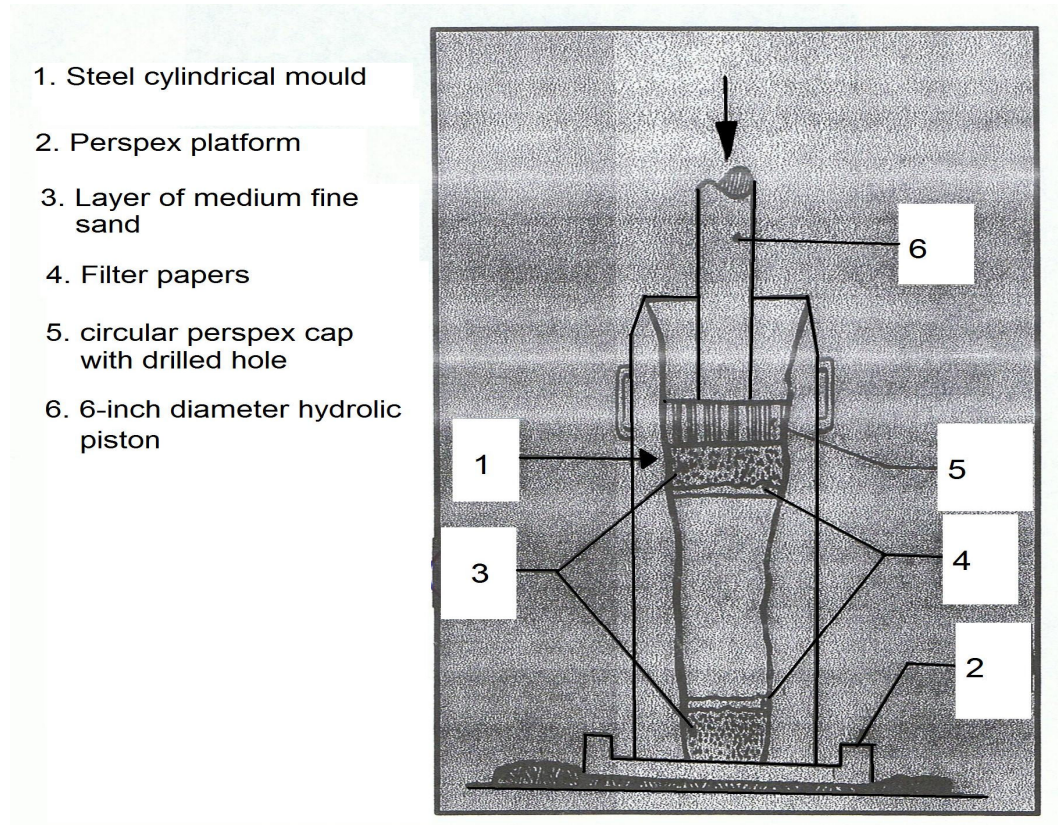


Figure 6.10. Typical arrangement of consolidation unit  
(after Lo et al, 2001)

For the plane shear test, the soil in the former was extruded using a perspex rectangular block, when the portion of the specimen which was coming out from the former suit to the size of the specimen required (72 mm x 72 mm x 36 mm), and the specimen was then cut by using a steel wire. The specimen was allowed to be intact initially for the purpose of critical state parameters determination and it was given an initial crack of a 30 mm wide with the thickness of 0.5 mm for simulating the shear strength characteristics of pre-crack specimen of unsaturated clay.



Figure 6.11. A view of consolidation unit machine

### 6.3.2. Preparation of plane strain test set up

The initial dimensions and the weight of the soil specimen are measured just before carrying out the compression test. The biaxial compression test has 2 different stages, those are preparing the test specimen in the plane strain test set up and shearing process. The assembly of preparing test specimen in the plane strain test set up may be stated in term of following stages.

#### Stage 1

The rubber membrane is slid over the top cap and O-rings are strapped around the top cap grooves, then the O-ring clamp is placed (Figure 6.12).

#### Stage 2

The rubber membrane is folded to a position where the mouth of the fold is about 10 mm from the edge of the top cap to leave enough membrane to be wrapped over the sleeve stretcher. The pore pressure line was then connected to the top cap and the rectangular porous plate was placed in position.

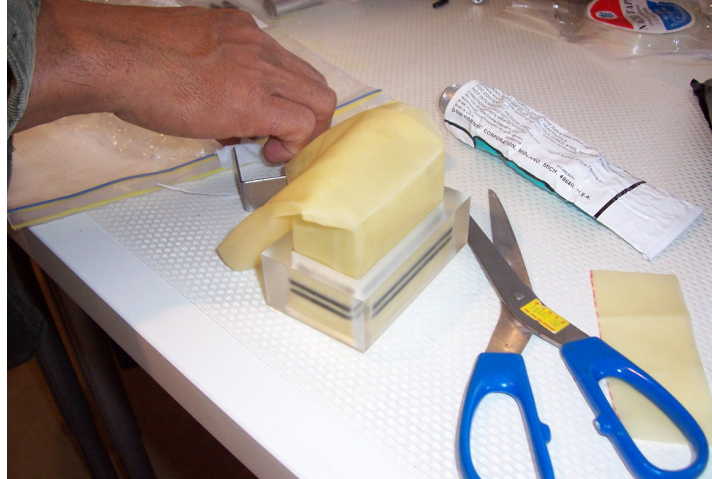


Figure 6.12. Inserting top cap to the rubber membrane

### Stage 3

The sleeve stretcher is slid over the rubber membranes until it is in line with the mouth of the rubber membranes fold. The rubber membrane then is unfolded upwards to wrap over the sleeve stretcher. The end of the rubber membranes are folded downwards to wrap over the sleeve stretcher. Air is then sucked out from the nozzle and the nozzle should be closed to prevent air to enter.

### Stage 4

Wet filter papers are put on both ends of the specimen. The test specimen is pushed until one of its ends sits on the porous stone which attached to the top cap. Another porous stone is placed on the top of the test specimen. The sleeve stretcher is then moved up carefully, allowing the folded rubber membranes at the bottom of the stretcher to unfold and wrap over the specimen. Once the membranes at the bottom of the stretcher have been fully extended, the membranes at the top are unfolded and the nozzle was opened to allow air to enter. Finally, the sleeve stretcher can be removed (Figure 6.13).

### Stage 5

Two O-rings are strapped around the O-ring collar and the collar is slowly moved over the test specimen. The rubber membranes are folded over the O-ring collar



and the whole set-up inverted onto the bottom pedestal and set in alignment. The rubber membranes are unfolded and wrapped around the bottom pedestal



Figure 6.13. Placing the test specimen in rubber membrane

#### Stage 6

The O-ring collar is moved downwards, until its bottom edge is aligned with the groove of bottom pedestal. The first O-ring is rolled out of the O-ring collar and strapped around the bottom pedestal along lower groove. The next O-ring then placed to the upper groove. The O-ring collar then removed. O-ring clamp then is put in the position around the bottom pedestal. (Figure 6.14)

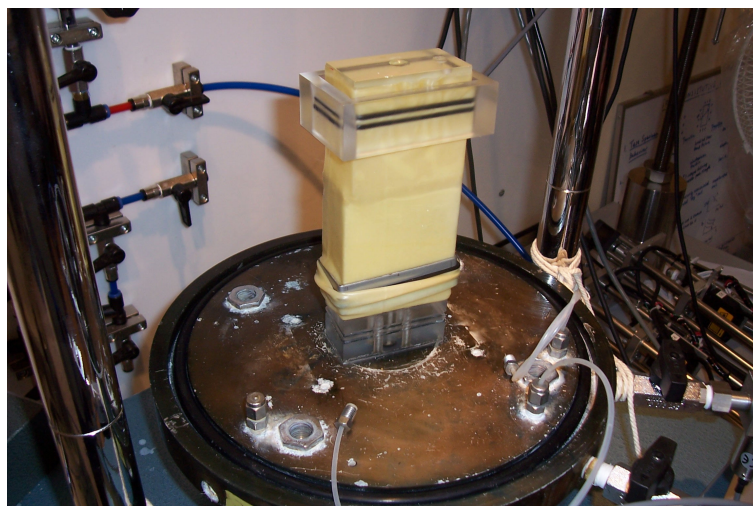


Figure 6.14. Rubber membrane slid over bottom pedestal

### Stage 7

The two rigid walls are placed on opposite side of the test specimen and seated on the O-ring clamp at the bottom pedestal. The four sets of tie rods and wing nuts are slotted to their respective notches and tightened. The cylindrical perspexes are mounted and the arrangement is ready to run the test (Figure 6.15).

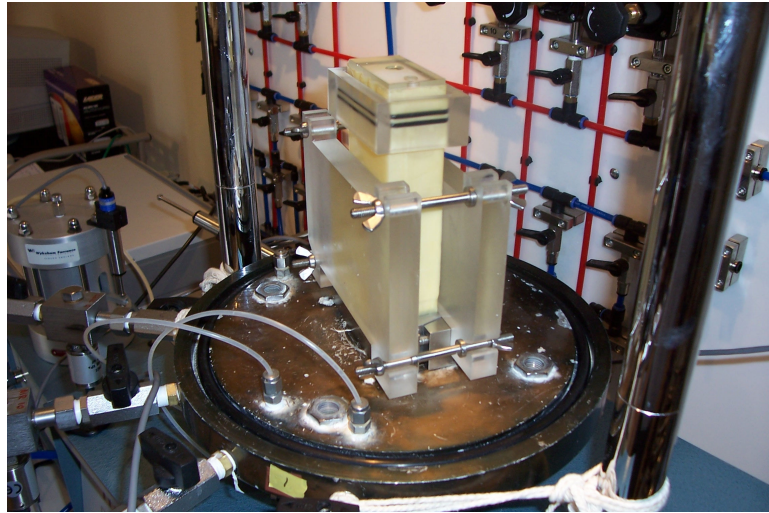


Figure 6.15. Perspex rigid wall assembled to the test specimen

## **6.4. Testing on saturated over consolidated clay**

### **6.4.1. Saturation and loading-unloading process**

Saturation and consolidation process are required before running compression test. The saturation process adopted here is based on BS Standard (Head, 1986). Firstly, the cell is filled up by water to enable the specimen to be pressurized laterally, supplied by a compressed air cylinder (Figure 6.16). The maximum consolidation pressure in the triaxial chamber to be applied to the specimens was 1000 kPa. To saturate the specimen, back pressure was used to allow the specimen to have pore pressure increase, which is similar to the cell pressure applied. The value of pore pressure coefficient,  $B$ , should be in the range of 0.95-1. A maximum of 700 kPa effective consolidation pressure was applied in four loading stages, those were 87.5 kPa, 175 kPa, 350 kPa and 700 kPa. Each loading was terminated until the 95 % consolidation was reached.





Figure 6.16. Biaxial testing arrangement

Once the specimen consolidated to the maximum pressure, it was allowed to swell isotropically to the desired over consolidation ratio (OCR). For example, if the desired OCR is 8, the isotropic swelling process is carried out in 4 steps of unloading process, that are 700 kPa, 350 kPa, 175 kPa and 87.5 kPa. During consolidation process, data were taken by setting the data logger reading similar to the method of oedometer test that is square root of time. When the process of consolidating the test specimen to the desired OCR had been completed, then it followed by the compression test either drained or undrained tests.

#### **6.4.2. Biaxial compression process**

The test specimen for drained condition (CD) is loaded axially by applying the loading through the loading machine, with the drainage line opened. Data were read every 10 minutes and for laser sensors the reading was taken every 3 mm long of the LVDT movement. The displacement-controlled loading rate of 0.004 mm/min was applied, corresponding to the rate of 0.35% per hour for the test specimen height of 72 mm. This loading rate was deduced based on the permeability of adopted kaolin clay (Bishop and Henkel, 1962). The drained compression test was terminated at the axial strain of about 20% or sooner. Once the test specimen had failed, it was taken out immediately for the purpose of moisture content determination. The information of plane strain compression test on heavily overconsolidated clay can be seen in Table 6.1.

Table 6.1. Plane strain compression tests on kaolin specimen

Test Name	Test Type	Initial moisture content (%)	OCR	B-value	Loading rate (mm/min)	CP (kPa)	BP (kPa)
OCR8CD	Drained	25.32	8	0.98	0.004	387	300
OCR20CD	Drained	25.75	20	0.97	0.004	335	300
OCR1CD	Undrained	24.67	1	0.97	0.008	1000	300
OCR4CU	Undrained	26.43	4	0.97	0.008	475	300
OCR10CU	Undrained	24.78	10	0.95	0.008	370	300
OCR16CU	Undrained	26.23	16	0.96	0.008	343.75	300

Similar to that of the drained test, the initial treatment described above also applied to the test specimen for undrained test. The test specimen was saturated and consolidated. The difference was the treatment on how the test specimen was sheared up to failure and the loading rate applied. The loading rate that applied for undrained test was 0.008 mm/min, which is equal to the loading rate of 0.7% per hour with the height of specimen of 72 mm (Bishop and Henkel, 1962). During the application of load, drainage line was closed and pore water pressure was measured and monitored. The data were recorded with the interval of 3 minutes.

## 6.5. Testing on partially saturated clay

### 6.5.1. Set up of the biaxial and triaxial test

Specimen preparation of partially saturated clay adopted the same way how saturated kaolin specimens were prepared, as mentioned in section 6.2 and section 6.3, except that a high air-entry disc (HAED) was also used in this test. The typical arrangement of biaxial device used for unsaturated testing can be seen in Figure 6.17.

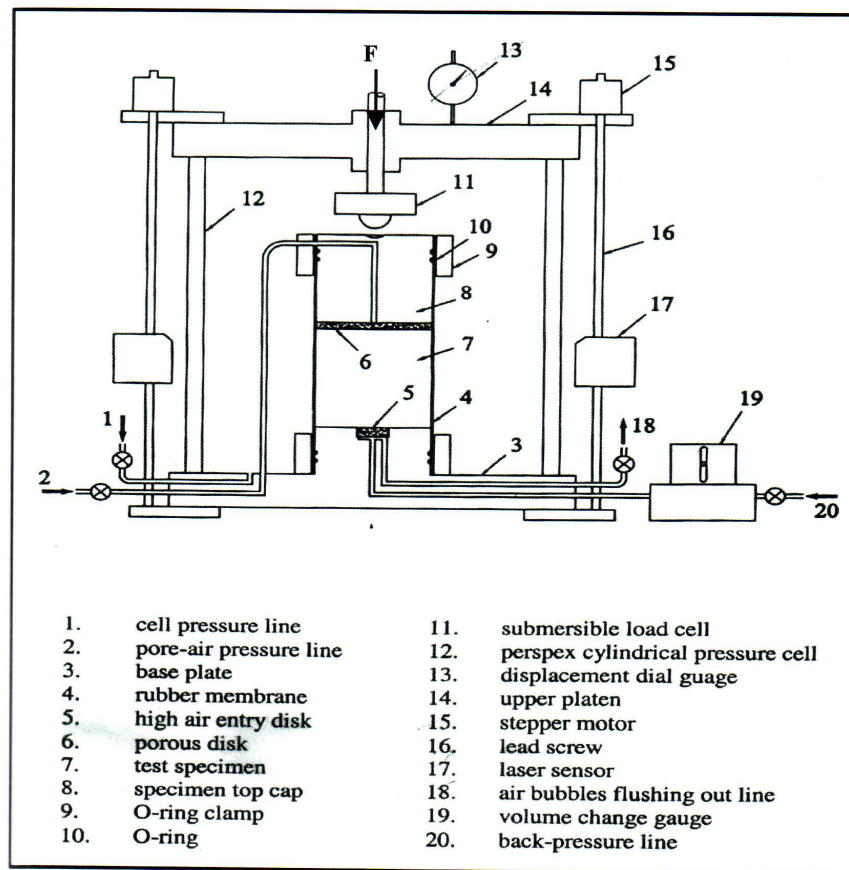


Figure 6.17. Typical arrangement for biaxial device for unsaturated testing  
(after Lo et al, 2001)

Two types of intact specimen and pre-crack specimen have been tested under plane strain condition as well as under triaxial test set up by unplacing the rigid wall. An initial intact prismatic specimen with the width of 36 mm, height of 72 mm, and thickness of 72 mm were placing in the apparatus as described below. The pre-crack specimens were formed a 30 mm diagonal pre-crack in the centre of the intact specimen to simulate the discontinuities in the specimen. Three specimen of IBM (intact specimen, biaxial), PCBM (Pre-crack specimen, biaxial) and ITM (intact specimen, triaxial) were tested under net normal stress of 0 and maximum matric suction of 500 kPa and three specimen of IBN (intact specimen, biaxial), PCBN (Pre-crack specimen, biaxial) and ITN (intact specimen, triaxial) were tested under matric suction of 0 and maximum net normal stress of 800 kPa. The specimen was first saturated until the B-value of the specimen reached the value of 0.95-0.98, followed by matric suction applied and loading compression

processed. Figure 6.18 shows the schematic diagram of plane strain condition of the pre-crack specimen on the testing of partially saturated clay.

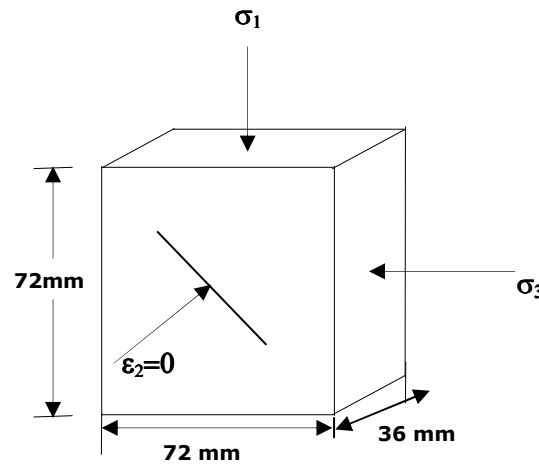


Figure 6.18. A schematic diagram of plane strain condition of the pre-crack specimen

The specimen was placed in the plane strain apparatus by the same way as saturated OC Clay specimen was treated. The rubber membrane was first placed over the test specimen with the aid of a sleeve stretcher. The rectangular porous plate was then placed on top of the specimen followed by the top assembly and the high air-entry disc (HAED). The rubber membrane was next slipped over the porous plate, the top assembly and the HAED and secured by the use of a set of O-rings and rectangular Perspex clamp. The specimen, together with the porous plate and the top assembly were then placed over the pedestal of the plane strain compression apparatus. The rubber membrane was next slipped over the pedestal and secured by the use of a set of O-rings and clamp set. Two rigid perspex plates were then placed and secured by the use of clamp set for biaxial test set up. The pressure cell, top assembly and laser sensor set-up were then installed.

### 6.5.2. Saturation and suction process

The initial void ratio and water content of the test specimen were first determined according to BS 1377 (British Standard Institution, 1990).

Constitutive surfaces of void ratio  $e$  and water content  $w$ , which provide the basis for determining the degree of saturation  $S$  and hence the pore pressure parameters,  $B_a$  and  $B_w$ , the volumetric deformation coefficients  $m_{1s}$ ,  $m_{1w}$  and  $m_{2w}$ , upon which the pore pressure parameters  $B_a$  and  $B_w$  also depend, are evaluated from the volume change indices  $C_t$ ,  $C_m$ ,  $D_t$  and  $D_m$  which are likewise obtained from constitutive surfaces. Based on foregoing subsequent 4.3.2 and 4.3.3 and similar to that of Figure 4.7, the constitutive surface of void ratio versus net normal stress and matric suction then are plotted as shown in Figure 6.19, while the constitutive surface of water content versus net normal stress and matric suction be depicted as presented in Figure 6.20.

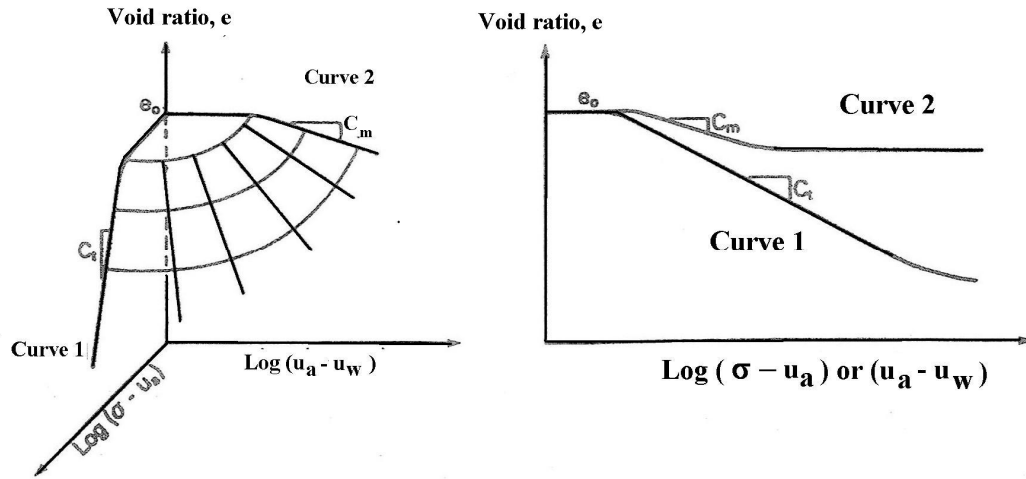


Figure 6.19. Constitutive surface of void ratio versus net normal stress and matric suction

To provide an initial net normal stress of  $(\sigma_3 - u_a) = 0$  and matric suction of  $(u_a - u_w) = 10$  kPa, a cell pressure of  $\sigma_3 = 600$  kPa, back pressure of  $u_w = 590$  kPa and pore-air pressure of  $u_a = 600$  kPa were applied to the IBM, PCBM and ITM specimen, which was in a saturated condition. Specimen of ITM was in triaxial test set up (Figure 6.21), while specimen of IBM and PCBM were set up under plane strain condition (Figure 6.22). As the matric suction was increased slowly, it was found that a small amount of recompression could take place due to prior swelling, after which a significantly greater amount of compression would occur as the specimen underwent primary consolidation. This trend would be reflected

by the slope of the curve on the constitutive surface which would initially be almost horizontal and then increase significantly. The matric suction at which desaturation started would not be obvious from the plots but could be found by making a plot of the effective saturation  $S_e$  versus the matric suction. The matric suction at which desaturation started would in fact be the air-entry value of the test specimen.

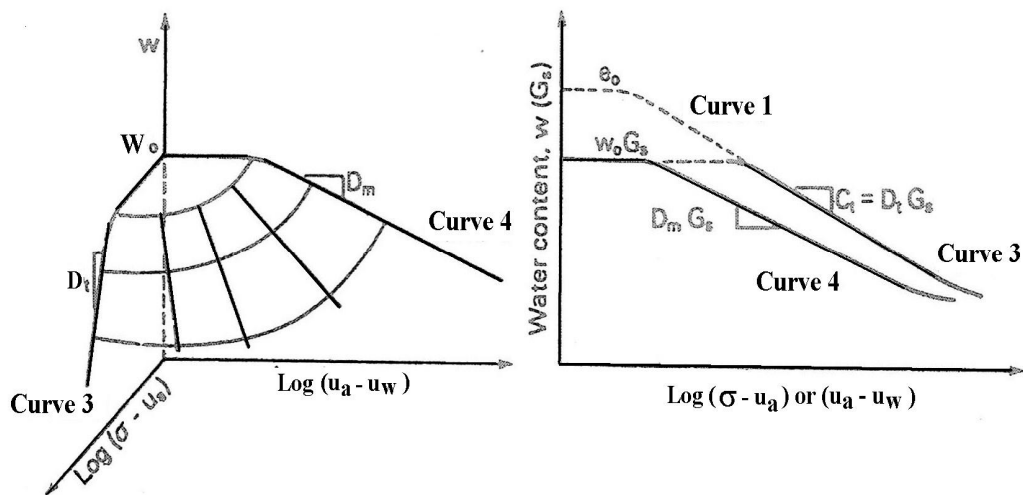


Figure 6.20. Constitutive surface of water content versus net normal stress and matric suction



Figure 6.21. Side view of the triaxial test set up

The volume change of the soil skeleton  $\Delta V_s$  was monitored continuously by laser sensors during the consolidation process. Measurements were taken at seven equally-spaced locations along each vertical line and the average of these measurements was taken as the displacement of the corresponding face. The mean value of the average displacements of the two opposite faces was taken to be the displacement along an axis normal to the faces, from which the lateral strain of the specimen could be computed. As the specimen properties and loading condition were taken to be isotropic, the volumetric strain and hence change in volume of the soil skeleton  $\Delta V_s$  could be determined from the lateral strain.

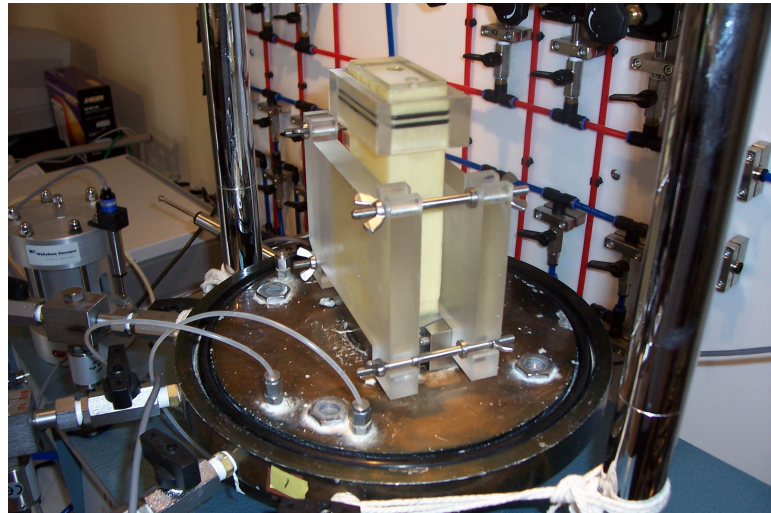


Figure 6.22. Side view of the plane strain test set up

Volume of water changes in the specimen  $\Delta V_w$  was also monitored continuously by the volume change gauge which was connected to the back-pressure line. Once the changes in the soil and water volumes had ceased, the test specimen was presumed to have fully consolidated under a matric suction of 10 kPa. Knowing  $\Delta V_s$  and  $\Delta V_w$  the void ratio  $e$  and water content  $w$  of the test specimen could be computed based on the fundamental phase relationships of soil. Next, the volume change gauge was set to bypass mode and the flushing line opened to a back pressure of 50 kPa. This was so as to flush out any bubbles that might accumulate below the high air-entry disc (HAED), so that a continuous water channel would be maintained between back pressure line and test specimen.

The flushing line was then closed when the flushing was complete and the volume change gauge set to flow mode.

The matric suction ( $u_a - u_w$ ) was next increased to 20 kPa by reducing the back pressure to  $u_w = 580$  kPa. The corresponding changes in the soil skeleton and water volumes,  $\Delta V_s$  and  $\Delta V_w$ , were monitored continuously until they had ceased, at which stage the corresponding void ratio  $e$  and water content  $w$  of the test specimen were computed from the cumulative changes in soil skeleton and water volumes. Air bubbles accumulating below HAED were flushed out as before. Thereafter, the entire procedure, that is from increasing the matric suction to the desired value up to flushing out the air bubbles, was repeated for matric suctions ( $u_a - u_w$ ) of 50, 100, 200, 300 and 500 kPa respectively, which were applied by reducing the back pressure accordingly, as shown in Table 6.2. The void ratio  $e$  and water content  $w$  could be determined by each increment of matric suction, and intersection curves of respective constitutive surfaces could be plotted as shown in figure 6.19 and 6.20.

Table 6.2. Stages of varying matric suction for IBM, PCBM dan ITM specimen

Back pressure (kPa)	590	580	550	500	400	300	100
Matric suction (kPa)	10	20	50	100	200	300	500

Another test specimen of IBN, PCBN, and ITN were prepared and the test apparatus set up similarly as before. In this case, however, the matric suction was maintained at zero during consolidation so that the specimen remained saturated throughout the test and no significant amount of air bubbles might be expected to collect below the HAED. Thus, a coarse porous disc was used in place of the HAED. To provide an initial net normal stress of  $(\sigma_3 - u_a) = 10$  kPa and matric suction of  $(u_a - u_w) = 0$ , a cell pressure of  $\sigma_3 = 110$  kPa, back-pressure of  $u_w = 100$  kPa and pore-air pressure of  $u_a = 100$  kPa were applied to the IBN, PCBN and ITN specimen, which were in a saturated condition. Specimen of ITN was in triaxial test set up (Figure 6.20), while specimen of IBN and PCBN were set up under plane strain condition (Figure 6.21). the saturated specimen. The changes in



soil skeleton and water volumes,  $\Delta V_s$  and  $\Delta V_w$ , were then monitored continuously and when these changes had ceased, the total changes in soil and water volumes were noted.

The net normal stress was first increased to 20 kPa by increasing the cell pressure to 120 kPa. The changes in soil and water volumes,  $\Delta V_s$  and  $\Delta V_w$  were then monitored continuously and when the changes had ceased, the total changes in soil and water volumes were noted. Thereafter, the entire above procedure was repeated for net normal stress of 50, 100, 200, 400 and 800 kPa, as shown in Table 6.3. As in the case of the first test specimen, the void ratio  $e$  and water content  $w$  were computed for each increment of net normal stress and the intersection curves of the corresponding constitutive surfaces plotted as shown in figure 6.19 and 6.20, although, in this case is for a matric suction of zero.

Table 6.3. Stages of varying net normal stress for IBN, PCBN dan ITN specimen

Cell pressure (kPa)	100	120	150	200	300	500	900
Net normal stress (kPa)	10	20	50	100	200	400	800

### 6.5.3. Compression process

The specimen was then compressed by elevating the base of the confining pressure cell at a constant velocity of 0.08 mm/m with the drainage line closed at net normal stress of 0 and matric suction of 500 kPa for IBM, PCBM, and ITM specimen and at matric suction of 0 and net normal stress of 800 kPa for IBN, PCBN, and ITN specimen. This loading rate was deduced based on the permeability of adopted kaolin clay suggested by Bishop and Henkel (1962). The data were recorded at 3 minute interval test and it was terminated at the axial strain of about 20 % or sooner. The specimen was then taken out immediately for the purpose of moisture content test. In the analysis of the behaviour of the brittle partially saturated clay, the pore pressure parameter would be required in order to the determined the pore pressure increments, matric suction, and volume changes

as can be seen the detail in chapter IV. The procedure was proposed by Fredlund and Rahardjo (1993), although adapted to biaxial conditions. Table 6.4 shows the information of compression test on partially saturated clay.

Table 6.4. Compression tests on partially saturated kaolin clay specimen

Test Name	Specimen type	Test Type	B-value	Matric suction (kPa)	Net normal stress (kPa)	CP (kPa)	BP (kPa)	PP (kPa)
IBM	Intact	Biaxial	0.94	500	0	100	600	600
PCBM	Pre-crack	Biaxial	0.95	500	0	100	600	600
ITM	Intact	Triaxial	0.95	500	0	100	600	600
IBN	Intact	Biaxial	0.94	0	800	900	100	100
PCBN	Pre-crack	Biaxial	0.96	0	800	900	100	100
ITN	Intact	Triaxial	0.94	0	800	900	100	100

## 6.6. Testing on fracture toughness of partially saturated clay

Mode I fracture tests for kaolin clay specimens were carried out by referring to ASTM standard, which is explained in ASTM-E 399. According to ASTM-E 399, the compact specimen should have  $W$  (width) equal to twice the thickness,  $B$ . Pre-crack length/width ratio,  $a/W$  lies between 0.45 and 0.55. The specimen design is such that all critical dimensions,  $a$ ,  $B$  and  $W-a$ , are approximately equal. ASTM – E 399 recommends that the user performs a preliminary validity check using:

$$B, a \geq 2.5 \left( \frac{K_{IC}}{\sigma_{YS}} \right)^2 \quad 0.45 \leq \frac{a}{W} \leq 0.55 \quad (6.1)$$

where  $\sigma_{YS}$  is yield stress of the specimen

The specimens used for these experiments have  $a = 36$  mm,  $B = 36$  mm, and  $W = 72$  mm. From the geometry of the specimens tested, it was clearly shown that the geometry of the tests specimen met the requirement which designated by ASTM standard. Figure 6.23 shows the typical geometry of mode I test specimen.

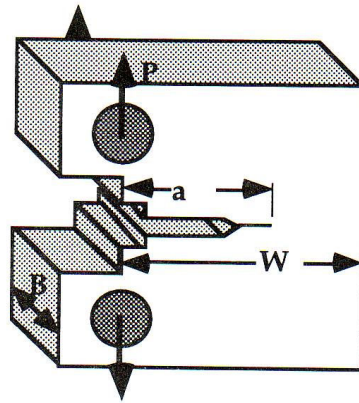


Figure 6.23. Typical geometry of Mode I test specimen (Anderson, 2005)

### 6.6.1. Specimen preparation

Specimen preparation of partially saturated clay adopted the same way how saturated kaolin specimens were prepared and set up in triaxial cell as outline in section 6.2 and section 6.3. It was then desaturated under a state of 300 kPa matric suction and zero net normal stress by applying a cell pressure of  $\sigma_3 = 350$  kPa, back pressure of  $u_w = 50$  kPa and pore-air pressure of  $u_a = 350$  kPa. The void ratio and water content of the test specimen after desaturation were determined in accordance with BS 1377 (British standard Institution, 1990).

When the volume changes  $\Delta V_s$  and  $\Delta V_w$  had ceased, the specimen was presumed to be in a homogenous state having these values of the stress variables. Knowing the initial water content, void ratio and volume changes of the specimen during consolidation, the degree of saturation, water content and void ratio of the specimen after desaturation could be determined from fundamental phase relationships of soil or computed via the constitutive surfaces for stress state of zero net normal stress and matric suction of 300 kPa. These values were taken to be representative of the state of the partially saturated soil prior to fracture testing.



Figure 6.24. Compact test specimen for Mode I test ( $K_{IC}$  test)

### 6.6.2. Mode I fracture test

The specimen was next taken from the triaxial cell for fracture testing. To ensure that the specimen would not absorb water from the back pressure line and swell when the pore air pressure was released, water from the back pressure was removed before the pore pressure was released. The specimen was then removed, the notch and two holes, as shown in Figure 6.24, were then form in it by the use of a sharp cutter which was supported vertically and mechanically pushed into the specimen, after which the test set up was assembled as shown in the Figure 6.25.



Figure 6.25. Mode I fracture test arrangement

The specimen was then secured to two steel loading clevises by using two steel pins. One of the clevises was connected to the moving arm of a 50 kN Wykeham Farrance triaxial testing machine, while the other was connected to the load cell of 10 kN capacity, which was in turn bolted to the opposite fixed end frame of the machine. A rate of displacement of 0.5 mm/min was then prescribed to the specimen via the loading clevises in order to minimize any inertial effects. All fracture tests data were recorded by the same data logger used in plane strain compression tests. Table 6.5 shows the information of the specimen prior to test the mode I fracture toughness on partially saturated clay.

Table 6.5. Mode I fracture toughness tests on partially saturated kaolin clay specimen

Test Name	Matric suction (kPa)	Net normal stress (kPa)	CP (kPa)	BP (kPa)	PP (kPa)
MS 300	300	0	350	50	350
MS 400	400	0	450	50	450
MS 500	500	0	550	50	550

#### **6.7. Test verification of finite element analysis on pre-crack partially saturated clay**

Two predictions could be drawn from the FE analysis, the crack propagation and pattern could theoretically be predicted for biaxial loading on the soil specimen, pre-consolidation under various boundary condition and also fracture toughness under various suctions. To verify the unified model theoretical crack propagation, it needs to compare the physical observation of crack propagation under varying biaxial loading condition. In this way the validity of the results obtained for  $C_m$ ,  $C_t$ ,  $D_m$ , and  $D_t$  and fracture toughness could be establish.

### **6.7.1. Specimen preparation and test apparatus set up**

Specimen preparation of partially saturated clay adopted the same way how saturated kaolin specimens were prepared and set up in triaxial cell as outline in section 6.2 and section 6.5. To obtain the most brittle specimen for biaxial loading, the specimen was consolidated under matric suction of 500 kPa and testing under plane strain test set up, as shown in Figure 6.2.2. The plane strain constraint was provided to simulate a 2-D problem. The void ratio and water content of the test specimen after desaturation were determined.

Since the specimen underwent consolidation under both applied net normal stress and matric suction, HAED was used throughout the consolidation process as it was able to function in both cases, whereas the standard porous disc would be ineffective in the case where matric suction applied. However, as a result of using HAED, a longer consolidation period was required, since the permeability of HAED is much lower than the conventional porous disc. Setting up was also similar to the steps as presented in the foregoing 6.5.1.

### **6.7.2. Test procedure for saturation, consolidation and loading the specimen**

Two intact specimens were tested similar to the ITM and IBN specimen in the foregoing 6.5 to obtain pore pressure and volume change parameter, and one pre-crack specimen was tested similar to the PCBM specimen in foregoing 6.5.1 to observe the crack propagation and pattern on the specimen.

Saturation and consolidation process adopted the same way how partially saturated kaolin specimens were tested, as mentioned in section 6.5.2 and 6.5.3. The saturation process adopted here is based on BS Standard (Head, 1985). The initial void ratio and water content of the test specimen were first determined according to BS 1377 (British Standard Institution, 1990). Constitutive surfaces of void ratio  $e$  and water content  $w$ , which provide the basis for determining the

degree of saturation  $S$  and hence the pore pressure parameters,  $B_a$  and  $B_w$ , the volumetric deformation coefficients  $m_{1s}$ ,  $m_{1w}$  and  $m_{2w}$ , upon which the pore pressure parameters  $B_a$  and  $B_w$  also depend, are evaluated from the volume change indices  $C_t$ ,  $C_m$ ,  $D_t$  and  $D_m$  which are likewise obtained from constitutive surfaces, as shown in Figure 6.19 and Figure 6.20.

The loading compression process for pre-crack specimen was carried out under undrained condition and the specimen was loaded monotonically with the velocity of 0.5 mm/min. This loading rate was established from the consolidation stage to be sufficient to sustain an undrained condition in the test specimen. During loading the volume change of soil and the axial displacement were recorded by an automatic data logger as described previously in sub sequent 6.2.4. The loading was applied until the specimen attained its ultimate condition.

## **CHAPTER 7**

### **RESULTS, ANALYSIS AND DISCUSSION**

#### **7.1. Introduction**

Laboratory test results, analysis and discussion are presented in this chapter. As stated in foregoing sub sequent 6.4, a total of six specimens under plane strain condition have been performed on saturated specimens of normally consolidated kaolin clay as well as over consolidated kaolin clay, under drained and undrained loading conditions, and a total of six specimens under plane strain as well as triaxial test set up have been performed on partially saturated specimens of brittle kaolin clay under drained loading condition. The main features of soil behaviour are presented according to the conventional laboratory testing of soil specimens. The trend of soil response, in different test set up of partially saturated brittle clay is also considered. The influence of discontinuities in varieties of normal stress and suction of partially saturated clay is also highlighted. Finally, the behaviour of partially saturated brittle clay using fracture mechanical approach is addressed.

The results analysis and discussion of the drained and undrained plane strain test of normally consolidated and over consolidated clay will be evaluated with in following sub section 7.2. The result of the intact specimens as well as pre-crack specimens in biaxial and triaxial test set up under different net normal stresses and maximum matric suctions will then be dealt in subsequent 7.3.



## 7.2. Behaviour of saturated over consolidated kaolin clay specimen

The plane strain compression test of normally consolidated as well as over consolidated clays is aimed to investigate the constitutive behaviour and failure patterns of these soils by the use of the new biaxial compression device that allow plane strain condition. Firstly, the kaolin specimen was isotropically consolidated to a certain level of consolidation pressure, in which in this study a maximum effective stress of 700 kPa was applied to each of the specimen. When the maximum effective stress had been reached the test specimen was allowed to swell isotropically to a certain effective stress, which depended upon the desired level of consolidation ratio. Following this the specimen was sheared under either drained or undrained condition.

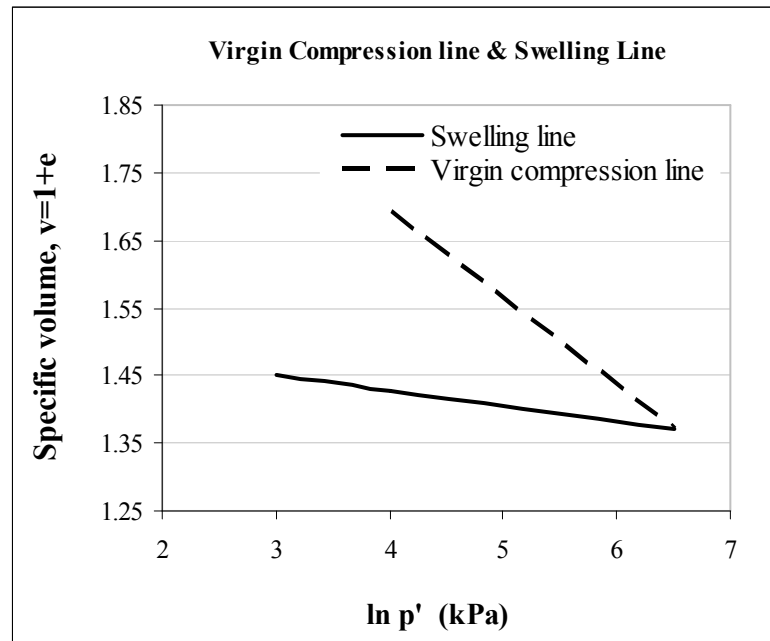


Figure 7.1. The virgin compression line and swelling line of kaolin clay specimen

Due to the loading and unloading process a curve was constructed which can be used to derive critical state parameters such as slope of critical state line  $\lambda$  and slope of swelling line  $\kappa$ . The plot of virgin compression line and swelling line as well as critical state line are depicted in Figure 7.1 and 7.2 respectively.

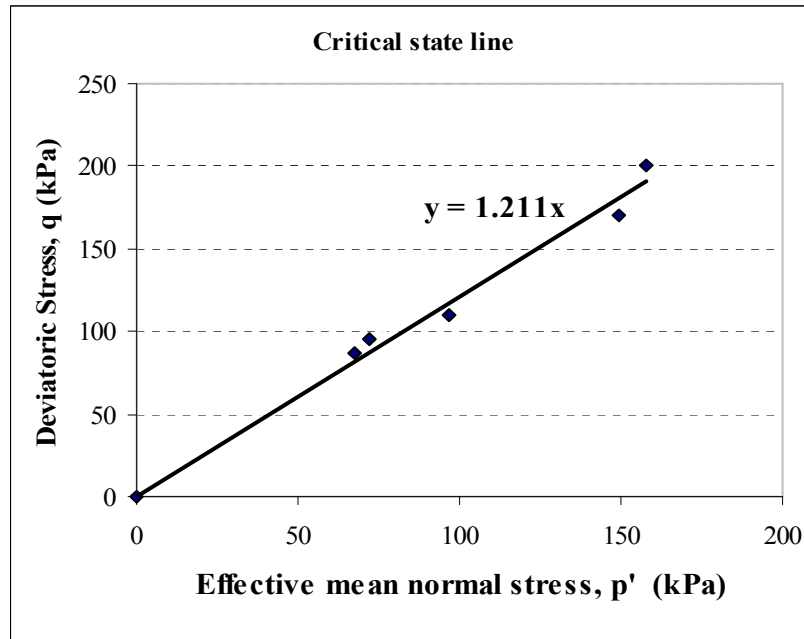


Figure 7.2. The Critical state line in  $p':q$  plane

The critical state represents a state in which a soil can be sheared indefinitely with no further change of effective stresses or specific volume. The slope of the critical state line in the  $p':q$  plane is denoted by  $M$ . The value of the critical state is determined by plotting the stress paths of shear tests on soil specimens in  $p':q$  plane and obtaining the stress ratio at the end of the test at very large strain, where the specimen has reached a so-called critical state, as shown in Figure 7.2.

The peak strengths of over consolidated clay specimens of kaolin clay have been observed to fall on the Hvorslev surface, which is obtained as a straight line in normalized  $p':q$  plane, as shown in Figure 7.3. The slope of the line denotes the value of parameter  $m_H$ . Some others parameter data of kaolin clay is summarised and presented in Table 7.1.

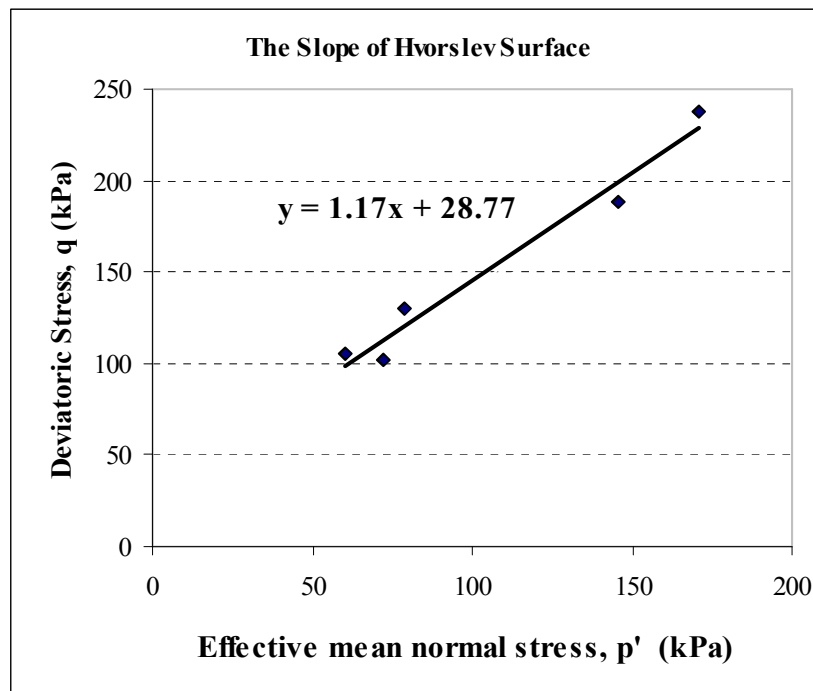


Figure 7.3. The Hvorslev surface in  $p'$ :  $q$  plane

Table 7.1. Material parameters of remoulded kaolin clay.

Parameter	Values
$\lambda$ , virgin compression line slope	0.129
$\kappa$ , swelling line slope	0.023
$N$ , specific volume at $p'=1$ kPa (NCL)	2.03
$\Gamma$ , specific volume at $p'=1$ kPa (CSL)	2.01
$M$ , critical state line slope	1.21
$m_H$ , Hvorslev surface slope	1.17
$\alpha$ , Hvorslev surface intercept, kPa	28.78
$G_s$ , Specific gravity	2.6
LL, Liquid limit (%)	53.5
PL, Plastic limit (%)	30.76
PI, Plasticity Index (%)	22.74

### 7.2.1. Normally consolidated-undrained plane strain tests

The test of normally consolidated-undrained plane strain was followed based on the ASTM standard. Firstly, the specimen was saturated by applying cell pressure and back pressure until it reached the B value of about 0.96-0.98. A consolidation process was then taken place with the applied effective stress of up to 700 kPa. Prior to shearing, the specimen was placed in the pressure cell under globally undrained conditions and the axial load was applied through the loading ram. The data were recorded at 5 minute interval and it was terminated at the axial strain of about 20 % or sooner to prevent localized deformation marking become visibly distorted. The deviatoric stress against the axial strain curves of the specimen the normally consolidated undrained test under confining pressure of 1000 kPa is presented in Figure 7.4, while the changes in pore pressure versus the axial strain is plotted in Figure 7.5.

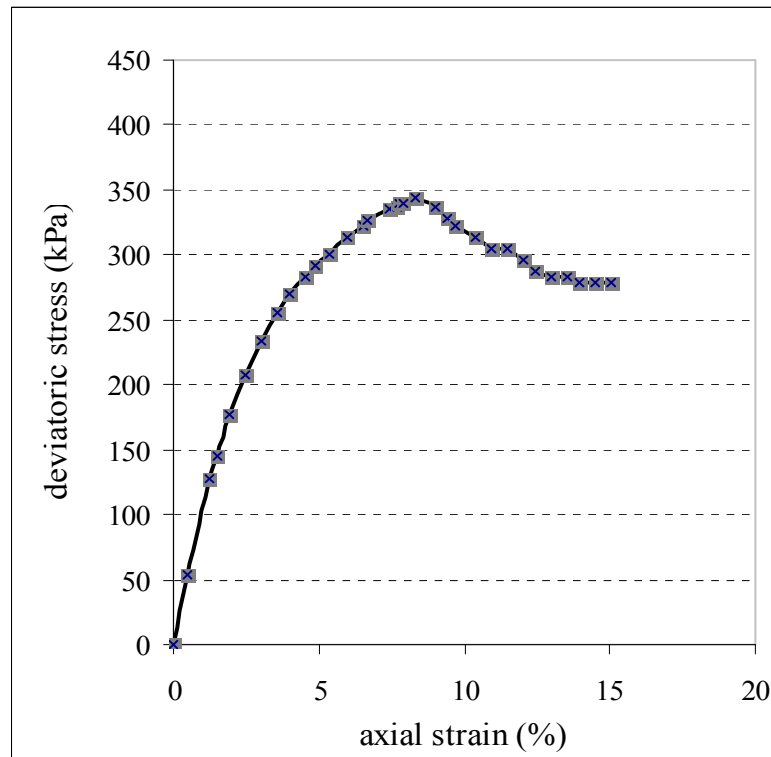


Figure 7.4. Deviatoric stress versus axial strain of NC clay specimen

As can be seen from the graph, the curves went up monotonically with the increasing vertical strain until it failed at the peak stress of 343 kPa which corresponds to an axial strain of about 8.3 %, followed by strain softening behaviour until it reaches critical state and remained at constant stress around 304 kPa starting from the axial strain of about 11.5 %. It is also clearly shown from the graph that the softening behaviour in normally consolidated clay under plain strain testing is different to the data that commonly obtained by triaxial apparatus, as mentioned in sub section 2.4 and Figure 2.14 (Mochizuki et al, 1993). In contrast to the data from the triaxial apparatus which the test specimen failed in bulging shape, in this plane strain result the failure of the specimen is splitting into two parts, as shown in Figure 7.4.

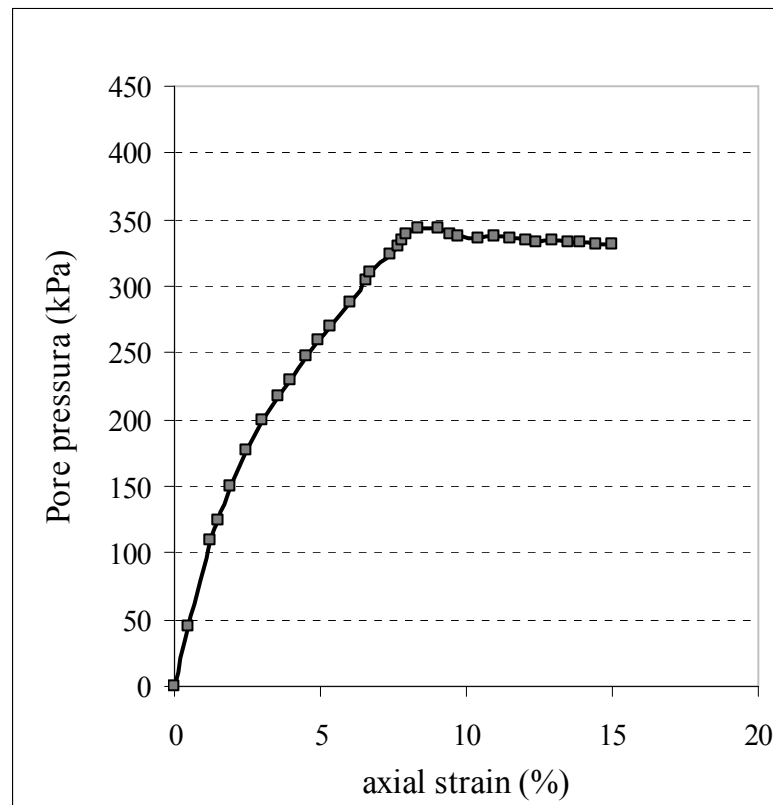


Figure 7.5. Pore pressure versus axial strain of NC clay specimen

### **7.2.2. Over consolidated-undrained plane strain tests**

As shown in foregoing Table 6.4 of Chapter VI, three undrained tests, OCR16CU, OCR10CU and OCR4CU, were carried out with the OCR values of 16, 10 and 4 respectively. Prior to shearing, the specimens were placed in the pressure cell, and an effective pressure of 100 kPa applied, under globally undrained conditions. Degrees of saturation of 95 % to 99 % were inferred for the soil specimens from pore water pressure response measured. Increments of back pressure of up to 200 kPa were then applied to the specimens, while opening the drainage line, in order to achieve a near 100% degree of saturation. The value of “B” for the very stiff to stiff soils, have been found by Black and Lee (1973) to range between 0.91 and 0.99. For all the specimens tested, the “B” values, at the end of the saturation stage, lay between 0.95 and 0.99. This resulted in effective cell pressures of 343.75 kPa, 370 kPa and 475 kPa being applied to the specimens in tests OCR16CU, OCR10CU and OCR4CU, respectively, as indicated in Table 6.1.

To impose an effective mean stress on the specimen that would provide the required OCR value, the applied cell pressure was then adjusted. The specimen was next allowed to consolidate under plane strain condition. As the imposed value for the mean effective stress was close to the pre-existing value of the soil sample, only minor volume changes were observed. All three undrained tests were performed with the drainage lines closed, under a displacement-controlled loading rate of 0.08mm/min, which is equal to the loading rate of 0.7% per hour with the height of specimen of 72 mm (Bishop and Henkel, 1962). Similar to that of normally consolidated clay test mentioned in preceding 7.2.1 earlier, the majority of the tests were stopped at axial strain of about 20% or less in cases where the specimen developed marked localized deformation and became visibly distorted.

Table 7.2. Moisture content variation in failed CU tests specimen

Test Name	Global moisture content at failure (%)	Moisture content within shear band at failure (%)	Moisture content difference (%)
OCR4CU	21.83	22.27	2.016
OCR10CU	23.18	23.61	1.855
OCR16CU	23.85	24.78	3.899

The specimen was immediately taken out after the completion of each test for moisture content determination. Representative portions of soil from the shear band, boundary and middle layer of the specimen were trimmed off and weighed for moisture content determination. The results are presented in Table 7.2. A comparison of the initial values of water content before shearing (as indicated in foregoing Table 6.1), and those after shearing (as indicated in preceding Table 7.2) shows that the water content of the undrained test specimen varied during the test. Moreover, the water content at failure, within the shear band, is correspondingly higher than the overall or global water content. The formation of shear zones, in the heavily over consolidated clay specimen, is likely to have caused local drainage and volume changes, so that the test was not strictly undrained. The result of biaxial compression test on over consolidated undrained test of kaolin clay specimen is summarised and presented in Table 7.3

Table 7.3. Result of biaxial compression test on undrained over consolidated clay

Test Name	$\sigma_3$ (kPa)	$q_f'$ (kPa)	$p_0'$ (kPa)	$p_f'$ (kPa)	$v_0$	$v_f$
OCR4CU	616	237.65	175	296.22	1.582	1.582
OCR10CU	336	129.63	70	202.21	1.598	1.598
OCR16CU	272	104.94	43.75	175.73	1.608	1.608

The deviatoric stress against the axial strain curves of the three specimens in the consolidated undrained test are presented in Figure 7.6, while the stress path

of the specimen shown in Figure 7.7. In general, the stress-strain curves went up monotonically with the increasing vertical strain until they reach peak stresses followed by strain softening behaviour until it reaches critical state. The increasing in axial strain without increasing shear stress then occurred to the specimens. This phenomenon is typical behaviour of over consolidated clay when it was sheared. The curves also showed that the specimen exhibited elastic as well as plastic behaviour.

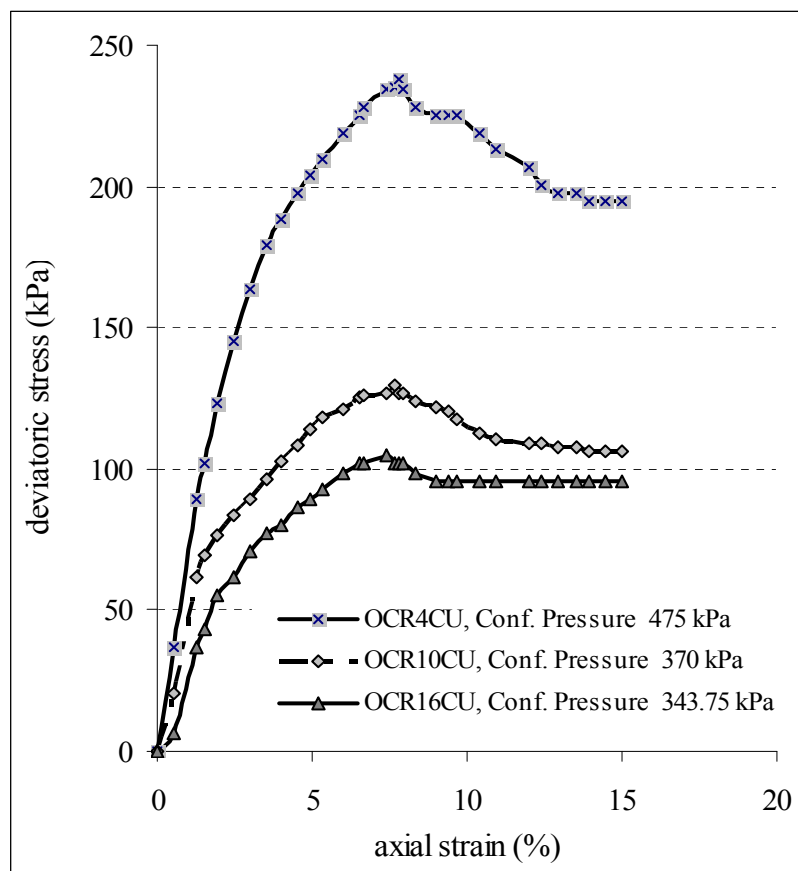


Figure 7.6. Deviatoric stress versus axial strain of CU specimen

The shear stress of specimen with the lower OCR value were higher along the vertical strain than that the shear stress of specimen with the higher OCR value. This was occurred because it was sheared under the lower confining pressure. The highest failure stress of 237.65 kPa at about 7.8 % its axial strain was reached by OCR4CU specimen, followed by OCR10CU specimen and



OCR16CU specimen with the peak stresses of 129.63 kPa, and 104.94 kPa at about 7.7% and 7.4 % axial strain, respectively. In general, it can be said that the higher the confining pressure the more strain hardening it would become. It was also displayed from the graph that the pronounced failure stress was reached by the specimen with the higher OCR value than the failure stress of specimen with the lower OCR value. Similar observations have been reported elsewhere (Mochizuki et.al., 1993; Lo et.al., 2000).

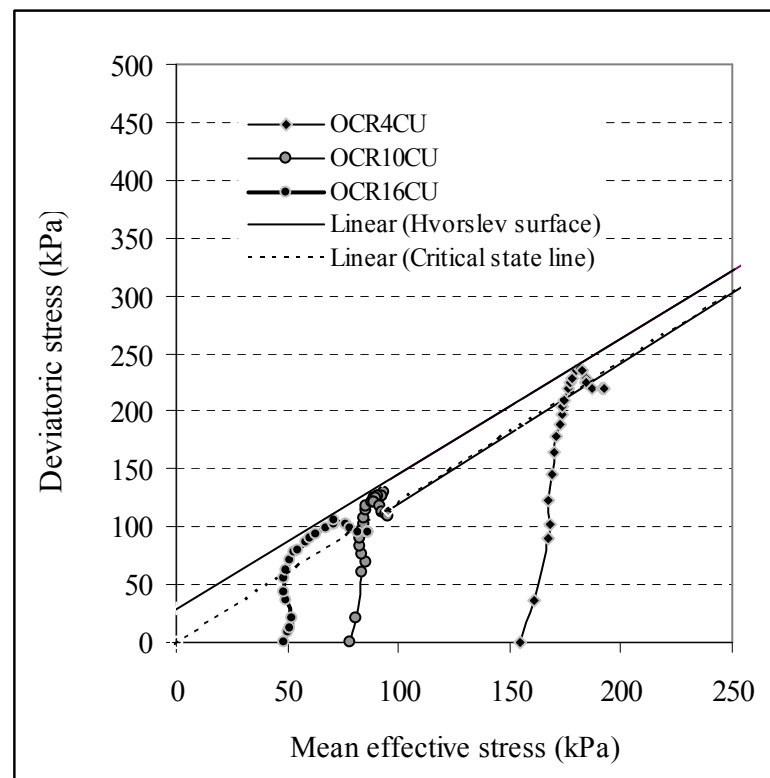


Figure 7.7. Deviatoric stress versus axial strain of CU specimen

Atkinson and Richardson (1987) studied the undrained behaviour of heavily over consolidated London clay, under triaxial compression loading, and reported that in nominally undrained tests, relatively, large hydraulic gradients were present near the shear zones that might lead to local drainage and volume changes, such that the tests would not, strictly have been undrained. The portion of the final state path in an undrained test, when prominent shear bands form, would not reach the ultimate point, corresponding to ultimate failure of a true

undrained test (Atkinson and Richardson, 1987). The peak point represents the end of the undrained test, which may occur when strong discontinuities develop and the specimen becomes severely distorted, or the limit of travel of the biaxial test device is reached. In such a test, during the initial portion of the state path, the strains are usually small. Shear banding is not likely to form, and there would probably be little volume change, resulting in practically undrained behaviour.

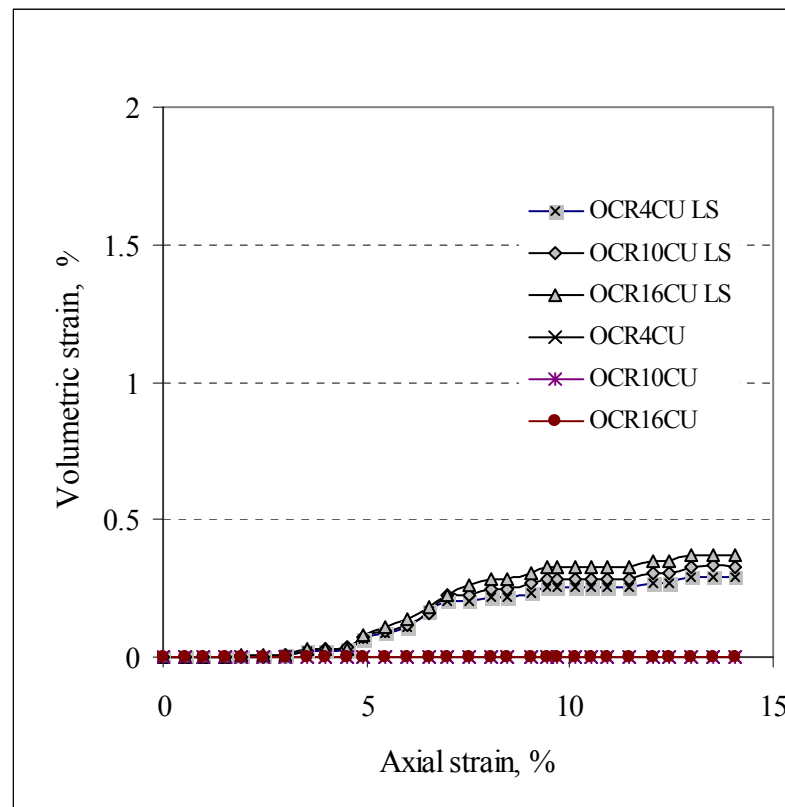


Figure 7.8. Volumetric strain versus axial strain of CU specimen

The volumetric strain-axial strain and specific volume-effective mean normal stress responses of the test specimens are plotted in Figure 7.8. As can be seen from the graph that almost zero volume change may be noted up to the initial loading stage, after which a slight expansive volumetric strain, about 0.2% to 0.46%, was measured by the laser sensor. Atkinson and Richardson (1987) suggested that such a small amount of volume change is likely to take place in the shear zone, as a result of local drainage, the degree of which would increase with higher OCR value. However, in considering the specimen as a whole, it might

seem that no volume change had occurred. The peak deviator stress would approximate the point at which volume changes develop relatively strong, and the reduction in deviator stress after the peak would be associated with continuing local drainage.

Excess pore pressure versus axial strain of specimen is shown in Figure 7.9. Positive excess pore pressure might be expected to be generated up to the elastic yield point, followed by a negative pore pressure, which reflects the dilatant behaviour in the undrained test of over consolidated clay. However, since the specimen did not reach the ultimate condition defined by a truly undrained test, only small amount of negative pore pressure was registered by the corresponding transducer. The response of the specimens in undrained tests of the present study seems to be consistent with the findings of Atkinson and Richardson (1987). The results are fairly typical for specimen of heavily over consolidated clay subjected to undrained compression.

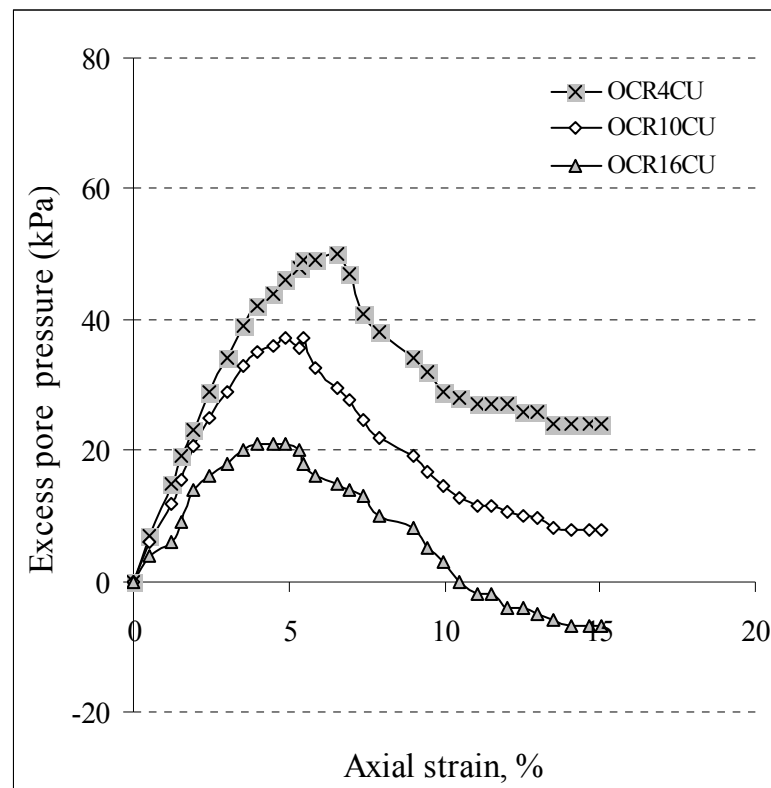


Figure 7.9. Excess pore pressure versus axial strain of CU specimen

### 7.2.3. Over consolidated-drained plane strain tests

Two drained tests, which are OCR8CD and OCR20CD, were carried out with the OCR values of 8 and 20, respectively. Prior to shearing, the specimens were placed in the pressure cell and saturated by increments of applied back pressure, in a similar manner as stated in preceding 6.2.1 for the undrained tests. A degree of saturation close to 99% was inferred for all the soil specimens, as shown in foregoing Table 6.1. The value of “B” for the very stiff to stiff soils, have been found by Black and Lee (1973) to range between 0.91 and 0.99. Once the required saturation was achieved, the applied cell pressure was adjusted to impose an effective mean stress on the specimen that would provide the desired OCR value. As indicated in Table 6.1, this resulted in effective cell pressures of 387 and 335 kPa being applied to the specimens in tests OCR8CD and OCR20CD, respectively.

The specimens were then allowed to consolidate under the plane strain conditions. As the imposed value of the mean effective stress was very close to the pre-existing value of the sample, only minor volume changes were observed. All there drained tests were performed with the drainage lines open, under a displacement-controlled loading rate of 0.004mm/min, which corresponds to a nominal axial strain rate of 0.35%/hour, for a specimen height of 72 mm. The appropriate rates have been deduced based on the permeability of the adopted kaolin clay (Bishop and Henkel, 1962). As mentioned earlier in sub sequent 7.2.1 and 7.2.2, the majority of the drained plane strain tests were also stopped at an axial strain of about 20%, or sooner, in case where the specimen developed strong localized deformation and became visibly distorted.

Table 7.4. Moisture content variation in failed CD tests specimen

Test Name	Global moisture content at failure (%)	Moisture content within shear band at failure (%)	Moisture content difference (%)
OCR8CD	22.71	23.18	2.070
OCR20CD	24.19	25.12	3.845

After the completion of each test, as in the case of the undrained tests, the specimen was straightaway taken out for moisture content determination. Representative portions of soil from the shear band, boundary and mid-section of the sheared specimen halves were trimmed off, and weighed for moisture content determination, the results of which are presented in Table 7.4. It is evident that the water content in the shear band was higher than the overall moisture content of the failed specimen, that is, maximum dilatancy occurred in the localized shear zone. In the drained tests, once part of the specimen had dilated, due to shear banding, the soil within the dilated region became less stiff than the surrounding soil. Further straining took place primarily in this softer and thus weaker soil, which continued to dilate until it reached the critical state. The result of biaxial compression test on drained over consolidated clay is summarised in Table 7.5

Table 7.5. Result of biaxial compression test on drained over consolidated clay

Test Name	$\sigma_3$ (kPa)	$q_f'$ (kPa)	$p_0'$ (kPa)	$p_f'$ (kPa)	$\nu_0$	$\nu_f$
OCR8CD	488	188.27	87.5	237.26	1.595	1.534
OCR20CD	264	101.85	35	241.95	1.613	1.48

Figure 7.10 shows the plots of deviatoric stress versus global axial strain. The stress-strain curves were obtained in accordance with the routine correction that uses the average sectional area of the specimen. The stress increases monotonically, up to about 7.8% and 5.5% axial strain for the specimen of OCR8CD and OCR20CD respectively, whereupon it decreases rapidly. For the drained tests on OCR clay, the stress path reaches its maximum on the Hvorslev yield surface, whereupon plastic deformation takes place. The soil specimen reaches its critical state after a certain amount of strain softening has taken place. The peak stresses for the two tests correspond to values of 188.27 kPa and 101.85 kPa, for the specimen of OCR8CD and OCR20CD respectively. It was also shown from the graph that specimen with higher OCR value reach the Hvorslev yield surface at a lower axial strain and peak deviatoric stress.

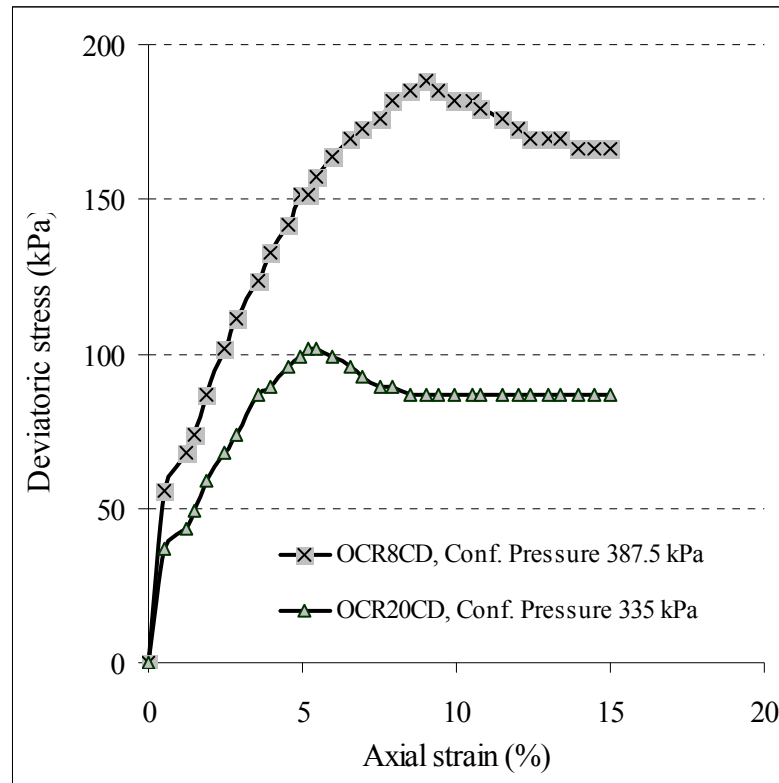


Figure 7.10. Deviatoric stress versus axial strain of CD specimen

The figure also includes the shear stress-strain plot from each test, depicted previously. Accordingly, a relatively uniform mode of deformation is maintained until peak point, whereupon the lateral displacement, and hence the lateral strain, increased rapidly, as indicated by the abrupt change in slope of the curve. The peak point, may be regarded as the onset of non-uniform deformation, or shear banding, whereas the peak stress point is associated with a fully-developed shear band across the specimen. Visual inspection, during the test, revealed that changes in the pre-marked gridlines, on the specimen, became visible as soon as the axial load reached its peak point. Shortly after that, a clear formation of the shear band was observed across the specimen. This was evident in all the tests. These observations are consistent with the development of a sliding surface, on which most of the deformation is concentrated (Viggiani et al., 1994). It is noteworthy that, as the OCR value gets higher, the peak stress has a greater tendency to occur at, or right after, the onset of strain localization.

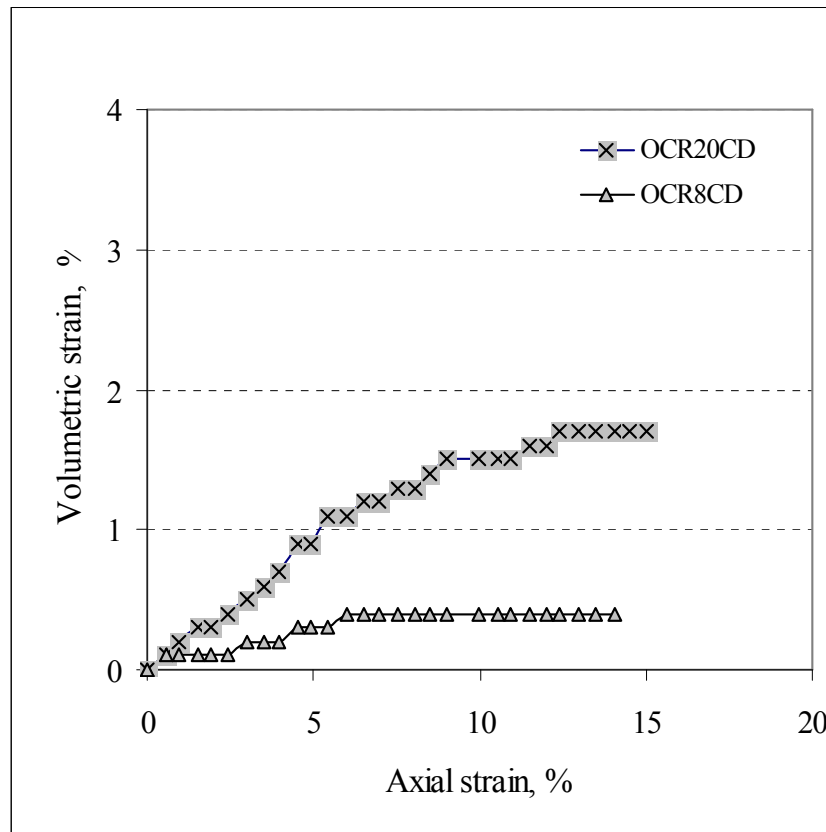


Figure 7.11. Volumetric strain versus axial strain of CD specimen

The global volumetric strain, computed from the volume of water expelled from the specimen (burette method), is plotted against the global axial strain in Figure 7.11. As can be seen from the graph, compressive volumetric strains are taken as positive. The specimen is compressed until the peak stress is attained, whereupon it starts to dilate, until it reaches the critical state, and further volumetric strains become negligible. This behaviour of volume change is consistent with routine observation of shear testing of clay specimens which are on the dry side of critical state. The burette method showed too small a volume expansion of the specimen. This is probably due to the fact that there was insufficient water intake into the voids of the expanding specimen. Mochizuki et al (1998) used no-contact “gap-sensors” to measure the lateral displacement of over consolidated sand specimens, tested under triaxial and plane strain conditions, and reported that the volumetric strains, computed from the lateral deformation of the sand specimen, also reflected greater dilatancy than that registered by the burette method.

In plane strain stress tests, the condition of zero strain ( $\epsilon_2 = 0$ ) along the out-of-plane axis is imposed on the specimen, which mobilizes the intermediate principal stress,  $\sigma_2$ . Evaluation of  $\sigma_2$  either by calculation or by direct measurement has been a problem of interest among researchers (Nagaraj and Somashekar, 1979; Vaid and Campanella, 1974). The mathematical determination of  $\sigma_2$  is expressed in terms of Poisson's ratio. The intermediate principal stress  $\sigma'_2$  is somewhere between  $\sigma'_1$  and  $\sigma'_3$ , and its exact value is difficult to measure in plane stress, but the test data available elsewhere (Potts and Zdravkovic, 1999). In the present study, total stress cells, flush with the surfaces of the rigid walls have been used to measure  $\sigma'_2$  directly.

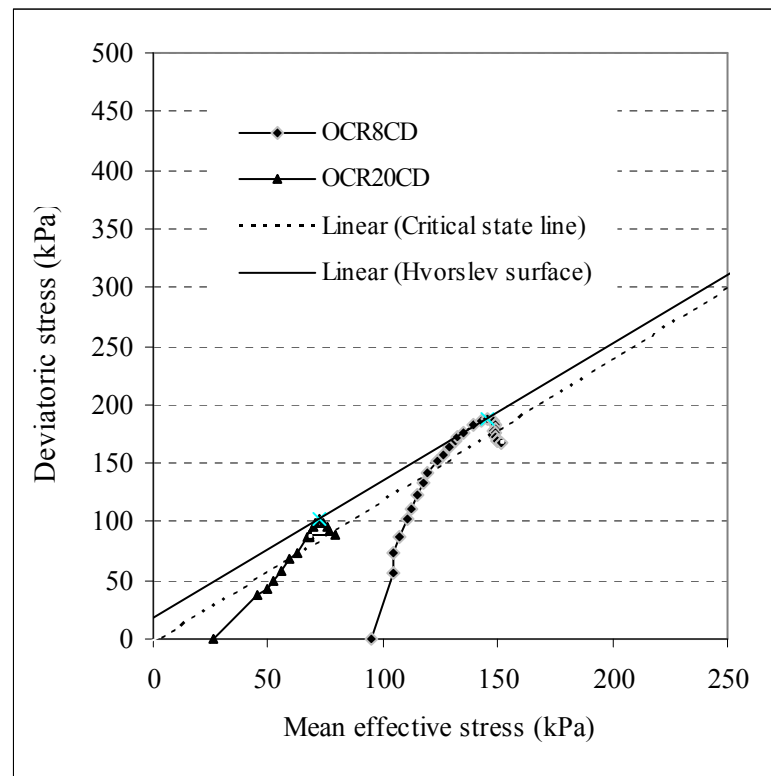


Figure 7.12. Stress Path of CD Specimens

In the foregoing drained tests, the clay specimen were subjected to axial compression, while the radial total stress was maintained constant and no significant excess pore water pressures were allowed to develop. Figure 7.12 depicts the stress paths of the two drained tests. Each stress path reaches the Hvorslev surface, at the yield point, whereupon it re-traces the drained path down,



to intersect the critical state line. The graph shows the drained stress path in the  $p':q$  plane, in which the specimen compresses along the swelling line up to the yield stress, from which it approaches the critical state line (CSL) by expanding in volume. Once the critical state is reached, unlimited shear strain takes place without any further change in deviatoric stress and specific volume. The CSL was obtained from the  $p':q$  plots of the sets of plane strain compression tests performed on the clay specimens as discussed in previous subsequent 7.2.1.

From the foregoing experimental results, it is evident that the fully-developed shear bands formed in the test specimen when their stress state reached the peak value. In most cases of drained shearing on soils, shear zones have been observed to occur at, or soon after peak state (Skempton and LaRochelle, 1965; Roscoe, 1970). When shear bands from the uniformity of deformation is disrupted and consequently, the assumption of a homogenous test specimen would be violated. This would, amongst other indications, be reflected in the water content distribution within the specimen, as shown in Table 7.4. The average water content denotes the overall moisture content of the saturated specimen after the test. As shown in Table 7.4, it is evident that the water content in the shear band is the maximum, which is consistent with the observation that the soil in this zone is the first to soften and dilate, and does so the most, right up to the critical state.

### **7.3. Behaviour of partially saturated kaolin clay specimen**

#### **7.3.1. Shear strength behaviour of partially saturated clay**

The typical result given by specimens tested under biaxial condition of IBM, IBN, PCBM, and PCBN as well as specimen observed under triaxial test set up of ITM and ITN will be discussed in the following discourse. The shear strain response of the specimen tested under matric suction 0 kPa and net normal stress 900 kPa are depicted in Figure 7.12, while stress-strain curves of the intact

specimen tested under net normal stress 0 kPa and matric suction 500 kPa are presented in Figure 7.13. The peak stress and strain of the specimen is summarised in Table 7.6.

The deviatoric stress against the axial strain curves of specimens presented in Figure 7.13 as well as in Figure 7.14 showed that the curves increased monotonically with the increasing of vertical strain until they reach peak stresses followed by strain softening behaviour. It is clearly shown from the graphs that the stress strain response of the specimens exhibit elastic behaviour. According to Lo et al (2005) this is the typical phenomenon of specimen of brittle, hard partly saturated soil specimen and demonstrated elastic failure only behaviour.

Table 7.6. The peak stress versus axial strain of partially saturated clay specimen

Suction Pressure	Specimen name	Peak stress (kPa)	Vertical strain (%)
Zero matric suction and Net normal stress of 900 kPa	IBM	228.395	3.9
	PCBM	124.519	3.3
	ITM	175.926	3.6
Zero net normal stress and Matric suction of 500 kPa	IBN	159.178	3.6
	PCBN	125.336	2.7
	ITN	139.464	3.0

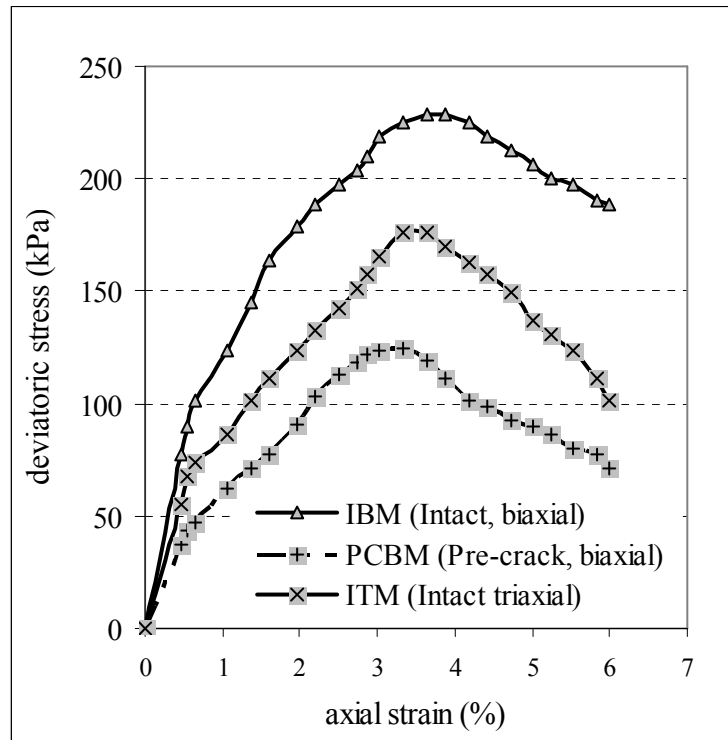


Figure 7.13. Deviatoric stress versus axial strain of specimen under matric suction 0 kPa and net normal stress 900 kPa

As can be seen in Figure 7.13, the shear strength of the intact specimen of IBM was greater along the vertical strain than that the specimen containing discontinuities or pre-crack specimen of PCBM. The highest failure stress of 228.395 kPa was reached by the intact specimen of IBM, and the lowest failure stress of 124.519 kPa was derived by the pre-crack specimen of PCBM. The presence of a fissure or discontinuity makes the soil weaker as the effective area offering resistance to shear is reduced. The shear strength along a surface of discontinuity is thereby less than that of the intact material. It is also shown from the graph that a lower axial strain of peak shear strength was occurred to the pre-crack specimen than the intact specimen. The results of the present work seem to be consistent with the observation reported by Mita (2004) and Lo et al (2000).

Mita (2004) and Lo et al (2000) studied the behaviour of heavily over consolidated kaolin clay containing of a 6 cm length of pre-crack and a 9 cm length of pre-crack compared to the intact specimen subjected to biaxial

compression loading and reported that the peak strength of the fissured specimens were correspondingly lower than the intact specimen before falling towards the same critical value. The observation also shown that if the shear displacement could be continued far enough, the shearing resistance for the specimens would fall to the same residual strength, which reflects the sliding resistance of the material.

The shear strength of the intact specimen tested under triaxial condition of test ITM is higher along the vertical strain than that the shear strength of intact specimen tested under plane strain condition of IBM. It is also shown that the earlier peak stress of specimen under triaxial test was reached at axial strain of about 3.6 % corresponding to the peak stress of 175.926 kPa than that the peak stress of intact specimen tested under plane strain at 3.9 % axial strain with the peak stress value of 228.395 kPa. Similar observation had been reported by Mochizuki et al (1993) who investigated the behaviour of dense, medium and loose sands under triaxial and biaxial condition. The stress strain curve was presented previously in Figure 2.14. It was concluded that when soil is tested under plane strain conditions, it, in general, exhibits a higher compressive strength and lower axial strain than that of axis symmetric condition.

Figure 7.14 presents the deviatoric stress versus strain of the partially saturated clay specimens under zero net normal stress and matric suction of 500 kPa. It can be seen from the graph that the shear strength of the intact specimen of IBN were higher along the vertical strain than that the fissured specimen of PCBM. The highest peak stress of 159.178 kPa at 3.6 % axial strain was reached by the intact specimen of IBN, and the lowest peak stress of 125.336 kPa at 2.7 % axial strain was derived by the fissured specimen of PCBN. Similar to that specimen under zero matric suction and net normal stress of 900 kPa discussed earlier, the occurrence of a fissured or discontinuity in the specimen makes the soil weaker as the effective area offering resistance to shear is reduced. The shear strength along a surface of discontinuity is thereby less than that of the intact material. The pre-crack specimen of test PCBN reached earlier peak strength before falling toward whereas the peak strength of the pre-crack specimen of

PCBN was correspondingly lower. This is in well agreement with the work reported by Mita (2004) and Lo et al (2000). Similar to the earlier discussion, compared to the intact specimen tested under triaxial condition of test ITN, not only had higher peak stress, but the specimen of test IBN also had higher shear strength along the vertical strain. This observation is in consistent with the results obtained by Lo et al (2000) and Mochizuki et al (1993).

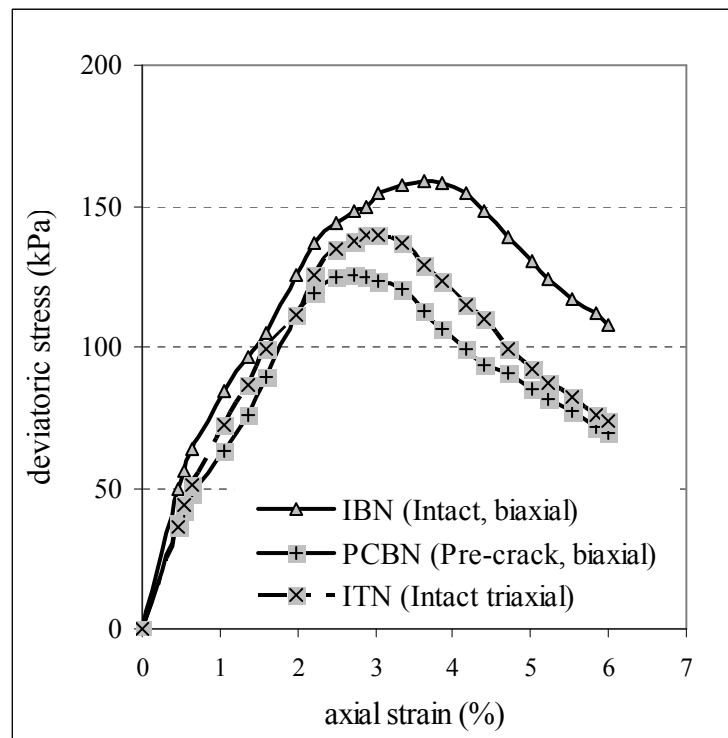


Figure 7.14. Deviatoric stress versus axial strain of specimen under net normal stress 0 kPa and matric suction 500 kPa

### 7.3.2. Volume change characteristic of partially saturated clay

The value of void ratio of the specimen with varying matric suction and net normal stress were obtained at different loading stages of the experiments. The results is summarised and tabulated in Table 7.7 and Table 7.7 respectively. From this results, the graph of void ratio against the log matric suction and log net normal stress have been plotted, as shown in Figure 7.15 and Figure 7.16 respectively.

Table 7.7. Void ratio variation with matric suction

Matric suction, MS (kPa)	Log MS	Void ratio (e)		
		IB	PCB	IT
20.0	1.30103	1.18994	1.18925	1.18736
50.0	1.69897	1.18985	1.18905	1.18729
100.0	2.00000	1.18670	1.18451	1.18658
200.0	2.30103	1.18307	1.17926	1.18134
300.0	2.47712	1.18091	1.17658	1.17832
500.0	2.69897	1.18005	1.17568	1.17730
Cm		0.0115	0.0160	0.0173

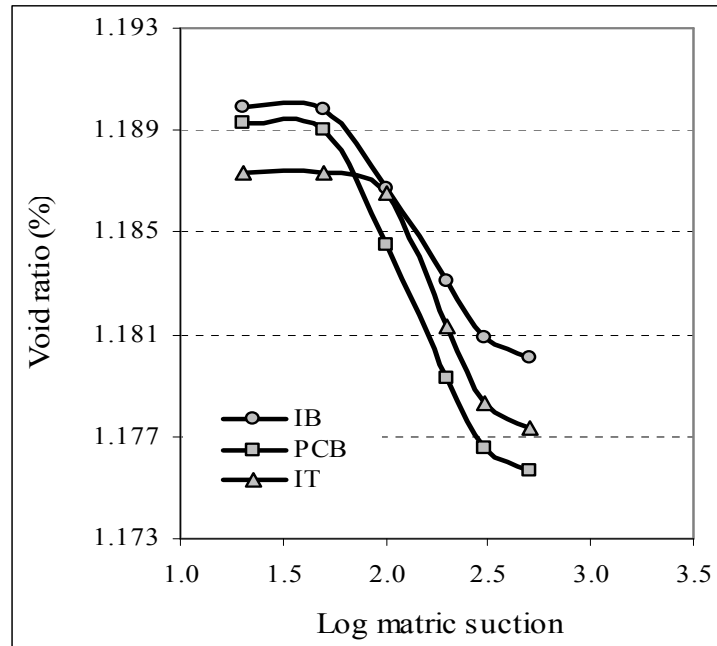


Figure 7.15. Void ratio against log matric suction of specimen  
zero net normal stress

The gradient of the best straight line of the graph, that is the linear portions of the constitutive surfaces, would be the  $C_m$  and  $C_t$ . The slope of the intersection curves are the volume change index  $C_m$  for the case that net normal stress set to zero, and  $C_t$  for the case of net normal stress set to zero. It can be shown from the graphs that the curves went down with the increasing of either matric suction or net normal stress.

Table 7.8. Void ratio variation with net normal stress

Net normal stress, NNS (kPa)	Log NNS	Void ratio (e)		
		IB	PCB	IT
20.0	1.30103	1.18991	1.18974	1.19271
50.0	1.69897	1.18807	1.18950	1.18872
100.0	2.00000	1.11915	1.18123	1.13631
200.0	2.30103	1.05264	1.10124	1.08190
300.0	2.47712	1.01800	1.05678	1.05000
500.0	2.69897	0.98970	0.99888	1.01270
800.0	2.90309	0.98368	0.94884	0.97937
Ct		0.2186	0.2573	0.2318

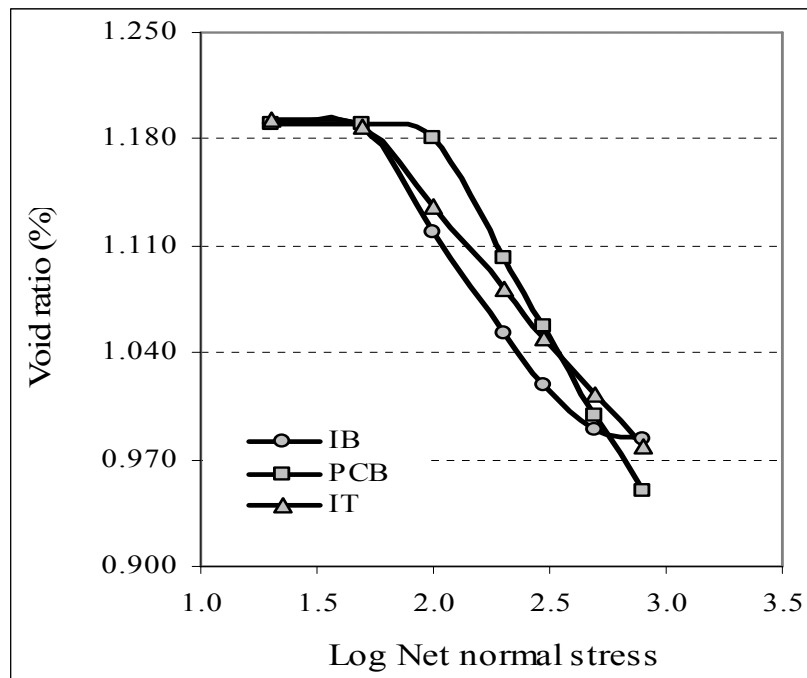


Figure 7.16. Void ratio against log net normal stress of specimen under zero matric suction

The constitutive surface of void ratio defined by the volume change index  $C_m$  corresponding to the matric suction it is equal to the slope of the shrinkage curve of a saturated soil. The constitutive surface of void ratio is defined by the

volume change index  $C_i$  corresponding to the net normal stress.  $C_i$  is the slope of the consolidation curve and is equal to the compressive index of a saturated soil. The volume change relationships of the kaolin clay specimens is summarised in Table 7.9. It clearly shown from the table that the specimens containing pre-crack of PCB had higher compressive index than that the intact specimen of IB. The reducing in effective area offering resistance to shear of specimen containing fissures makes the specimen had lower compressive strength than that the intact specimen. It is also shown from the table that the specimen tested under biaxial condition exhibits a higher compressive strength than that the specimen tested under triaxial test set up.

Table 7.9. Volume change index of the specimen correspond to void ratio

Specimen Type	Matric suction	Net normal stress
	$C_m$	$C_t$
Intact, Biaxial (IB)	0.0115	0.2186
Pre-crack, Biaxial (PCB)	0.0160	0.2573
Intact, Triaxial (IT)	0.0173	0.2318

Figure 7.17 – Figure 7.22 plot the constitutive surfaces of void ratio versus log net normal stress and log matric suction of the specimen. The constitutive surfaces of void ratio of intact specimen under biaxial test were shown in Figure 7.17 and Figure 7.18, while the pre-crack specimen under biaxial test curves were depicted in Figure 7.19 and Figure 7.20, and the intact specimen under triaxial test curves presented in Figure 7.21 and Figure 7.22. As clearly shown from the graphs, the slope of consolidation curve  $C_i$  is greater than the slope of the shrinkage curve  $C_m$ . This is consistent with the theory presented by previous researchers (Fredlund et al, 2000; Fredlund and Rahardjo, 1993) as discussed in sub sequent 4.3.2 and sub sequent 6.4.2 and consistent with figure 6.19 and Figure 6.20.



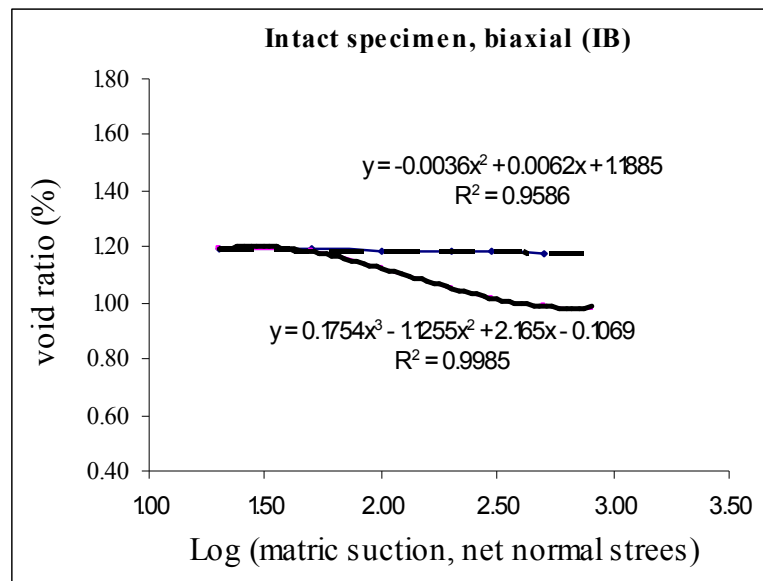


Figure. 7.17. Constitutive surface of void ratio versus net normal stress and matric suction of IB specimen (Intact, biaxial test)

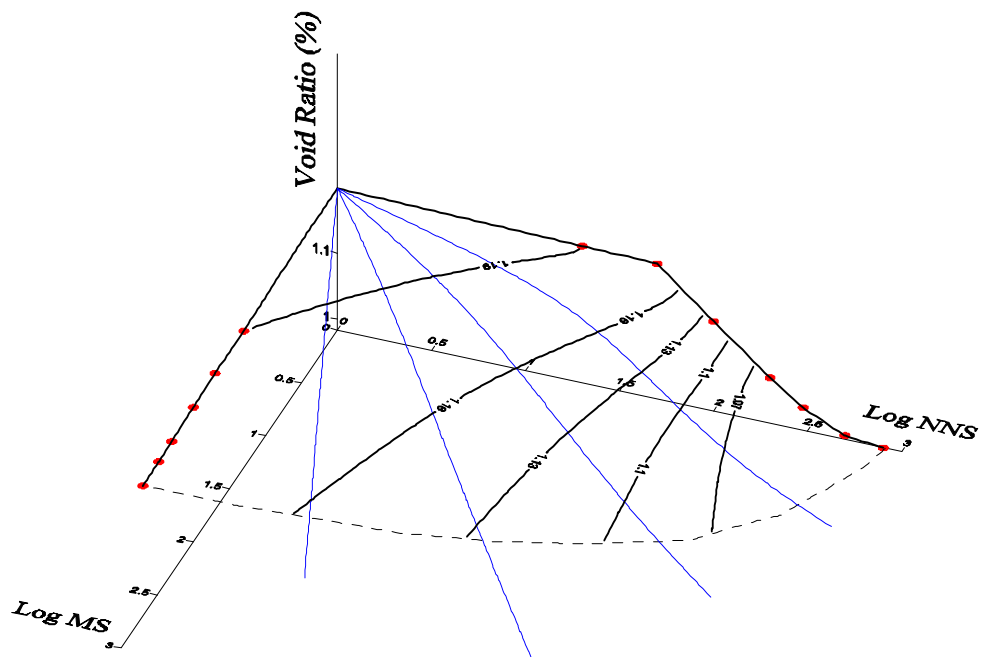


Figure. 7.18. A-three dimensional constitutive surface of void ratio versus net normal stress and matric suction of IB specimen (Intact, biaxial test)

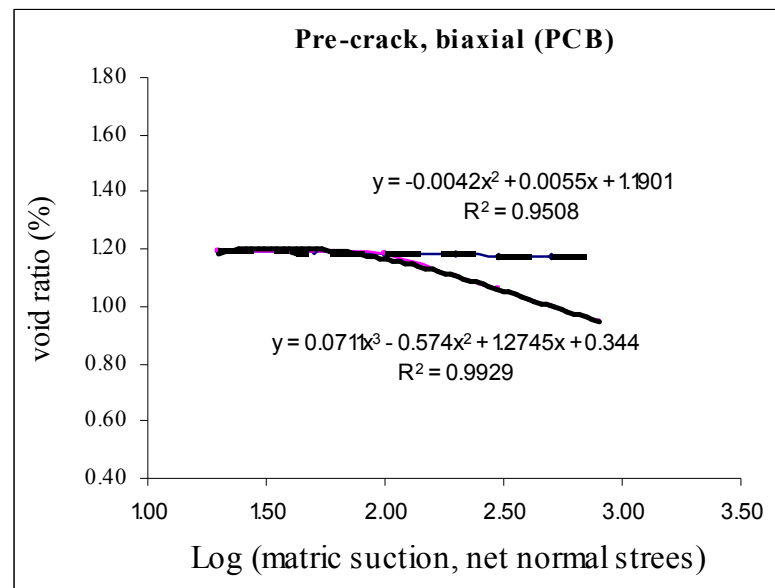


Figure. 7.19. Constitutive surface of void ratio versus net normal stress and matric suction of PCB specimen (Pre-crack, biaxial test)

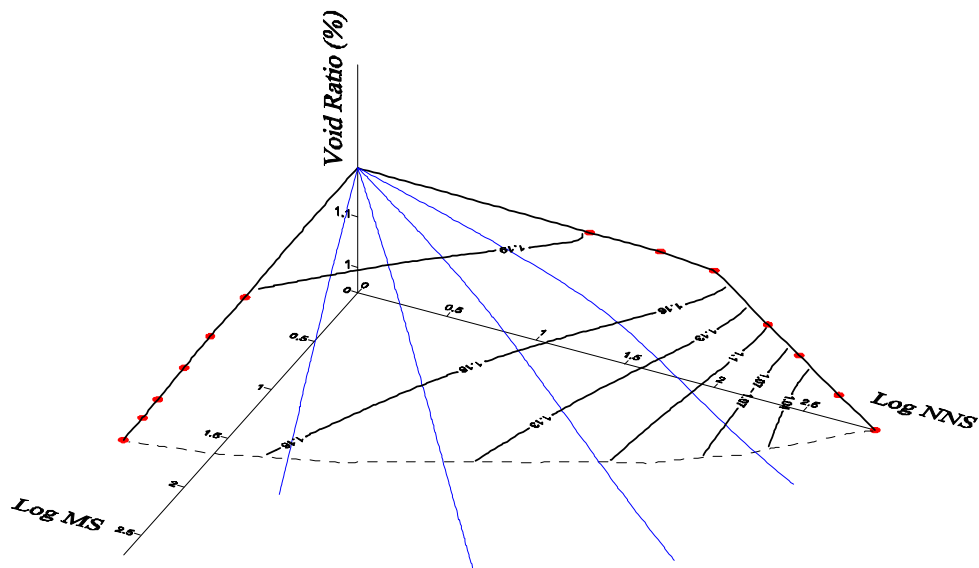


Figure. 7.20. A-three dimensional constitutive surface of void ratio versus net normal stress and matric suction of PCB specimen (Pre-crack, biaxial test)

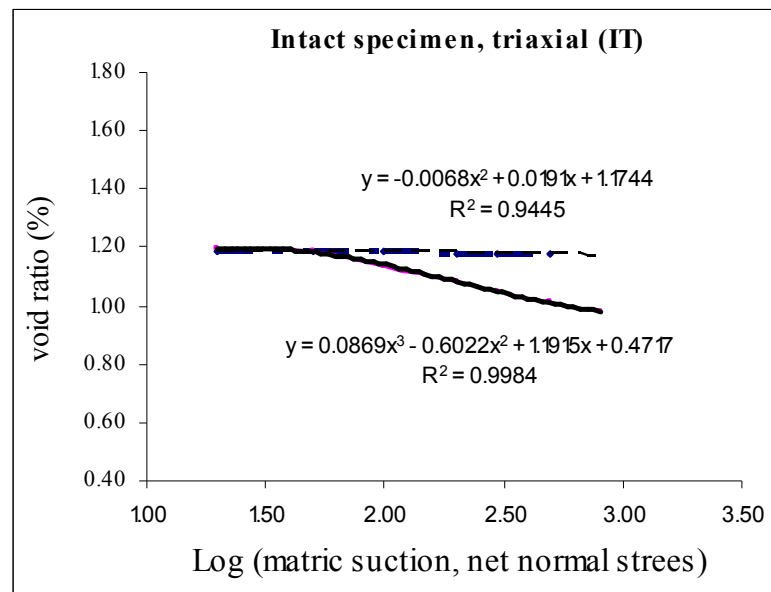


Figure. 7.21. Constitutive surface of void ratio versus net normal stress and matric suction of IT specimen (Intact, triaxial test)

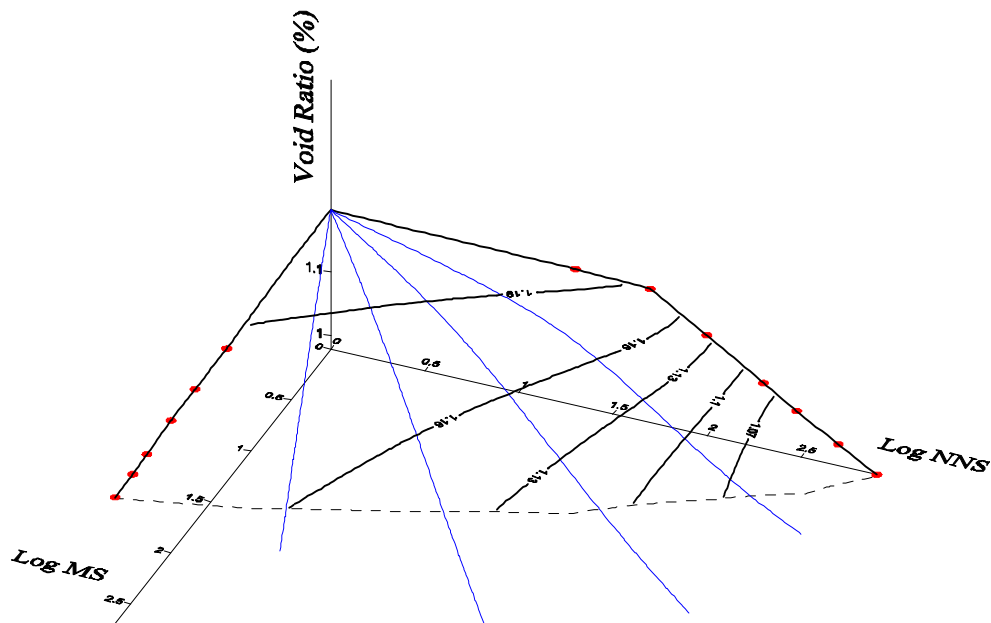


Figure. 7.22. A-three dimensional constitutive surface of void ratio versus net normal stress and matric suction of IT specimen (Intact, triaxial test)

Similarly, the water content of the specimen with varying matric suction and net normal stress were obtained at different loading stages of the experiments. The results is summarised and tabulated in Table 7.10 and Table 7.11. From this results, the graph of water content against log matric suction log net normal stress have been depicted, as shown in Figure 7.23 and Figure 7.24 respectively.

Table 7.10. Water content variation with matric suction

Matric suction, MS (kPa)	Log MS	Water content (%)		
		IB	PCB	IT
20.0	1.30103	0.253350	0.251738	0.261600
50.0	1.69897	0.252151	0.251217	0.259971
100.0	2.00000	0.236769	0.220802	0.237940
200.0	2.30103	0.219182	0.185720	0.207912
300.0	2.47712	0.208102	0.168413	0.189820
500.0	2.69897	0.195215	0.161784	0.170121
Dm		0.0548	0.0708	0.0899

Table 7.11. Water content variation with net normal stress

Net normal stress, NNS (kPa)	Log NNS	Water content (%)		
		IB	PCB	IT
20.0	1.30103	0.253350	0.261434	0.258500
50.0	1.69897	0.253112	0.259601	0.254640
100.0	2.00000	0.251020	0.243510	0.236688
200.0	2.30103	0.234534	0.221230	0.217201
300.0	2.47712	0.224353	0.207920	0.205679
500.0	2.69897	0.211905	0.191905	0.192350
800.0	2.90309	0.210005	0.187919	0.191212
Dt		0.0560	0.0677	0.0623

The value of compressive index  $D_m$  obtained by determining the gradient

of the linear portion of the curve of the water content against the log of matric suction. The constitutive surface of water content is defined by the water content index  $D_m$  corresponding to the matric suction as plotted in Figure 7.23. The value of water content index  $D_t$  obtained by determining the gradient of the linear portion of the curve of the water content against log net normal stress and is equal to the shrinkage of a saturated soil, is depicted in Figure 7.24.

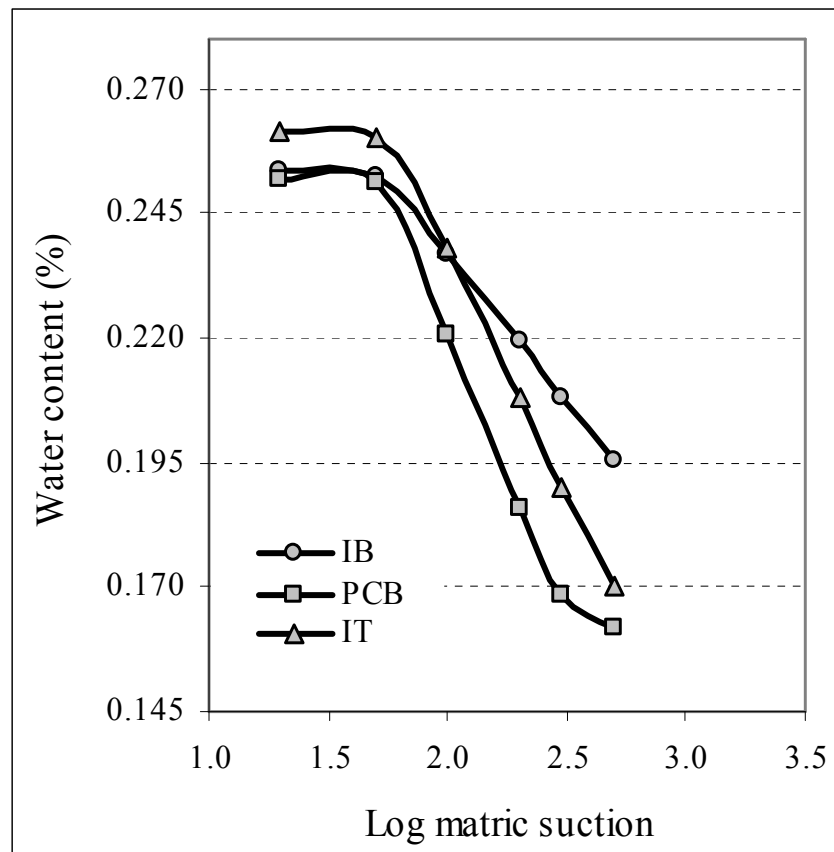


Figure 7.23. Water content against log matric suction of specimen under zero net normal stress

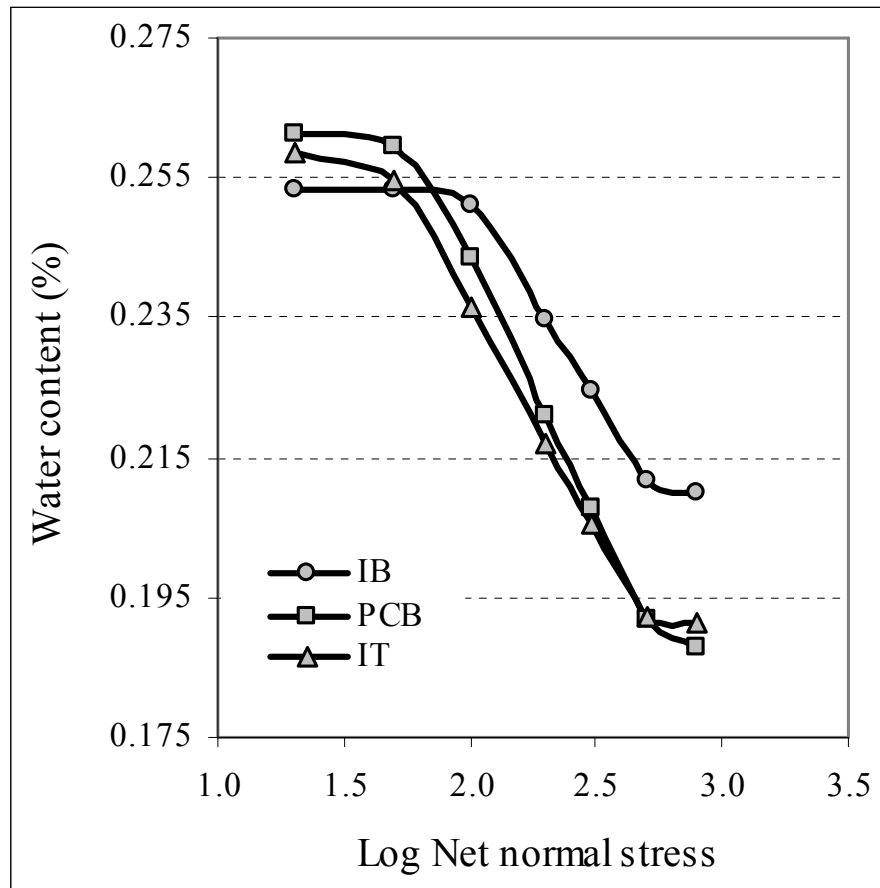


Figure 7.24. Water content against log net normal stress of specimen under matric suction zero

The volume change relationships of the kaolin clay specimens correspond to matric suction and net normal stress is summarised in Table 7.12. From the table it can be seen that the specimens containing pre-crack of PCB had higher compressive index than that the intact specimen of IB, while the intact specimen tested under triaxial test set up of IT had greater compressive index than that of intact specimen tested under biaxial condition. Similar to the curve of the volume change result in Figure 7.17 –Figure 7.22, and consistent with the stress-strain behaviour of the specimens shown in Figure 7.13 and Figure 7.14, the existence of discontinuities caused by crack or fissure on the pre-crack specimen makes the specimen weaker than that the intact specimen. The slope of the compressive index of the specimen indicated that the specimen containing pre-crack had lower strength than that the intact specimen.

Table 7.12. Volume change index of the specimen correspond to water content

Specimen Type	Matric suction	Net normal stress
	Dm	Dt
Intact, Biaxial (IB)	0.0548	0.0560
Pre-crack, Biaxial (PCB)	0.0708	0.0677
Intact, Triaxial (IT)	0.0899	0.0623

The constitutive surfaces of water content against log net normal stress and log matric suction of the specimen were presented in Figure 7.25 – Figure 7.30. The constitutive surfaces of water content of intact specimen under biaxial test were shown in Figure 7.25 and Figure 7.26, while the pre-crack specimen under biaxial test curves were depicted in Figure 7.27 and Figure 7.28, and the intact specimen under triaxial test curves presented in Figure 7.29 and Figure 7.30. The estimation of the volume change constitutive surfaces for unsaturated soil for the case of monotonic loading was studied by Fredlund et al (2000). The results of these studies seem to be in well agreement with the theory postulated by Fredlund et al (2000) presented in foregoing Figure 4.11 and Figure 4.12 and the work published by Fredlund and Rahardjo (1993) shown in foregoing Figure 4.7.

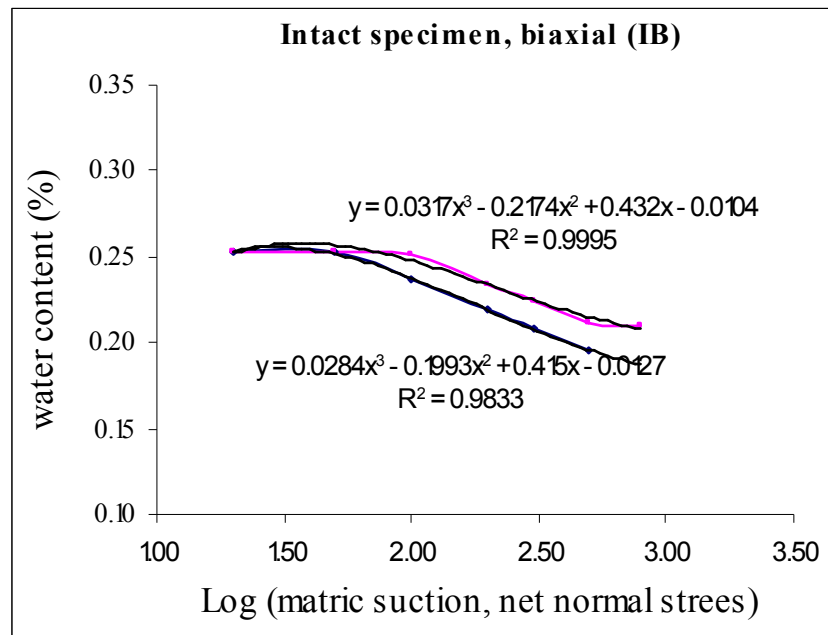


Figure. 7.25. Constitutive surface of water content versus net normal stress and matric suction of IB specimen (Intact specimen, biaxial test)

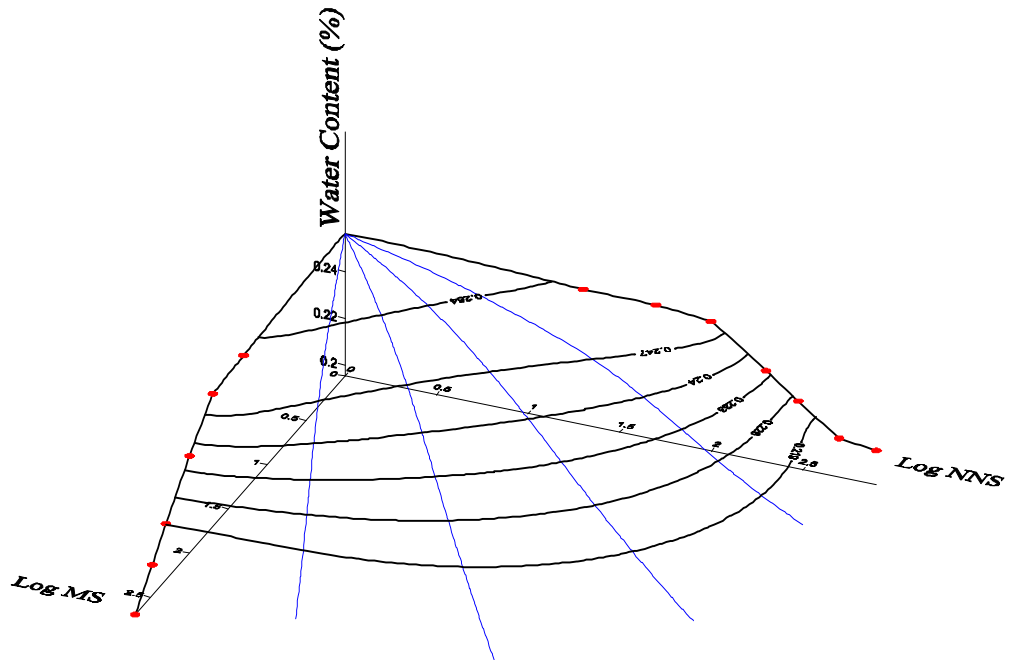


Figure. 7.26. A-three dimensional constitutive surface of water content versus net normal stress and matric suction of IB specimen (Intact specimen, biaxial test)



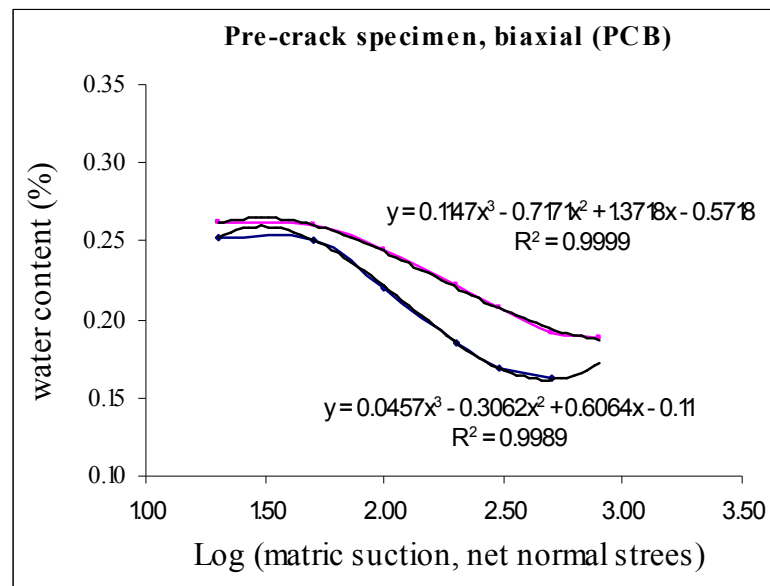


Figure. 7.27. Constitutive surface of water content versus net normal stress and matric suction of PCB specimen (Pre-crack specimen, biaxial test)

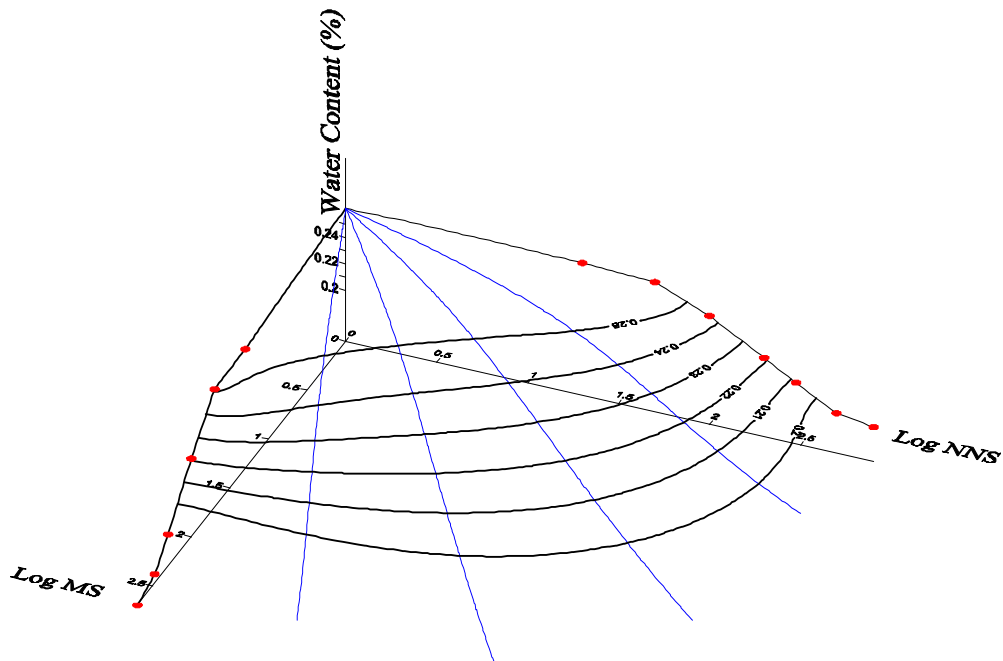


Figure. 7.28. A-three dimensional constitutive surface of water content versus net normal stress and matric suction of PCB specimen (Pre-crack specimen, biaxial test)

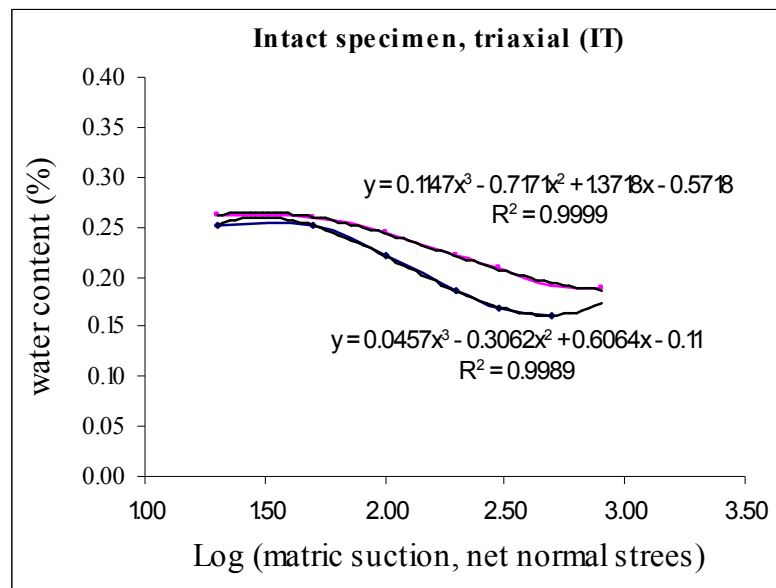


Figure. 7.29. Constitutive surface of water content versus net normal stress and matric suction of IT specimen (Intact specimen, triaxial test)

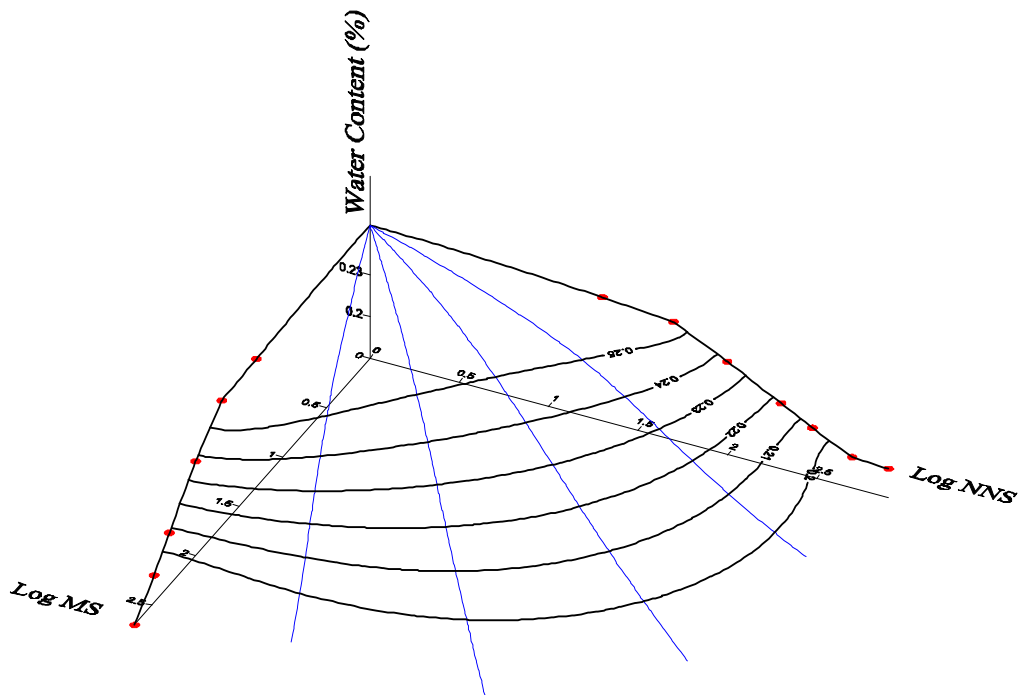


Figure. 7.30. A-three dimensional constitutive surface of water content versus net normal stress and matric suction of IT specimen (Intact specimen, triaxial test)

#### 7.4. Fracture toughness of partially saturated kaolin clay specimen

Mode I fracture test on partially saturated kaolin clay was carried out to obtain fracture load, which is used to determine the value of fracture toughness mode I by multiplying it with the stress intensity factor. The stress intensity factor is calculated based on Taada et al (2000) as follows:

$$K_I = \frac{P}{B\sqrt{W}} f\left(\frac{a}{W}\right) \quad (7.1)$$

where:

$$f\left(\frac{a}{W}\right) = \frac{2 + \frac{a}{W}}{(1 - \frac{a}{W})^{\frac{3}{2}}} \left[ 0.886 + 4.64\left(\frac{a}{W}\right) - 13.32\left(\frac{a}{W}\right)^2 + 14.72\left(\frac{a}{W}\right)^3 - 5.6\left(\frac{a}{W}\right)^4 \right] \quad (7.2)$$

The typical configuration of the specimen is shown in foregoing Figure 6.23, which the dimension parameters are  $a = 36$  mm,  $B = 36$  mm, and  $W = 72$  mm.

Result of Mode I fracture test and fracture toughness of specimen tested is presented in Table 7.12, while the relationship of the load against displacement is plotted in Figure 7.31. As shown from the graph that the fracture load obtained from the experimental is 10.5 N. Theoretically the graph should have a linear upslope when the specimen was undergoing the fracture test. However, due to the slack between the specimen holes and loading pins, the graph took the line up non linearly. Result of mode I fracture test of the specimen under matric suction of 500 kPa is presented in Table 7.13.

Table 7.13. Result of mode I fracture test of partially saturated clay specimen

Matric suction (kPa)	Fracture load, $F_c$ (N)	Stress intensity factor, $K_I \left( mm^{-\frac{3}{2}} \right)$	Fracture toughness, $K_{IC} (MPa\sqrt{mm})$
500	10.5	0.224	0.235

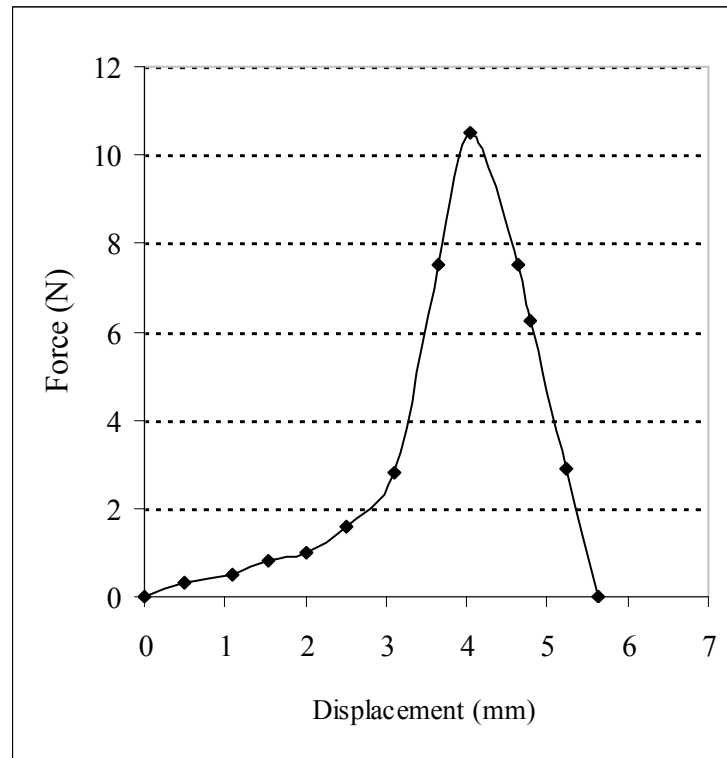


Figure. 7.31. Force against displacement of mode I fracture test of the partially saturated kaolin clay specimen under 500 kPa

## 7.5. Crack propagation analysis on pre-crack partially saturated kaolin clay specimen

### 7.5.1. Finite element analysis on crack development

The finite element analysis under plane strain condition on the pre-crack partially saturated kaolin clay specimen was carried out based on the procedure outline in the preceding sub sequent 5.5.6. The software package ABAQUS version 6.6 (Simulia Inc., 2006) was used to generate the finite element mesh of the model and to simulate the crack propagation and pattern of partially saturated kaolin clay specimen.

The analysis was initiated by making geometry of the test specimen in plane strain condition. Eight-node isoparametric plane strain elements were chosen to build the mesh with the mid-side nodes of elements surrounding the

crack tips moved to the quarter point of each element side, so that a square root singular deformation field at the crack tip might simulated. Finite element mesh of specimen is shown in Figure 7.32.

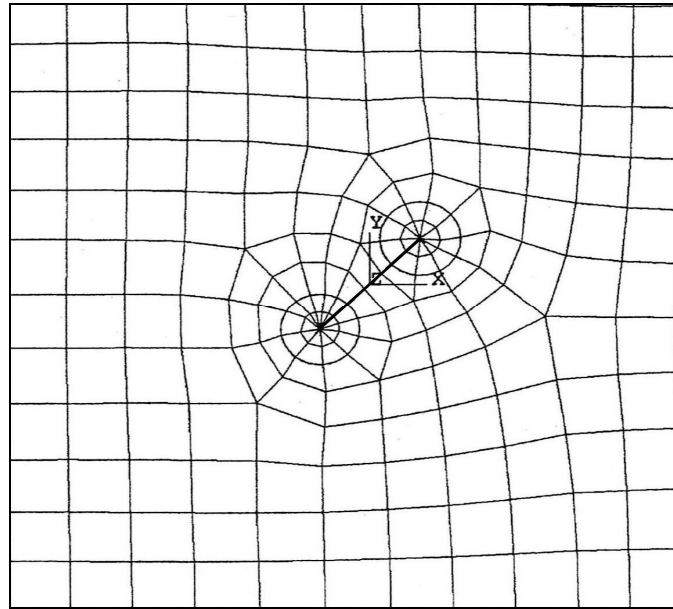


Figure. 7.32. Finite element mesh of the pre-crack partially saturated specimen on plane strain test

Four nodal displacements as mentioned in the preceding sub sequent 5.5.5 would be used to calculate stress intensity factor. Following the procedure as detailed in 5.5.4 and 5.5.6 then is used to check the fracture criteria. The fracture criteria met when a pair of load and displacement determined based on the particular loading arrangement that have caused the crack to develop had been obtained. The next step is to extend the crack virtually by setting the new crack tip at an angle of  $-70.5^\circ$  to the direction of the pre-crack from the tip location, due to its pure shearing loading mode of fracture. The length of virtual extension  $l$  is 1 mm, as shown in Figure 7.33. This process is repeated until the crack grows by itself without further load increase. As shown in Figure 7.33, the trend of the crack development was vertical. The analysis revealed load, axial strain and displacement. Figure 7.36 plots the stress strain curve of the specimen based on results of analytical work compare to the experimental results.

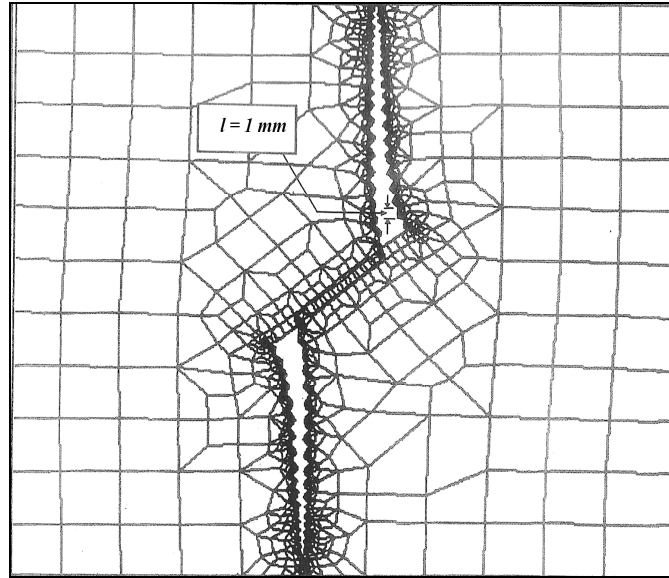


Figure. 7.33. Crack pattern of the specimen using finite element analysis

### 7.5.2. Experimental verification on crack development

The volume change relationship of the partially saturated kaolin clay specimens are plotted in Figures 7.34 and Figures 7.35. The corresponding experimentally determined volumetric deformation indices are summarised in Table 7.14. Knowing the volume change indices  $C_t$  and  $C_m$  and the water content indices  $D_t$  and  $D_m$ , the constitutive surfaces of water content  $w$  and void ratio  $e$  may be established as outlined in preceding sub sequent 4.3.2.

Table 7.14. Result of volumetric deformation indices of specimen

$G_s$	$e_0$	$w_0 G_s$	$C_t$ or $D_t G_s$	$D_t$	$C_m$	$D_m$
2.6	1.192	0.6578	0.2186	0.0623	0.0173	0.0899

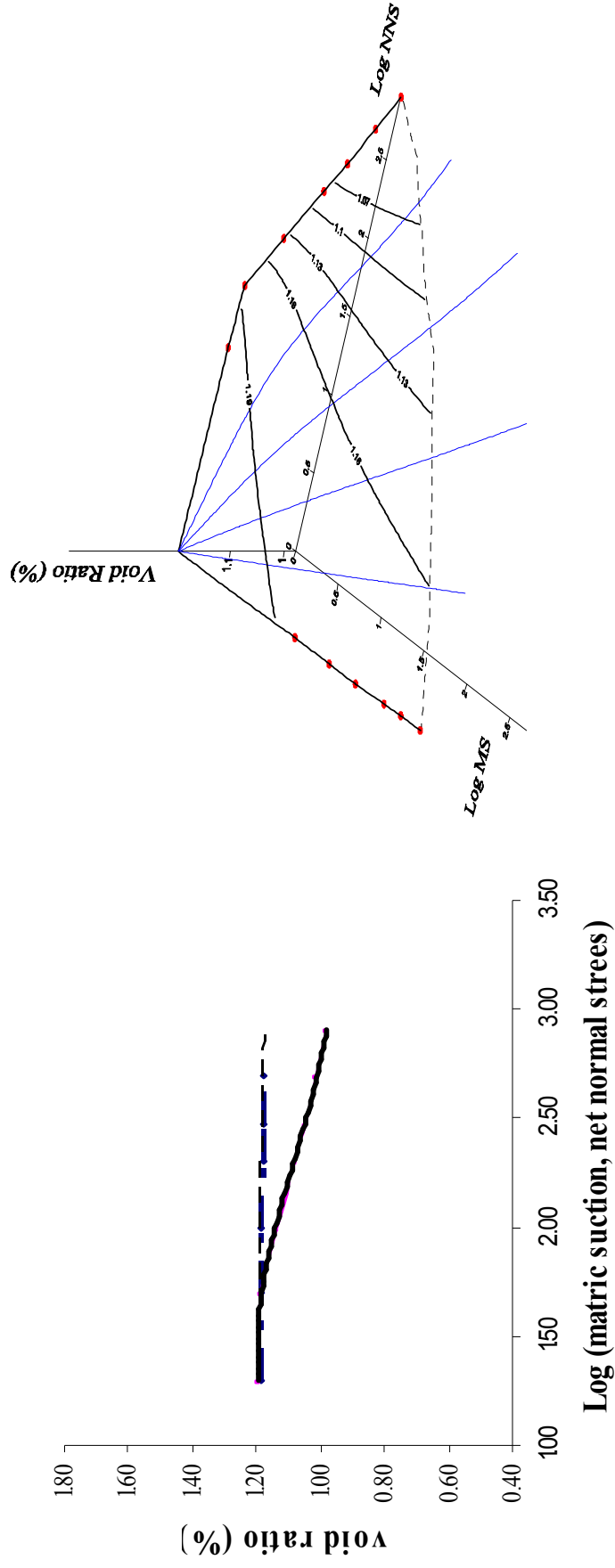


Figure. 7.34. Constitutive surface of void ratio versus net normal stress and matrix suction

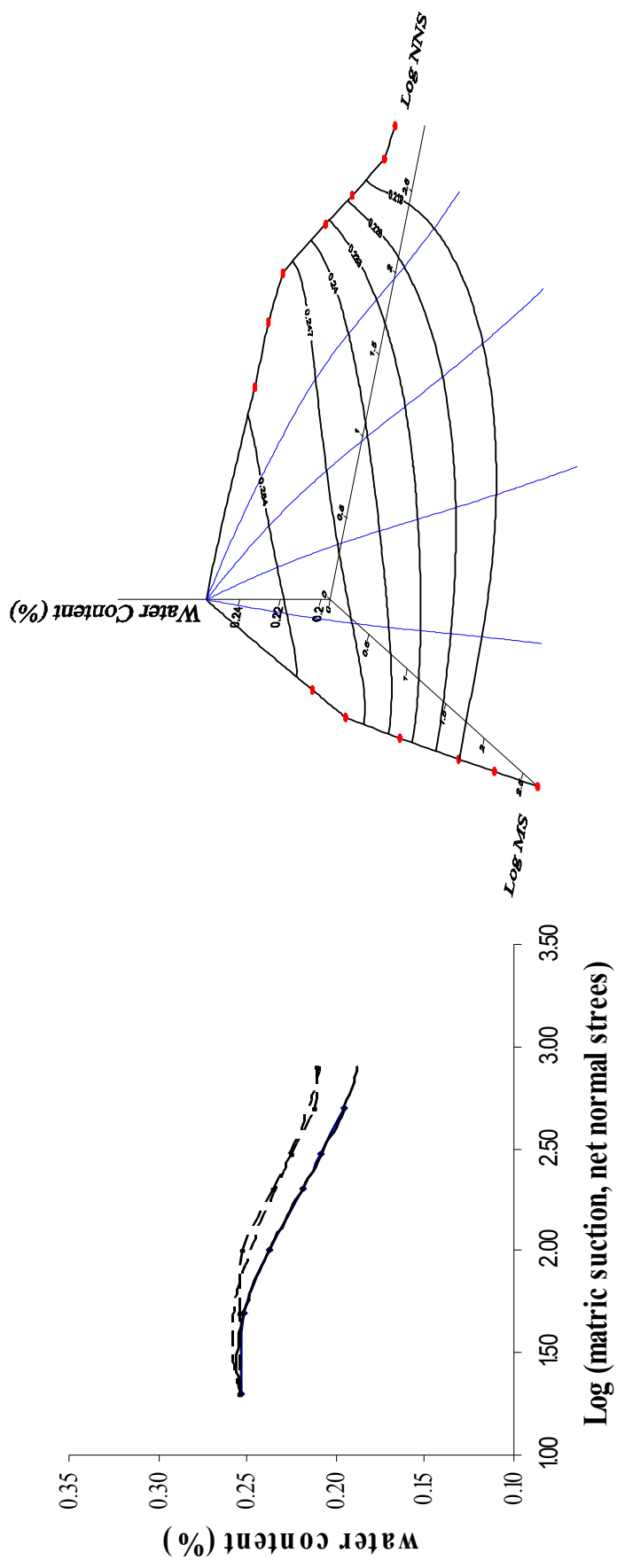


Figure. 7.35. Constitutive surface of water content versus net normal stress and matric suction



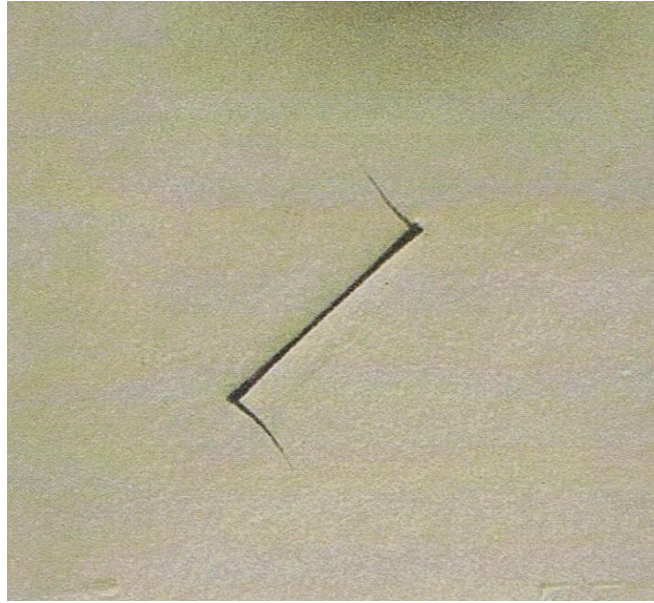


Figure. 7.36. Crack pattern of the pre-crack partially saturated specimen under plane strain compression test

From biaxial loading test, the crack propagation was observed after the specimen had fractured, as presented in Figure 7.36, while the stress strain curve obtained from the loading test compare to the analytical calculation was depicted in Figure 7.37. As shown in Figure 7.36 it is evident that the crack propagation was developed vertical and indeed of the same pattern as predicted by the use of unified model shown in Figure 7.33. Vesga (2005) observed the mechanical of crack propagation in clay subjected to dynamic loading. In the study, various angle of crack was investigated. It was concluded that the specimen with an initial pre-crack at 45 degree would be the weakest of all the specimens, at which in this condition the crack growth vertical. Similar observation also reported by Boon and Suen (2001) and Lo (2001).

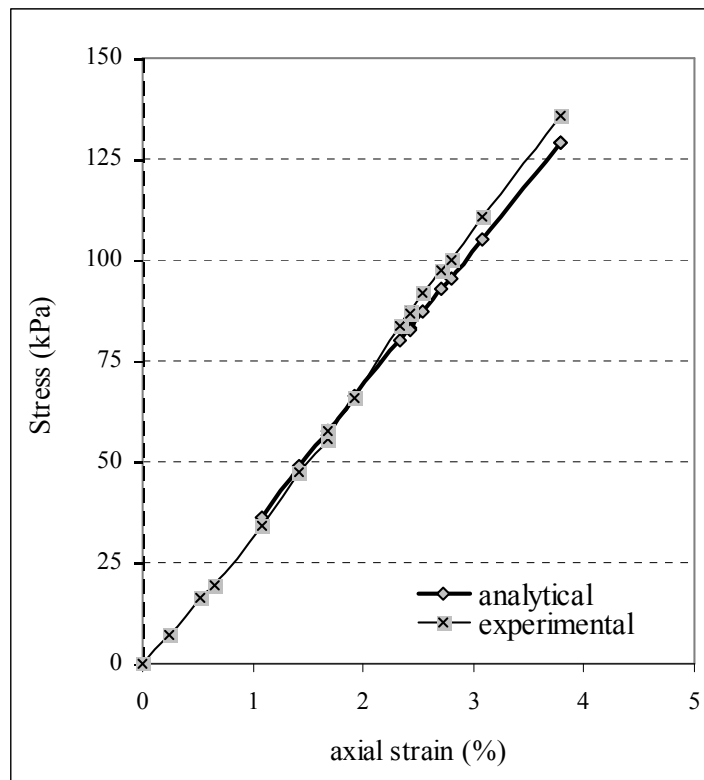


Figure. 7.37. Stress against strain curves resulted from experimental and analytical work

The stress strain relation shows that in general it is reflected the behaviour of the kaolin clay specimen is in elastic regime. It is also clear that the curve obtained from analytical work is in a good accordance with the result from laboratory testing. The result of the present study seems consistence with the work of Vesga (2005), Boon and Suen (2001) and Lo (2001).

## **CHAPTER 8**

### **CONCLUSIONS AND RECOMMENDATIONS**

#### **8.1. Conclusions**

From the analyses presented in this thesis, it can be concluded that:

- (i) The new biaxial compression apparatus, with its plane strain device, which has been used in the present research has been able to produce realistic test results of the constitutive behaviour of clayey soil in saturated and partially saturated conditions that are in accordance with known soil behaviour.
- (ii) Due to its simplicity and toughness, malfunction or inaccuracy of the test result caused by leakage and other deficiencies are minimized. This device is not only easy to set up but it also easy to carry out the testing with minimum disturbances. A new system to measure lateral displacement and volume change using laser micro sensors is also able to detect the onset of such localized deformation.
- (iii) The results of the undrained test on over consolidated clay specimens indicate that there was local drainage concentrated in the shear band. This was indicated by the difference between the water content within the shear band and the global water content. As a consequent, the undrained shear strength of over consolidated clay specimen was reduced.
- (iv) The occurrence of shear band formation in over consolidated clay specimens had detected in the plane strain test by sudden increases in the lateral deformation. The presence of the shear localisation in over

consolidated clay subjected to load had caused discontinuity and non-uniform deformation within the specimen. It is evidence that the continuum model ceased to perform well in the post peak region.

- (v) The application of a new system to measure lateral displacement using laser micro sensors is also able to establish the volume change of partially saturated clay specimen, due to the presence of the air, has been examined. The results obtained were realistic and resembled existing data accumulated by other researcher.
- (vi) It has been found from the stress strain behaviour of the partially saturated clay specimen tested either under triaxial test set up or under biaxial test set up that the typical of brittle hard clay and exhibit elastic only behaviour were shown in all the specimens.
- (vii) The results of partially saturated clay specimens indicate that shear strength of the intact specimens were higher than that the pre-crack specimens along the axial strain. It is also shown that the earlier and lower peak strength was occurred to the pre-crack specimens than the intact specimen. Furthermore, the lower compressive strength of specimen containing discontinuities was indicated by their higher volume change index than the intact specimen's.
- (viii) In general, the partially saturated kaolin clay specimens tested under plane strain condition exhibit higher shear strength as well as compressive strength than that the specimen tested under triaxial test set up.
- (ix) The crack propagation of partially saturated clay specimen with pre-crack subjected to low cell pressure proposed by the model has been verified by experiment, in other word, the experimental and analytical results were a close match. It has been found that the unified model used in this study can predict crack pattern reasonably well.

## 8.2. Recommendations

To finalize the present study, following recommendations may be proposed:

- (i) The applied of a pressure generator like GDS pressure generator for each pressures line to supply confining pressure, cell pressure, back pressure and flushing line of the new biaxial device used in this project is proven to be better than generating pressure from one compressor and distributing the pressure through pressure line. The new biaxial device used in the present study could be extended to have more capacity for future work for the use of wider range of materials to be tested.
- (ii) Due to the existence of discontinuities or shear band during shear testing in over consolidated clay specimens, only the pre-shear band localisation portion of the load-displacement and stress strain curve represents true material behaviour. This confirmed that the soil constitutive model based on continuum mechanics ceased to apply. Future work to solve this problem involving fracture mechanics approach based on the unified model (Lo et al, 1996) and elastoplastic shear fracture model (Lo et al, 2005) would need to be channelled.
- (iii) Investigation involving different orientations of the pre-crack and intact specimen of partially saturated clay may be done. The actual ground would undoubtedly have inherent microscopic cracks in all directions, but would be unlikely to have very distinct pre-crack. Further projects of varying specimen configurations and crack length, may be used to generate more results for interpolation and prediction as required.
- (iv) The mode I fracture testing had only been done in this project. Further work on different mode loading fracture tests under varying matric suctions and net normal stresses need to be investigated to give a more comprehensive result.
- (v) The scope of the present work does not include the investigation of the effects of different cell pressures on the fracture load and crack pattern of partially saturated clay, which may be predicted by the model. Future work may be addressed into this area.

## REFERENCES

- Adachi T. and Oka F. (1982). Constitutive equations for sands and over consolidated clay and assigned works for sand. Proc. of Int. workshop on constitutive relations for soils, Grenoble, pp 141-157.
- Adachi T., Oka F. and Kojima K. (1987). Visco-plastic constitutive model of soft rocks with strain softening. Proc. of 2<sup>nd</sup> Int. Conf. Constitutive laws for Engineering materials: Theory and applications, Arizona, pp 659-666.
- Akai K. Adachi T., and Nishi K. (1987). Elastoplastic properties of soft sedimentary rock (porous tuff). Proc. of JSCE, pp 83-95.
- Alonso E. E., Gens A., Josa A. (1990). A constitutive model for partially saturated soils. *Geotechnique*, Vol 40 (3), pp 405-430.
- Alonso E. E., Gens A., Hight D. W. (1987). Special problems soils. General report. Proc. 9<sup>th</sup> Europe Conf. on Soil Mech., Dublin, Vol 3. pp 1087-1146.
- Al-Tabbaa A. (1987). Permeability and stress-strain response of speiswhite kaolin. PhD thesis, University of Cambridge, Cambridge, UK.
- Al-Tabbaa A. and Wood D.M. (1989). An experimental based “bubble” model for clay. Int. Conf. on Numerical Models in Geomechanics, A. Pietruszczak and G.N. Pande (eds.), Balkema, pp 91-99.
- Alshibli K.A., Akbas I. S. (2007). Strain localization in clay: plane strain versus triaxial loading conditions. *Geotechnical Geological Eng.*, No 25, pp 45-55.
- Alshibli K.A., Godbold D. L., and Hoffman K. (2004). The Louisiana Plane strain apparatus for soil testing. *Geotechnical Testing Journal*, Vol 27, No 4, pp 337-346, ASTM, US.
- Alshibli K.A. and Sture S. (2000). Shear bands formation in plane strain experiments of sand. *Journal of Geotechnical and Geoenvironmental Engineering*, Vol 126, No 6, Paper no 21167
- American Society for Testing and Materials (1996). Standard test method for measurement of fracture toughness of metallic materials. ASTM E 1820-96, Philadelphia.
- Anderson T.L. (2005). *Fracture mechanics: fundamental and applications*, 3<sup>rd</sup> ed., CRC Press, London.
- Atkinson J.H., Richardson D. and Stallebrass S.E. (1990). Effect of recent stress history on the stiffness of overconsolidated soil. *Geotechnique*, Vol 40, No 4, pp 531-540.
- Atkinson J.H. and Richardson D. (1987). The effect of local drainage in shear in shear zones on the undrained strength of overconsolidated clay. *Geotechnique*, Vol 37, No 3, pp 393-403.
- Atkinson J.H. and Bransby P.L. (1982). *The mechanics of soils : an introduction to critical state soil mechanics*. McGraw-Hill, London.
- Atkinson J.H. and Salfors G. (1991). Experimental determination of stress-strain-time characteristics in laboratory and in situ tests. Proc. of the 10th European Conf. on Soil Mechanics and Foundation Eng. Florence, Vol 3, pp 915-956.

- Banerjee P. K. and Stipho A. S. (1979). An elastic-plastic model for undrained behaviour of heavily over consolidated clays. *Int. Journal for numerical and analytical method in Geomechanics*, Vol 3, pp 97-103.
- Banks-Sills L. and Arcan M. (1984). Mode II fracture toughness testing with application to PMMA in *Application of Fracture Mechanics to Materials and structure*, ed by G. C. Sih, pp 337-334, Kluwer, Boston.
- Baudet B.A. (2001). Modelling effects of structure in soft natural clays. PhD thesis, City University, London, UK.
- Barsoum R.S.( 1976). On the use of isoparametric finite elements in linear fracture mechanics. *Int. Journal for Numerical Methods in Eng.*, Vol 10, pp 25-37.
- Bathe K.J. (1996). *Finite Element Procedures*. Practice-Hall, Inc, New Jersey.
- Baver L. D., Gardner W. L. and Gardner W. L. (1972). *Soil physics*. Fourth edition. John Willey and Sons, Inc. New York.
- Belding D.F. and Mitchell K.J.(1991). *Foundations of Analysis*. Practice-Hall, Inc, New Jersey.
- Biot MA (1941) General theory of three-dimensional consolidation. *Journal of Applied Physics*, Vol 12, pp 155–164.
- Bishop A. W. (1981). Thirty five years of soil testing. *Proc. of 10<sup>th</sup> ICSMFE*, Stockholm, pp 185-193.
- Bishop A.W. (1967). Progressive failure with special reference to the mechanism causing it. *Proc.of Int. Conf. on Geotechnical Eng.*, Oslo, pp 142-150.
- Bishop A.W.and Green G.E. (1965). The influence of end restraint on the compression strength of cohesionless soil. *Geotechnique*, Vol 15, No 3, pp 243-266.
- Bishop A. W., Webb D.L. and Lewin P.I. (1965). Undisturbed samples of London Clay from the Ashford common Shaft: strength-effective stress relationship. *Geotechnique*, Vol 15, No 1, pp 1-31.
- Bishop A. W. and Blight G. E. (1963). Some aspect of effective stress in saturated and partially saturated soils. *Geotechnique*, Vol 13, No 3, pp 177-197.
- Bishop A. W. and Henkel D. J. (1962). *The measurement of soil properties in the triaxial test*, Arnold, London.
- Bishop A. W. (1959). The principle of effective stress. *Tek. Ukleblad.*, Vol 39, pp 859-863.
- Bizzarri A., Allersma H. G. B., Koehorst B. A. N. (1995). Preliminary tests on soft clay with a biaxial apparatus. *Proc. of the 1995 Int. Symposium on Compression and Consolidation of Clayey Soils. Part 1 (of 2)*, Hiroshima, Japan.
- Bjerrum L. (1967). 7<sup>th</sup> Rankine Lecture: Engineering geology of Norwegian normally-consolidated marine clays as related to settlements of buildings. *Geotechnique*, Vol 17, No 2, pp 81-118.
- Bjerrum L. (1973). Problems of soil mechanics and construction on soft clays and structurally unstable soils (collapsible, expansive and others). *Proc.of the 8<sup>th</sup> Int.Conf.on Soil Mech. and Foundation Eng.*, Moscow, Vol. 3, pp 111-159.
- Boon, T. W. and Suen, T. B. (2001). Fracture testing of brittle soil. B. Eng thesis, National University of Singapore.
- Broek D. (1986). *Elementary engineering fracture mechanics*. 4<sup>th</sup> edn, Kluwer,

Dordrecht.

- Brooks R. H. and Corey A. T. (1964). Hydraulic properties of porous media. Hydrology paper no 3, Civil Eng. Dept, Colorado Univ., Fort Collins, Colo
- Burland J.B. (1990). 30th Rankine Lecture : On the compressibility and shear strength of natural clays. *Geotechnique*, Vol 40, No 3, pp 329-378.
- Burland J.B. (1989). Ninth Laurits Bjerrum Memorial Lecture: "Small is beautiful"-the stiffness of soils at small strains. *Canadian and Geotechnical Journal*, Vol 26, pp 499-516.
- Buzzard R.J., Gross B. and Srawley J.E.(1986). Mode II fatigue crack growth specimen development. In *Fracture Mechanics*, ASTM\_STP 905, ed by J.H. Underwood et al, 17, pp 329-346.
- Callisto L., Gajo A. and Muir Wood D. (2002). Simulation of triaxial and true triaxial tests on natural reconstituted Pisa clay. *Geotechnique*, Vol 52, No 9, pp 649-666.
- Carl B.B. (1959). *The History of the Calculus and its conceptual development*, Dover Publications, Inc, New York.
- Chandler R.J. (1999). Clay sediments in depositional basins: the geotechnical strains. *Geotechnique*, Vol 51, No 3, pp 245-255.
- Cheung Y. K and Yeo M.F. (1979). *A Practical Introduction to Finite Element Analysis*, Pitman Publishing Ltd, London.
- Chandler R.J. (1973). A study of structural discontinuities in stiff clays using polarizing microscope. *Proc. Int. Symp. on Soil Structure*, Gothenburg, Sweden, pp 78-85.
- Chiu H. and Johnson I. (1981). The application of critical state concepts to Melbourne mudstone. *Proc. of 4<sup>th</sup> ANZ Conf. on Geomechanics*, Perth, pp 234-240.
- Chudnovsky A., Saada A.S, and Lesser A.J.(1988). Micromechanisms of deformation in fracture of overconsolidated clays. *Canadian Geotechnical Journal*, Vol 25, pp 213-221.
- Clayton C.R.I. and Heymann G. (2001). Stiffness of geomaterials at very small strains. *Geotechnique*, Vol 30, pp 336-339.
- Coleman J. D. (1962). Stress strain relations for partly saturated soil. *Geotechnique*, Vol 12, No 4, pp 348-350.
- Coop M. R., Atkinson J. H. and Taylor R. N. (1995). Strength and stiffness of structured and unstructured soils. *Proc. of the 11<sup>th</sup> European Conf. on Soil*.
- Cornforth C. N. (1964). Some experiment on the influence of strain conditions on the strength of soil. *Geotechnique*, Vol 14, No 2, pp 143-167.
- Cotecchia F. and Chandler R. J. (1997). The influence of structure on the pre-failure behaviour of a natural clay. *Geotechnique*, Vol 47, No 3, pp 523-544.
- Cotterell and Rice J. R. (1980). Slightly curved or kinked cracks, *Int. Journal of Fracture*, Vol 16, No 2, pp 155.
- Covarrubias S.W. (1969). *Cracking of Earth and Rockfill Dams*, Harvard Soil. Mechanics Series, 82.
- Cui Y. J. and Delage P. (1996). Yielding and plastic behaviour of unsaturated compacted silt. *Geotechnique*, Vol. 46, No 2, pp 291-311.
- Croney D. (1952). The movement and distribution of water in soils. *Geotechnique*, Vol 3, No 1, pp 1-66.



- Dafalias Y.F. and Popov E.P. (1976). Plastic internal variables formalism of cyclic complex loadings. *Acta Mechanica*, Vol 21, pp 173-192.
- Dafalias Y.F. and Herrmann (1980). A bounding surface soil plasticity model. *Mechanics-Transient and Cyclic Loads*, G.N. Pande and O.C. Zienkiewicz (eds.). John Wiley and Sons Ltd.
- Dasari G. R. (1996). Modelling the variation of soil stiffness during sequential excavation. PhD thesis, Cambridge University, UK.
- Desai C. S. and Salami M. R. (1987). A constitutive model and associated testing for soft rock. *Int. J. Rock Mech. Min. Sci. and Geomech.*, Vol 24, No 5, pp 299-307.
- Dimaggio F. L. and Sandler I. S. (1971). Material model for granular soils. *J. EM Div., ASCE*, (97), pp 935-950.
- Drucker D. C. and Prager W. (1952). Soil mechanics and plastic analysis of limit design. *Q. Applied. Mathematic.*, (10), pp 157-164.
- Drucker D. C. and Gibson R. E. and Henkel D. J. (1957). Soil mechanics and work hardening theories of plasticity. *Trans. ASCE*, (122), pp 338-346.
- Drescher A., Vardoulakis I. and Han C. (1990). A biaxial apparatus for testing soils. *Geotechnical Testing Journal*, GTJODJ, Vol 13, pp 226-234
- Elliot G. M. and Brown E. T. (1986). Further development of a plasticity approach to yield in porous rock. *Int. J. Rock Mech. Min. Sci. and Geomech.*, Vol 23, No 2, pp 519-527.
- Erdogan F. and Sih G.C. (1963). On the crack extension in plate under plane loading and transverse shear, *Journal of Basic Engineering*, 85, pp 519-527.
- Fang H.G., Mikroudis G.K. and Pamukcu S. (1989). Fracture Behaviour of compacted fine-grained soils. *Fracture Mechanics: Perspectives and Directions*, Wei, R.P., and Gangloff, R.P., eds. ASTM STP 1020, pp 659-667.
- Fauziah M. and Nikraz H. (2007). Biaxial testing of overconsolidated clay. *Proceeding of The 1<sup>st</sup> Int. con. of Eur. Asian Civil Eng. Forum*, pp 148-153.
- Fauziah M. and Nikraz H. (2007). Stress-strain behaviour of overconsolidated clay under plane strain condition. *Proc. 10<sup>th</sup> ANZ conf. on Geomech.*, pp 148-153
- Finno R. J. and Rhee Y. (1993). Consolidation, pre-and post peak shearing response from internally instrumented biaxial compression device. *Geotechnical Testing Journal*. ASTM, Vol 16, No 4, pp 496-501.
- Finn W.D.L., Wade N.H. and Lee K.L. (1968). Volume change in triaxial and plane strain tests. *ASCE*, No. SM6, pp 297-308.
- Fookes P.G. and Denness B. (1969). Observational studies of fissure patterns in Cretaceous sediments of South-East England, *Geotechnique*, Vol 19, pp 453-477
- Fredlund D.G., Fredlund M.D. and Wilson G. W. (2000). Estimation of Volume change function for unsaturated soils. *Unsaturated soil for Asia*. Rahardjo, Toll and Leong (Eds), Balkema, Rotterdam, pp 663-668.
- Fredlund D.G., Fredlund M.D. and Barbour S. L. (1995). The relationship of the unsaturated soil shear strength to the soil-water characteristic curve. *Canadian Geotech Journal*, Vol 32, pp 440-448.

- Fredlund D.G. and Rahardjo H (1993). Soil mechanics for unsaturated soil. John Willey & Sons, Inc. New York.
- Fredlund D.G. and Morgenstern N. R., (1977). State state variable for unsaturated soil. *Journal of Geotechnical Engineering ASCE*, 103 (5), pp 447-466.
- Fredlund D.G. and Morgenstern N. R., (1976). Constitutive relation for volume change in unsaturated soil. *Canadian Geotechnique Journal*, Vol 13, No 3, pp 261-276.
- Fredlund D.G. (1975). A Diffused air volume indicator for unsaturated soils. *Canadian Geotech. Journal*, Vol 12, pp 121-139.
- Gajo A. and Muir Wood D. (2001). A new approach to anisotropic, bounding surface plasticity: general formulation and simulations of natural and reconstituted clay behaviour. *Int. Journal for Numerical and Analytical Methods in Geomechanics*, Vol 25, pp 207-241.
- Ganendra D. and Potts D. M. (1995). Discussion on 'Evaluation of constitutive model for overconsolidated clays' by A.J. Whittle. *Geotechnique*, Vol 45, No 1, pp 169-173.
- Gens A (1982). Stress-strain and strength of a low plasticity clay. PhD Thesis, Imperial College, University of London.
- Gens A. and Potts D. M. (1987). The use of critical state models in numerical analysis of geotechnical problems: A review. *Computational plasticity* (eds. Owen, Hinton and Onate), Pineridge Press, pp 1491-1525.
- Georgopoulos, I.-O. and Vardoulakis, I. (2005). *The Handbook of Geotest Geo Biax*. National Technical University of Athens.
- Gerogiannopoulos N.G. and Brown E. T. (1978). The critical state concept applied to rock. *Int. J. Rock Mech. Min. Sci. and Geomech.*, Vol 15, Pp 1-10.
- Ghorbel S. and Leroueil S. (2006). An elastoplastic model for unsaturated soil. *Proc. of 4<sup>th</sup> Int. Conf. on unsaturated soils*, Carefree, Arizona, pp 1908-1919.
- Graham J., Noonan M.L. and Lew K.V. (1983). Yield states and stress-strain relationships in a natural plastic clay. *Canadian Geotechnical Journal*, Vol 20, pp 502-516.
- Grammatikopoulou A. (2004). Development, Implementation and Application of Kinematic Hardening Models for Overconsolidated Clays. PhD Thesis, Imperial College, London.
- Green G.E. and Reades D.W.(1975). Boundary conditions, anisotropy and sample shape effects on the stress-strain behaviour of sand in triaxial compression and plain strain. *Geotechnique*, Vol 25, No 2, pp 333-356.
- Green G.E. (1971). Strength and deformation of sand measured in an independent stress control cell. *Stress-strain behaviour of soils*, Proc. Roscoe Memorial Symp, Cambridge, pp 285-323.
- Green G.E. and Reades D. W. (1975). Boundary conditions, anisotropy and sample shape effects on the stress-strain behaviour of sand in triaxial compression and plane strain. *Geotechnique*, Vol 25, No 2, pp 333-356.
- Griffith A.A. (1920). The phenomena of rupture and flow in solids. *Philosophical transactions of the royal Society*, London, A221, pp 163-198.
- Hambly E.C. and Roscoe K.H.(1969). Observation and prediction of stresses and strains during plane strain of "wet" clays. *7<sup>th</sup> ICSMFE*, Mexico, Vol 2, pp 173-181.

- Han C. and Drescher A.(1993). Shear bands in biaxial tests on dry coarse sand. *Soils and Foundations*, Japanese Society of Soil Mechanics and Foundation Engineering, Vol 33, No 1, pp118-132
- Han C and Vardoulakis I.G.(1991). Plane strain compression experiments on water-saturated fine-grained sand. *Geotechnique*, Vol 41, No 1, pp 49-78.
- Hardin B.O. (1978). The nature of stress-strain behavior for soils. *Proceedings of Specialty Conference on Earthquake Engineering and Soil Dynamics*, ASCE, Pasadena, California, pp 3-90.
- Hardin B.O. and Black W.L. (1969). Closure to: Vibration modulus of normally consolidated clay. *Journal of the Soil Mechanics and Foundations Division*, ASCE, Vol 95, No SM3, pp 1531-1537.
- Hardin B.O. and Black W.L. (1968). Vibration modulus of normally consolidated clay. *Journal of the Soil Mechanics and Foundations Division*, ASCE, Vol 94, No 2, pp 353-369.
- Hashiguchi K. (1985). Two- and three-surface models of plasticity. *Proc. 5th Int.Con. on Numerical Methods in Geomechanics*, Nagoya, pp 285-292.
- Hayashi K. and Nemat-Nasser S. (1981). Energy release rate and crack kinking under combined loading. *ASME Journal of Applied Mech*, Vol 48, pp 520–524.
- Head K.H.(1986). *Manual of Soil Laboratory Testing*. Vol 3, Pentech Press, London
- Hayashi H. and Nemat-Nasser S (1981). Energy-release rate and crack kinking under combined loading. *ASME Journal of Applied mechanics*, 48, pp 520-524.
- He M. Y. and Hutchinson J. W. (1989). Kinking of a crack out of an interface. *ASME Journal of Applied Mechanics*, 56, pp 270-278.
- Henkel D. J. (1956). The effect of overconsolidation on the behaviour of clays during shear. *Geotechnique*, Vol 6, pp 139-150.
- Henkel D. J. (1959). The relationships between the strength pore-water pressure and volume change characteristics of saturated clays. *Geotechnique*, Vol 9, pp. 119-135.
- Henkel D. J. (1960). The relationship between the effective stress and water content in saturated clays. *Geotechnique*, Vol 10, pp 41-54.
- Heymann G. (1998). The stiffness of soils and weak rocks at very small strains. *Geotechnique*, Vol 47, No 3, pp 665-691.
- Hirari H. and Masao, S. (1982). Proposal of a yield function and description of plastic behaviour of soft rock. *Proc. JSCE*, (320), pp 159-164.
- Houlsby G. T., Wroth C. P. and Wood D. M. (1982). Predictions of the results of laboratory tests on clay using a critical state model. *Proc. Int. workshop on constitutive behaviour of soils*, Grenoble, Balkema , pp 99-121.
- Huang W., Pu J. and Chen Y. (1981). Hardening rule and yield function for soils. *Proc. 10<sup>th</sup> ICSMFE*, (1), pp 631-634.
- Hvorslev M. J. (1960). Physical components of the shear strength of saturated clays. *Proceedings of the Research Conference on Shear Strength of Cohesive Soils*, ASCE, Boulder, CO, pp 169-273.
- Horslev M.J.(1937). *Über die Festigkeitseigenschaften Gestörter, Bindiger Böden*, Copenhagen.
- Ichikawa Y. Kyoya T. and Kwamoto T. (1988). Incremental theory of elasticity and plasticity under cyclic loading. *Proc. of Int. Conf. on Constitutive laws*

- for engineering materials, Tuckson. pp 451-462.
- Ichikawa Y. Yamabe T. Obara Y. Ito F. and Kwamoto T. (1987). Brittle ductile fracture of a tuffaceous rock and plasticity theory. Proc. of 6<sup>th</sup> Int. Conf. on numerical methods in Geomechanics, pp 327-334.
- Ingraffea A.R.(1987). Theory of crack initiation and propagation in rock. In Fracture Mechanics of Rocks, ed by B.K. Atkinson, pp 71-110, Academic Press, London.
- Irwin G. R. (1957). Analysis of stresses and strains near the end of a crack traversing a plate, Trans. ASME, Journal of Applied Mechanics, Vol 24, pp 361-364.
- Irwin G. R. (1958). Fracture. In Handbuch der Physik, Vol 6, ed by S. Flungge, pp 551-590. Springer, Berlin.
- ISSMFE subcommittee on constitutive laws of soils (1985). Constitutive laws of soils. ed. S. Muruyama, Jap. Soc. SMFE, pp 25-65.
- ISSMFE technical committee on soft rocks and indurated soils (1989). Recent advances in soft rock research. Report of ISSMFE technical committee on soft and indurate soils and Proc. of discussion session, (5), XII ICSMFE, Rio de Janeiro, pp 1-21.
- Jakobson B.(1957). Some Fundamental properties of sand. 4<sup>th</sup> ICSMFE, London, Vol 1, pp 167-171.
- Jamiolkowski M., Lancellotta R. and Lo Presti D.C.F. (1995). Remarks on the stiffness at small strains of six Italian clays. Pre-Failure Deformation of Geomaterials, Shibuya, Mitachi and Miura (eds.), Balkema, Vol 2, pp 817-836.
- Janbu N. (1963). Soil compressibility as determined by oedometer and triaxial tests. Proc. 2nd European Conf. on Soil Mechanics, Wiesbaden, Vol 1, pp 19-24.
- Jardine R.J. (1995). One perspective of the pre-failure deformation characteristics of some geomaterials. Pre-Failure Deformation of Geomaterials, Shibuya, Mitachi and Miura (eds.), Balkema, Vol 2, pp 855-886.
- Jardine R. J., Potts D. M., Fourie A. B. and Burland J. B. (1986). Studies of the influence of nonlinear stress-strain characteristics in soil-structure interaction. Geotechnique, Vol 36, No 3, pp 377-396.
- Jayatilaka S. (1993). Fracture of Brittle Solids, 2nd Edn, Cambridge University Press Great Britain.
- Johnston I. W. and Novello E.A. (1985). Cracking and critical state concepts for soft rocks. Proc. 11<sup>th</sup> Int. Conf. on Soil Mech. And Found. Eng., Vol 2, San Francisco, pp 515-518.
- Jovicic V. and Coop M.R. (1998). The measurement of stiffness anisotropy in clays with bender element tests in the triaxial apparatus. Geotechnical Testing Journal, Vol 21, No 1, pp 3-10.
- Jovicic V. (1997). The measurement and interpretation of small strain stiffness of soils. PhD thesis, City University, London, UK.
- Kavvasdas M. and Amorosi A. (2000). A constitutive model for structured soils. Geotechnique, Vol 50, No 3, pp 263-273.
- Kjellman W. (1936). Report on apparatus for consummate investigation of the mechanical properties of soils. 1<sup>st</sup> ICSMFE, Cambridge, Vol 2, pp 16-20.

- Lee K.L.(1970). Comparison of plane strain and triaxial tests of sand. Journal of the Soil Mechanics and Foundation Division. ASCE, Vol 96, No 5, SM3.
- Lee K.L. and Seed H.B.(1964). Discussion on use of free end in triaxial testing on clays. ASCE, Vol 91, No SM 6, pp 173-177.
- Leonards G. A. and Ramiah B.K. (1959). Time effects in the consolidation of clays ASTM Special Technical Publication, No 254, pp 116-130.
- Leroueil S. and Barbarosa P. S. (2000). Combined effect of fabric, bonding and partial saturation on yielding of soils. In Rahardjo, Toll & Leong (eds), Asian Conf. on unsaturated soils, Singapore, Rotterdam: Balkema, pp 527-532.
- Lo K.W., Nikraz R.H.,Tamilselvan T. and Zhao M.M.(2005). An Elastoplastic fracture model for soil and soft rock. Proc of the 11th International Conference on Fracture, Turin, Italy.
- Lo K.W. (2001). Constitutive behaviour of brittle hard soil-soft rock. Research Report No RP950629, Departement of Civil Engineering, National University of Singapore.
- Lo K.W., Mita K.A., and Tamilselvan T. (2000). Plane strain testing of overconsolidated clay. Research Report, Departement of Civil Engineering, National University of Singapore.
- Lo K. W. and Tamilselvan T. (1998). Crack kink analysis – an aberration of fracture mechanics. Research Report No CE025/98. Department of Civil Engineering, National University of Singapore.
- Lo K. W. and Tamilselvan T. (1997). The unified equivalent stress intensity factor,  $K_0$ . In Advances in Fracture Reseach, Vol. 4, ed by B. L. Karihallo, Y. W. Mai, M. I. Ripley and R. O. Ritchie, pp 2031-2038, Pergamon, Great Britain.
- Lo K.W., Lai M.O. and Tamilselvan T. (1997). True shear and mixed mode fracture toughness testing of materials. In Advances in Fracture Research, Vol 5, ed., B.L.Karihaloo, Y.W.Mai, M.I. Ripley and R.O.Ritchie, Pergamon, Great Britain.
- Lo K. W. and Tamilselvan T., Zhao M. M. and Chua K. H. (1996). A new treatise on fracture mechanics. Reseach Report No CE017/96, Department of Civil Engineering, National University of Singapore.
- Lo K.W., Tamilselvan, T., Chua K.H. and Zhao M.M.(1996). A Unified model for fracture mechanics. In Engineering Fracture Mechanics, Vol.54, No. pp.189-210.
- Lo K.W., Chua K.H. and Tamilselvan, T.(1993). A fracture mechanical model for hard soil. In Geotechnical Engineering of hard soils-soft rocks, Vol.1, ed. by A. Anagnostopoulos, F. Schlosser, N. Kalteziotis and R. Frank, pp 647-652.
- Lorenz H., Neumeuer H. and Gudehus G. (1965). Test concerning compaction and displacements performed on samples of sand in the state of plane deformation. 6<sup>th</sup> ICSMFE, Montreal, Vol 1, pp 293-297.
- Marach N.D., Duncan J.M., Chan C.K. and Seed H.B.(1981). Plane strain testing of sand, laboratory shear strength of soil. ASTM STP 740, pp 294-302.
- Maekawa H. and Miyakita K. (1983). Mechanical properties of diatomaceous soft rock. Proc. JSCE, (334), pp 135-143.
- Maatouk A., Leroueil S. and La Rochelle P. (1995). Yielding and critical state of

- acollapsible unsaturated silty soil. *Geotechnique*, Vol 45, No 3, pp465-477.
- Matyas E. L. (1967). Air and water permeability of compacted soils. In *Materials. Special technical publication*, Vol 417, pp 160-175.
- Mita K. A. (2003). Constitutive testing of soil on the dry side of critical state', national University of Singapore, PhD. Thesis.
- Mitchell J. K. (1993). *Fundamental of soil behaviour*. Second edition. John Willey and Sons, Inc. New York.
- Mochizuki A., Min C. and Takahashi S.A (1993). A method for plane strain testing of sand. *Journal of Japanese Geotechnical Society*, No 475, pp 99-107.
- Mochizuki A., Mikasa M. and Takahashi S. (1988). A new independent principal stress control apparatus. In *Advanced Triaxial Testing of Soil and Rock*. ASTM STP 97, Donaghe et al., Eds., American Society for Testing and Materials, Philadelphia, pp 844-858.
- Montanez J. E. C. (2002). Suction and volume changes of compacted sand-bentonite mixtures. PhD thesis, Imperial College, University of London, London, UK.
- Morgenstern N. (1977). Slope and excavation in heavily over consolidated clays, *Proc. of 9th Int. Conf. on Soil Mechanics and Foundation Engineering*, State of the Art Report, Tokyo, Japan, Vol 2, pp 567-581.
- Morris P.H., Graham J., and Williams D.J. (1992). Crack depth in drying clays using fracture mechanics. *ASCE's Geotechnical Special Publication No 43*, Vallejo, L. E., and Liang, R.Y., eds, pp 40-53.
- Mroz Z., Norris V. A. and Zienkiewicz O. C. (1978). An anisotropic hardening model for soils and its application to cyclic loading. *Int. Jurnal of Numerical Analitic*, Vol 2, pp 203-221.
- Mroz Z., Norris V. A. and Zienkiewicz O. C. (1979). Application of an anistropic hardening model in the analysis of elasto-plastic deformation of soils. *Geotechnique*, Vol 29, pp 1-24.
- Mroz Z., Norris V. A. and Zienkiewicz O. C. (1981). An anisotropic critical state model for soils subject to cyclic loading. *Geotechnique*, Vol 31, pp 451-469.
- Nagaraj T. S. and Somashekar B. V. (1979). Stress deformation and strength of soils in plane strain. *Proc. of 6<sup>th</sup> Asian Reginal Conf. on Soil mechanics and Foundation engineering*, Singapore, Vol I, pp 43-46
- Naylor D. J. (1985). A continuous plasticity version of the critical state model. *Int. J. Num. Meth. Eng.*, Vol 21, pp 1187-1204.
- Nelson I. (1978). Constitutive models for use in numerical computations. *Proc. Seminar Dynam. Meth. Soil and Rock Mechanics*, Karlsruhe, Vol 2, pp 45-97.
- Novello E. A. and Johnston I. W. (1995 ). *Geotechnical materials and the critical state*. *Geotechnique*, Vol 45, No 2, pp 223-235.
- Nyaoro D. L. (1989). Analysis of soil-structure interaction by finite elements. PhD thesis, Imperial College, University of London.
- Nuismer R.J. (1975). An energy release rate criterion or mixed mode fracture, *International Journal of fracture*, Vol 11, pp 245-250.
- Ohmaki S. (1979). A mechanical model for the stress-strain behaviour of normally consolidated cohesive soil. *Soils and Foundations*, Vol 19, No 3, pp 29-44.
- Ohmaki S. (1980). A stress-strain relationship of normally consolidated cohesive

- soils and generalized stress conditions. *Soils and Foundations*, Vol 21, No 1, pp 29-43.
- Ohta H. and Wroth C. P. (1976). Anisotropy and stress reorientation in clay under load. 2<sup>nd</sup> Int. Conf. Numerical Meth. Geomech., Blacksburg, (1), pp 319-328.
- Ohta H., Nishihara A and Morita Y. (1985). Undrained stability of  $K_0$  consolidated clays. Proc 11<sup>th</sup> ICSMFE, Vol 2, San Fransisco, pp 613-617.
- Oka F. and Washizu H. (1981). Constitutive equations for sands and overconsolidated clays under dynamic loads based on elasto-plasticity. Proc. int. Conf. Recent advances in Geotech. Earthquake Eng. and Soil dynamics (ed. S. P. Prakash), St. Louis, pp 71-74.
- Okamoto T. (1985). Application of deformation model with no yield surface to various overconsolidated geologic materials. 5<sup>th</sup> Int. Conf. on Numer. Methods in Geomechanic, Nagoya, Japan, pp, pp 301-308.
- Ortigo J. A. R. (1995). Soil mechanics in the light of critical state theories, An introduction, A. A. Balkema, Rotterdam.
- Palmer A.C. and Rice J.R. (1973). The growth of slip surfaces in the progressive failure of over consolidated clay, Proc. of the Royal Society of London, Series A332, pp 527-548.
- Panasyuk V. V. (1997). Some stages of the development of fracture mechanics in the Ukraine. In *Fracture Research in Retrospect*, ed by H. P. Rossmannith, pp 351-367, Balkema, Rotterdam.
- Parry R. G. H. and Nadarajah V. A. (1973). A volumetric yield locus for lightly overconsolidated clay. *Geotechnique*, Vol 23, pp 450-453.
- Parry R. H. G. (1960). Triaxial compression and extension tests on remoulded caturated clays. *Geotechnique*, Vol 10, pp 166-180.
- Pender M. J. (1978). A model for the behaviour of overconsolidated soil. *Geotechnique*, Vol 280, pp 1-25.
- Pender M. J. (1982). A model for the cyclic loading of a overconsolidated soil. In *soil mechanics-transient cyclic loads*, (eds. G. N. Pande and O. C. Zienkiewicz), Wiley (Chichester), pp 283-311.
- Peters J.F., Lade P.V. and Bro A. (1988). Shear band formation in triaxial and plane strain tests. In *advanced Triaxial Testing of Soil and Rocks*. ASTM STP 977, ASTM, Philadelphia, pp 604-627.
- Pietruszczak St. and Mroz Z. (1983). On hardening anisotropy of  $K_0$ -consolidated clays. *Int. J. Numer. Anal. Geomech.*, (7), pp 19-38.
- Poorooshab H. B., Holubec I., and Sherbourne A. N. (1966). Yielding and flow of sand in triaxial compression. *Canadian Geotech. Journal*, Vol 3, No 4, pp 179–190.
- Potts D. M., Axelsson K., Grande L., Schweiger, H., Long M., Sagaseta C., Dolezalova, M., Anagnostou G, De La Fuente, P., Laue J., Herle I. and Battelino D. (2002). *Guidelines for the use of adfanced numerical analysis*. Thomas Telford Publishing, London.
- Potts D. M. and Zdravkovic L. (1999). *Finite element anaysis in geotechnical engineering: Theory*. Thomas Telford, London.
- Potts D. M. (1985). Behaviour of clay during cyclic during cyclic loading. *Developments in soil mechanics and foundation eng.* (eds. Banerjee and Butterfield), Elsevier, pp 105-138.

- Potts D. M. and Gens, A. (1984). The effect of the plastic potential in boundary value problems involving plane strain deformation. *Num, Anal. Meth. Geomech.*, Vol 8, pp 259-286.
- Prevost J. H. (1977). Mathematical modeling of monotonic and cyclic undrained clay behaviour. *International Journal for Numerical and Analytical Methods in Geomechanics*, Vol 1, pp 195-216.
- Prevost J. H. (1978a). Anisotropic undrained stress-strain behaviour of clays. *Eng Division, ASCE*, Vol 104, pp 1075-1090.
- Price A. M. and Farmer I. W. (1979). Application of yield models to rock. Technical note, *Int. J. Rock Mech. Min. Sci. and Geomech. Abstr.*, Vol 160, pp 157-159.
- Price A. M. and Farmer I. W. (1981). The Hvorsley surface in rock deformation. *Int. J. Rock Mech. Min. Sci. and Geomech*, Vol 180, pp 229-234.
- Rampello S. and Silvestri F. (1993). The stress-strain behaviour of natural and reconstituted samples of two overconsolidated clays. *Geotech. Eng. of Hard Soils-Soft Rocks*, Anagnostopoulos et al. (eds.), Balkema, Rotterdam, pp 769-778.
- Read H. E. and Hegemier G. P. (1984). Strain-softening of rock. *Soil and concrete – A review article*, *Mech. Mat.*, Vol 3, No 4, pp 271-294.
- Rendulic L. (1936). Relation between void ratio and effective principle stress for a remoulded silty clay. *Proc. of 1<sup>st</sup> Int. Conf. on Soil mechanics and foundation engineering*, Cambridge, pp 48-51.
- Richart F.E., Hall J.R. and Woods R.D. (1970). *Vibrations of soils and foundations* Prentice-Hall, Inc., Englewood Cliffs, New Jersey.
- Ridley A. M. (1993). The measurement of soil moisture suction. Phd thesis, Imperial College, London.
- Roscoe K. H. (1970). The influence of strains in soil mechanics. 10<sup>th</sup> Rankie Lecture. *Geotechnique*, Vol 20, No 2, pp 129-170.
- Roscoe K. H and Burland J. B. (1968). On the generalized stress-strain behaviour of 'wet' clay. *Engineering Plasticity*, Cambridge University Press, Cambridge, pp 535-609.
- Roscoe K. H and Poorooshab H. B. (1963). A theoretical and experimental study of strains in triaxial compression tests for normally consolidated clays. *Geotechnique*, Vol 13, pp 12-38.
- Roscoe K. H., Schofield A. N. and Thuairejah A. (1963). Yielding of clays in stress wetter than critical. *Geotechnique*, Vol 13, pp 211-240.
- Roscoe K. H., Schofield A. N. and Wroth C. P. (1958). On the yielding of soils. *Geotechnique*, Vol 8, pp 22-52.
- Rowe P.W. (1971). Theoretical meaning and observed values of deformation parameters for soils. *Proc. of the Roscoe Memorial Symposium on Stress-strain behaviour of Soils*, pp 143-194.
- Rowe P.W. and Barden L. (1964). Importance of Free Ends in Triaxial Testing. *ASCE*, Vol 90, No SMI, January, pp1-27.
- Saada A.S., Bianchini G.F., and Liang L. (1994). Cracks, bifurcation and shear bands propagation in saturated clays. *Geotechnique*, Vol 44, No 1, pp 35-64.
- Saada A. S., Chudnovsky A. and Kennedy M. R. (1985). A fracture mechanics study of stiff clays. *Proc. of 11<sup>th</sup> International conference on soil*



- mechanics and foundation engineering, san Francisco, pp 637-640.
- Sekiguchi H. and Ohta H. (1977). Induced anisotropy and time dependency in clays. 9<sup>th</sup> ICSMFE, Tokyo, Spec. Session 9, pp 163-175.
- Schanz T. and Alabdullah J. (2007). Testing Unsaturated Soil for Plane Strain Conditions: A New Double Wall Biaxial Device. Book: Experimental Unsaturated Soil Mechanicss. Book series: Springer Proceedings in Physics, Springer, Berlin Heidelberg, Vol 112, pp 169-178, ISSN: 0930-8989, ISBN: 978-3-540-69873-9 (Online)
- Schofield A.N. and Wroth C.P. (1968). Critical State Soil Mechanics. Mc Graw Hill, London
- Sharma R. S. (1998). Mechanical behaviour of unsaturated highly expansive clay. PhD thesis, Cambridge University, UK.
- Sih G.C. (1973). Some basic problems in fracture mechanics and new concept. Engineering Fracture mechanics, 5, pp 365-377.
- Sih G.C., Paris P. C. and Erdogan F. (1962). Crack tip stress intensity factors for plane extension and plate bending problems, Journal of Applied Mechanics, 29, pp 306-312.
- Simulia Inc (2006). ABAQUS Version 6.6. USA.
- Skempton A. W., Scuster R.L. and Petley D.J. (1969). Joint and fissure in the London clay at Wrysbury and Edgeware. Geotechnique, Vol 47, No 2, pp 235-254.
- Skempton A. W. and La Rochelle P. (1965). The Bradwell slip: a short-term failure in London clay. Geotechnique, Vol 15, No 3, pp 221-242.
- Smith P.R. (1992). Properties of high compressibility clays with reference to construction on soft ground. PhD thesis, Imperial College, University of London, London, UK.
- Stallebrass S. E. and Taylor R. N. (1997). The development and evaluation of a constitutive model for the prediction of ground movements in overconsolidated clay. Geotechnique, Vol 47, No 2, pp 235-254.
- Taylor D.W. (1941). 7<sup>th</sup> Progress report on shear strength to US Engineers. Massachusetts Institute of Technology.
- Terzhagi K. (1936). The shear strength of saturated soils. Proc. of. 1<sup>st</sup> Conf. on Soil mechanics and foundation engineering, Cambridge, Vol 1, pp 54-56.
- Thangayah, T. S. (1998). A model for mixed mode fracture. PhD thesis, National University of Singapore.
- Timoshenko S. P. and Goodier J. N. (1970). Theory of elasticity, 3rd Edn, McGraw-Hill, New York.
- Vaid Y. P. and Campanella R. G. (1974). Triaxial and plane strain behaviour of natural clay. ASCE, Jnl. Geotechnical Eng., Vol 100, No 3, pp 207-218.
- Vallejo L.E., Alaasmi A. and Yoo H.(1993). Behaviour under compression of stiff clay with multiple cracks. Proc. of International symposium on hard soils-soft rocks, Athen, pp 825-830.
- Vallejo L.E.(1989). Fissure parameters in stiff clays under compression. Journal of geotechnical engineering, Vol 115, No 9, pp1303-1317.
- Vallejo L.E.(1988). The brittle and ductile behaviour of clay samples containing a crack under mixed mode loading. Theoretical and Applied Fracture Mechanics, Vol 10, pp73-78
- Vallejo L.E.(1987). The influence of fissure in a stiff clays. Geotechnique, Vol 37,

- No 1, pp 69-82.
- Vallejo L.E.(1986). Mechanics of crack propagation in stiff clays. In Geotechnical aspect of stiff and hard clay, pp 14-27.
- Vallejo L.E.(1985). Fissure interaction and the progressive failure of slopes. Proc. of 11<sup>th</sup> International conference on soil mechanics and foundation engineering, San Fransisco, pp 2353-2356.
- Vanapalli S. K., Fredlund D.G, Pufahl D. E. and Clifton A. W. (1996). Model for prediction of shear strength with respect to soil suction. Canadian Geotech. Journal, Vol 33, pp 379-392.
- Vardoulakis I. (1980). Shear band inclination and shear modulus of sand in biaxial tests. International Journal for Numerical and Analytical Methods in Geomechanics, Vol 4, No 2, pp 103-119.
- Vardoulakis I. and Goldscheider, M. (1981). Biaxial apparatus for testing shear bands in soils. Proc. 10<sup>th</sup> ICSMFE, Stockholm, Balkema, Rotterdam. Vol 4/61, pp 819-824.
- Vaughan P. R. (1997). Engineering behaviour of weak rocks: some answer and some questions. Geotech. Engineering of hard soils-soft rocks (eds. Anagnostopoulos et al.), Rotterdam, Balkema, pp 1741-1765.
- Vermeer P. A. (1982). A simple shear band analysis using compliances. Proc. IUTAM Conf., Deformation and failure of granular materials (eds. P. A. Vermeer and H.J. Luger), Delft, Balkema (Rotterdam), pp 493-499.
- Vermeer P. A. (1998). Non-associated plasticity for soils, concrete and rock. Physics of dry granular media (eds. H. J. Herman et al.), Kluwer Academic Publisher, pp 163-196.
- Vesga L. F. (2005). Mechanics of crack propagation in clays under dynamic loading. Phd Thesis, University of Pittsburg, Pennsylvania, USA.
- Viggiani G. and Atkinson J.H. (1995). Stiffness of fine-grained soil at very small strains. Geotechnique, Vol 45, No 2, pp 249-265
- Viggiani G, Finno R.J. and Harris W.W. (1994). Experimental Observations of strain localisation in plane strain compression of a stiff clay. In Localisation and Bifurcation Theory for Soils and Rocks, Chambon et.al., Eds., Balkema, Rotterdam, pp189-198.
- Wang J. J. , Zhu J. G. , Chiu C.F. and Zhang H. ( 2007). Engineering Geology, Vol 94, No 1-2, pp 65-75.
- Weibull, W. (1939). A statistical theory of the strength of materials. Proc. Royal Swedish Institute for Engineering Research. Stockholm, Sweden, Vol 151, No.1.
- Westergaard H. M.(1939). Bearing pressures and cracks, ASME Journal of Apllied Mechanics, Vol 6, pp 49-53.
- Wheeler S. J. and Sivakumar V. (1995). An elastic critical state framework for unsaturated soil. Geotechnique, Vol 45, No 1, pp 35-53.
- Whittle A.J. (1993). Evaluation of a constitutive model for overconsolidated clays. Geotechnique, Vol 43, No 2, pp 289-313.
- Whittle A. J. (1987). A constitutive model for overconsolidated clays. Geotechnique, Vol 43, No 2, pp 289-313.
- Wilde P. (1983). Elastic-plastic behaviour in plane strain problems for granular media. Ing-Arch., Vol 53, pp 85-100.
- Williams A.A.B., and Jennings J.E. (1977). The in-situ shear behaviour of fissured

- soils, Proc. of the 9th Int. Conf. on Soil Mechanics and Foundation Engineering, Tokyo, Japan, Vol 2, pp 169-176.
- Wood C. C. (1958). Shear strength and volume change characteristics of compacted soil under conditions of plane strain. Ph.D. thesis, University of London.
- Wroth C. P. and Houlsby G. T. (1980). A critical state model for predicting the behaviour of clays. Proc. Workshop on Limit equilibrium, plasticity and generalized stress-strain in geotechnical engineering, Montreal, pp 592-627.
- Wroth C. P. and Houlsby G. T. (1985). Soil mechanics-property characterization and analysis procedures. Proc. 11<sup>th</sup> Int. conf. SMFE, (1), San Fransisco, pp 1-55.
- Yatomi C., Yashima A., Lizuka A. et al. (1989). General theory of shear bands formation by a non coaxial Cam-Clay model. Soils and Foundation, Vol 29, No 29, No 3, pp 41-53.
- Zdravkovic L., Potts D.M and Hight D.W. (2002). The effect of strength anisotropy on the behaviour of embankments on soft ground. Geotechnique, Vol 52, No 6, pp 447-457.
- Zdravkovic L., Potts D.M and Jardine R.J. (2001). A parametric study of the pull-out capacity of bucket foundations in soft clay. Geotechnique, Vol 51, No 1, pp 55-67.
- Zhong, K. (2003). Mixed mode I-II-III fracture criterion and its application to cement mortar. PhD thesis, National University of Singapore.
- Zhao X. H., Sun H. and Lo K.W.(2002). An elastoplastic damage model of soil. Geotechnique, Vol 52, No 7, pp533-536.
- Zienkiewicz O.C., Chan A.H.C., Pastor M., Schrefler B.A. and Shiomi T. (1999). Computational geomechanics with special reference to earthquake engineering, John Wiley & Sons, Chichester, UK.
- Zienkiewicz O. C. and Taylor R. L. (1989). The finite element method, 4th Edn, McGraw-Hill, UK.
- Zienkiewicz O. C. and Naylor D. J. (1973). Finite elements studies of soils and porous media. Lect. Finite Elements in Continuum Mechanics (eds. Oden and de Arantes). UAH press, pp 459-493.
- Zytynski M., Randolph M. F., Nova R. and Wroth C. P. (1978). Short communications on modelling the unloading-reloading behaviour of soils. International Journal for Numerical and Analytical Methods in Geomechanics, Vol 2, pp 87-94.

*“Every reasonable effort has been made to acknowledge the owners of copyright material. I would be pleased to hear from any copyright owner who has been omitted or incorrectly acknowledge.”*

## **APPENDICES**

**Papers resulted from the project**

## INFLUENCE OF DISCONTINUITIES ON THE BEHAVIOUR OF PARTIALLY SATURATED COMPACTED CLAY

Miftahul Fauziah

Research student, Civil Engineering Department, Curtin University of Technology

Email: [miftahul.fauziah@postgrad.curtin.edu.au](mailto:miftahul.fauziah@postgrad.curtin.edu.au)

Lecturer, Civil Engineering and Planning Department, Islamic University of Indonesia

Email : [miftah@ftsp.uui.ac.id](mailto:miftah@ftsp.uui.ac.id)

Hamid R Nikraz

Civil Engineering Department, Curtin University of Technology

Email: [H.Nikraz@exchange.curtin.edu.au](mailto:H.Nikraz@exchange.curtin.edu.au)

---

### ABSTRACT

*The partially saturated soil behaviour is quite different from those of fully saturated soil because of the presence of matric suction pressure. Although soils are generally assumed fully saturated below the groundwater table, they may be semi saturated near the state of full saturation under certain conditions. Results obtained with the strength theory of saturated soil could not be directly applied to solve the partially saturated soil problems, in particular to the soil containing discontinuities. It has been observed that discontinuities are known to develop when such geological materials are subject to loading. In the case of strong rock, on the other hand, there has been considerable interest in the application of fracture mechanics to account for such discontinuities. Moreover, the mechanical properties of soil that usually conducted by the use of triaxial apparatus rather than biaxial device will be addressed according to the fact that field problems involving geotechnical structures are often truly or close to plane strain situation. This paper will disseminate the result of some experimental testing on the effect of discontinuities on the properties of partially saturated compacted kaolin clay specimen under triaxial and biaxial condition. A modification of the conventional triaxial apparatus was used in this study. A high air-entry disc (HAED) was used as the interface between the unsaturated soil and the pore water pressure measuring system. Two types of intact specimen and pre-crack specimen have been tested under biaxial as well as triaxial condition. It was concluded that the discontinuities on the specimen weaken the shear strength as well as compressive strength of the specimen.*

Keywords: *discontinuities, partly saturated, matric suction, triaxial and biaxial*

### INTRODUCTION

The behaviour of partially saturated soil is different from those of fully saturated soil because of the influence of suction. Partially saturated soils form the largest category of materials that cannot be classified by classical saturated soil mechanics concepts. Results obtained with the strength theory of saturated soil could not be directly applied to solve the partially saturated soil problems. Although soils are generally assumed fully saturated below the groundwater table, they may be semi saturated near the state of full saturation under certain conditions. The situation of partial saturation may be caused by several factors, such as variation of water table level due to natural or manmade processes.

Generally, Partially saturated soil is characterized by three phases, soil solids, water, and air. The presence of a fourth independent phase, a so called air-water interface or contractile skin was

introduced by Fredlund and Morgenstern in 1977. Based on multiphase continuum mechanics, they proposed a theoretical stress analysis of an partially saturated soil (Fredlund and Morgenstern, 1993). The analysis concluded that any two of three possible normal stress variables can be used to describe the stress state of an unsaturated soil. In contrast to saturated soil, it is possible to relate the behaviour of the soil to the effective stress only. The presence of matric suction pressure is the main difference between saturated and unsaturated soil mechanics. It has been observed that several stability problems, involving soils used as construction materials, are due to water content changes and therefore to matric suction changes that occur periodically in nature.

The present modeling of brittle soil and weak rock is based on principles of continuum mechanics in spite of the fact that discontinuities are known to develop when such geological materials are subject to loading. In the case of strong rock, on the other

hand, there has been considerable interest in the application of fracture mechanics to account for such discontinuities (Ingraffea, 1987). Many studies have been conducted on detailed aspect of such discontinuities, but these are of limited practical application in an actual situation. The existence of cracks and fissures, which are the result of mechanical, thermal and volume-change-induced stresses, such soils are non uniform and therefore not amenable to analysis by continuum mechanics. On the other hand, fracture mechanical theory may be used to advantage to replicate their behavior.

Atkinson and Bransby (1982) proposed the conventional failure criteria for soils which might be partly appropriate to yield-dominant behaviour, but not this category of brittle fracture. In practice, there is the possibility that soil behaves more like a brittle material. The soil ruptures suddenly under compressive loading like soft rock, starting from the weakest crack in it. A basic premise of fracture theory is that crack like imperfections are inherent in engineering materials. These defects have the tendency to make stresses higher, which eventually trigger off fractures when a material body is subjected to a critical load or undergoes damage under cyclic loading. This present state of fracture mechanical theory has been summarized by Anderson (2004). Lo et al (2005) modeled brittle overconsolidated clay accordingly and thereby provided a rational basis for the prediction of such soil behaviour.

Most laboratory experiments on soils for the purposes of evaluating constitutive behaviour and stability properties of soil are performed under axisymmetric or conventional triaxial conditions. However, most geotechnical field problems such as landslide problems, failure of soils beneath shallow foundations, and failure of retaining structures are truly or close to biaxial situations. Mochizuki et al (1993) reported that when soil is tested under plane strain conditions, it, in general, exhibits a higher compressive strength and lower axial strain. Behaviour of fined grained sands tested under biaxial conditions has been reported (Alshibli et al, 2004; Alshibli and Sture, 2000; Bizzarri, 1995; Han and Vardoulakis, 1991; Hans and Drescher, 1993; Marach et al, 1984; and Mochizuki et al, 1993). The plane strain testing of clay has only been initiated recently (Fauziah and Nikraz, 2008; Fauziah and Nikraz, 2007; Lo et al, 2000; Drescher et.al (1990)) and published data of such tests especially for brittle clay material is very limited.

This paper will present the experimental study of the behaviour of pre-crack partially saturated clay specimens compare to the intact specimen by the use of biaxial compression apparatus as well as triaxial

test set-up, although the behaviour of overconsolidated clay (Fauziah and Nikraz, 2007) and fracture characteristics of brittle clay may also be determined by this test apparatus. Description of the apparatus, specimen preparation, testing method, procedure and data analysis will be presented in the following discussion. Some results of the testing will be compared with the known soil behaviour and previous working.

## DISCRIPTION OF THE DEVICE

A conventional triaxial apparatus was modified for the purpose of biaxial testing in this study. The biaxial arrangement is placed in a cell, with the height of 300 mm, 200 mm internal diameter and 30 mm wall thickness. Figure 1 shows the schematic diagram of the biaxial compression device

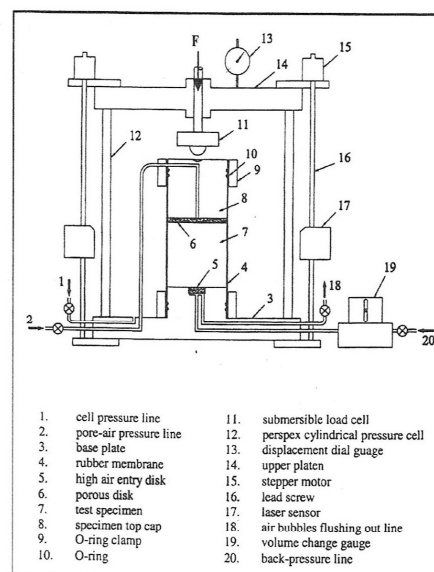


Figure 1 A schematic diagram of the plane strain device

A prismatic specimen with the size of 36 mm wide, 72 mm high, and 72 mm thick, so that the aspect ratio is 2, is placed on the base pedestal where it was restrained laterally by two rigid perspex plates to restrain its out-of plane movement which make  $\epsilon_2=0$ . Therefore, only major ( $\sigma_1$ ) and minor ( $\sigma_3$ ) principal stresses acting on the soil specimen (Figure 2).

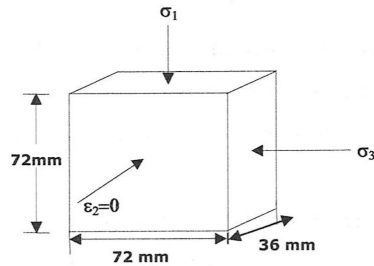


Figure 2 A schematic diagram of plane strain condition

To prevent any air from passing through the disc into the measuring system, a high air-entry disc (HAED) was used as the interface between the partly saturated soil and the pore water pressure measuring system. All surfaces which are in contact with the specimen were lubricated to avoid the likelihood of scratching and reduced friction. An LVDT (Linear Vertical Displacement Transducer) was used to measure the axial displacements of the test specimen. The global volume change of the water saturated soil specimen was monitored by the use of an automatic volume change unit which is connected to the back-pressure line. A data acquisition system consisting of an MPX 300 data logger and a set of microcomputer were used to record the displacement, loads, pressure and volume change reading of the specimen. WINHOST 2.0 package software was used to convert digital bit data from the ADU (Analogue digital Unit) to engineering units based on the calibration of the relevant measuring unit, which was done before running the plane strain test. A more detail description of this biaxial compression device can be found in previous working reported by Fauziah and Nikraz (2008) and Fauziah and Nikraz (2007).

#### MATERIAL PREPARATION AND METHOD

The material used in this study was commercial Kaolin clay, a product of UNIMIN PTY LTD, Australia. The basic characteristics of the material are shown in Table 1.

Table 1. Basic characteristics of kaolin clay

Type of test	Value
Liquid limit (ASTM D-4318)	53.5 %
Plastic limit (ASTM D-427)	30.76 %
Plasticity Index	22.74 %
Specific Gravity (ASTM D-854)	2.60

It took few weeks to complete the preparation of soil specimen. Initially, a kaolin clay sample was slurried to a uniform consistency of 1 ½ times its liquid limit using an electrical soil mixer. This slurry was obtained by mixing 8 kg of kaolin powder with 6 kg of water using the electric mixer for about 2 hours. Before pouring the kaolin slurry to the consolidation unit, the inner wall of the cylinder mould was greased to ease the extrusion of the sample from the mould at the end of consolidation. A steel cylindrical mould with the height of 600 mm and 150 mm in diameter was used to consolidate the slurry using a hydraulic tester in over a period of one to two weeks which the maximum of 300 kPa was applied in three stages.

To apply the pressure evenly to the slurry, two circular perspexes were placed at both ends of the slurry in the mould. The slurry was allowed to consolidate by its own weight and small pressure was applied to prevent the slurry being squeezed out between the circular perspexes and the mould. A higher vertical pressure was applied when there was no further settlement change. The soil was then extruded from the mould into lubricated formers when the consolidation process had completed. Following this, the specimen and the former were wrapped in plastic film sheeting after sealing both their faces with liquid wax. To obtain even pore water pressure, the specimens were placed in the dehumidifier for at least 2 days until it is tested.

In the plane strain test set-up, the rubber membrane was first placed over the test specimen with the aid of a sleeve stretcher. The rectangular porous plate was then placed on top of the specimen followed by the top assembly and the high air-entry disc (HAED). The rubber membrane was next slipped over the porous plate, the top assembly and the HAED and secured by the use of a set of O-rings and rectangular Perspex clamp. The specimen, together with the porous plate and the top assembly were then placed over the pedestal of the plane strain compression apparatus. The rubber membrane was next slipped over the pedestal and secured by the use of a set of O-rings and clamp set. Two rigid perspex plates were then placed and secured by the use of clamp set for biaxial test set up (Figure 3). For triaxial test set up the rigid plates were uninstalled to specimen. The pressure cell, top assembly and laser sensor set-up were then installed.

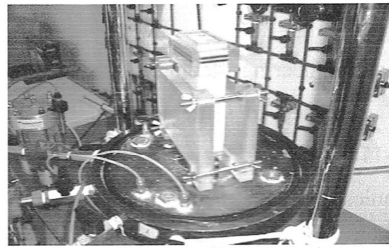


Figure 3 Side view of biaxial test set up

## TESTING METHOD AND PROCEDURE

Two types of intact specimen and pre-crack specimen have been tested under biaxial and triaxial condition. The pre-crack specimen were made by adding the 3 cm diagonal precrack in the center of the intact specimen to make the discontinuities in the specimen. Three specimen of IBM (intact specimen, biaxial), PCBM (Pre-crack specimen, biaxial) and ITM (intact specimen, triaxial) were tested under net normal stress of 0 and maximum matric suction of 500 kPa and three specimen of IBN (intact specimen, biaxial), PCBN (Pre-crack specimen, biaxial) and ITN (intact specimen, triaxial) were tested under matric suction of 0 and maximum net normal stress of 800 kPa. The specimen was first saturated until the B-value of the specimen reached the value of 0.95-0.98, followed by matric suction applied and loading compression processed.

A cell pressure of 600 kPa, back pressure of 590 kPa and pore pressure of 600 kPa were applied to provide an initial net normal stress of 0 and matric suction of 10 to the IBM, PCBM, and ITM specimens. The volume change of the soil skeleton was monitored continuously by the laser sensors. The change in volume of water in the specimen was also monitored continuously by the volume change gauge which was connected to the back-pressure line. Once the changes in the soil and water volumes had ceased, the test specimen was presumed to have fully consolidated under a matric suction of 10 kPa. The matric suction was next increased to 20 kPa by reducing the back pressure to 580 kPa. The corresponding changes in the soil skeleton and water volumes were monitored continuously until they had ceased, at which stage the corresponding void ratio and the water content of the test specimen were computed from the cumulative changes in soil skeleton and water volumes. The entire procedure, that is from increasing the matric suction to the desired value up to flushing out the air bubbles, was repeated for matric suctions of 50, 100, 200, 300, and

500 kPa respectively, which were applied by reducing the back pressure accordingly.

Another test apparatus were set up for IBN, PCBN, and ITN specimens similarly as before, except that the head was replaced with a porous disc. A cell pressure of 110 kPa, back-pressure of 100 kPa and pore-air pressure of 100 kPa were then applied to the specimen to provide an initial net normal stress of 10 kPa and matric suction of 0. The changes in soil skeleton and water volumes were then monitored continuously and when these changes had ceased, the total changes in soil and water volumes were noted. The net normal stress was first increased to 20 kPa by increasing the cell pressure to 120 kPa. Thereafter, the entire above procedure, starting from applying the net normal stress up to when the changes in soil and water volumes ceased, was repeated for net normal stresses of 50, 100, 200, 300, 500 and 800 kPa.

The specimen was then compressed by elevating the base of the confining pressure cell at a constant velocity of 0.08 mm/m with the drainage line closed at at net normal stress of 0 and matric suction of 500 kPa for IBM, PCBM, and ITM specimen and at matric suction of 0 and net normal stress of 800 kPa for IBN, PCBN, and ITN specimen. This loading rate was deduced based on the permeability of adopted kaolin clay suggested by Bishop and Henkel (1962).

The data were recorded at 3 minute interval test and it was terminated at the axial strain of about 20 % or sooner. The specimen was then taken out immediately for the purpose of moisture content test. In the analysis of the behaviour of the brittle unsaturated clay, the pore pressure parameter would be required in order to the determined the pore pressure increments and the matric suction. The pore pressure parameters were deduced from the volumetric deformation coefficient, which was obtained by laboratory testing. This procedure was proposed by Fredlund and Rahardjo (1993), although adapted to biaxial conditions.

## TEST RESULT AND DISCUSSION

The typical result given by specimens tested under biaxial condition of IBM, IBN, PCBM, and PCBN as well as specimen observed under triaxial test set up of ITM and ITN will be discussed in the following discourse. The strain softening response of the intact and pre-crack specimen tested under biaxial test set up are depicted in Figure 4 and stress-strain curves of the intact specimen tested under biaxial and triaxial condition presented in Figure 5. The peak stress and strain of the specimen is summarised in Table 2.



Table 2. The peak stress vs axial strain

Specimen name	Peak stress (kPa)	Vertical strain (%)
IBN	159.178	3.64
PCBN	125.336	2.73
ITN	139.464	3.03
IBM	228.395	3.87
PCBM	124.519	3.33
ITM	175.926	3.33

In general, the shear stress curves increase monotonically with the increasing vertical strain until they reach peak stresses followed by strain softening behaviour. According to Lo et al (2005) this is the typical phenomenon of specimen of brittle, hard partly saturated soil specimen and exhibit elastic only.

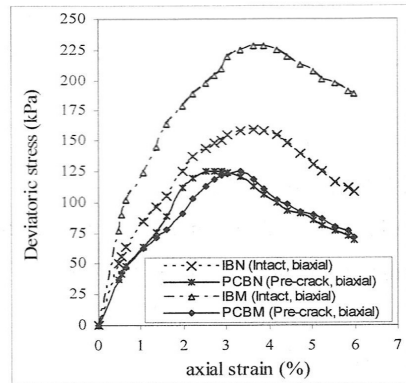


Figure 4 Stress strain behaviour of intact and pre-crack specimen under biaxial testing

As can be seen in Figure 4, the shear strength of the intact specimen of IBM and IBN were higher along the vertical strain than that the specimen containing discontinuities or precrack of PCBN and PCBM specimen. The highest failure stress of 228.395 kPa was reached by the intact specimen of IBM, and the lowest failure stress of 124.519 kPa was derived by the pre-crack specimen of PCBM. The presence of a fissure or discontinuity makes the soil weaker as the effective area offering resistance to shear is reduced. The shear strength along a surface of discontinuity is thereby less than that of the intact material. It is also shown from the graph that the pronounced peak shear strength were occurred to the precrack specimen than the intact specimen. Similar observation of pre-crack overconsolidated clay had been reported elsewhere (Lo et al, 2000).

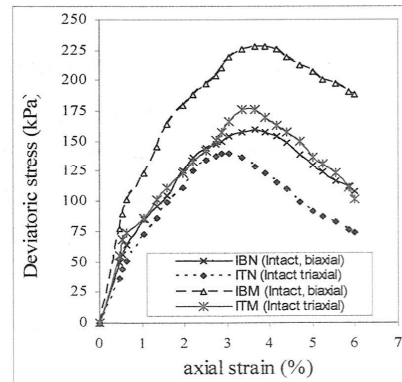


Figure 5 Stress strain of intact specimen under biaxial and triaxial testing

The shear stress versus axial strain curves of intact specimen under biaxial and triaxial testing were presented in Figure 5. The graph shows that under the same matric suction and net normal stress the biaxial specimen of IBM had higher shear stress along the strain than that the specimen of ITM which was tested at triaxial test set up, as well as the IBN specimen compared to the ITN specimen. The triaxial specimen also reached earlier peak strength at 3.03 % and 3.33 % axial strain for ITM and ITN respectively than that the biaxial specimen of IBM and ITM at 3.87 % and 3.64 % respectively. This result seem to be consistent with the founding of Mochizuki et al (1993).

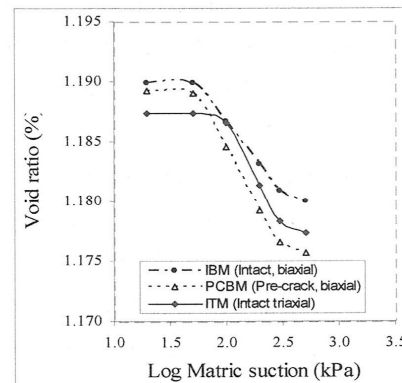


Figure 6: Void ratio versus matric suction of IBM, PCBM and ITM specimens

Figure 6 and Figure 7 present the constitutive surface of void ratio versus log net normal stress and log matric suction of the specimen. The slope of the intersection curves are the volume change index  $C_m$

and water content index  $D_m$  respectively for the case that net normal stress set to zero, whereas the slope of the intersection curves are the volume change index  $C_i$  and water content index  $D_i$  when the matric suction set to zero.  $C_i$  is the slope of the consolidation curve and is equal to the compressive index of a saturated soil, while  $C_m$  is the slope of the shrinkage curve. The change in void ratio of the IBM, PCBM and ITM specimen in relation with matric suction depicted in Figure 6, while water content changes of the IBN, PCBN and ITN specimen in connection with net normal stress changes presented in Figure 7. It can be shown from the graphs that the curves went down with the increasing of either matric suction or net normal stress for all of the specimens.

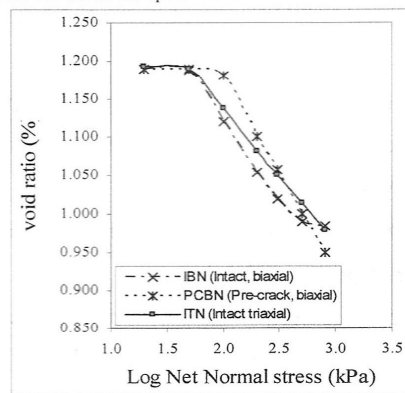


Figure 7 Void ratio versus matric suction of IBN, PCBN and ITN specimens

The value of the volume change index of the IBM, PCBM and ITM specimens were calculated as 0.011, 0.016, and 0.017 respectively. The value of the  $C_i$  of the IBN, PCBN and ITN specimens are 0.219, 0.257 and 0.232 respectively. The higher slope of ITN and ITM curves than that of IBN and ITM curve indicated that the specimen tested at biaxial condition had higher compressive strength than that of specimen tested under triaxial test set up. This is in well agreement with the observation reported by Mochizuki et al (1993). It is also clearly shown that the specimens containing precrack of PCBM and PCBN had higher compressive index than that the intact specimens of IBM and ITN.

The change in water content of the specimen in relation with matric suction and net normal stress depicted in Figure 8 and Figure 9. The constitutive surface of water content is defined by the compressive index  $D_m$  and  $D_i$  corresponding to the matric suction and net normal stress respectively. The value of compressive index obtained by

determining the gradient of the linear portion of the curve of the water content against the log of matric suction for  $D_m$  and the log of net normal stress for  $D_i$ .

As can be seen from the graph that the curve went down with the increasing of either matric suction or net normal stress for all the specimens. The curve also indicated that the higher gradient value of 0.071 and 0.068 were reached by precrack specimens of PCBM and PCBN respectively than that the gradient value of intact specimens of IBM and IBN which were 0.55 and 0.056 respectively (Figure 8). Similar to the curve of the volume change result on Figure 6 and Figure 7, and consistent with the stress-strain behaviour of the specimens shown on Figure 4 and Figure 5, the existence of the crack or discontinuities on the specimen not only weaken its shear strength as well as its compressive strength but they also quicken the failure of the specimen.

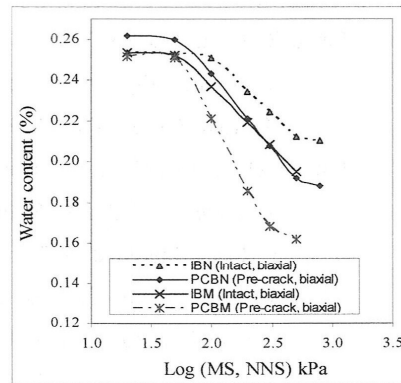


Figure 8 Water content change of intact and pre-crack specimen under biaxial testing

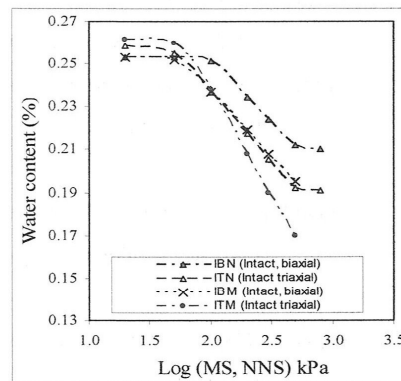


Figure 9 Water content change of intact specimen under biaxial and triaxial testing

The water content change of intact specimen under biaxial and triaxial testing were plotted in Figure 9. The graph shows that under the same matric suction and net normal stress the biaxial specimen of IBM had lower slope than that the specimen of ITM which was tested at triaxial test set up, as well as the IBN specimen to the ITN specimen. This result indicated that in general specimen tested under plane strain condition exhibits a higher compressive strength than that the specimen tested under triaxial test set up.

## CONCLUSION

The following conclusion might be drawn from this experimental study.

1. The typical of brittle hard clay and exhibit elastic only behaviour were shown by all the specimen tested.
2. Shear strength of the intact specimen were higher along axial strain than that the intact specimen. It is also shown that the pronounced and lower value of peak shear strength were occurred to the precrack specimen than the intact specimen.
3. The weaken compressive strength of the specimen containing discontinuities were indicated by their higher volume change index than the intact specimen's.
4. Under the same matric suction and net normal stress the specimen tested under plane strain condition exhibits a higher compressive strength than that the specimen tested under triaxial test set up.

## ACKNOWLEDGMENT

The authors generously give acknowledgment to Professor Kwang Wei Lo from National University of Singapore and Dr Min Min Zhao for their valuable advice and support and also to Dr. Pontjo Utomo and Mr. Paisar Syakur, for their assistance, commitment and care.

## REFERENCES

- Alshibli, K.A. and Sture, S., 2000, Shear bands formation in plane strain experiments of sand, *Journal of Geotechnical and Geoenvironmental Engineering*, v 126, n.6, June, ASCE, Paper no.21167, ASCE, USA.
- Alshibli, K.A., Godbold, D. L., and Hoffman, K., 2004, The Louisiana Plane strain apparatus for soil testing, *Geotechnical Testing Journal*, v 27, n 4, July, p 337-346, ASTM, US.
- Anderson, T.L., 2004, *Fracture mechanics: fundamental and applications*, 3<sup>rd</sup> ed., CRC Press, London, UK.
- Atkinson, J.H. and Bransby, P.L., 1982, *The mechanics of soils : an introduction to critical state soil mechanics*. McGraw-Hill, New York, US.
- Atkinson, J.H. and Richardson, D., 1987, The effect of local drainage in shear in shear zones on the undrained strength of overconsolidated clay. *Geotechnique*, 37 (3), 393-403, Thomas telford, UK.
- Bizzarri, A., Allersma, H. G. B., Koehorst, B. A. N., 1995, Preliminary tests on soft clay with a biaxial apparatus, *Proceedings of the 1995 International Symposium on Compression and Consolidation of Clayey Soils. Part 1 (of 2)*, May 10-12 1995, Hiroshima, Japan.
- Fauziah, M. and Nikraz, H., 2007, Biaxial testing of overconsolidated clay, *Proceeding of The 1<sup>st</sup> International Conference of European Asian Civil Engineering Forum*, Universitas Pelita Harapan, 27-28 September 2007, Jakarta, Indonesia.
- Fauziah, M. and Nikraz, H., 2007, Stress-strain behaviour of overconsolidated clay under plane strain condition, *Proceeding of The 10<sup>th</sup> Australia New Zealand conference on geomechanics*, Australian Geomechanics Society, 21-25 October 2007, Brisbane, Australia.
- Fauziah, M. and Nikraz, H., 2008, The behaviour of unsaturated compacted clay under plane strain condition, *Proceeding of The 3<sup>rd</sup> International conference on Geo-Environment and Landscape Evolution*, Wessex Institute of Technology, 16-18 Jun 2008, The New Forest, UK.
- Fauziah, M. and Nikraz, H., 2008, Volume change behaviour of unsaturated compacted clay under plane strain condition strain condition, *The Australian Earth Science Convention*, Geological Society of Australia, 20-25 July 2008, Perth, Australia.
- Fredlund, DG and Rahardjo, H (1993). “ *Soil mechanics for unsaturated soil*, John Wiley & Sons, Inc, US
- Grammatikopoulou, A., 2004, *Development, Implementation and Application of Kinematic Hardening Models for Overconsolidated Clays*, Phd Thesis, Imperial College, London.
- Han, C. and Drescher, A., 1993, Shear bands in biaxial tests on dry coarse sand. *Soils and Foundations*, Japanese Society of Soil

- Mechanics and Foundation Engineering*, Vol.33, No.1, pp.118-132, JSSMFE, Japan.
- Han, C and Vardoulakis, I.G., 1991, Plane strain compression experiments on water-saturated fine-grained sand, *Geotechnique*, Vol. 41, No.1, pp.49-78, Thomas telford, UK.
- Head, K.H., 1986, *Manual of Soil Laboratory Testing*. Vol 3, Pentech Press, London, UK.
- Ingraffea, AR (1987). "Theory of crack initiation and propagation in rock", *In Fracture Mechanics of Rocks*, ed by B.K. Atkinson, pp.71-110, Academic Press, London, UK.
- Lo, K.W., Nikraz, R.H., Tamiselvan, T. and Zhao, M.M., 2005, An elastoplastic shear fracture model for soil and soft rock, *Proc of the 11th International Conference on Fracture*, ICF XI, ASTM, 20-25 March 2005, Turin, Italy.  
[www.icf11.com/proceeding/TOPIC/topic.htm](http://www.icf11.com/proceeding/TOPIC/topic.htm)
- Lo, K.W., Mita, K.A., and Tamiselvan, T., 2000, *Plane Strain Testing of Overconsolidated Clay*, Research Report, Department of Civil Engineering, National University of Singapore.
- Mochizuki, A., Min, C. and Takahashi, S.A., 1993, A method for plane strain testing of sand. *Journal of Japanese Geotechnical Society*, No.475, pp.99-107, JGT, Japan.
- Marach, N.D., Duncan, J.m., Chan, C.K. and Seed, H.B., 1981, *Plane strain testing of sand, laboratory shear strength of soil*. ASTM STP 740, pp.294-302.
- Viggiani, G., Finno, R.J. and Harris, W.W., 1994, *Experimental Observations of strain localisation in plane strain compression of a stiff clay*. In *Localisation and Bifurcation Theory for Soils and Rocks*, Chambon et.al., Eds., , pp.189-198, Balkema, Rotterdam.

# **The Proceedings of The Nineteenth (2009) International OFFSHORE AND POLAR ENGINEERING CONFERENCE**

Osaka, Japan, June 21-26, 2009

**VOLUME II, 2009**

## **GEOTECHNICAL AND GEOENVIRONMENTAL ENGINEERING**

**Plenary Presentation, Cyclic Loading and Liquefaction, In-Situ Test, Seepage and Soil Improvement, Consolidation and Embankment, Soil Properties and Centrifuge, Foundation, Pile and Caisson, Landslide and Stability, Modeling and Simulation, Geohazard and Geoinformatics**

ISBN 978-1-880653-53-1 (Vols. 1-4 Full Proceedings Set)

ISSN 1098-6189 (Vols. 1-4 Full Proceedings Set)

Indexed by Engineering Index, Compendex and Others

[www.isopec.org orders@isopec.org](http://www.isopec.org/orders@isopec.org)

Edited by:

**Jin S. Chung**, ISOPE, Cupertino, California, USA

**Wan C. Kan**, ExxonMobil Development Co., Houston, TX, USA

**Sangchul Bang**, South Dakota School of Mines and Technology, Rapid City, SD, USA

**Kazunori Uchida**, Kobe University, Kobe, Japan

**Hermann Moshagen**, BHM Engineering Services, Trondheim, Norway

Presented at:

The Nineteenth (2009) International Offshore and Polar Engineering Conference held in Osaka, Japan, June 21-26, 2009

Organized by:

International Society of Offshore and Polar Engineers

Sponsored by:

International Society of Offshore and Polar Engineers (ISOPE) with cooperating societies and associations

The publisher and the editors of its publications assume no responsibility for the statements or opinions expressed in papers or presentations by the contributors to this conference or proceedings.

**International Society of Offshore and Polar Engineers (ISOPE)**  
**P.O. Box 189, Cupertino, California 95015-0189 USA**

## **CONTENT**

### **GEOTECHNICAL AND GEOENVIRONMENTAL ENGINEERING**

#### **Soil Properties and Centrifuge**

**156** **Shear Strength Characteristics of Landslide Soils, Asato Landslide, Okinawa, Japan**

Sho Kimura, Seiichi Gibo, Shinya Nakamura and Shriwantha Buddhi Vithana

**162** **Evaluation of Deformation Modulus of Cemented Sands Using Cone Tip Resistance**

Moon-Joo Lee, Sung-Kun Choi, Hyunwook Choo and Woojin Lee

**168** **Electrical Resistivity and Cone Tip Resistance Monitoring by Using Cone Resistivity Penetrometer**

Hyung-Koo Yoon, Joon Han Kim, Raehyun Kim and Jong-Sub Lee

**172** **Temperature-Compensated Micro Cone Penetrometer by Using FBG Sensor**

Raehyun Kim, Woojin Lee, Shinwhan An, Hyung-Koo Yoon and Jong-Sub Lee

**177** **Biaxial Testing on the Properties of Pre-cracked Partially Saturated Clay**

Miftahul Fauziah and Hamid Reza Nikraz

**183** **Centrifuge Experiments Investigating the Use of Jetting in Spudcan Extraction**

Christophe Gaudin, Britta Bienen and Mark J. Cassidy

**191** **Centrifuge Model Tests on Suction Piles in Sand Under Inclined Loading**

K.O. Kim, Y.S. Kim, Y. Cho, S. Bang and K. Jones

## **Biaxial Testing on the Properties of Pre-cracked Partially Saturated Clay**

*Miftahul Fauziah<sup>1)</sup> and Hamid Reza Nikraz<sup>2)</sup>*

<sup>1)&2)</sup> Civil Engineering Department, Curtin University of Technology,  
Perth, Western Australia, Australia

<sup>1)</sup> Civil Engineering and Planning Faculty, Universitas Islam Indonesia  
Yogyakarta, Indonesia

### **ABSTRACT**

This paper presents the result of the biaxial testing on the properties of precrack partially saturated clay specimen. A modification of the conventional triaxial apparatus was used in this study. Cell pressure from the triaxial compression test and a rigid loading platen are used to apply the minor and major principle stresses to the specimen. A high air-entry disc (HAED) was used as the interface between the partially saturated soil and the pore water pressure measuring system. Experimental results proved that the existence of crack or fissure in soil influence the mechanical properties of the specimen tested.

**KEY WORDS:** Partially saturated; matric suction; pre-crack; biaxial; triaxial.

### **INTRODUCTION**

The behavior of partially saturated soil is quite different from those of fully saturated soil because of the influence of suction. Partially saturated soils form the largest category of materials that cannot be classified by classical saturated soil mechanics concepts. Results obtained with the strength theory of saturated soil could not be directly applied to solve the partly saturated soil problems. Although soils are generally assumed fully saturated below the groundwater table, they may be semi saturated near the state of full saturation under certain conditions. The situation of partial saturation may be caused by several factors, such as variation of water table level due to natural or manmade processes.

Partially saturated soil is generally characterized by three phases, soil solids, water, and air. The presence of a fourth independent phase, a so called air-water interface or contractile skin was introduced (Fredlund and Morgenstern, 1977). Based on multiphase continuum mechanics, a theoretical stress analysis of an unsaturated soil has been presented (Fredlund and Morgenstern, 1977; Fredlund and Morgenstern, 1976). The analysis concluded that any two of three possible normal stress variables can be used to describe the stress state of an unsaturated soil. This is in contrast to saturated soil, where it is possible to relate the

behaviour of the soil to the effective stress only. The presence of matric suction pressure is the main difference between saturated and unsaturated soil mechanics. It has been observed that several stability problems, involving soils used as construction materials, are due to water content changes and therefore to matric suction changes that occur periodically in nature.

For the purposes of evaluating constitutive behaviour and stability properties of soil, most laboratory experiments on soils in particular to the clayey soils are performed under axisymmetric or conventional triaxial conditions. However, most geotechnical field problems such as landslide problems, failure of soils beneath shallow foundations, and failure of retaining structures are truly or close to biaxial situations. Mochizuki-Min and Takahashi (1993) reported that when soil is tested under plane strain conditions, it, in general, exhibits a higher compressive strength and lower axial strain. Behaviour of fined grained sands tested under biaxial conditions has been reported (Alshibli-Godbold and Hoffman 2004; Alshibli and Sture, 2000; Bizzarri, 1995; Han and Vardoulakis, 1991; Hans and Drescher, 1993; Lee, 1970; Marach-Duncan-Chan and Seed, 1984; Mochizuki-Min and Takahashi, 1993). The plane strain testing of clay has only been initiated recently (Fauziah and Nikraz, 2008; Fauziah and Nikraz, 2007; Lo-Mita and Thangayah, 2000; Drescher et.al (1990)) and published data of such tests especially for hard clay material is very limited.

The present modeling of brittle soil and weak rock is based on principles of continuum mechanics in spite of the fact that discontinuities are known to develop when such geological materials are subject to loading. In the case of strong rock, on the other hand, there has been considerable interest in the application of fracture mechanics to account for such discontinuities (Inggraffea, 1987). Many studies have been conducted on detailed aspect of such discontinuities, but these are of limited practical application in an actual situation. The existence of cracks and fissures, which are the result of mechanical, thermal and volume-change-induced stresses, such soils are non uniform and therefore not amenable to analysis by continuum mechanics. On the other hand, fracture mechanical theory may be used to advantage to replicate their behavior.

The conventional failure criteria for soils (Atkinson and Bransby, 1982) may be partly appropriate to yield-dominant behaviour, but not this category of brittle fracture. In practice, there is the possibility that soil behaves more like a brittle material. The soil ruptures suddenly under compressive loading like soft rock, starting from the weakest crack in it. A basic premise of fracture theory is that crack like imperfections are inherent in engineering materials. These defects have the tendency to make stresses higher, which eventually trigger off fractures when a material body is subjected to a critical load or undergoes damage under cyclic loading. This present state of fracture mechanical theory has been summarized (Anderson, 2004). Lo-Nikraz-Thangayah and Zhao (2005) modeled brittle overconsolidated clay accordingly and thereby provided a rational basis for the prediction of such soil behaviour.

The behaviour of pre-crack partially saturated clay specimens by the use of biaxial compression apparatus will be presented in this paper, although the behaviour of overconsolidated clay (Fauziah and Nikraz, 2007) and fracture characteristics of brittle clay may also be determined by this test apparatus. Details of the apparatus, specimen preparation and data evaluation will be presented in the following discussion. Some results of the testing will be compared with the known soil mechanical concept.

#### BIAXIAL TEST EQUIPMENT

The biaxial apparatus used in this experimental study was a modification of the conventional triaxial apparatus. The biaxial arrangement is placed in a cell, with the height of 300 mm, 200 mm internal diameter and 3 mm wall thickness. A prismatic specimen of initial width of 36 mm, height of 72 mm, and thickness of 72 mm, so that the aspect ratio is 2, is placed on the base pedestal where it is restrained laterally by two rigid perspex plates to restrain its out-of plane movement which make  $\epsilon_2=0$ . Therefore, only major ( $\sigma_1$ ) and minor ( $\sigma_3$ ) principal stresses acting on the soil specimen (Figure. 1 and Figure. 2). Previous researchers (Taylor, 1941; Rowe and Barden, 1964; Lee and Seed, 1964; Bishop and Green, 1965) found that if the specimen aspect ratio (height to width) was bigger than 2, the effect of loading platen friction and the restraint of loading frame would be negligible and the specimen would maintain constant strength.

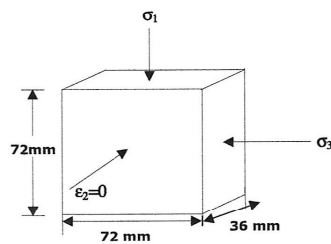


Figure. 1 A schematic diagram of biaxial condition

A high air-entry disc (HAED) was used as the interface between the unsaturated soil and the pore water pressure measuring system. This was to prevent any air from passing through the disc into the measuring system, provided that the matric suction did not exceed the air-entry value of the disc. To avoid the likelihood of scratching and reduced

friction, all surfaces which are in contact with the specimen were lubricated. The cell was filled with water to enable the specimen to be pressurized laterally using the pressure generator for applying confining pressure, which was supplied by a compressed air cylinder, connected to gas-water pressure accumulator equipped with pressure gauges and regulators. A 50 kN capacity of Wykeham Farrance displacement-controlled compression machine was used for the application of axial load of the biaxial testing.

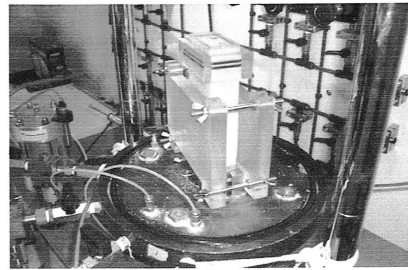


Figure. 2 Side view of biaxial test set up (Fauziah and Nikraz, 2008)

A submersible load cell of 5 kN capacity was used to measure the axial load of the specimen. A 35-mm range LVDT (Linear Vertical Displacement Transducer) which was attached on top of the top cover of the cell was used to measure the axial displacements of the test specimen. To measure the applied cell pressure, back pressure pore pressure and flush pressure of the specimen four pore pressure transducers were used and mounted to the base plate of the cell. An automatic volume change unit which is connected to the back-pressure line was used to monitor the global volume change of the water-saturated soil specimens.

A data acquisition system consisting of an MPX 300 data logger and a set of microcomputer were used to record the displacement, loads, pressure and volume change reading of the specimen. WINHOST 2.0 package software was used to convert digital bit data from the ADU (Analogue digital Unit) to engineering units based on the calibration of the relevant measuring unit, which was done before running the plane strain test.

#### SPECIMEN PREPARATION

Biaxial experimental testing has been performed on remoulded kaolin clay specimens. The material used in this study was commercial Kaolin clay, with a specific gravity  $G_s = 2.6$ , Liquid Limit  $LL = 53.5\%$  and plastic limit  $PL = 30.76\%$ . It took few weeks to complete the preparation of soil specimen.

Firstly, slurry of kaolin clay was mixed to a uniform consistency of  $1 \frac{1}{2}$  times its liquid limit using an electrical soil mixer. This slurry was obtained by mixing 8 kg of kaolin powder with 6 kg of water using the electric mixer for about 2 to 3 hours. A steel cylindrical mould with the height of 600 mm and 150 mm in diameter was used to consolidate the slurry using a hydraulic tester. To ease the extrusion of the sample from the mould at the end of consolidation, the inner wall of the cylinder mould was greased before pouring the kaolin slurry to the consolidation unit. A layer of sand and geosynthetic were placed on the top and the bottom of the slurry to accelerate the consolidation process. To apply



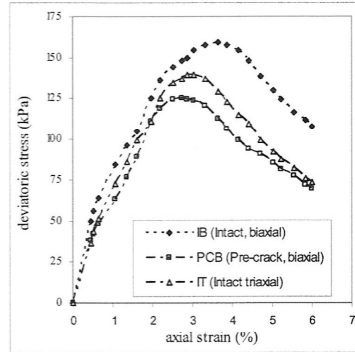


Figure. 4 Stress-strain behavior of the specimen

The presence of a crack or discontinuity makes the soil weaker as the effective area offering resistance to shear is reduced. The shear strength along a surface of discontinuity is thereby less than that of the intact material. The pre-crack specimen of test PCB reached earlier peak strength before falling toward whereas the peak strength of the pre-crack specimen of PCB was correspondingly lower. Compared to the intact specimen tested under triaxial condition of test IT, not only had higher peak stress, but the specimen of test IB also had higher shear strength along the vertical strain. Similar observation had been reported elsewhere (Lo-Mita and Thangayah, 2000 and Mochizuki-Min and Takashi, 1993).

The volume change relationships of the kaolin clay specimens is summarised in Table 1. The constitutive surface of void ratio is defined by the volume change index  $C_m$  and  $C_i$  corresponding to the matric suction and net normal stress respectively.  $C_i$  is the slope of the consolidation curve and is equal to the compressive index of a saturated soil, while  $C_m$  is the slope of the shrinkage curve. The value of compressive index obtained by determining the gradient of the linear portion of the curve of the water content against the log of matric suction for  $D_m$  and the log of net normal stress for  $D_i$ . The constitutive surface of water content is defined by the water content index  $D_m$  and  $D_i$  corresponding to the matric suction and net normal stress respectively. It clearly shown from the table that the specimens containing pre-crack of PCB had higher compressive index than that the intact specimen of IB. The reducing in effective area offering resistance to shear of pre-crack specimen makes it had lower compressive strength than that the intact specimen.

Table 1. Volume change index of the specimen

Specimen Type	Void ratio (e)		Water content (%)	
	$C_m$	$C_i$	$D_m$	$D_i$
IB	0.0115	0.2186	0.0548	0.0560
PCB	0.0160	0.2573	0.0708	0.0677
IT	0.0173	0.2318	0.0899	0.0623

Constitutive surface of void ratio versus log net normal stress and log matric suction of the specimen were plotted in Figures. 6-8. The slope

of the intersection curves are the volume change index  $C_m$  and water content index  $D_m$  respectively for the case that net normal stress set to zero, whereas the slope of the intersection curves are the volume change index  $C_m$  and water content index  $D_m$  when the matric suction set to zero. It can be shown from the graphs that the curves went down with the increasing of either matric suction or net normal stress for all of the specimens.

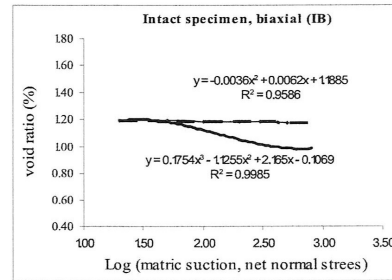


Figure. 5 Constitutive surface of void ratio versus net normal stress and matric suction of IB specimen (Intact, biaxial test)

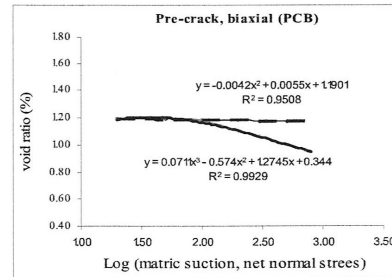


Figure. 6 Constitutive surface of void ratio versus net normal stress and matric suction of PCB specimen (Pre-crack specimen, biaxial test)

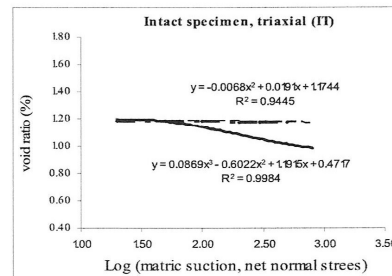


Figure. 7 Constitutive surface of void ratio versus net normal stress and matric suction of IT specimen (Intact specimen, triaxial test)

the pressure evenly to the slurry, two circular perspexes were placed at both ends of the slurry in the mould.

A vertical pressure of 300 kPa was applied on the top of the slurry to allow the consolidation process in over a period of one to two weeks which the maximum pressure of 300 kPa was applied in three stages. The slurry was allowed to consolidate by its own weight to prevent the slurry being squeezed out between the circular perspexes and the mould. A higher vertical pressure was applied when there was no further settlement change. Once the consolidation process completed the soil was extruded from the mould into lubricated formers. Following this, the specimen and the former were wrapped in plastic film sheeting after sealing both their faces with liquid wax. To obtain even pore water pressure, the specimens were placed in the dehumidifier for at least 2 days until it is tested.

The specimen in the former was then extruded using a hydrolic perspex rectangular block. The specimen was allowed to be intact initially, while for the pre-crack specimen it was given a 30 mm pre-crack in the center of the specimen. In the plane strain test set-up, the rubber membrane was first placed over the test specimen with the aid of a sleeve stretcher. The rectangular porous plate was then placed on top of the specimen followed by the top assembly and the high air-entry disc (HAED). The rubber membrane was next slipped over the porous plate, the top assembly and the HAED and secured by the use of a set of O-rings and rectangular Perspex clamp. The specimen, together with the porous plate and the top assembly were then placed over the pedestal of the plane strain compression apparatus. The rubber membrane was next slipped over the pedestal and secured by the use of a set of O-rings and clamp set. Two rigid perspex plates were then placed and secured by the use of clamp set. The pressure cell, top assembly and laser sensor set-up were then installed. The cell was then filled with water to enable the specimen to be pressurized laterally by the use of the pressure generator for applying confining pressure. Figure. 3 shows the biaxial testing arrangement.

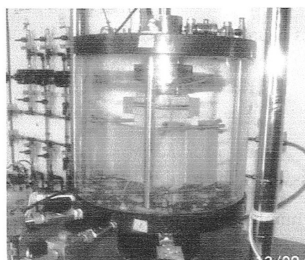


Figure. 3 Biaxial testing arrangement (Fauziah and Nikraz, 2007)

#### TEST PROCEDURES

Three types of specimens of IB (intact specimen, biaxial), PCB (Pre-crack specimen, biaxial) and IT (intact specimen, triaxial) were tested under net normal stress of 0 and maximum matric suction of 500 kPa and matric suction of 0 and maximum net normal stress of 800 kPa. Firstly, the specimen was saturated until the B-value of the specimen reached the value of 0.95-0.98, followed by matric suction applied and loading compression processed.

A cell pressure of 600 kPa, back pressure of 590 kPa and pore pressure of 600 kPa were applied to the specimen to provide an initial net normal stress of 0 and matric suction of 10. The volume change of the soil skeleton  $\Delta V_s$  was monitored continuously by the laser sensors. The change in volume of water in the specimen  $\Delta V_w$  was also monitored continuously by the volume change gauge which was connected to the back-pressure line. Once the changes in the soil and water volumes had ceased, the test specimen was presumed to have fully consolidated under a matric suction of 10 kPa. The matric suction was next increased to 20 kPa by reducing the back pressure to 580 kPa. The corresponding changes in the soil skeleton and water volumes were monitored continuously until they had ceased, at which stage the corresponding void ratio  $e$  and the water content of the test specimen were computed from the cumulative changes in soil skeleton and water volumes. The entire procedure, that is from increasing the matric suction to the desired value up to flushing out the air bubbles, was repeated for matric suctions of 50, 100, 200, 300, and 500 kPa respectively, which were applied by reducing the back pressure accordingly.

Another test apparatus set up similarly as before, except that the head was replaced with a porous disc. A cell pressure of 110 kPa, back-pressure of 100 kPa and pore-air pressure of 100 kPa were then applied to the specimen to provide an initial net normal stress of 10 kPa and matric suction of 0. The changes in soil skeleton and water volumes were then monitored continuously and when these changes had ceased, the total changes in soil and water volumes were noted. The net normal stress was first increased to 20 kPa by increasing the cell pressure to 120 kPa. Thereafter, the entire above procedure, starting from applying the net normal stress up to when the changes in soil and water volumes ceased, was repeated for net normal stresses of 50, 100, 200, 300, 500 and 800 kPa.

The specimen was then compressed by elevating the base of the confining pressure cell at a constant velocity of 0.08 mm/m with the drainage line closed at matric suction of 0 and net normal stress of 800 kPa. This loading rate was deduced based on the permeability of adopted kaolin clay suggested by Bishop and Henkel (1962). The data were recorded at 3 minute interval test and it was terminated at the axial strain of about 20 % or sooner. Following this, the specimen was taken out immediately for the purpose of moisture content test. In the analysis of the behaviour of the brittle unsaturated clay, the pore pressure parameter would be required in order to determine the pore pressure increments and the matric suction. The pore pressure parameters were deduced from the volumetric deformation coefficient, which was obtained by laboratory testing. This procedure was proposed by Fredlund and Rahardjo (1993), although adapted to biaxial conditions.

#### RESULTS AND DISCUSSION

Figure. 4 shows the strain softening response of the IB, PCB, and IT specimen tested at matric suction of 0 and net normal stress of 800 kPa. In general, the shear stress curves increase monotonically with the increasing vertical strain until they reach peak stresses followed by strain softening behaviour. According to Lo-Nikraz-Tamiselvan and Zhao (2005) this is the typical phenomenon of specimen of brittle, hard partly saturated soil specimen and exhibit elastic only. The highest failure stress of 159.178 kPa was reached by the intact specimen of IB, and the lowest failure stress of 125.336 kPa was derived by the pre-crack specimen of PCB.

Constitutive surface of water content versus net normal stress and matric suction of the specimen were depicted in Figures. 9-11. Similar to the curve of the volume change result in Figures. (9-11), and consistent with the stress-strain behaviour of the specimens shown in Figure 4, the existence of discontinuities cause by crack or fissure on the specimen makes the specimen weaker than that the intact specimen. The slope of the compressive index of the specimen indicated that the specimen containing pre-crack had lower strength than that the intact specimen.

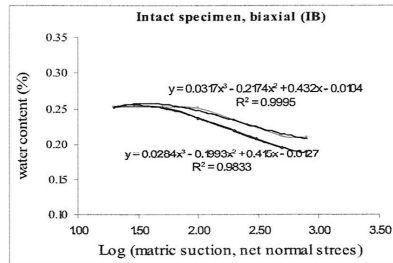


Figure. 9 Constitutive surface of water content versus net normal stress and matric suction of IB specimen (Intact specimen, biaxial test)

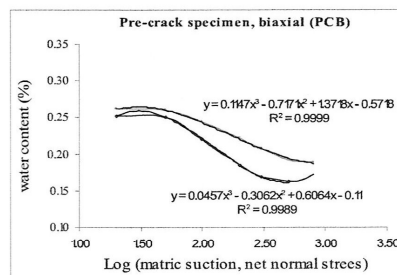


Figure. 10 Constitutive surface of water content versus net normal stress and matric suction of PCB specimen (Pre-crack, biaxial test)

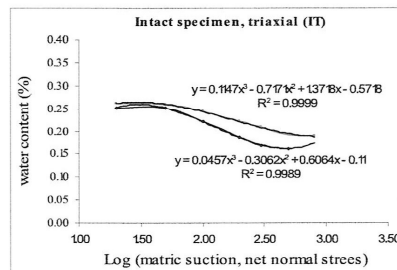


Figure. 11 Constitutive surface of water content versus net normal stress and matric suction of IT specimen (Intact specimen, triaxial test)

## CONCLUSIONS

Experimental results proved that the existence of crack or fissure in soil influence the mechanical properties of the specimen tested. The result of shear strength curves indicated that the specimens were the typical of brittle and exhibit elastic only failure. A pronounced failure and lower shear strength as well as compressive strength were reached by pre-crack specimen than the intact specimen. It is also noted that shear strength and compressive strength of the intact specimen under triaxial testing was lower than specimen tested under biaxial condition.

## ACKNOWLEDGEMENTS

The authors wish to express their gratitude to Professor Kwang Wei Lo from National University of Singapore and Dr Min Min Zhao for their valuable advices and support. Additionally, the authors would like to thank Dr. Pontjo Utomo and Mr. Paisar Syakur, for their assistance and care

## REFERENCES

- Alshibli, KA, Godbold, DL and Hoffman, K (2004). "The Louisiana Plane strain apparatus for soil testing", *Geotechnical Testing Journal*, ASTM, Vol 27, No 4, pp 337-346.
- Alshibli, KA and Sture, S (2000). "Shear bands formation in plane strain experiments of sand", *Journal of Geotechnical and Geoenvironmental Engineering*, ASCE, Paper no.21167.
- Anderson, TL (2004). "Fracture mechanics: fundamental and applications", CRC Press, London.
- Atkinson, JH and Bransby, PL (1982). "The mechanics of soils : an introduction to critical state soil mechanics", McGraw-Hill, New York.
- Bishop, AW and Green, GE (1965). "The influence of end restraint on the compression strength of cohesionless soil", *Geotechnique*, Vol 15, No 3, pp 243-266.
- Bishop, AW and Henkel, DJ (1962). "The measurement of soil properties in the triaxial test", Arnold, London.
- Bizzarri, A, Allersma, HGB, Koehorst, BAN (1995). "Preliminary tests on soft clay with a biaxial apparatus, *Proceedings of the 1995 International Symposium on Compression and Consolidation of Clayey Soils. Part 1 (of 2)*.
- Drescher, A, Vardoulakis, I and Han, C (1990). "A biaxial apparatus for testing soils", *Geotechnical Testing Journal*, GTJODJ, Vol 13, pp 226-234.
- Fauziah, M and Nikraz, H (2007). "Biaxial testing of overconsolidated clay, *Proceeding of The 1st International Conference of European Asian Civil Engineering Forum*, Pelita harapan University, pp 124-130.
- Fauziah, M and Nikraz, H (2007). "Stress-strain behaviour of overconsolidated clay under plane strain condition", *Proceeding of 10th Australia New Zealand conference on geomechanics*, AGS, pp 148-153.
- Fauziah, M and Nikraz, H (2008). "The behaviour of unsaturated compacted clay under plane strain condition", *Proceeding of the 3rd International Conference on Evaluation, Monitoring, Simulation, Management and Remediation of the Geological Environment and Landscape*, WIT Press UK, pp 77-86.
- Fauziah, M and Nikraz, H (2008). "Plane strain testing on properties of unsaturated compacted clay", *Proceeding of Geo-Chiang Mai 2008, An International Conference on Geotechnical Engineering*, CI-Premier CO Singapore, pp 157-164.
- Fredlund, DG and Rahardjo, H (1993). "Soil mechanics for unsaturated soil", John Wiley & Sons, Inc.

- Fredlund, DG and Morgenstern, NR (1976). "Constitutive relation for volume change in unsaturated soil", *Canadian Geotechnique Journal*, Vol 17, No 3, pp 261-276.
- Fredlund, DG and Morgenstern, NR (1977). "Stress state variables for unsaturated soils", *Journal of Geotechnical Engineering*, ASCE, Vol 103, No 5, pp 447-466.
- Green, GE and Reades, DW (1975). "Boundary conditions, anisotropy and sample shape effects on the stress-strain behaviour of sand in triaxial compression and plain strain", *Geotechnique*, Vol 25, No 2, pp 333-356.
- Han, C. and Drescher, A (1993). "Shear bands in biaxial tests on dry coarse sand", *Soils and Foundations, Japanese Society of Soil Mechanics and Foundation Engineering*, Vol 33, No 1, pp 118-132.
- Han, C and Vardoulakis, IG (1991). "Plane strain compression experiments on water-saturated fine-grained sand", *Geotechnique*, Vol 41, No 1, pp 49-78.
- Ingraffea, AR (1987). "Theory of crack initiation and propagation in rock", *In Fracture Mechanics of Rocks*, ed by B.K. Atkinson, pp 71-110, Academic Press, London.
- Lee, KL (1970). "Comparison of plane strain and triaxial tests of sand", *Journal of the Soil Mechanics and Foundation Division*, ASCE, Vol 96, No 3, pp 901-923.
- Lee, KL and Seed, HB (1964). "Discussion on use of free end in triaxial testing on clays", *ASCE*, Vol 91, No 6, pp 173-177.
- Lo, KW, Mita, KA, and Thangayah, T (2000). "Plane Strain Testing of Overconsolidated Clay", *Research Report*, Department of Civil Engineering, National University of Singapore.
- Lo, KW, Nikraz, RH, Thangayah, T and Zhao, MM (2005). "An elastoplastic shear fracture model for soil and soft rock", *Proc of the 11th International Conference on Fracture*, 2005  
www.icf11.com/proceeding/TOPIC/topic.htm
- Marach, ND, Duncan, JM, Chan, CK and Seed, HB (1984). "Plane strain testing of sand", *laboratory shear strength of soil*, ASTM STP 740, pp 294-302.
- Mochizuki, A, Min, C and Takahashi, SA (1993). "A method for plane strain testing of sand", *Journal of Japanese Geotechnical Society*, No 475, pp.99-107.
- Rowe, PW and Barden, L (1964). "Importance of Free Ends in Triaxial Testing", *ASCE*, Vol.90, No.1, pp.1-27.
- Taylor, DW (1941}. "*7th Progress report on shear strength to US Engineers*, Massachusetts Institute of Technology.
- Viggiani, G, Finno, RJ and Harris, WW (1994). "Experimental Observations of strain localisation in plane strain compression of a stiff clay", *In Localisation and Bifurcation Theory for Soils and Rocks*, Chambon et.al., Eds., Balkema, Rotterdam, pp 189-198.

# GEO-CHIANGMAI

focusing on New Developments in

- Soil & Rock Engineering
- Engineering Geology &
- Environmental Geotechnique

10-12 December 2008, Chiangmai, Thailand

Conference Advisory Committee (International)

## Conference Chairman

Dr Aniruth Thongchai

Head, Dept of Civil Engineering

Chiangmai University, Thailand

## Deputy Chairman

- Dr Chitchai Anantasech, Dept of Civil Engineering,  
Chiangmai University, Thailand

## Conference Past Chairmen

- Dr David Toll, University of Durham, UK (Singapore, 2006)
- Prof Xinghua Wang, Changsha University (Changsha China, 2007)

Conference Committee

Director: Er John S Y Tan, CI-Premier Conference, Singapore

## Members:

- Dr Jing-Cai Jiang, The University of Tokushima, Japan
- Dr Hasan Kamal, Kuwait Inst. of Scientific Research, Kuwait
- Mr Jack Oostveen, Delft University of Tech., The Netherlands
- Dr Jun Sugawara, Inst. of Slope Technology Co., Ltd, Japan
- Dr Kem Yah, PC Geo-Management Sdn Bhd, Malaysia
  - Dr M Zakaria Hossain, Mie University, Japan
- Prof Jun-Jie Zheng, Texas A & M University, USA

\*\*\*\*\*

## Support Organisations

Korean Geo-synthetics Society, Korea

Society of ISRM and IAEG, Singapore

## Managed by:

CI-Premier Conference Organisation, Singapore

### **Honorary Chairman:**

- Prof S L Lee, National University of Singapore, Singapore

### **Members:**

- Prof XingHua Wang (Chairman of GT07) will guide the Committee in the Advisory Committee
- Prof Isabel Pinto, Portugal; continues as one of the Editors of the Proceedings of the Conference

### **Advisors:**

- Dr. Hj. Affendi Abdullah, Ranhill Bersekutu Sdn. Bhd, Malaysia
  - Prof A A Balasubramaniam, Griffiths University, Australia
- Dr Ian Jefferson, University of Birmingham, United Kingdom
  - Prof Isabel Pinto, University of Coimbra, Portugal
  - Prof Han-Yong Jeon, Inha University, Korea
- Dr YingXin Zhou, President, Society for ISRM and IAEG, Singapore
  - Dr Myint Win Bo, DST Consulting Engineers, Canada

### **Themes:**

- 01-Geo mechanics
- 02-Soil mechanics
- 03-Geotechnical investigations & interventions
- 04-Structured foundations
- 05-Earthworks design
- 06-Lateral earth support structures
- 07-Ground subsidence & heave
- 08-Geosynthetics, geomembranes & geotextiles
- 09-Landslides and slope stability
- 10-Anchored structures (soil & rock anchors)
- 11-Design of rock structures
- 12-Environmental impact analysis
- 13-Geologic hazards predictions and risk mapping
- 14-Construction methods, qc and assurance
- 15-Case histories & practical examples
- 16-Other related topics
- 17-Soil contamination
- 18-Tunnels
- 19-Soil vibrations
- 20-Rock mechanics
- 21-Ground Improvement

# Plane Strain Testing on Properties of Unsaturated Compacted Clay

Miftahul Fauziah<sup>1</sup> & Hamid.R.Nikraz<sup>2</sup>

<sup>1</sup> Research student at Department of Civil Engineering  
Curtin University of Technology also lecturer at Indonesian Islamic  
University  
Indonesia

<sup>2</sup>Departement of Civil Engineering  
Curtin University of Technology  
Western Australia

## Abstract

The presence of matric suction pressure is the main difference between saturated and unsaturated soil. It has been observed that several stability problems involving soil as structure material are due to water content changes and therefore to matric suction changes in soil. Experimental tests to determinate the mechanical properties of soil usually are tested using triaxial apparatus, in spite of the fact that field problems involving geotechnical structures are often close to plane strain situations. This paper presents the result of the experimental testing on the properties of compacted kaolin clay specimen containing precrack in plane strain condition. The biaxial device, which was used in this study, is a modification of the conventional triaxial apparatus. Cell pressure from the triaxial compression test and a rigid loading platen are used to apply the minor ( $\sigma_3$ ) and major ( $\sigma_1$ ) principle stresses, respectively, to the clay specimen. The specimen is mounted inside the device, which fully restrains any out-of-plane deformation by the use of a pair of rigid perspex wall. A high air-entry disc (HAED) was used as the interface between the unsaturated soil and the pore water pressure measuring system. The volume change of the sample was measured by local strain devices, while the water volume change was recorded by a volume gauge. The experimental result shows that the discontinuities on the specimen weaken the shear strength and the compressive strength of the specimen and the test result in a good agreement with known soil behaviour.

Keywords: unsaturated soil, matric suction, clay, crack, biaxial and triaxial.

## 1. Introduction

Most of the manmade structures such as shallow foundations, retaining walls, cuts in slopes, etc are generally sited on the surface of the earth and above the water table. Although soils are generally assumed fully saturated below the groundwater table, they may be semi saturated near the state of full saturation under certain conditions. The situation of partial saturation may be caused by several factors, such as variation of water table level due to natural or manmade processes. The behaviour of unsaturated soil is quite different from those of saturated soil because of the influence of suction. Results obtained with the strength theory of saturated soil could not be directly applied to solve the problems related to the unsaturated soil.

Unsaturated soils form the largest category of materials that cannot be classified by classical saturated soil mechanics concepts. Any soil near the ground surface in a relatively dry environment will be subjected to negative pore-water pressure and possible desaturation. An unsaturated soil is generally characterized by three phases, soil solids, water, and air. The presence of a fourth independent phase, a so called air–water interface or contractile skin was introduced by Fredlund, and Morgenstern (1977) [1]. Based on multiphase continuum mechanics, a theoretical stress analysis of an unsaturated soil is presented by Fredlund and Morgenstern [1, 2]. The analysis

concluded that any two of three possible normal stress variables can be used to describe the stress state of an unsaturated soil. This is in contrast to saturated soil, where it is possible to relate the behaviour of the soil to the effective stress only. The presence of matric suction pressure is the main difference between saturated and unsaturated soil mechanics. It has been observed that several stability problems, involving soils used as construction materials, are due to water content changes and therefore to matric suction changes that occur periodically in nature.

Most laboratory experiments on soils in particular to the clayey soils are performed under axisymmetric or conventional triaxial conditions for the purposes of evaluating constitutive behaviour and stability properties. However, most geotechnical field problems such as landslide problems, failure of soils beneath shallow foundations, and failure of retaining structures are cases that can generally be considered as plane strain. Mochizuki et.al [3] reported that when soil is tested under plane strain conditions, it, in general, exhibits a higher compressive strength and lower axial strain. Most of the plane strain apparatus used by previous researchers (Mochizuki et.al.[3], Han and Vardoulakis [4], Green and Reades [5], Drescher et.al.[6], and Viggiani et.al.) had the common feature of using rigid walls and tie-rods to impose a zero strain boundary condition in one of the principle axes. This method was found to be satisfactory, and friction between the rigid wall and test specimen could be adequately mitigated. Taylor [8], Rowe and Barden [9], Lee and Seed [10] and Bishop and Green [11] found that if the aspect ratio (height to width) was bigger than 2, the effect of loading platen friction and the restraint of loading frame would be negligible.

The Behaviour of fined grained sands tested under plane strain conditions has been reported by Mochizuki et.al.[3], Han and Vardoulakis [4], Hans and Drescher [12], Lee, K. L. [13], Marach et. al. [15], Alshibli, K.A. and Sture, S. [16] and Alshibli et. al. [17] and the plane strain testing of clay has been initiated recently (Drescher [18], Fauziah, M and Nikraz, H.R. [19, 20], Lo et. al. [21], Bizzari, A. [22]). However published data of such tests especially for hard clay material and unsaturated soil are relatively rare. Lo et.al [23] presented a fracture model for soil and soft rock accordingly and thereby provided a rational basis for the prediction of such soil behaviour. This paper presents the behaviour of unsaturated compacted clay specimens containing precrack by the use of plane strain compression apparatus, although the behaviour of overconsolidated clay (Fauziah, M and Nikraz, H.R. [19, 20]) and fracture characteristics of brittle clay may also be determined by this test apparatus. Details of the apparatus, specimen preparation and data evaluation are presented in the following discussion. Some results of the testing will be compared with the known soil mechanical concept.

## **2. Description of the apparatus**

A schematic diagram of the biaxial device used in this study is shown in Figure 1. The testing apparatus used in this experimental study was a modification of the conventional triaxial apparatus. The biaxial arrangement is placed in a cell, with the height of 300 mm, 200 mm internal diameter and 30 mm wall thickness. A specimen of initial width of 36 mm, height of 72 mm, and thickness of 72 mm (Figure 2), so that the aspect ratio is 2, is placed on the base pedestal where it is restrained laterally by two rigid Perspex plates to restrain its out-of plane movement. A high air-entry disc (HAED) was used as the interface between the unsaturated soil and the pore water pressure measuring system. This was to prevent any air from passing through the disc into the measuring system, provided that the matric suction did not exceed the air-entry value of the disc. To offset the likelihood of scratching and reduced friction, all surfaces which are in contact with the specimen are lubricated. The cell is filled with water to enable the specimen to be pressurized laterally using the pressure generator for applying confining pressure.

The axial load of the specimen was measured by the use of a 5 kN capacity of submersible load cell. A 35-mm range LVDT (Linear Vertical Displacement Transducer) which was attached on top of the top cover of the cell was used to measure the axial displacements of the test specimen. Four pore pressure transducers were used and mounted to the base plate of the cell to measure the applied cell pressure, back pressure pore pressure and flush pressure of the specimen. The global volume change of the



water-saturated soil specimens are monitored by an automatic volume change unit which is connected to the back-pressure line. To record the displacement, loads, pressure and volume change reading a data acquisition system consisting of data logger and a set of microcomputer were used. Package software was used to convert digital bit data from the ADU (Analogue digital Unit) to engineering units based on the calibration of the relevant measuring unit, which was done before running the plane strain test.

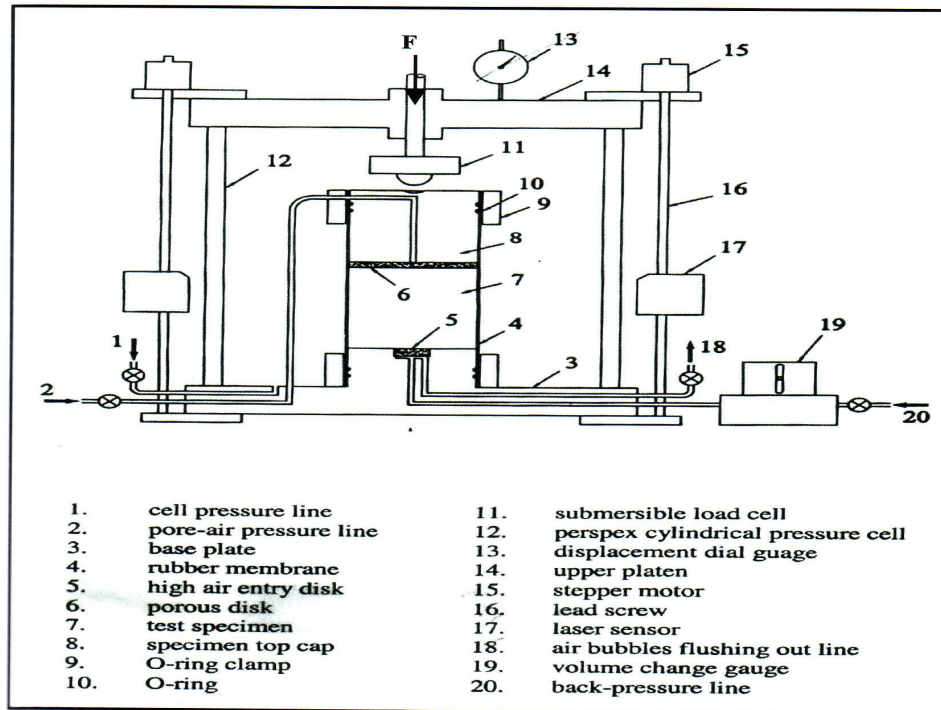


**Figure 1: A schematic diagram of the Plane strain device**

### 3. Material Preparation

The material used in this study was commercial Kaolin clay. The basic characteristics of the material are shown in Table 1.

Table 1: Characterization and classification test of the material

Type of test	Value
Liquid limit (ASTM D-4318)	53.5 %
Plastic limit (ASTM D-427)	30.76 %
Plasticity Index	22.74 %
Specific Gravity (ASTM D-854)	2.60

The preparation of soil specimen took a few weeks to complete. Initially, a kaolin clay sample was slurried to a uniform consistency of 1 ½ times its liquid limit using an electrical soil mixer. This slurry was obtained by mixing 8 kg of kaolin powder with 6 kg of water using the electric mixer for about 2 hours. Before pouring the kaolin slurry to the consolidation unit, the inner wall of the cylinder mould was greased to ease the extrusion of the sample from the mould at the end of consolidation. Figure 2 presents a schematic diagram of consolidation unit of kaolin slurry for preparing the specimens. A steel cylindrical mould with the height of 600 mm and 150 mm in diameter was used to consolidate the slurry using a hydraulic tester in over a period of one to two weeks which

the maximum of 300 kPa was applied in three stages. To apply the pressure evenly to the slurry, two circular perspexes were placed at both ends of the slurry in the mould. The slurry was allowed to consolidate by its own weight and small pressure was applied to prevent the slurry being squeezed out between the circular perspexes and the mould. A higher vertical pressure was applied when there was no further settlement change. The soil was then extruded from the mould into lubricated formers when the consolidation process had completed. Following this, the specimen and the former were wrapped in plastic film sheeting after sealing both their faces with liquid wax. To obtain even pore water pressure, the specimens were placed in the dehumidifier for at least 2 days until it is tested

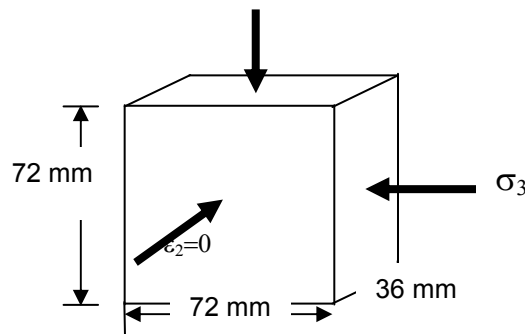


Figure 2: A schematic diagram of the specimen

In the plane strain test set-up, the rubber membrane was first placed over the test specimen with the aid of a sleeve stretcher. The rectangular porous plate was then placed on top of the specimen followed by the top assembly and the high air-entry disc (HAED). The rubber membrane was next slipped over the porous plate, the top assembly and the HAED and secured by the use of a set of O-rings and rectangular Perspex clamp. The specimen, together with the porous plate and the top assembly were then placed over the pedestal of the plane strain compression apparatus. The rubber membrane was next slipped over the pedestal and secured by the use of a set of O-rings and clamp set. Two rigid perspex plates were then placed and secured by the use of clamp set (Figure3). The pressure cell, top assembly and laser sensor set-up were then installed.

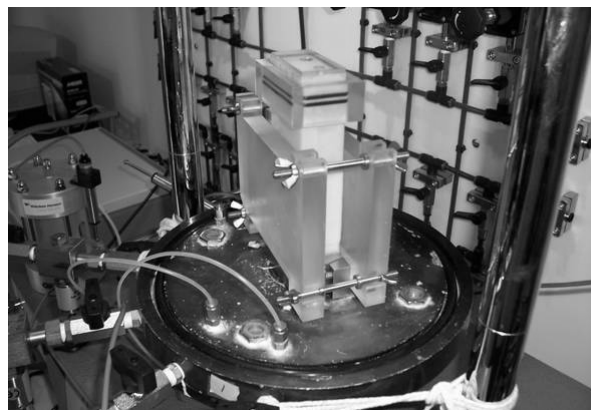


Figure 3: Side view of plane strain test set up

#### 4. Method and Test Procedure

Three specimens of MI, MC, and MT were tested under net normal stress of 0 and various matric suction and two specimens of NI and NC were tested under matric suction of 0 and various net normal stress. The specimen in test MC and NC had pre crack length of 30 mm, the specimen in test MI and NI were “intact”, and the specimen in test MT was “intact” specimen under tri axial test set up.

To provide an initial net normal stress of 0 and matric suction of 10, a cell pressure of 600 kPa, back pressure of 590 kPa and pore pressure of 600 kPa were then applied to the MI, MC, and MT specimens. The volume change of the soil skeleton  $\Delta V_s$  was monitored continuously by the laser sensors based on measurements taken at time intervals of 15 minutes. As the specimen properties and loading configuration were taken to be isotropic, the volumetric strain and hence change in volume of the soil skeleton  $\Delta V_s$  could be determined from the lateral strain. The change in volume of water in the specimen  $\Delta V_w$  was also monitored continuously by the volume change gauge which was connected to the back-pressure line. Once the changes in the soil and water volumes had ceased, the test specimen was presumed to have fully consolidated under a matric suction of 10 kPa. To flush out any air bubbles that might accumulate below the high air entry disc (HAED), the volume change gauge was set to by pass mode and the flushing line opened to a back-pressure of 50 kPa. Once the flushing was complete, the flushing line was closed and the volume change gauge set to flow mode. The matric suction was next increased to 20 kPa by reducing the back pressure to 580 kPa. The corresponding changes in the soil skeleton and water volumes were monitored continuously until they had ceased, at which stage the corresponding void ratio  $e$  and the water content of the test specimen were computed from the cumulative changes in soil skeleton and water volumes. Air bubbles accumulating below the HAED were then flushed out as before. The entire procedure, that is from increasing the matric suction to the desired value up to flushing out the air bubbles, was repeated for matric suctions of 50, 100, 200, 300, and 500 kPa respectively, which were applied by reducing the back pressure accordingly.

Other tests were prepared for NI and NC specimens and the test apparatus set up similarly as before, except that the head was replaced with a porous disc. A cell pressure of 110 kPa, back-pressure of 100 kPa and pore-air pressure of 100 kPa were then applied to the specimen to provide an initial net normal stress of 10 kPa and matric suction of 0. The changes in soil skeleton and water volumes were then monitored continuously and when these changes had ceased, the total changes in soil and water volumes were noted. The net normal stress was first increased to 20 kPa by increasing the cell pressure to 120 kPa. Thereafter, the entire above procedure, starting from applying the net normal stress up to when the changes in soil and water volumes ceased, was repeated for net normal stresses of 50, 100, 200, 300, 500 and 800 kPa. The specimen was then loaded by elevating the base of the confining pressure cell at a constant velocity of 0.08 mm/m with the drainage line closed at net normal stress of 0 and matric suction of 500 kPa for MI, MC and MT specimens and at matric suction of 0 and net normal stress of 800 kPa for NI and NC specimens. This loading rate was deduced based on the permeability of adopted kaolin clay suggested by Bishop and Henkel [24]. The data were recorded at 3 minute interval test and it was terminated at the axial strain of about 20 % or sooner. Following this, the specimen was taken out immediately for the purpose of moisture content test. In the analysis of the behaviour of the brittle unsaturated clay, the pore pressure parameter would be required in order to determine the pore pressure increments and the matric suction. The pore pressure parameters were deduced from the volumetric deformation coefficient, which was obtained by laboratory testing. This procedure was proposed by Fredlund and Rahardjo [25], although adapted to plane strain conditions.

#### 5. Test Result and Discussion

The typical result given by three specimens of MI, MC and MT and two specimens of NI and NC will be present in the following discussion.

The relationship between shear stress and vertical strain of the MI, MC, and MT specimen tested at matric suction of 500 kPa presented at Figure 3. In general, the shear stress curves increase monotonically with the increasing vertical strain until they reach peak stresses of 228.395 kPa 124.519 kPa and 175.926 kPa at about 3.87 %, 3.33 % and 3.64 % axial strain for MI, MC, and MT specimens respectively followed by strain softening behaviour. The results are fairly typical for specimen of brittle, hard partly saturated soil specimen and exhibit elastic only. This is in accordance with the model proposed by Lo et.al [23]. The highest failure stress was reached by the “intac” specimen of MI, and the lowest result was derived by the pre-crack specimen of MC. The presence of a fissure or discontinuity makes the soil weaker as the effective area offering resistance to shear is reduced. The shear strength along a surface of discontinuity is thereby less than that of the intact material. Compared to the “intact” specimen tested under triaxial condition of test MT, not only had higher peak stress, the specimen of test MI also had higher shear strength along the vertical strain. This is in consistent with the founding of Mochizuki et.al [3].

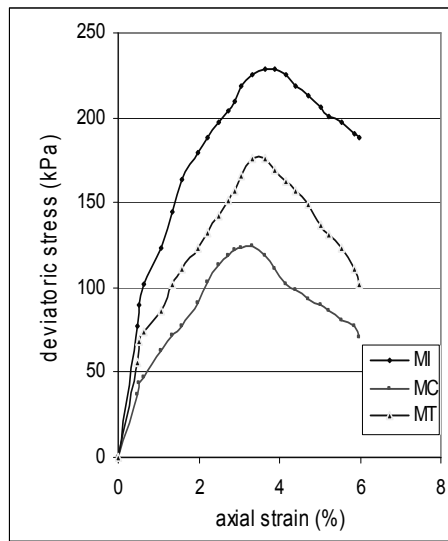


Figure 4: Stress-strain behaviour of MI, MC and

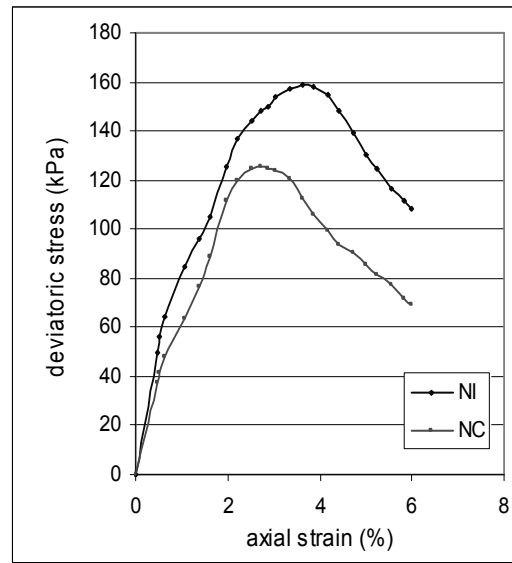


Figure 5: Stress-strain behaviour of NI and

The volume change relationships of the specimens were plotted in Figure 6 and Figure 7. The constitutive surface of void ratio is defined by the volume change index  $C_m$  and  $C_t$  corresponding to the matric suction and net normal stress respectively.  $C_t$  is the slope of the consolidation curve and is equal to the compressive index of a saturated soil, while  $C_m$  is the slope of the shrinkage curve. Regardless of specimen type, the void ratio decreased sharply with increasing of either matric suction or net normal stress at all specimens. The value of the volume change index of the MI, MC and MT specimens were calculated as 0.011, 0.016, and 0.017 respectively. The value of the  $C_t$  of the NI and NC specimens are 0.219 and 0.257. It clearly shown that the specimens containing precrack of MC and NC had higher compressive index than that the intact specimens of MI and NI.

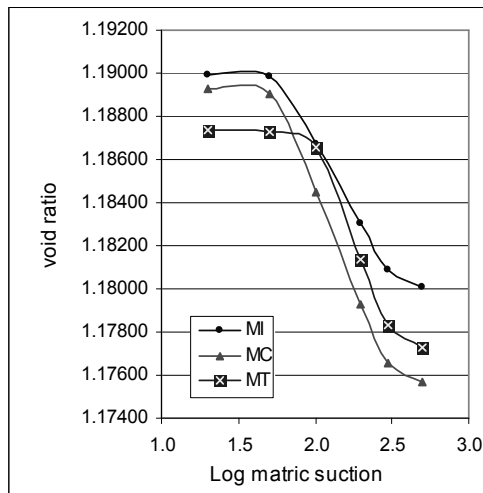


Figure 6: Void ratio versus matric

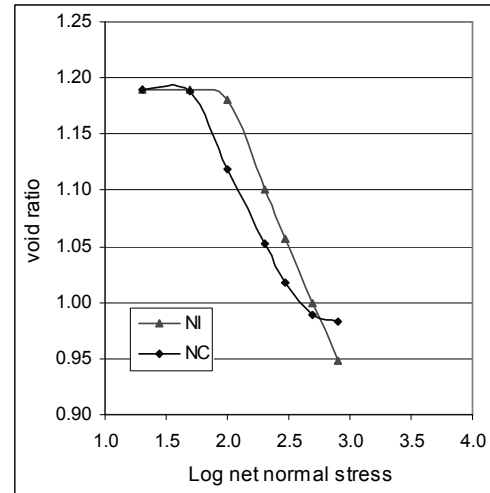


Figure 7: Void ratio versus net normal

Figure 8 shows the relationship between water content (%) (y-axis, 0.16 to 0.27) and log matric suction (x-axis, 1.0 to 3.5) for three specimens: MI (triangles), MC (circles), and MT (crosses). The curves show a decrease in water content as matric suction increases. The specimen containing precrack (MT) has a higher water content than the intact specimens (MI and MC). Figure 9 shows the relationship between water content (%) (y-axis, 0.16 to 0.27) and log net normal stress (x-axis, 1.0 to 3.5) for two specimens: NI (triangles) and NC (circles). The curves show a decrease in water content as net normal stress increases. The specimen containing precrack (NC) has a lower water content than the intact specimen (NI).

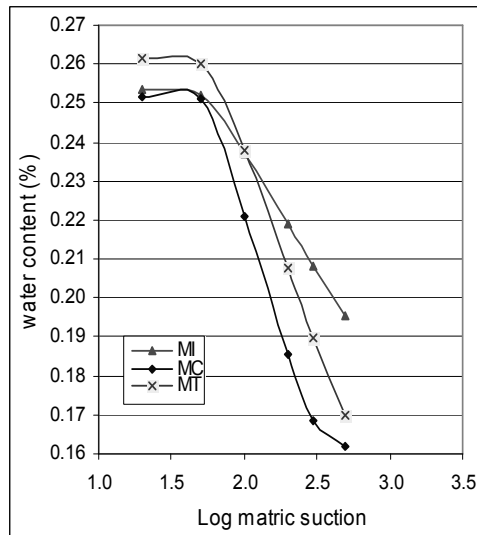


Figure 8: Water content versus matric suction of MI, MC and MT specimens

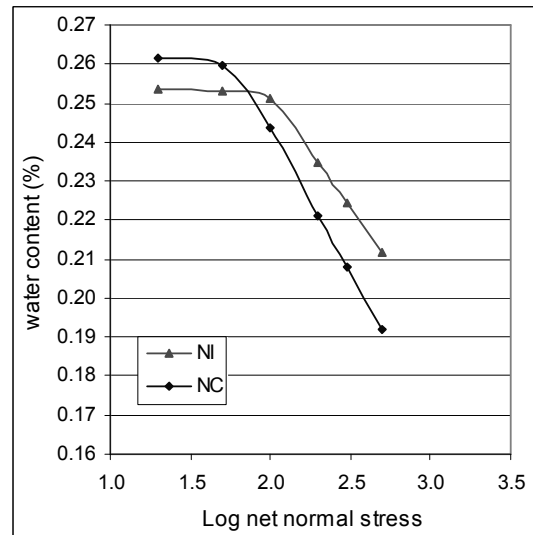


Figure 9: Water content versus net normal stress of NI and NC specimens

The following conclusions may be drawn from this experimental study.

- (1) The shear test result showed that the specimen tested is typical for specimen of brittle, hard partly saturated soil specimen and exhibit elastic only.
- (2) The discontinuities on the specimen weaken the shear strength and the compressive strength of the specimen.

## 7. Acknowledgement

The authors generously give acknowledgment to all those involved in the project, especially to Professor Kwang Wei Lo from National University of Singapore and Dr Min Min Zhao for their valuable advice and support and also to Mr. Pontjo Utomo and Mr. Paisar Syakur, for their assistance, commitment and care.

## References

- [1] Fredlund, D.G. and Morgenstern, N. R., Stress state variables for unsaturated soils, *Journal of Geotechnical Engineering*, ASCE, 1977, 447-466
- [2] Fredlund, D.G. and Morgenstern, N. R., Constitutive relation for volume change in unsaturated soil, *Canadian Geotechnique Journal*, 1976, 261-276
- [3] Mochizuki, A., Min, C. and Takahashi, S.A., A method for plane strain testing of sand, *Journal of Japanese Geotechnical Society*, 1993, 99-107
- [4] Han, C and Vardoulakis, I.G., Plane strain compression experiments on water-saturated fine-grained sand, *Canadian Geotechnique Journal*, 1991, 49-78
- [5] Green, G.E. and Reades, D.W., Boundary conditions, anisotropy and sample shape effects on the stress-strain behaviour of sand in triaxial compression and plain strain, *Geotechnique*, 1975, 333-356
- [6] Drescher, A., Vardoulakis, I. and Han, CA Biaxial Apparatus for Testing Soils, *Geotechnical Testing Journal*, GTJODJ, 1990, 226-234
- [7] Viggiani, G., Finno, R.J. and Harris, W.W., Experimental observations of strain localisation in plane strain compression of a stiff clay, *In Localisation and Bifurcation Theory for Soils and Rocks*, Chambon et.al., Balkema, 1994
- [8] Taylor, D.W., *7<sup>th</sup> Progress report on shear strength to US Engineers*, Massachusetts Institute of Technology, 1941
- [9] Rowe, P.W. and Barden, L., *Importance of free ends in triaxial testing*, *Journal of Geotechnical Engineering*, ASCE, 1964, 1-27
- [10] Lee, K.L. and Seed, H.B., Discussion on use of free end in triaxial testing on clays, *Journal of Geotechnical Engineering*, ASCE, 196, 173-177
- [11] Bishop, A.W. and Green, G.E., The influence of end restraint on the compression strength of cohesionless soil, *Geotechnique*, 1965, 243-266
- [12] Han, C. and Drescher, A., Shear bands in biaxial tests on dry coarse sand, *Soils and Foundations*, *Japanese Society of Soil Mechanics and Foundation Engineering*, 1993, 118-132
- [13] Lee, K.L., Comparison of plane strain and triaxial tests of sand, *Journal of the Soil Mechanics and Foundation Division*, ASCE, 1970,
- [14] Marach, N.D., Duncan, J.m., Chan, C.K. and Seed, H.B., Plane strain testing of sand, *laboratory shear strength of soil*, ASTM STP 740, 1984, 294-302
- [15] Mochizuki, A., Min, C. and Takahashi, S.A., A method for plane strain testing of sand, *Journal of Japanese Geotechnical Society*, 1993, 99-107
- [16] Alshibli, K.A. and Sture, S., Shear bands formation in plane strain experiments of sand, *Journal of Geotechnical and Geoenvironmental Engineering*, ASCE, 2000, Paper no.21167
- [17] Alshibli, K.A., Godbold, D. L., and Hoffman, K., The Louisiana Plane strain apparatus for soil testing, *Geotechnical Testing Journal*, ASTM, 2004, 337-346
- [18] Drescher, A., Vardoulakis, I. and Han, C., A Biaxial sapparatus for testing soils, *Geotechnical Testing Journal*, GTJODJ, 1990, 226-234
- [19] Fauziah, M. and Nikraz, H, Biaxial testing of overconsolidated clay, *Proceeding of The 1<sup>st</sup> International Conference of European Asian Civil Engineering Forum*, Pelita harapan University, 2007,
- [20] Fauziah, M. and Nikraz, H., Stress-strain behaviour of overconsolidated clay under plane strain condition, *Proceeding of 10<sup>th</sup> Australia New Zealand conference on geomechanics*, 2007, 148-153

- [21] Lo, K.W., Mita, K.A., and Tamiselvan, T., Plane strain testing of overconsolidated clay, *Research Report*, Department of Civil Engineering National University of Singapore, 2000
- [22] Bizzarri, A., Allersma, H. G. B., Koehorst, B. A. N., Preliminary tests on soft clay with a biaxial apparatus, *Proceedings of the 1995 International Symposium on Compression and Consolidation of Clayey Soils. Part 1 (of 2)*, 1995
- [23] Lo, K.W., Nikraz, R.H., Tamiselvan, T. and Zhao, M.M., An elastoplastic shear fracture model for soil and soft rock, *Proc of the 11th International Conference on Fracture*, 2005 [www.icf11.com/proceeding/TOPIC/topic.htm](http://www.icf11.com/proceeding/TOPIC/topic.htm)
- [24] Bishop, A.W. and Henkel, D.J., *The measurement of soil properties in the triaxial test*, Arnold, London, 1962.
- [25] Fredlund, D.G. and Rahardjo, H., *Soil mechanics for unsaturated soil*, John Willey & Sons, Inc, 1993

THIRD INTERNATIONAL CONFERENCE ON EVOLUTION,  
MONITORING, SIMULATION, MANAGEMENT AND  
REMEDICATION OF THE GEOLOGICAL ENVIRONMENT AND  
LANDSCAPE

Geo-Environment and Landscape Evolution III

CONFERENCE CHAIRMEN

**U. Mander**

*University of Tartu, Estonia*

**C.A. Brebbia**

*Wessex Institute of Technology, UK*

**J. F. Martín-Duque**

*Complutense University, Spain*

INTERNATIONAL SCIENTIFIC ADVISORY COMMITTEE

M. Antrop

D. Gilmanov

M. Mirzaeian

M. Noormets

**Organised by**

*Wessex Institute of Technology, UK*

*Complutense University, Spain*

**Sponsored by**

*WIT Transactions on The Built Environment*



# Contents

## Section 1: Remediation and restoration

Silica sand slope gullyng and mining in Central Spain: erosion processes and geomorphic reclamation of contour mining <i>M. A. Sanz, J. F. Martín-Duque, C. Martín-Moreno, A. Lucía, J. M. Nicolau, J. Pedraza, L. Sánchez, R. Ruiz &amp; A. García</i> .....	3
The problem of flow by-pass at permeable reactive barriers <i>H. Klammler &amp; K. Hatfield</i> .....	15
Planning of flood defence management and rehabilitation of the natural habitat in the downstream part of the river Tiber <i>L. de Santoli, D. Astiaso Garcia &amp; A. C. Violante</i> .....	25

## Section 2: Environmental modelling

The potential impact of agricultural management change on soil restoration of the cereal-growing regions of central Spain <i>D. L. Boellstorff</i> .....	37
The nugget-effect approaches of SAKWeb <sup>®</sup> for environmental modelling <i>J. Negreiros, M. Painho, A. C. Costa, P. Cabral &amp; T. Oliveira</i> .....	47
Occurrence of <i>Pseudomonas aeruginosa</i> in Kuwait environment <i>A. Akbar, D. AL-Otaibi, H. Drobiova, C. Obwekue &amp; E. Al-Saleh</i> .....	57
The water balance analysis of Kordan Basin (north west of Iran) <i>H. Moghimi</i> .....	65
The behaviour of unsaturated compacted clay under plane strain condition <i>M. Fauziah &amp; H. R. Nikraz</i> .....	77

## The behaviour of unsaturated compacted clay under plane strain condition

M. Fauziah<sup>1</sup> & H. R. Nikraz<sup>2</sup>

<sup>1</sup>Research student at Department of Civil Engineering,  
Curtin University of Technology, Western Australia,  
also lecturer at Indonesian Islamic University, Indonesia

<sup>2</sup>Departement of Civil Engineering Curtin University of Technology,  
Western Australia

### Abstract

The behaviour of unsaturated soil is quite different from those of saturated soil because of the influence of suction. Although soils are generally assumed fully saturated below the groundwater table, they may be semi saturated near the state of full saturation under certain conditions. The situation of partial saturation may be caused by several factors, such as variation of water table level due to natural or manmade processes. This study was undertaken to delineate the effects of soil water suction on the behaviour of kaolin clay under plane strain condition, as more geotechnical problems in the field such as slope failure, earth retaining structures, and shallow foundation basically occur in plane strain conditions rather than tri axial condition. The biaxial apparatus, which was used in this study, is a modification of the conventional tri axial apparatus. Cell pressure from the tri axial compression test and a rigid loading platen are used to apply the minor ( $\sigma_3$ ) and major ( $\sigma_1$ ) principle stresses, respectively, to the clay specimen. The specimen is mounted inside the device, which fully restrains any out-of-plane deformation by the use of a pair of rigid perspex wall. The volume change of the sample was measured by local strain devices and laser sensor while the water volume change was recorded by a volume gauge. Results from the tests were compared with the theoretical analysis within the elasto-plastic critical state model for unsaturated soil.

*Keywords:* biaxial, partly saturated, matric suction, volume change.



## 1 Introduction

An unsaturated soil is generally characterized by three phases, soil solids, water, and air. The presence of a fourth independent phase, a so called air-water interface or contractile skin was introduced by Fredlund and Morgenstern [7]. Based on multiphase continuum mechanics, a theoretical stress analysis of an unsaturated soil is presented by Fredlund and Morgenstern [6, 7]. The analysis concluded that any two of three possible normal stress variables can be used to describe the stress state of an unsaturated soil. This is in contrast to saturated soil, where it is possible to relate the behaviour of the soil to the effective stress only. The presence of matric suction pressure is the main difference between saturated and unsaturated soil mechanics. It has been observed that several stability problems, involving soils used as construction materials, are due to water content changes and therefore to matric suction changes that occur periodically in nature.

The mechanical properties of soil usually are tested by the use of tri axial apparatus. However, field problems involving geotechnical structures are often plane strain situations and hence data obtained from tri axial testing would not apply. It would be more appropriate using data from plane strain compression testing. In addition to foundations, retaining walls and cuts in slope and other light structures are generally designed such that they are under unsaturated conditions as they remain above the water table. Mochizuki et al. [16] reported that when soil is tested under plane strain conditions, it, in general, exhibits a higher compressive strength and lower axial strain. Most of the plane strain apparatus used by previous researchers [3, 10, 11, 16, 19], had the common feature of using rigid walls and tie-rods to impose a zero strain boundary condition in one of the principle axes. This method was found to be satisfactory, and friction between the rigid wall and test specimen could be adequately mitigated. Several researchers, [1, 13, 18, 27] found that if the aspect ratio (height to width) was bigger than 2, the effect of loading platen friction and the restraint of loading frame would be negligible.

The Behaviour of fined grained sands tested under plane conditions has been reported [9, 10, 12, 16, 17] and the plane strain testing of clay has been initiated recently [3–5, 14]. However published data of such tests especially for hard clay material and unsaturated soil are very limited. Lo et al. [15] presented a fracture model for soil and soft rock accordingly and thereby provided a rational basis for the prediction of such soil behaviour.

This study will present the behaviour of unsaturated clay specimens by the use of plane strain compression device, although the fracture characteristics of brittle clay may also be determined by this test apparatus. Details of the apparatus, specimen preparation and data evaluation are presented in the following discussion. Some results of the testing will be compared with the known soil mechanical concept.



## 2 Plane strain compression test

### 2.1 Description of the plane strain compression test

A conventional triaxial apparatus was modified for the purpose of plane strain testing in this study. The plane strain arrangement is placed in a cell, with the height of 300 mm, 200 mm internal diameter and 30 mm wall thickness. A specimen of initial width of 36 mm, height of 72 mm, and thickness of 72 mm, so that the aspect ratio is 2, is placed on the base pedestal where it is restrained laterally by two rigid perspex plates to restrain its out-of plane movement. A high air-entry disc (HAED) was used as the interface between the unsaturated soil and the pore water pressure measuring system. This was to prevent any air from passing through the disc into the measuring system, provided that the matric suction did not exceed the air-entry value of the disc. To offset the likelihood of scratching and reduced friction, all surfaces which are in contact with the specimen are lubricated. The cell is filled with water to enable the specimen to be pressurized laterally using the pressure generator for applying confining pressure. Figure 1 shows the plane strain arrangement.

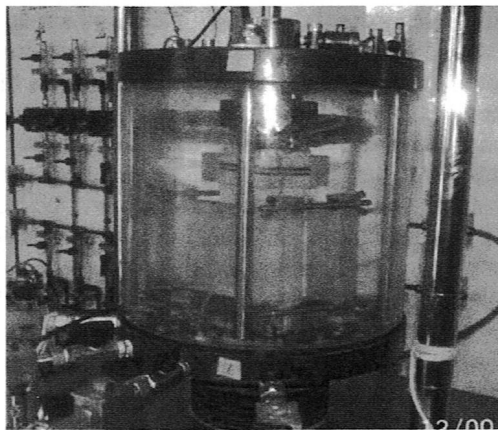


Figure 1: The plane strain arrangement.

To measure the axial load of the specimen, a 5 kN capacity of submersible load cell was used. The axial displacements of the test specimen are measured by 35-mm range LVDT (Linear Vertical Displacement Transducer) which was attached on top of the top cover of the cell. Four pore pressure transducers were used and mounted to the base plate of the cell to measure the applied cell pressure, back pressure pore pressure and flush pressure of the specimen. The global volume change of the water-saturated soil specimens are monitored by an automatic volume change unit which is connected to the back-pressure line. For the purpose of recording the displacement, loads, pressure and volume change reading a data acquisition system consisting of data logger and a set of microcomputer were used. Package software was used to convert digital bit data from the ADU (Analogue



This loading rate was deduced based on the permeability of adopted kaolin clay suggested by Bishop and Henkel [2]. During shearing the suction in the specimen was maintained at a constant matric suction of 500 kPa. The data were recorded at 3 minute interval test and it was terminated at the axial strain of about 20% or sooner. Following this, the specimen was taken out immediately for the purpose of moisture content test.

In the analysis of the behaviour of the brittle unsaturated clay, the pore pressure parameter would be required in order to determine the pore pressure increments and the matric suction. The pore pressure parameters were deduced from the volumetric deformation coefficient, which was obtained by laboratory testing. This procedure was proposed by Fredlund and Rahardjo [8], although adapted to plane strain conditions.

### 3 Test result and discussion

The typical result given by three drained test NC, PC, and NR will be present in the following discussion. The specimen in test PC had pre crack of length 3 mm cm, the specimen in test NC was "intact", and the specimen in test NR was "intact" specimen under tri axial test set up. The soil states of remoulded kaolin clay specimen are summarized in Table 2.

Table 2: Value of state parameters of the specimen.

Test Name	Initial condition			After shearing		
	$w$ (%)	$E$	$S_r$	$w$ (%)	$e$	$S_r$
NC	24.43	0.688	92.323	17.72	0.613	75.158
PC	24.47	0.730	87.153	18.01	0.693	67.570
NR	23.36	0.719	84.473	17.13	0.692	64.361

Note :  $w$ , water content;  $e$ , void ratio;  $S_r$ , Degree of saturation.

Figure 3 shows the relationship between shear stress and vertical strain at the same matric suction of 500 kPa. The shear stress increase monotonically with the increasing vertical strain up to the peak stress of 124.519 kPa, 175.926 kPa and 228.395 kPa at about 3.33%, 3.64% and 3.87% axial strain for PC, NC, and NR, respectively, then followed by strain softening behaviour to critical state. The results are fairly typical for specimen of brittle, hard partly saturated soil specimen and exhibit elastic-only fracture. This is in accordance with the model proposed by Lo et al. [15]. The "intact" specimen of test NC showed a higher peak strength than that of the fissured specimen of test PC. The presence of a fissure or discontinuity makes the soil weaker as the effective area offering resistance to shear is reduced. The shear strength along a surface of discontinuity is thereby less than that of the intact material. Compared to the "intact" specimen



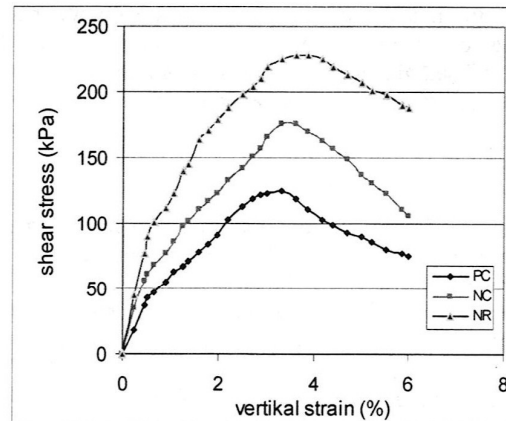


Figure 3: Stress-strain behaviour of the specimen.

testing without rigid wall of test NR, not only had higher peak stress, the specimen of test NC also had higher shear strength along the vertical strain. This is in well agreement with the founding of Mochizuki et al. [16].

Figure 4 presents the influence of matric suction on volume change of the specimen. In general it is clearly shown that for all specimens, the volumetric strain was rising with the increasing of the matric suction. The compressive volumetric strains are taken as positive. The tendency in plane strain test seems to be compressive volume change. Similar to the stress-strain of specimen test on Figure 3, because of the presence of the crack or discontinuities on the PC specimen, it makes the specimen weaker than that the "intact" specimen of NC.

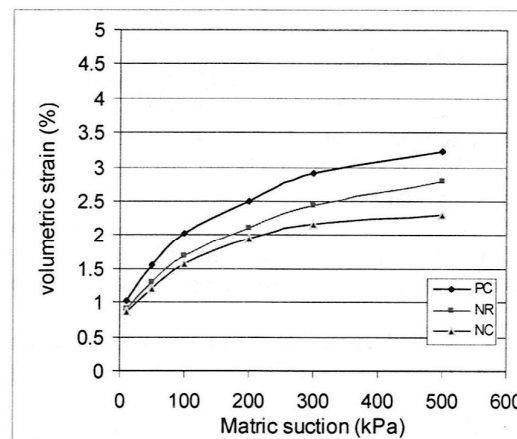


Figure 4: Influence of matric suction on volumetric strain of the specimen.

The specimen of PC had the lowest compressive strength than that the other specimen. Compared to the specimen under the tri axial of test NR, the bi axial specimen of test NC had higher shear strength along the vertical strain. This is consistent with the founding of Mochizuki et al. [16].

#### 4 Conclusions

The following conclusions may be drawn from this experimental study.

- (1) The apparatus have been able to provide the test result that in accordance with known soil behaviour.
- (2) The shear test result showed that the specimen tested is typical for specimen of brittle, hard partly saturated soil specimen and exhibit elastic-only fracture.
- (3) The discontinuities of the specimen affected to the shear strength and the compressive strength of the specimen.

#### Acknowledgements

We would like to thank all those involved in the project, especially to Associate Professor Kwang Wei Lo and Dr. Min Min Zhao for valuable advice and Mr. Pontjo Utomo and Mr. Paisar Syakur, both research students at Curtin University of Technology, for their assistance, commitment and care.

#### References

- [1] Bishop, A.W. and Green, G.E., The influence of end restraint on the compression strength of cohesionless soil, *Geotechnique*, 15 (3), pp. 243–266, 1965.
- [2] Bishop, A.W. and Henkel, D.J., *The measurement of soil properties in the triaxial test*, 2<sup>nd</sup> Ed., Arnold, London, 1962.
- [3] Drescher, A., Vardoulakis, I. and Han, C., A Biaxial apparatus for testing soils, *Geotechnical Testing Journal*, GTJODJ, 13, pp. 226–234, 1990.
- [4] Fauziah, M. and Nikraz, H., Biaxial testing of overconsolidated clay, *Proceeding of The 1<sup>st</sup> International Conference of European Asian Civil Engineering Forum*, Jakarta, Indonesia, 2007.
- [5] Fauziah, M. and Nikraz, H., Stress-strain behaviour of overconsolidated clay under plane strain condition, *Proceeding of 10<sup>th</sup> Australia New Zealand conference on geomechanics*, pp. 148–153, Brisbane, Australia, 2007.
- [6] Fredlund, D.G. and Morgenstern, N.R., Constitutive relation for volume change in unsaturated soil, *Canadian Geotechnique Journal*, 13 (3), pp. 261–276, 1976.
- [7] Fredlund, D.G. and Morgenstern, N.R., Stress state variables for unsaturated soils, *Journal of Geotechnical Engineering ASCE*, 103 (5), pp. 447–466, 1977.



- [8] Fredlund, D.G. and Rahardjo, H., Soil mechanics for unsaturated soil, John Wiley & Sons, Inc, 1993.
- [9] Han, C. and Drescher, A., Shear bands in biaxial tests on dry coarse sand, Soils and Foundations, Japanese Society of Soil Mechanics and Foundation Engineering, 33 (1), pp. 118–132, 1993.
- [10] Han, C. and Vardoulakis, I.G., Plane strain compression experiments on water-saturated fine-grained sand, Geotechnique, 41(1), pp. 49–78, 1991.
- [11] Green, G.E. and Reades, D.W., Boundary conditions, anisotropy and sample shape effects on the stress-strain behaviour of sand in triaxial compression and plain strain, Geotechnique, Vol.25, No.2, pp. 333–356, 1975.
- [12] Lee, K.L., Comparison of plane strain and triaxial tests of sand, Journal of the Soil Mechanics and Foundation Division. ASCE, 96(3), 1970.
- [13] Lee, K.L. and Seed, H.B., Discussion on use of free end in triaxial testing on clays, ASCE, 91 (6), pp. 173–177, 1964.
- [14] Lo, K.W., Mita, K.A. and Tamiselvan, T., Plane strain testing of overconsolidated clay, Research Report, Department of Civil Engineering, National University of Singapore, 2000.
- [15] Lo, K.W., Nikraz, R.H., Tamiselvan, T. and Zhao, M.M., An elastoplastic shear fracture model for soil and soft rock, Proc of the 11th International Conference on Fracture, Turin, Italy, 2005, [www.icf11.com/proceeding/TOPIC/topic.htm](http://www.icf11.com/proceeding/TOPIC/topic.htm)
- [16] Mochizuki, A., Min, C. and Takahashi, S.A., A method for plane strain testing of sand, Journal of Japanese Geotechnical Society, 475, pp. 99–107, 1993.
- [17] Marach, N.D., Duncan, J.M., Chan, C.K. and Seed, H.B., Plane strain testing of sand, laboratory shear strength of soil, ASTM STP 740, pp. 294–302, 1981.
- [18] Rowe, P.W. and Barden, L., Importance of free ends in triaxial testing, ASCE, 90 (1), pp.1–27, 1964.
- [19] Viggiani, G., Finno, R.J. and Harris, W.W., Experimental observations of strain localisation in plane strain compression of a stiff clay, In Localisation and Bifurcation Theory for Soils and Rocks, Chambon et al., Eds., Balkema, Rotterdam, pp. 189–198, 1994.
- [20] Taylor, D.W., 7<sup>th</sup> Progress report on shear strength to US Engineers, Massachusetts Institute of Technology, 1941.







# COMMON GROUND

## PROCEEDINGS OF THE 10TH AUSTRALIA NEW ZEALAND CONFERENCE ON GEOMECHANICS


### VOLUME 1

EDITORS: JAY AMERATUNGA, BRETT TAYLOR AND MATTHEW PATTEN

AUSTRALIAN GEOMECHANICS SOCIETY AND  
THE NEW ZEALAND GEOTECHNICAL SOCIETY INC

HILTON HOTEL, BRISBANE, QUEENSLAND, AUSTRALIA  
21 - 24 OCTOBER 2007

CONFERENCE PATRON

**coffey**  geotechnics

THIS IS A REGIONAL CONFERENCE OF THE INTERNATIONAL SOCIETY FOR SOIL MECHANICS  
AND GEOTECHNICAL ENGINEERING (ISSMGE)

THE AUSTRALIAN GEOMECHANICS SOCIETY IS JOINTLY SPONSORED BY:  
ENGINEERS AUSTRALIA AND THE AUSTRALASIAN INSTITUTE OF MINING AND METALLURGY

## CONTENTS

	COMMON GROUND COMMITTEE	1-25
	CONFERENCE SPONSORS AND SUPPORTERS	1-27
	REVIEWERS	1 - 29
KEYNOTE ADDRESS	THE CONTINUING PROBLEMS ASSOCIATED WITH EXPANSIVE AND COLLAPSING SOILS Peter W. Mitchell	1-32
INTERNATIONAL LECTURE	THE RELIABILITY OF THE GEOTECHNICAL ENTERPRISE John T. Christian	1-42
JOHN JAEGAR MEMORIAL LECTURE	THE MECHANICS OF INTERNAL EROSION AND PIPING OF EMBANKMENT DAMS AND THEIR FOUNDATIONS Robin Fell	1-60
NEW ZEALAND GEOMECHANICS LECTURE	A GEOMECHANICS VIEW ON HEAVY DUTY PAVEMENTS D.V. Toan	1-96

## VOLUME I - ANALYTICAL AND NUMERICAL METHODS

ANALYTICAL AND NUMERICAL METHODS	A RIVER EDGE RETENTION SYSTEM IN THE SOFT SOILS OF LAUNCESTON A Ahmed-Zeki, A Lecocq, R Longey	1 - 118
ANALYTICAL AND NUMERICAL METHODS	FINITE ELEMENT MODELLING OF LOAD SHED AND NON-LINEAR BUCKLING SOLUTIONS OF CONFINED STEEL TUNNEL LINERS A Bedi, D A Jenkins	1 - 124
ANALYTICAL AND NUMERICAL METHODS	PSEUDO-STATIC ANALYSIS OF PILES IN LIQUEFIED SOILS: A CASE STUDY OF A BRIDGE FOUNDATION H J Bowen, M Cubrinovski, M E Jacka	1 - 130
ANALYTICAL AND NUMERICAL METHODS	IMPLEMENTING ANISOTROPY INTO A CONSTITUTIVE MODEL FOR COMPACTED UNSATURATED SOILS F Ciavaglia, D M Wood, A Russell	1 - 136
ANALYTICAL AND NUMERICAL METHODS	ENHANCED NUMERICAL ANALYSIS OF GROUND BEHAVIOUR INFLUENCED BY TREE ROOT SUCTION B Fatahi, B Indraratna, H Khabbaz	1 - 142
ANALYTICAL AND NUMERICAL METHODS	STRESS-STRAIN BEHAVIOUR OF OVERCONSOLIDATED CLAY UNDER PLANE STRAIN CONDITION M Fauziah, H Nikraz	1 - 148
ANALYTICAL AND NUMERICAL METHODS	MODELLING THE STRESS-STRAIN RESPONSE OF A CEMENTED REGIONAL CLAY M K Islam, A Siddique, M I K Ullah	1 - 154
ANALYTICAL AND NUMERICAL METHODS	NUMERICAL IMPLEMENTATION OF A HYDRO-MECHANICAL MODEL FOR PARTIALLY SATURATED SOILS M A Habte, N Khalili	1 - 160
ANALYTICAL AND NUMERICAL METHODS	DEM MODELING OF CRUSHED STONE MATERIAL - EMPHASIS ON THE GRAIN SIZE DISTRIBUTION AND POROSITY D Lee, N Cho, C Yoo	1 - 166

## Stress-strain behaviour of overconsolidated clay under plane strain condition

Miftahul Fauziah

Department of Civil Engineering,  
Curtin University of Technology, WA, Australia  
Hamid Nikraz

Department of Civil Engineering,  
Curtin University of Technology, WA, Australia

Keywords: plane strain, triaxial, overconsolidated clay

### ABSTRACT

The present modelling of soil failure in common usage tend to view the stress-strain behaviour of soil based on principles of continuum mechanics. The behaviour of soil is routinely interpreted from triaxial testing; whereas, testing of soil using the biaxial device would be more useful information, as more geotechnical problems basically occur in these situations. A new biaxial compression device has been used to investigate the stress-strain behaviour of overconsolidated clay. The plane strain apparatus, which was used in this study, is a modification of the conventional triaxial apparatus. Cell pressure from the triaxial compression test and a rigid loading platen are used to apply the minor ( $\sigma_3$ ) and major ( $\sigma_1$ ) principle stresses, respectively, to the clay specimen. The specimen is mounted inside the device, which fully restrains any out-of-plane deformation by the use of a pair of rigid Perspex wall. Some results of the testing are presented and compared with the known soil mechanical model. The device has been able to provide test results that are reasonably consistent with known soil behaviour.

### 1 INTRODUCTION

The failure of soil is an important basis of its mechanical behaviour. Experimental tests to determine constitutive behaviour of soil are based on the premise that the specimen deforms uniformly in spite of the fact that laboratory evidence of localization phenomena has existed for some time. The occurrence of such failure zones, therefore, affects the experimental techniques as well as the numerical implementation of the constitutive equations of soil.

Routine soil testing mainly using triaxial apparatus is carried out to obtain its mechanical properties in the laboratory. However, field problems involving geotechnical structures are often plane strain situations and hence data obtained from triaxial testing would not apply. It would be more appropriate using data from biaxial compression testing. Mochizuki et al. (1993) reported that when soil is tested under plane strain conditions, it, in general, exhibits a higher compressive strength and lower axial strain. Plane strain testing of soil was performed firstly by Kjellman (1936). Hambly and Roscoe (1969) who adopt this testing device found the "corner junction" problem. Wood (1958) and Cornforth (1964) proposed a long rectangular specimen for ease of controlling the plane strain condition. However, inaccuracy in the measurements of stresses and strains caused by the friction force arising from axial loading surface was found by Finn et al. (1968), Lee (1970) and Marach et al. (1981) when they adopted this method. A plane strain test device using a rectangular sample of 84 mm x 76 mm x 53 mm was developed by Green (1971). However, Bishop (1981) pointed out that Green's method, which had the  $\sigma_2$  loading surface suspended by wires, could not perform as expected. Most of the plane strain apparatus (Green and Reades, 1975; Mochizuki et al., 1993; Drescher, 1990; Han and Vardoulakis, 1991; Viggiani et al., 1994) had the common feature of using rigid walls and tie-rods to impose a zero strain boundary condition in one of the principle axes. This method was found to be satisfactory, and friction between the rigid wall and test specimen could be adequately mitigated. Taylor (1941), Rowe and Barden (1964), Lee and Seed (1964) and Bishop and Green (1965) found that if the aspect ratio (height to width) was bigger than 2, the effect of loading platen friction and the restraint of loading frame would be negligible.

The present study deals with the strain-stress of overconsolidated clay specimens by the use of biaxial compression device, although the fracture characteristics of brittle clay may also be determined by this test apparatus. Details of the apparatus, specimen preparation and data evaluation are presented in the following discussion. Some results of the testing will be compared with the known soil mechanical concept.

## 2 BIAXIAL COMPRESSION TEST

### 2.1 Testing apparatus

The testing apparatus used in this study was a modification of the conventional triaxial apparatus. The biaxial arrangement is placed in a cell, with the height of 300 mm, 200 mm internal diameter and 30 mm wall thickness. A specimen of initial width of 36 mm, height of 72 mm, and thickness of 72 mm, so that the aspect ratio is 2, is placed on the base pedestal where it is restrained laterally by two rigid Perspex plates to restrain its out-of plane movement. All biaxial surfaces which are in contact with the specimen are lubricated to offset the likelihood of scratching and reduced friction. The cell is filled with water to enable the specimen to be pressurized laterally by the use of the pressure generator for applying confining pressure.

A 5 kN capacity of submersible load cell is used to measure the axial load of the specimen. The axial displacements of the test specimen are measured by 35- mm range LVDT (Linear Vertical Displacement Transducer) attached on top of the top cover of the cell. For the purposed of measuring the applied cell pressure, back pressure and pore pressure of the specimen three pore pressure transducers were used and mounted to the base plate of the cell. The global volume change of the water-saturated soil specimens are monitored by an automatic volume change unit which is connected to the back-pressure line.

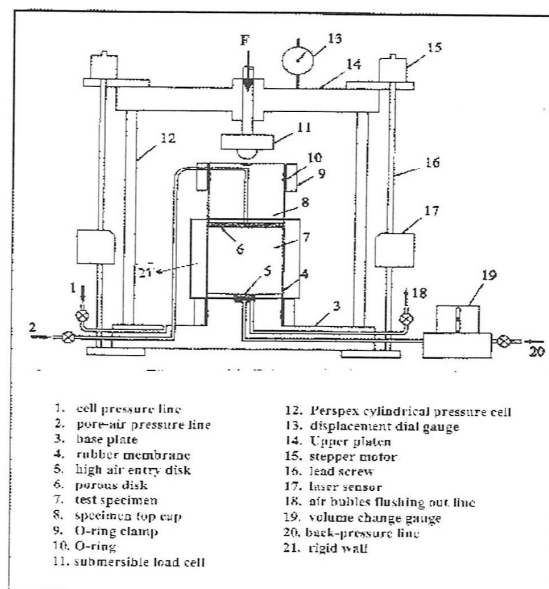


Figure 1 : Schematic diagram of the biaxial device

To record the displacement, loads, pressure and volume change reading a data acquisition system consisting of data logger and a set of microcomputer were used. A package software is used to

convert digital bit data from the ADU (Analogue digital Unit) to engineering units based on the calibration of the relevant measuring unit, which was done before running the plane strain test. A schematic diagram of the biaxial device used in this study is shown in Figure 1. The difference between triaxial and biaxial apparatus is that the specimen for biaxial test is restrained laterally by two rigid perspex plates, which make  $\varepsilon_2=0$ . Therefore, only major ( $\sigma_1$ ) and minor ( $\sigma_3$ ) principal stresses acting on the soil specimen.

## 2.2 Specimen preparation

Plane strain experiments have been performed on remoulded kaolin clay specimens. The source of clay used in this study was kaolin clay, with a specific gravity  $G_s = 2.6$ , Liquid Limit  $LL = 53.5\%$  and plastic limit  $PL = 30.76\%$ .

It took a few weeks to complete the preparation of soil specimens. Initially, a kaolin clay sample was slurried to a uniform consistency of 1 ½ times its liquid limit using an electrical soil mixer. A steel cylindrical mould with the height of 600 mm and 150 mm in diameter was used to consolidate the slurry using a hydraulic tester in over a period of one to two weeks which the maximum of 300 kPa was applied in three stages. Two circular perspexes were placed at both ends of the slurry in the mould to apply the pressure evenly to the slurry. The slurry was allowed to consolidate by its own weight and small pressure was applied to prevent the slurry being squeezed out between the circular perspexes and the mould. A higher vertical pressure was applied when there was no further settlement change. Once consolidated, the soil was extruded from the mould into lubricated formers. Following this, the specimen and the former were wrapped in a plastic film sheeting after sealing both their faces with liquid wax, and then left in the dehumidifier for at least 2 days until it is tested.

## 2.3 Tests procedures

The standard procedure either for consolidated-drained test (CD) and consolidated-undrained test (CU) triaxial testing was applied before the biaxial compression test was carried out (Head, 1986). Firstly, the specimen was saturated until the B-value of the specimen reached the value of 0.95-0.98; then it was consolidated by applying a back pressure of 300 kPa and the maximum of 700 kPa effective consolidation pressure, and followed by unloading process to reach the desire OCR in three stages. The specimen was then sheared by elevating the base of the confining pressure cell at a constant velocity of 0.04 mm/m for drained test (CD) and 0.08 mm/m for undrained test (CU). The specimen is loaded axially with the drainage line opened for CD specimen and closed for CU specimen. The Data were recorded at 5 minute interval and it was terminated at the axial strain of about 20 % or sooner. The primary data acquisition comprised the axial load, axial displacement, pore pressure, applied cell pressure, and volume change. From these data, the axial stress ( $\sigma_1$ ), axial Strain ( $\varepsilon_1$ ), deviatoric stress, ( $q$ ), effective mean normal stress ( $p'$ ), and other quantities of the following graphs have been determined.

## 3 TEST RESULTS AND DISCUSSION

The typical result given by two CD specimens, and two CU specimens, there were OCR20CD, OCR8CD, OCR16CU and OCR4CU for specimen with the value OCR of 20, 8, 16, and 4 respectively, will be discussed in the following discourse.

The strain softening response of the two specimens in the drained test are showed in Figure 2. The stress increases monotonically up to about 5.5 % and 7.8 % axial strain for OCR20CD and OCR8CD, respectively. A reduction in the shear strength after they reached peak stresses followed by strain softening to reach the critical state is the typical behaviour of overconsolidated clay when it is sheared. Compared to the specimen with the OCR of 8, the specimen with the OCR of 20 has lower stress because it was sheared under the lower confining pressure. Figure 3 shows the volumetric strain with axial strain of the drained specimens. The compressive volumetric strains are taken as positive. The tendency in plane strain test seems to be compressive volume change. Similar observations have been reported elsewhere (Mochizuki et.al., 1993; Lo et.al., 2000).

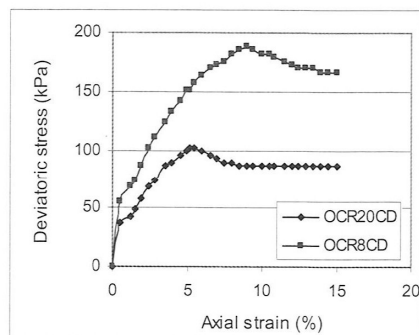


Figure 2: Stress-strain behaviour (CD test)

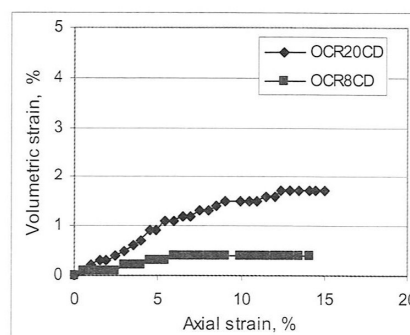


Figure 3: Volume change (CD test)

The stress-strain behaviour of CU specimens can be seen in Figure 4. Similar to the stress-strain of CD test on Figure 2, because of the lower confining pressure when sheared, the specimen with higher OCR (OCR16CU) has lower stress than the lower OCR specimen (OCR4CU). The maximum deviatoric stress of the specimens was reached on the value of about 7.4 % and 7.8 % axial strain for OCR16UD and OCR4UD, respectively. Changes in excess pore pressure against axial strain are depicted in Figure 5. The response of the specimens in undrained tests of the present study seems to be consistent with the findings of Atkinson and Richardson (1987). The results are fairly typical for specimen of heavily overconsolidated clay subjected to undrained compression.

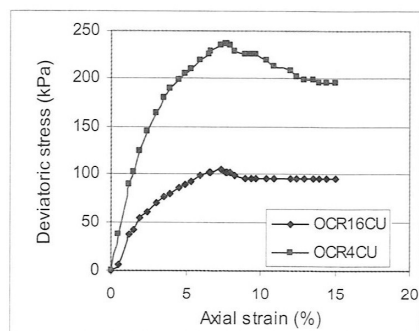


Figure 4: Stress-strain behaviour (CU test)

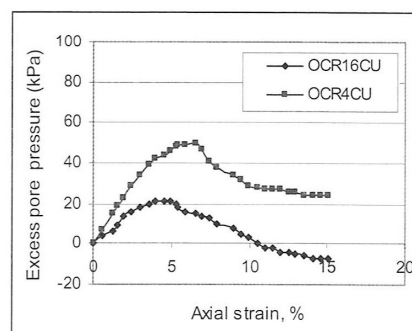


Figure 5: Excess pore pressure changes (CU test)

The stress path of the plane strain compression test is depicted in Figure 6. For drain loading condition, the specimen yields on the Hvorslev surface, where it reaches a peak shear stress and thereafter starts to dilate and soften, finally attaining the critical state. The result of this study seems to be consistent with the known mechanical concept which was founded by Hvorslev and reinvestigated by Parry in 1960 (in Atkinson and Bransby, 1982).

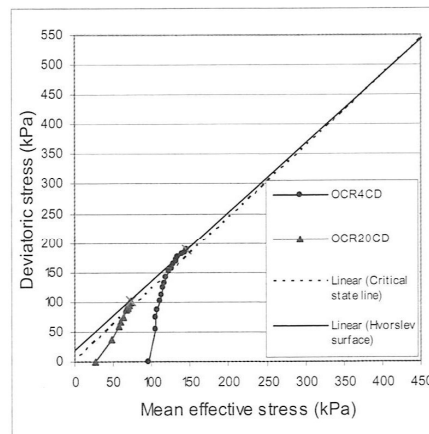


Figure 6: Stress path of drained specimens

#### 4 CONCLUSIONS

The biaxial compression apparatus used in this study for the purpose of conducting plane strain tests has been able to provide test results that are in accordance with generally observed behaviour and known soil behaviour. Failure behaviour of overconsolidated specimens on the Hvorslev surface is shown in the test results.

#### ACKNOWLEDGEMENTS

We would like to thank all those involved in the project, especially to Associate Professor Kwang Wei Lo and Dr. Min Min Zhao for valuable advice and supports and Mr. Pontjo Utomo and Mr. Paisar Syakur, both research students at Curtin University of Technology, for their assistance, commitment and care.

#### REFERENCES

- Atkinson, J.H. and Bransby, P.L.(1982). *The mechanics of soils : an introduction to critical state soil mechanics*. McGraw-Hill, New York
- Atkinson, J.H. and Richardson,D.(1987). *The effect of local drainage in shear in shear zones on the undrained strength of overconsolidated clay*. Geotechnique, 37 (3), 393-403
- Bishop, A.W.and Green, G.E.(1965). *The influence of end restraint on the compression strength of cohesionless soil*. Geotechnique, Vol.15, No.3, pp.243-266
- Cornforth, C.N.(1964). *Some experiment on the influence of strain conditions on the strength of soil*. Geotechnique, Vol.14, No.2, pp.143-167
- Drescher, A., Vardoulakis, I. and Han, C.(1990). *A biaxial apparatus for testing soils*. Geotechnical Testing Journal, GTJODJ, Vol.13, pp.226-234
- Finn, W.D.L., Wade, N.H. and Lee, K.L.(1968). *Volume change in triaxial and plane strain tests*. ASCE, No.SM6, December, pp.297-308
- Hambly, E.C. and Roscoe, K.H.(1969). *Observation and prediction of stresses and strains during plane strain of "wet" clays*.7<sup>th</sup> ICSMFE, Mexico, Vol.2, pp.173-181

- Han, C. and Drescher, A.,(1993). *Shear bands in biaxial tests on dry coarse sand*. *Soils and Foundations*. Japanese Society of Soil Mechanics and Foundation Engineering, Vol.33, No.1, pp.118-132
- Han, C and Vardoulakis, I.G.(1991). *Plane strain compression experiments on water-saturated fine-grained sand*. *Geotechnique*, Vol. 41, No.1, pp.49-78
- Head, K.H.(1986). *Manual of Soil Laboratory Testing*. Vol 3, Pentech Press, London
- Green, G.E. and Reades, D.W.(1975). *Boundary conditions, anisotropy and sample shape effects on the stress-strain behaviour of sand in triaxial compression and plain strain*. *Geotechnique*, Vol.25, No.2, pp.333-356
- Kjellman, W. (1936). *Report on apparatus for consummate investigation of the mechanical properties of soils*. 1<sup>st</sup> ICSMFE, Cambridge, Vol.2, pp.16-20
- Lee, K.L.(1970). *Comparison of plane strain and triaxial tests of sand*. *Journal of the Soil Mechanics and Foundation Division*. ASCE, Vol.96,May, No. SM3
- Lee, K.L. and Seed, H.B.(1964). *Discussion on use of free end in triaxial testing on clays*. ASCE, Vol.91, No.SM 6, November, pp.173-177
- Lo, K.W., Mita, K.A., and Tamiselvan, T.(2000). *Plane Strain Testing of Overconsolidated Clay*, Research Report, Department of Civil Engineering, National University of Singapore
- Mochizuki, A., Min, C. and Takahashi, S.A (1993). *A method for plane strain testing of sand*. *Journal of Japanese Geotechnical Society*, No.475, pp.99-107
- Marach, N.D., Duncan, J.m., Chan, C.K. and Seed, H.B.(1981). *Plane strain testing of sand, laboratory shear strength of soil*. ASTM STP 740, pp.294-302
- Roscoe, K.H. and Burland, J.B.(1968). *On the originalized stress-strain behaviour of wet clay*. *Eng.Plasticity*. Cambridge Univ. Press, pp.535-609
- Rowe, P.W. and Barden, L. (1964). *Importance of Free Ends in Triaxial Testing*. ASCE, Vol.90, No.SMI, January, pp.1-27
- Viggiani, G., Finno, R.J. and Harris, W.W.(1994). *Experimental Observations of strain localisation in plane strain compression of a stiff clay*. In *Localisation and Bifurcation Theory for Soils and Rocks*, Chambon et.al., Eds., Balkema, Rotterdam, pp.189-198



ISBN 978-979-1053-01-3

The 1<sup>st</sup> International Conference of EACEF  
(*European Asian Civil Engineering Forum*)

# PROCEEDING

The FUTURE DEVELOPMENT in  
STRUCTURAL and CIVIL ENGINEERING  
BASED on RESEARCH and  
PRACTICAL EXPERIENCE

26 – 27 September 2007

at the  
Universitas Pelita Harapan  
Lippo Karawaci, Jakarta  
INDONESIA

## Editors

Wiryanto Dewobroto (*Chief editor*)  
Harianto Hardjasaputra (*Geotechnic / Structure*)  
Jack Wijayakusuma (*Material*)  
Fransikus Mintar Sihontang (*Infrastructure*)  
Manliand R. Adventus (*Construction Management*)

## Graphic Design

Eston

## THE COMMITTEES

### ***International Scientific Committee***

Prof. Dr.-Ing. Karl-Heinz Reineck	Universität Stuttgart, Germany
Prof. Dr.-Ing. Pieter A. Vermeer	Universität Stuttgart, Germany
Prof. Dr.-Ing. Jurgan Hothan	Universität Hannover, Germany
Prof. Jenn-Chuan Chern, Ph.D	NTU, Taiwan
Prof. Chan Weng Tat, Ph.D	NUS, Singapore
Prof. Dr.-Ing. Harianto Hardjasaputra	UPH, Indonesia
Dr. FX. Supartono	HAKI, Indonesia
Dr.-Ing. Andreas Triwiyono	UGM, Indonesia

### ***Organizing Committee***

Department of Civil Engineering, Universitas Pelita Harapan

- \* Prof. Dr.-Ing. Harianto Hardjasaputra
- \* Dr.-Ing. Jack Wijayakusuma
- \* Dr.Ir. Manliand Ronald Adventus, MT.
- \* Ir. David B. Soelaiman, Dipl. HE.
- \* Ir. Wiryanto Dewobroto, MT.
- \* Ir. Fransiskus Mintar Sihontang, MT.
- \* Kristopher, ST.

### ***Supporters***

- \* Department of Civil Engineering, University of Pelita Harapan
- \* Master of Civil Engineering, University of Pelita Harapan
- \* Institute for Lightweight Structures Conceptual and Structural Design (ILEK), Universität Stuttgart, Germany
- \* Indonesian Society of Civil and Structural Engineers (HAKI)
- \* German Academic Exchange Service (DAAD)

### ***Main Sponsor***

1. PT. Indocement Tunggul Prakarsa Tbk.
2. PT. Optima Solusindo Informatika
3. PT. Lippo Karawaci

### ***Sponsor***

4. PT. Jasa Ferrie Pratama
5. PT. Gelora Bangun Lestari
6. PT. Franki Pile Indonesia
7. Majalah Proyeksi
8. PT. Multistran Engineering
9. PT. Indonesia Nihon Seima
10. PT. Surya Bangun Persada Indah
11. PT. Wiratman & Associates
12. PT. Classic Carpet
13. Oriental Sheet Piling

**BIAXIAL TESTING of OVERCONSOLIDATED CLAY**Miftahul Fauziah<sup>1</sup>, Hamid R Nikraz<sup>2</sup><sup>1</sup> PhD student, Curtin University of Technology, Western Australia,

E-mail : miftahul.fauziah@postgrad.curtin.edu.au

<sup>2</sup> Curtin University of Technology, Western Australia

E-mail : H.Nikraz@exchange.curtin.edu.au

**ABSTRACT :** The failure of soil is an important basis of its mechanical behaviour. The behaviour of soil is routinely interpreted from triaxial testing, whereas more geotechnical problems in the field such as slope failure, earth retaining structures, and shallow foundation are basically occur in biaxial conditions. Therefore, testing of soil using the biaxial device would be more useful information. A new biaxial compression device has been used to investigate the behaviour of overconsolidated clay. The plane strain apparatus, which was used in this study, is a modification of the conventional triaxial apparatus. Cell pressure from the triaxial compression test and a rigid loading platen are used to apply the minor ( $\sigma_3$ ) and major ( $\sigma_1$ ) principle stresses, respectively, to the clay specimen. The specimen is mounted inside the device, which fully restrains any out-of-plane deformation by the use of a pair of rigid perspex wall. Some results of the testing are presented and compared with the known soil mechanical model. The device has been able to provide test results that are reasonably consistent with known soil behaviour. Failure behaviour of overconsolidated specimens on the Hvorslev surface is showed in the test results.

**KEYWORDS:** biaxial, triaxial, overconsolidated clay

**1. INTRODUCTION**

Experimental tests to determine constitutive behaviour of soil are based on the premise that the specimen deforms uniformly in spite of the fact that laboratory evidence of localization phenomena has existed for some time. The occurrence of such failure zones, therefore, affect the experimental techniques as well as the numerical implementation of the constitutive equations of soil.

Triaxial apparatus is usually used to carried out to obtain mechanical properties of soil in the laboratory. However, field problems involving geotechnical structures are often plane strain situations and hence data obtained from triaxial testing would not apply. It would be more appropriate using data from biaxial compression testing. Mochizuki et al. (1993) reported that when soil is tested under plane strain conditions, it, in general, exhibits a higher compressive strength and lower axial strain.

Plane strain testing of soil was performed firstly by Kjellman (1936). Hambly and Roscoe (1969) who adopt this testing device found the "corner junction" problem. Wood (1958) and Cornforth (1964) proposed a long rectangular specimen for ease of controlling the plane strain condition. However, inaccuracy in the measurements of stresses and strains caused by the friction force arising from axial loading surface was found by Finn et.al. (1968), Lee (1970) and Marach et.al (1981), when they adopted this method.

A plane strain test device using a rectangular sample of 84 mm x 76 mm x 53 mm was developed by Green (1971). However, Bishop (1981) pointed out that Green's method, which had the  $\sigma_2$  loading surface suspended by wires, could not perform as expected. Most of the plane strain apparatus (Green and Reades, 1975; Mochizuki et.al., 1993; Drescher, 1990; Han and Vardoulakis, 1991; Viggiani et.al., 1994) had the common feature of using rigid walls and tie-rods to impose a zero strain boundary condition in one of the principle axes. This method was found to be satisfactory, and friction between the rigid wall and test specimen could be adequately mitigated. Taylor (1941), Rowe and Barden (1964), Lee and Seed (1964) and Bishop and Green (1965) found that if the aspect ratio (height to width) was bigger than 2, the effect of loading platen friction and the restraint of loading frame would be negligible.

Behaviour of fined grained sands tested under plane conditions has been reported recently (Han and Vardoulakis, 1991; Hans and Drescher, 1993; Mochizuki et.al., 1993). The plane strain testing of clay

has only been initiated recently (Drescher et.al., 1990) and published data of such tests especially for hard clay material is very limited. In the field of fracture, Lo et.al. (1993) and Lo et.al. (1997) modeled brittle overconsolidated clay accordingly and thereby provided a rational basis for the prediction of such soil behaviour.

The behaviour of overconsolidated clay specimens by the use of biaxial compression device will presented in this study, although the fracture characteristics of brittle clay and the behaviour of unsaturated clay specimens may also be determined by this test apparatus. Details of the apparatus, specimen preparation and data evaluation are presented in the following discussion. Some results of the testing will be compared with the known soil mechanical concept.

## 2. BIAXIAL COMPRESSION TEST

### 2.1. Testing Apparatus

A conventional triaxial apparatus was modified for the purpose of biaxial testing in this study. The biaxial arrangement is placed in a cell, with the height of 300 mm, 200 mm internal diameter and 30 mm wall thickness. A specimen of initial width of 36 mm, height of 72 mm, and thickness of 72 mm, so that the aspect ratio is 2 (Taylor, 1941; Rowe and Barden, 1964; Lee and Seed, 1964; Bishop and Green, 1965) is placed on the base pedestal. A schematic diagram of the biaxial device used in this study is shown in Figure 1.

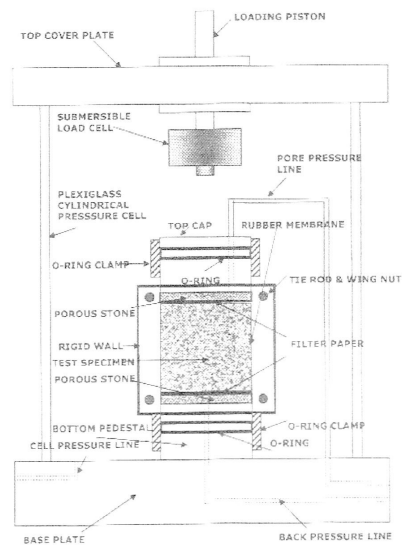


Figure 1 Schematic Diagram of The Biaxial Device

To allow some flexibility in the height of specimen the ordinary cylindrical rubber membrane measured 45 mm in diameter and 200 mm length was used. The rubber membrane is secured to the rectangular loading platens by the used of the O-rings with the diameter of 45 mm and the wall thickness of 3 mm and O-ring clamp. The rectangular sintered bronze porous stone plate of 5 mm thickness, 36 mm width, 72 mm length and 5 mm thick were used, which the same porosity to the standard porous stone for triaxial device.

The specimen is restrained laterally by two rigid Perspex plates to impose zero strain boundary condition in one of the principal axes. All biaxial surfaces which are in contact with the specimen are lubricated to offset the likelihood of scratching and reduced friction. The cell is filled with water to enable the specimen to be pressurized laterally by the use of the GDS pressure generator for applying confining pressure.

To measure the axial load of the specimen a 5 kN capacity of Wykeham Farrance WF 17109 submersible load cell is used. The axial displacements of the test specimen are measured by 35- mm range LVDT (Linear Vertical Displacement Transducer) attached on top of the top cover of the cell. For the purpose of measuring the applied cell pressure, back pressure and pore pressure of the specimen three pore pressure transducers were used and mounted to the base plate of the cell. The global volume change of the water-saturated soil specimens are monitored by an automatic volume change unit which is connected to the back-pressure line.

A data acquisition system consisting of an MPX 300 data logger and a set of microcomputer were used to record the displacement, loads, pressure and volume change reading. A WINHOST 2.0 package software (VJ Technology product) is used to convert digital bit data from the ADU (Analogue digital Unit) to engineering units based on the calibration of the relevant measuring unit, which was done before running the plane strain test.

#### a. Specimen Preparation

Plane strain experiments have been performed on remoulded kaolin clay specimens. The clay used in this study was kaolin clay, which is a product of UNIMIN PTY LTD, Australia, with a specific gravity  $G_s = 2.6$ , Liquid Limit  $LL = 53.5\%$  Plasticity Index  $PI = 22.74\%$  and plastic limit  $PL = 30.76\%$ .

The preparation of soil specimens took a few weeks to complete. Firstly, a kaolin clay sample was slurried to a uniform consistency of 1 ½ times its liquid limit using an electrical soil mixer. This slurry was obtained by mixing 8 kg of kaolin powder with 6 kg of water using the electric mixer for about 2 hours. Before pouring the kaolin slurry to the consolidation unit, the inner wall of the cylinder mould was greased to ease the extrusion of the sample from the mould at the end of consolidation. Figure 2 shows a schematic diagram of consolidation unit of kaolin slurry for preparing the specimens.

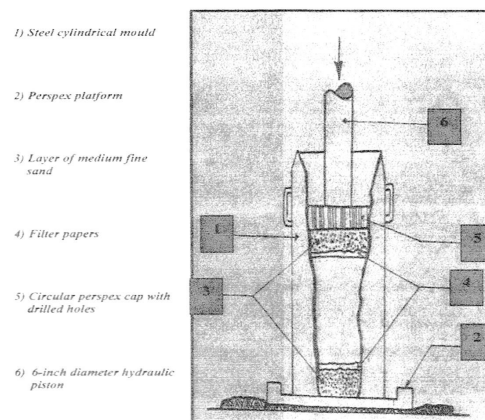


Figure 2 A schematic diagram of Consolidation unit of Kaolin Slurry

A steel cylindrical mould with the height of 600 mm and 150 mm in diameter was used to consolidate the slurry using a hydraulic tester in over a period of one to two weeks which the maximum of 300 kPa was applied in three stages. Two circular perspexes were placed at both ends of the slurry in the mould to apply the pressure evenly to the slurry. The slurry was allowed to consolidate by its own weight and small pressure was applied to prevent the slurry being squeezed out between the circular perspexes and the mould. A higher vertical pressure was applied when there was no further settlement change.

The soil was extruded from the mould into lubricated formers when the consolidation process completed. Following this, the specimen and the former were wrapped in plastic film sheeting after sealing both their faces with liquid wax. To obtain even pore water pressure, the specimens were placed in the dehumidifier for at least 2 days until it is tested.

#### b. Test Procedures

The standard procedure either for consolidated-drain test (CD) and consolidated-undrained test (CU) triaxial testing was applied before the biaxial compression test was carried out (Head, 1986). Initially, the specimen was saturated until the B-value of the specimen reached the value of 0.95-0.98; then it was consolidated by applying a back pressure of 300 kPa and the maximum of 700 kPa effective consolidation pressure in four loading stages. Each loading was terminated once the 95 % consolidation was reached, and followed by three stages unloading process to reach the desire OCR.

The specimen was then sheared by elevating the base of the confining pressure cell at a constant velocity of 0.04 mm/m for drained test (CD) and 0.08 mm/m for undrained test (CU). This loading rate was deduced based on the permeability of adopted kaolin clay (Bishop and Henkel, 1962). The specimen is loaded axially with the drainage line opened for CD specimen and closed for CU specimen. The time required to complete shearing the specimens were about 8 hours for drained

The data were recorded at 3 minute interval for CU test and at 10 minute interval for CD test and it was terminated at the axial strain of about 20 % or sooner. Following this, the specimen was taken out immediately for the purpose of moisture content test.

The primary data acquisition comprised the axial load, axial displacement, pore pressure, applied cell pressure, and volume change. From these data, the axial stress ( $\sigma_1$ ), axial Strain ( $\epsilon_1$ ), deviatoric stress, ( $q$ ), effective mean normal stress ( $p'$ ), and other quantities of the following graph have been determined. Table 1 shows the information about the test of overconsolidated clay.

Table 1. Biaxial compression test on overconsolidated clay

Test Name	Test Type &	OCR	B-value	Loading rate (mm/min)	CP (kPa)	BP (kPa)
OCR8CD	Drained	8	0.98	0.004	387	300
OCR20CD	Drained	20	0.97	0.004	335	300
OCR4CU	Undrained	4	0.97	0.008	475	300
OCR10CU	Undrained	10	0.95	0.008	370	300
OCR16CU	Undrained	16	0.96	0.008	343.75	300

### 3. TEST RESULT AND DISCUSSION

The result of testing on material parameter of remoulded kaolin clay can be seen in Table 2.

Table 2. Material parameters of remoulded kaolin clay.

$\lambda$ , virgin compression line slope	$\kappa$ , swelling line slope	N, specific volume at $p'=1$ kPa (NCL)	$\Gamma$ , specific volume at $p'=1$ kPa (CSL)	$M$ , critical state line slope	$m_H$ , Hvorslev surface slope
0.129	0.023	2.03	2.01	1.21	1.17

The typical result given by two CD specimens, and three CU specimens, there were OCR20CD, OCR8CD, OCR16CU, OCR10CU and OCR4CU for specimen with the value OCR of 20, 8, 16, and 4

respectively, will be discussed in the following discourse. The result of biaxial compression test on overconsolidated clay can be seen in Table 3.

Table 3. Result of biaxial compression test on overconsolidated clay

Test Name	$\sigma_3$ (kPa)	$q_f'$ (kPa)	$p_0'$ (kPa)	$p_f'$ (kPa)	$V_0$	$V_f$
OCR8CD	488	188.27	87.5	237.26	1.595	1.534
OCR20CD	264	101.85	35	241.95	1.613	1.48
OCR4CU	616	237.65	175	296.22	1.582	1.582
OCR10CU	336	129.63	70	202.21	1.598	1.598
OCR16CU	272	104.94	43.75	175.73	1.608	1.608

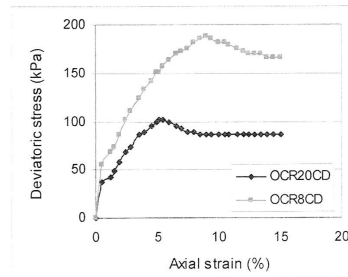


Figure 3 Stress-strain Behaviour (CD test)

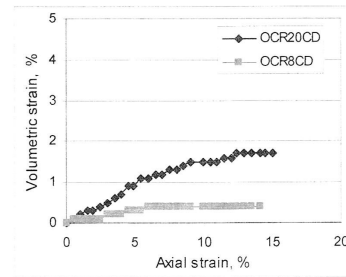


Figure 4 Volume Change (CD test)

The strain softening response of the two specimens in the drained test can be seen in Figure 3. The stress increases monotonically up to the peak deviatoric stress of 101.85 kPa and 188.27 kPa at about 5.5 % and 7.8 % axial strain for OCR20CD and OCR8CD, respectively. A reduction in the shear strength after they reached peak stresses followed by strain softening to reach the critical state is the typical behaviour of overconsolidated clay when it is sheared. Compared to the specimen with the OCR of 8, the specimen with the OCR of 20 has lower stress because it was sheared under the lower confining pressure. Figure 4 shows the volumetric strain with axial strain of the drained specimens. The compressive volumetric strains are taken as positive. The tendency in plane strain test seems to be compressive volume change. Similar observations have been reported elsewhere (Mochizuki et al., 1993; Lo et al., 2000).

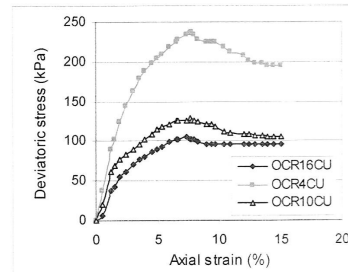


Figure 5 Stress-strain Behaviour (CU test)

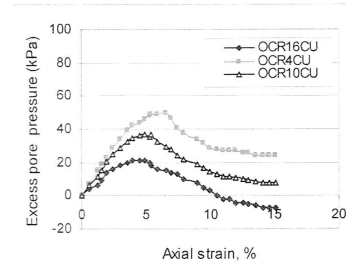


Figure 6 Excess Pore Pressure Changes (CU test)

The stress-strain behaviour and excess pore pressure changes of CU specimens can be seen in Figure 5 and Figure 6. Similar to the stress-strain of CD test on Figure 3, because of the lower confining pressure when sheared, the specimen with higher OCR has lower stress than the lower OCR specimen.

The maximum deviatoric stress of the CU specimens was reached on the value of 237.65 kPa, 129.63 kPa, and 104.94 kPa at about 7.4 %, 7.7 % and 7.8 % axial strain for OCR16UD, OCR10UD and OCR4UD, respectively. Changes in excess pore pressure against axial strain are depicted in Figure 6. The response of the specimens in undrained tests of the present study seems to be consistent with the findings of Atkinson and Richardson (1987). The results are fairly typical for specimen of heavily overconsolidated clay subjected to undrained compression.

The stress path of the plane strain compression test is depicted in Figure 7. For drain loading condition, the specimen yields on the Hvorslev surface, where it reaches a peak shear stress and thereafter starts to dilate and soften, finally attaining the critical state. The failure state of overconsolidated clay specimens laid on the Hvorslev surface while the critical state line is the locus of the critical state of the specimens. The result of this study seems to be consistent with the known mechanical concept which was founded by Hvorslev and reinvestigated by Parry in 1960 (in Atkinson and Bransby, 1982).

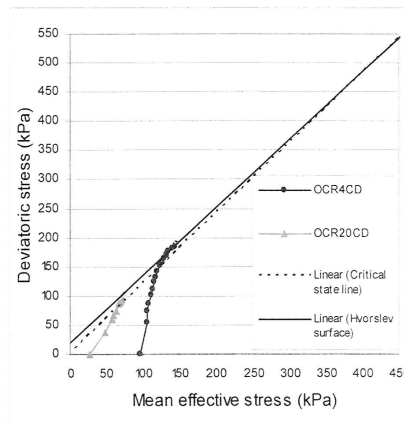


Figure 7 Stress Path of Drained Specimens

#### 4. CONCLUSIONS

The biaxial compression apparatus used in this study for the purpose of conducting plane strain tests has been able to provide test results that are in accordance with generally observed behaviour and known soil behaviour. Failure behaviour of overconsolidated specimens on the Hvorslev surface is shown in the test results.

#### 5. ACKNOWLEDGEMENTS

We would like to thank all those involved in the project, especially to Associate Professor Kwang Wei Lo and Dr. Min Min Zhao for valuable advice and Mr. Pontjo Utomo and Mr. Paisar Syakur, both research students at Curtin University of Technology, for their assistance, commitment and care.

#### 6. REFERENCES

- Atkinson, J.H. and Bransby, P.L.(1982). **"The Mechanics of Soils : An Introduction to Critical State Soil Mechanics"** McGraw-Hill, New York.
- Atkinson, J.H. and Richardson,D.(1987). **"The Effect of Local Drainage in Shear in Shear Zones on The Undrained Strength of Overconsolidated Clay"** Geotechnique, 37 (3), 393-403.



- Bishop, A.W. and Green, G.E. (1965). **"The Influence of End Restraint on The Compression Strength of Cohesionless Soil"** Geotechnique, Vol.15, No.3, pp.243-266.
- Cornforth, C.N. (1964). **"Some Experiment on The Influence of Strain Conditions on the Strength of Soil"** Geotechnique, Vol.14, No.2, pp.143-167.
- Drescher, A., Vardoulakis, I. and Han, C. (1990). **"A Biaxial Apparatus for Testing Soils"** Geotechnical Testing Journal, GTJODJ, Vol.13, pp.226-234.
- Finn, W.D.L., Wade, N.H. and Lee, K.L. (1968). **"Volume Change in Triaxial and Plane Strain Tests"** ASCE, No.SM6, December, pp.297-308.
- Hambly, E.C. and Roscoe, K.H. (1969). **"Observation and Prediction of Stresses and Strains During Plane Strain of 'Wet' Clays"**. 7<sup>th</sup> ICSMFE, Mexico, Vol.2, pp.173-181.
- Han, C. and Drescher, A. (1993). **"Shear Bands in Biaxial Tests on Dry Coarse Sand. Soils and Foundations"** Japanese Society of Soil Mechanics and Foundation Engineering, Vol.33, No.1, pp.118-132.
- Han, C. and Vardoulakis, I.G. (1991). **"Plane Strain Compression Experiments on Water-saturated Fine-grained Sand"** Geotechnique, Vol. 41, No.1, pp.49-78.
- Head, K.H. (1986). **"Manual of Soil Laboratory Testing"** Vol 3, Pentech Press, London.
- Green, G.E. and Reades, D.W. (1975). **"Boundary Conditions, Anisotropy and Sample Shape Effects on The Stress-strain Behaviour of Sand in Triaxial Compression and Plain Strain"** Geotechnique, Vol.25, No.2, pp.333-356.
- Kjellman, W. (1936). **"Report on Apparatus for Consummate Investigation of The Mechanical Properties of Soils"** 1<sup>st</sup> ICSMFE, Cambridge, Vol.2, pp.16-20.
- Lee, K.L. (1970). **"Comparison of Plane Strain and Triaxial Tests of Sand"** Journal of the Soil Mechanics and Foundation Division. ASCE, Vol.96, May, No. SM3.
- Lee, K.L. and Seed, H.B. (1964). **"Discussion on Use of Free End in Triaxial Testing on Clays"** ASCE, Vol.91, No.SM 6, November, pp.173-177.
- Lo, K.W., Mita, K.A., and Tamiselvan, T. (2000). **"Plane Strain Testing of Overconsolidated Clay"** Research Report, Department of Civil Engineering, National University of Singapore.
- Mochizuki, A., Min, C. and Takahashi, S.A. (1993). **"A Method for Plane Strain Testing of Sand"** Journal of Japanese Geotechnical Society, No.475, pp.99-107.
- Marach, N.D., Duncan, J.m., Chan, C.K. and Seed, H.B. (1981). **"Plane strain testing of sand, laboratory shear strength of soil"** ASTM STP 740, pp.294-302.
- Roscoe, K.H. and Burland, J.B. (1968). **"On the Originalized Stress-strain Behaviour of Wet Clay"** Eng. Plasticity, Cambridge Univ. Press, pp.535-609.
- Rowe, P.W. and Barden, L. (1964). **"Importance of Free Ends in Triaxial Testing"** ASCE, Vol.90, No.SMI, January, pp.1-27.
- Viggiani, G., Finno, R.J. and Harris, W.W. (1994). **"Experimental Observations of Strain Localisation in Plane Strain Compression of a Stiff clay"** In Localisation and Bifurcation Theory for Soils and Rocks, Chambon et.al., Eds., Balkema, Rotterdam, pp.189-198